THE JOURNAL OF THE INSTITUTE OF Metals

WITH THE BULLETIN AND METALLURGICAL ABSTRACTS

Principal Contents:

PRICE: TEN SHILLINGS AND SIXPENCE

JULY 1953

KIMON *master engraver of coins*

The metal artificers of old would recognise a deep kinship with to-day's skilled workmen at Capper Pass—though they would marvel at the metallurgical techniques used nowadays to extract maximum quantities of metals of the highest purity from complex and low grade materials.

You are invited to send samples or detailed analyses of your complex and low grade ores and residues containing Tin or Lead or tin combined with lead, copper, antimony, bismuth and silver.

The fine art of 'celature' came to its apex in Sicily about the year 400 B.C., and found its most famous exponent in the Athenian, Kimon. In this ten-drachma coin the goddess Arethusa is seen full face with dolphins leaping through her tresses, and the artist has proudly set his signature on her headband. The Dolphin motif typifies the Greeks' love of the sea.

CAPPER PASS *master extractors of metals*

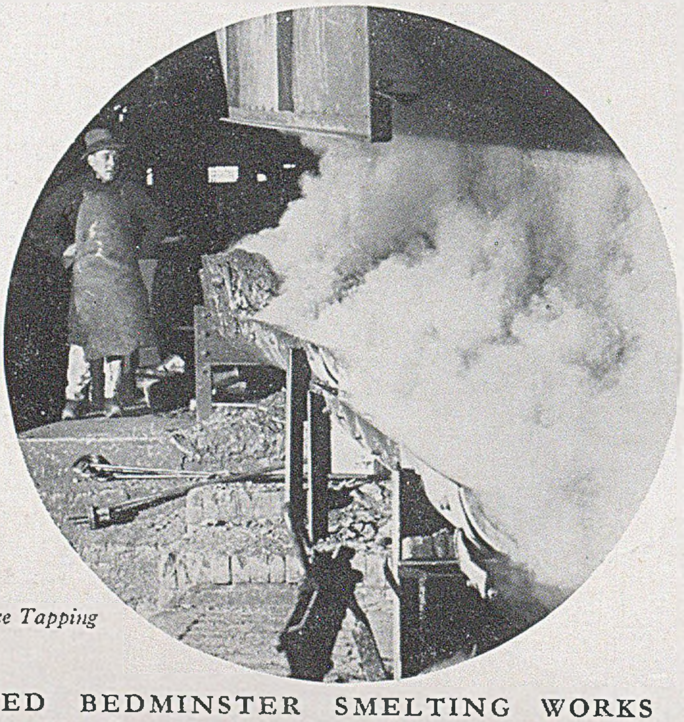

Blast Furnace Tapping

CAPPER PASS & SON LIMITED BEDMINSTER SMELTING WORKS BRISTOL


FIRTH
BROWN
TURBINE
DISC
FORGINGS
THOS. FIRTH & JOHN BROWN LTD.
SHEFFIELD.

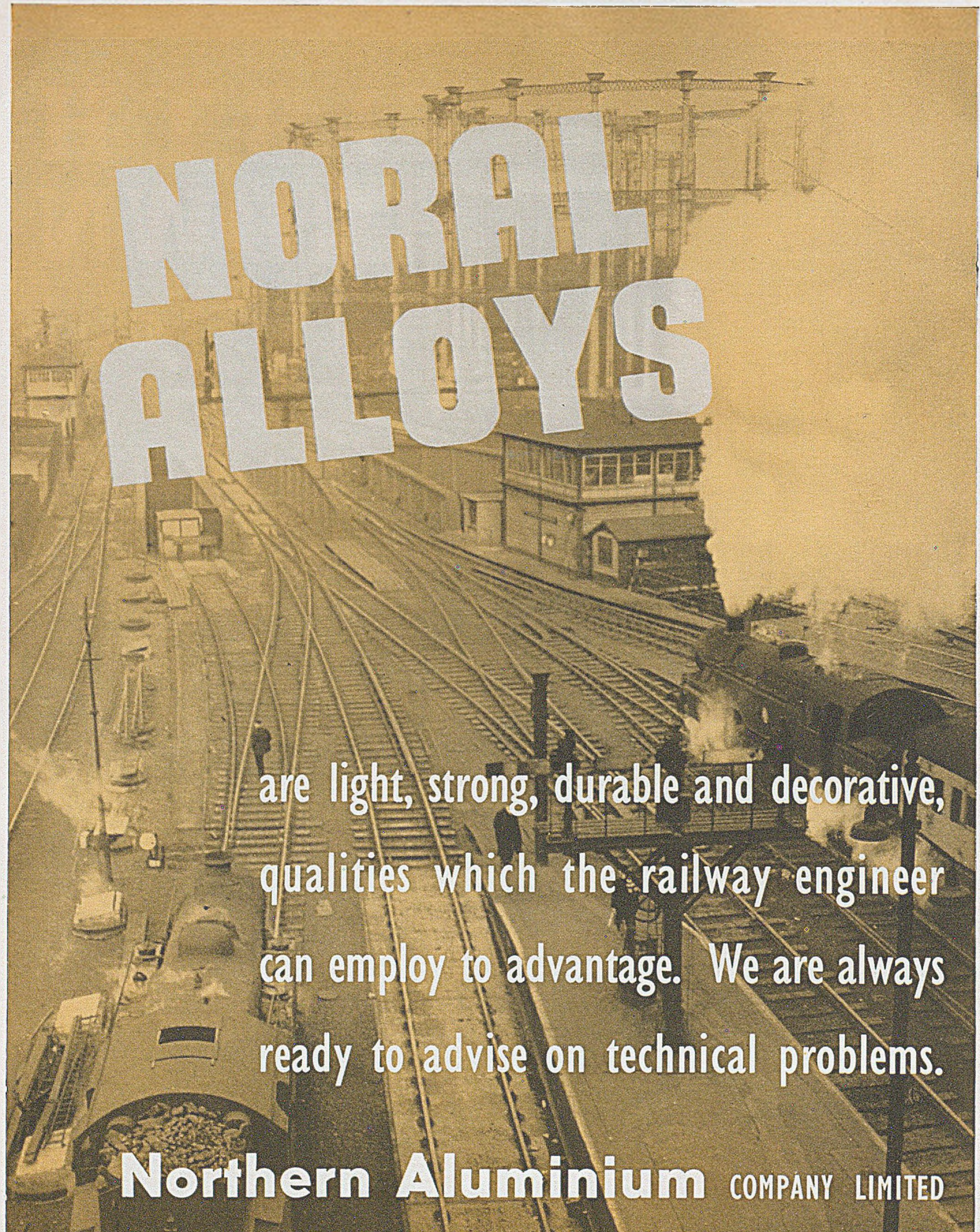

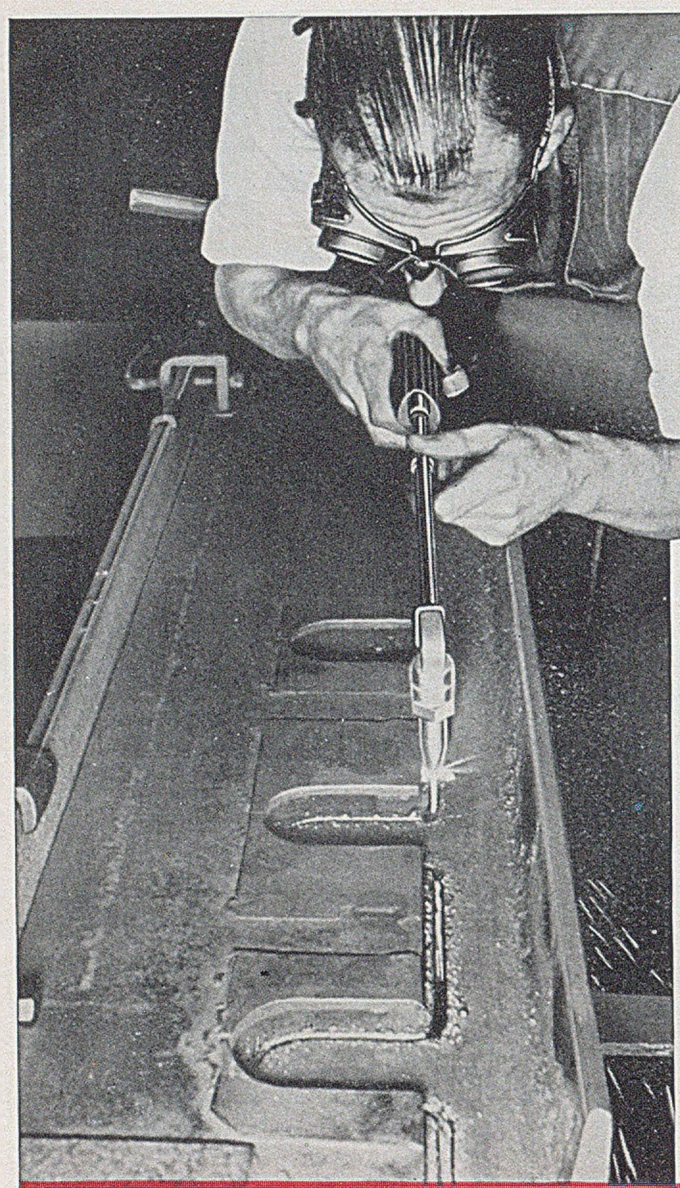

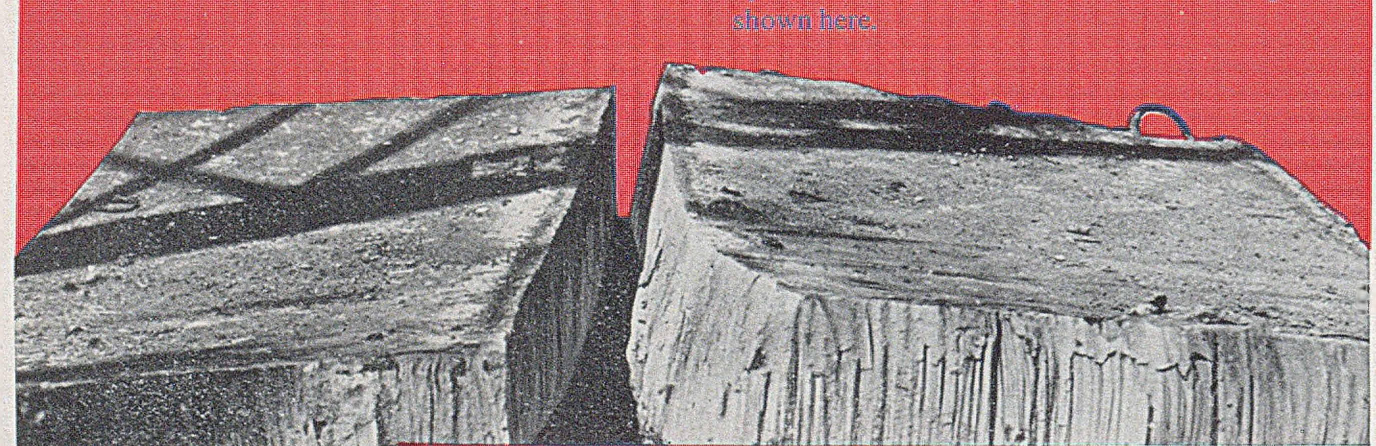

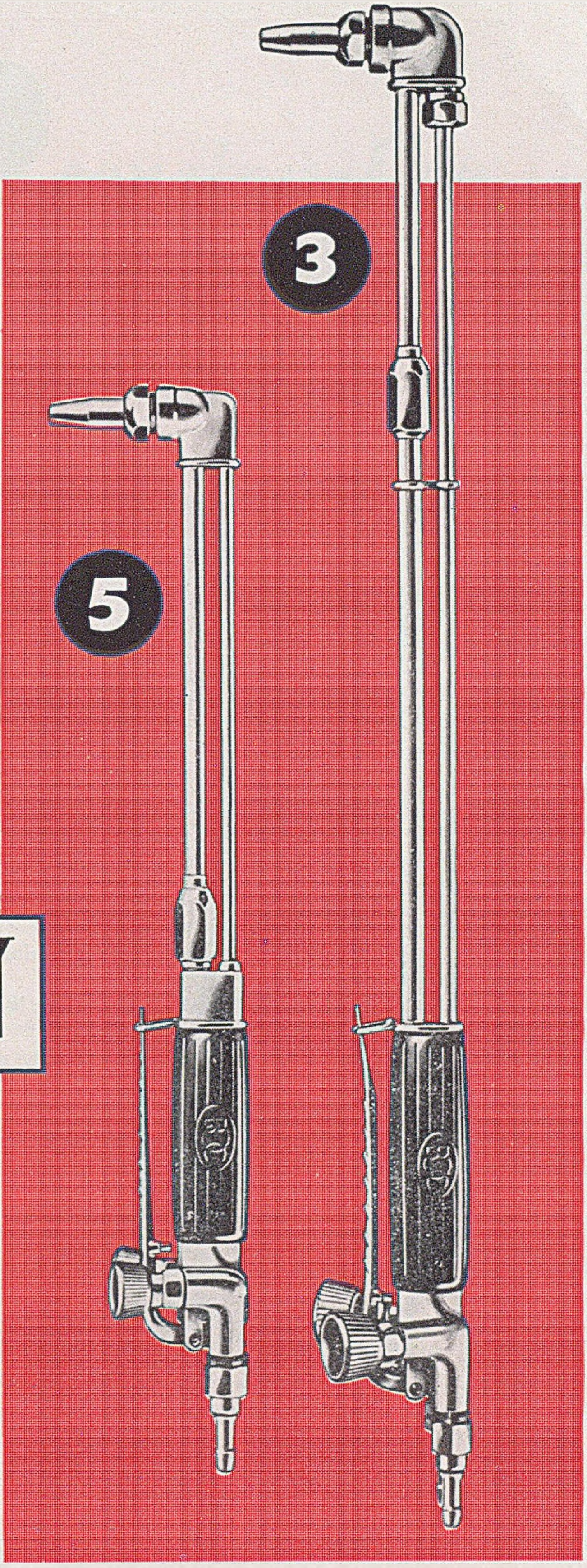
3
5

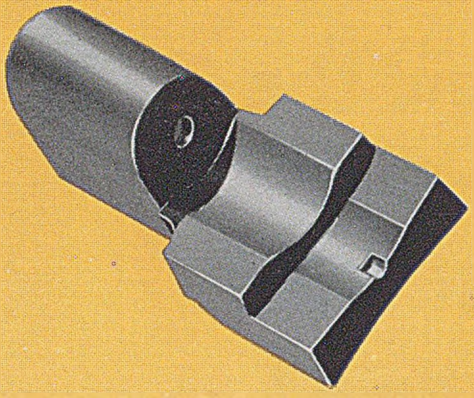

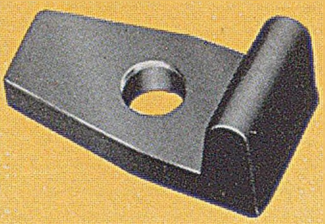

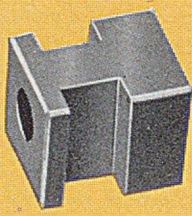

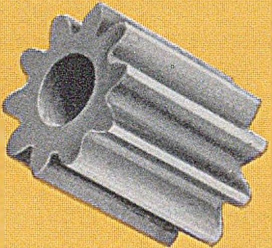

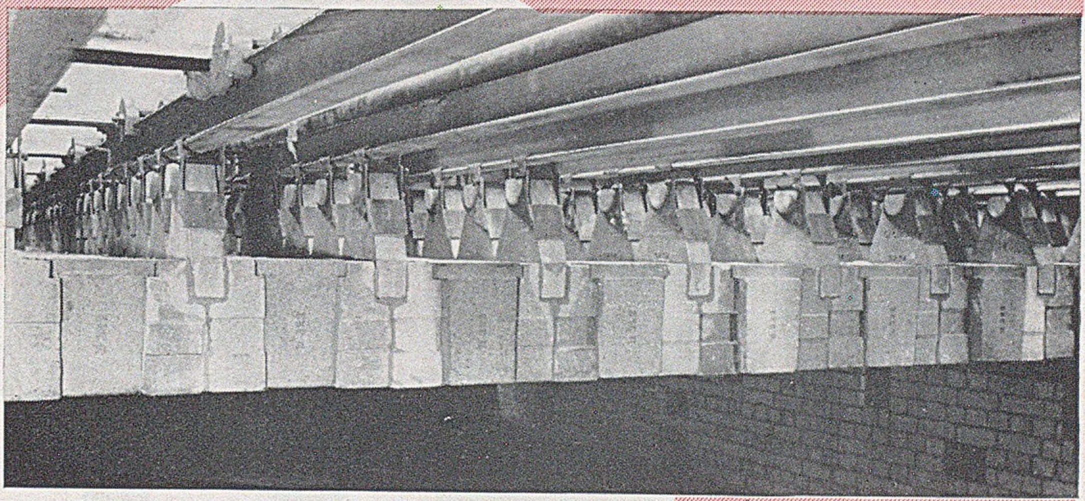

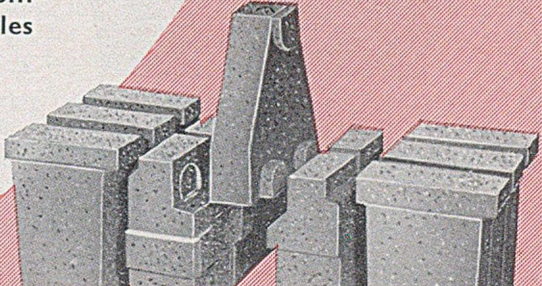


HANNA

FATIGUE TESTING EQUIPMENT

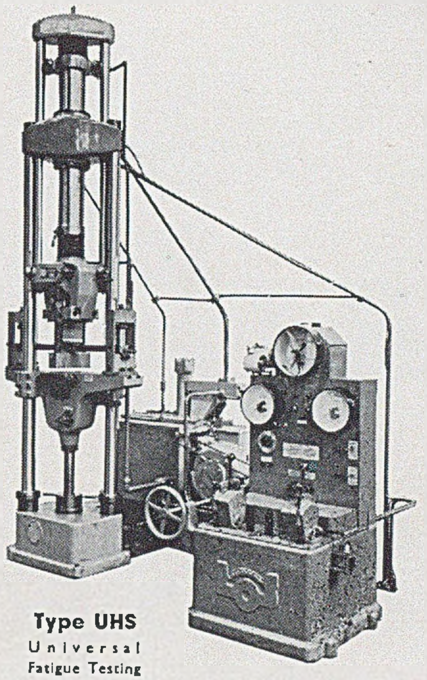

Type UHS
Universal
Fatigue Testing
Machine

FOR MATERIALS

Losenhausenwerk Models UHW Universal Fatigue Testing Machines are suitable for tensile, compression and bending tests on material specimens under fluctuating loads plus/minus oscillation loads.

Manufactured in two sizes of 6 and 20 tons dynamic load capacity.

FOR COMPONENTS AND STRUCTURAL MEMBERS

Losenhausenwerk Models UHS Universal Fatigue Testing Machines are suitable for tensile, compression and bending tests on materials, components, structural members, and built-up machine assemblies under static loads, fluctuating loads, plus/minus oscillating and alternating dynamic loads.

Manufactured in sizes having maximum static load capacities of 20, 40, 60, 100 and 200 tons and maximum dynamic load capacities of 10, 20, 40, 60 and 100 tons respectively.

Losenhausenwerk Models UHP Universal Testing Machines of 6, 10, 20, 40, 60, 100 and 200 tons maximum static load capacity may be fitted with a Pulsator Unit either at the time of ordering or at a later date making them suitable for fluctuating load tests in either tension or compression up to a maximum dynamic load of approximately half the maximum static load capacity. They are not however suitable for alternating load tests from tension to compression.

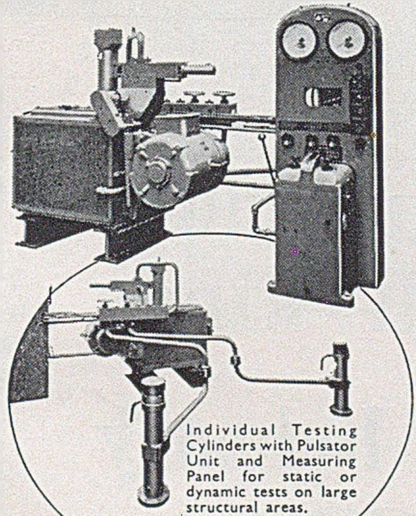

Individual Testing Cylinders with Pulsator Unit and Measuring Panel for static or dynamic tests on large structural areas.

FOR LARGE STRUCTURAL AREAS

When structural assemblies are of such dimensions that they cannot be accommodated in any of the machines previously described and where it is necessary to apply static or dynamic loads at points widely separated over a structural area, **Losenhausenwerk Individual Testing Cylinders** may be connected through a distributor to a Losenhausenwerk Pulsator Unit and Pump as shown in the illustration. Typical applications of this type of installation are for static and fatigue tests on aeroplane wings, tail planes, etc., and in building research.

These individual testing cylinders are manufactured for maximum static loads of 2, 6, 10, 20, 40, 60 or 100 tons with maximum dynamic load capacities equal to half the static load capacity. Losenhausenwerk Pulsator Units are manufactured in sizes of 50, 100, 200, 300, 800 cubic cm./volume. Models 50 to 300 with 330, 500, 600, 660 and 1000 strokes per minute and model 800 with 200, 300, 400 and 600 strokes per minute.

The complete Losenhausenwerk range in addition to the equipment described includes Vibration Machines, Vibration Tables, Universal Testing Machines, Building Material Testing Machines, Creep Testing Machines, Chain Testing Machines, Spring Testing Machines, Pendulum Impact Testing Machines and Balancing Machines.

WICKMAN *of* COVENTRY

LONDON · BRISTOL · BIRMINGHAM · MANCHESTER
LEEDS · GLASGOW · NEWCASTLE · BELFAST

297F85

Bogie, Roller and Rotary Hearth Furnaces, Rectangular and Tubular Batch Furnaces, Bell Type Furnaces, Chain, Mesh Belt and Continuous Conveyor Furnaces, Rotary Drum Furnaces, Pit Furnaces, Pusher Furnaces, Gravity Feed Furnaces, **Air Circulating Ovens**, Drying Ovens and Walking Beam Furnaces.

Air Circulating Ovens

Illustrated is an ageing oven, supplied to a prominent aircraft manufacturing concern, to take up to 24 feet long light alloy sections and working on the batch principle of operation. The sections are truck-loaded into the oven, the truck running on rails. A centre door, half-way along the chamber, enables the oven to be split into two 12 foot sections, each section having independent temperature control, thus saving electricity costs by using only half the capacity of the unit.

Each half of the oven is provided with its own external heater battery and large volume circulating fan. From the view of the chamber will be seen the series of heater ducts mounted on each side wall. The fans are of the centrifugal type with the impellor shaft mounted in ring oiled bearings, the inner bearing being watercooled. The total rating is 150 kW. Two sets of switchgear and oil circuit breakers are mounted on the outside wall of the oven casing. Each section of the unit is equipped with its own independent dial-type indicating controller.

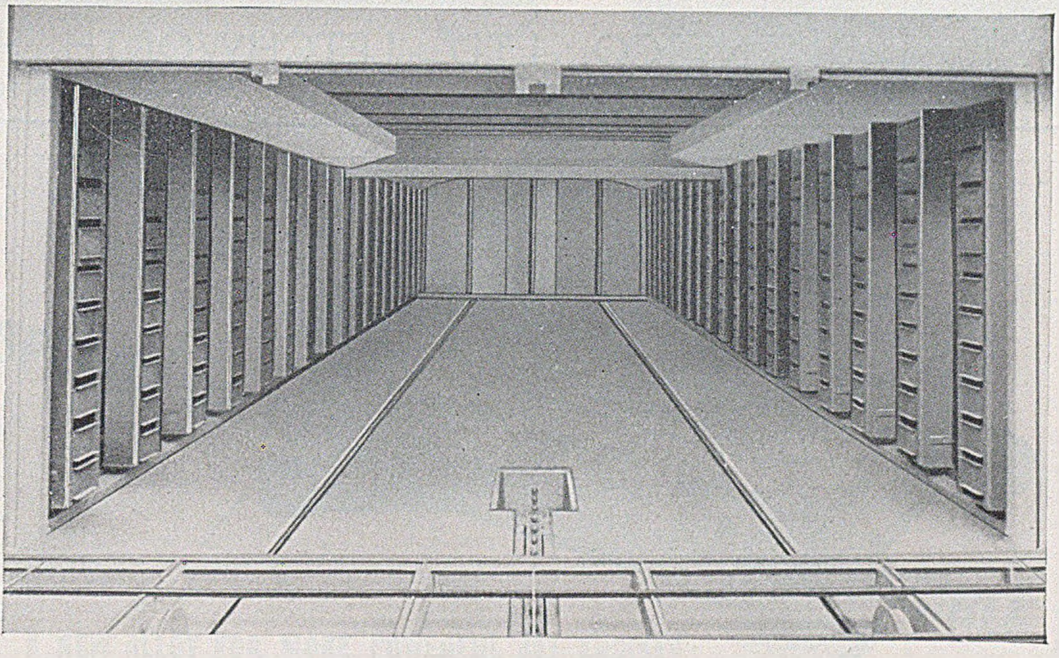

Consult **G·W·B**

on every aspect of heat-treatment

G.W.B. ELECTRIC FURNACES LTD.
Dibdale Works, Dudley, Worcs. Phone: Dudley 4284/5
Proprietors: GIBBONS BROS. LTD. and WILD-BARFIELD ELECTRIC FURNACES LTD.

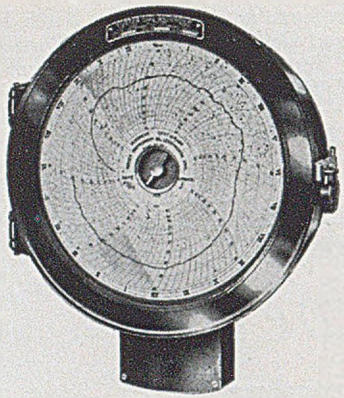

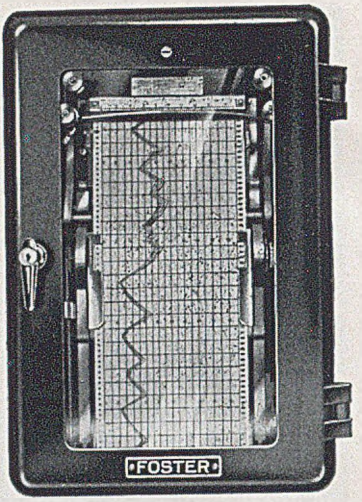

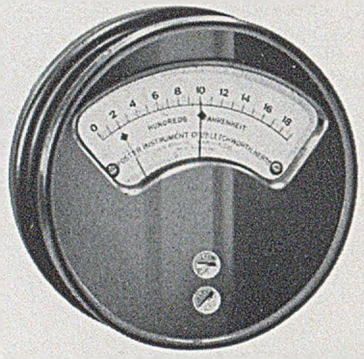

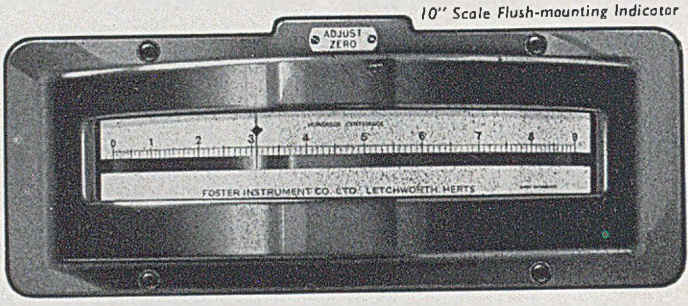

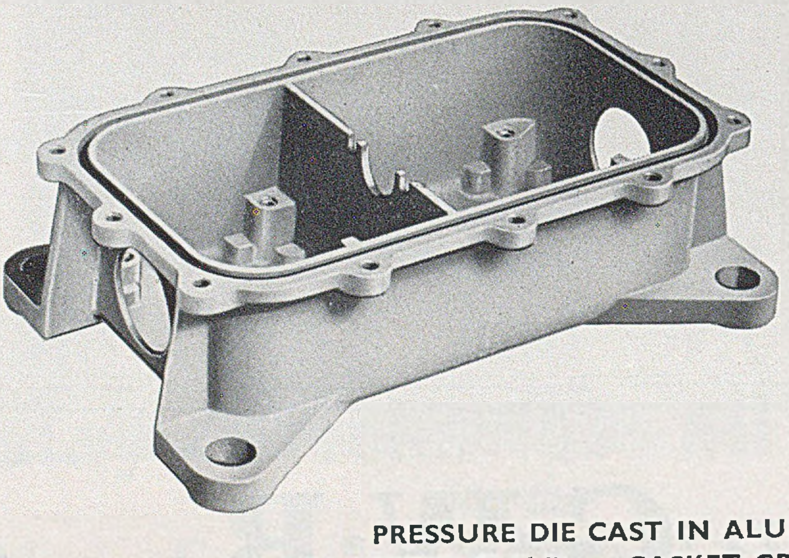

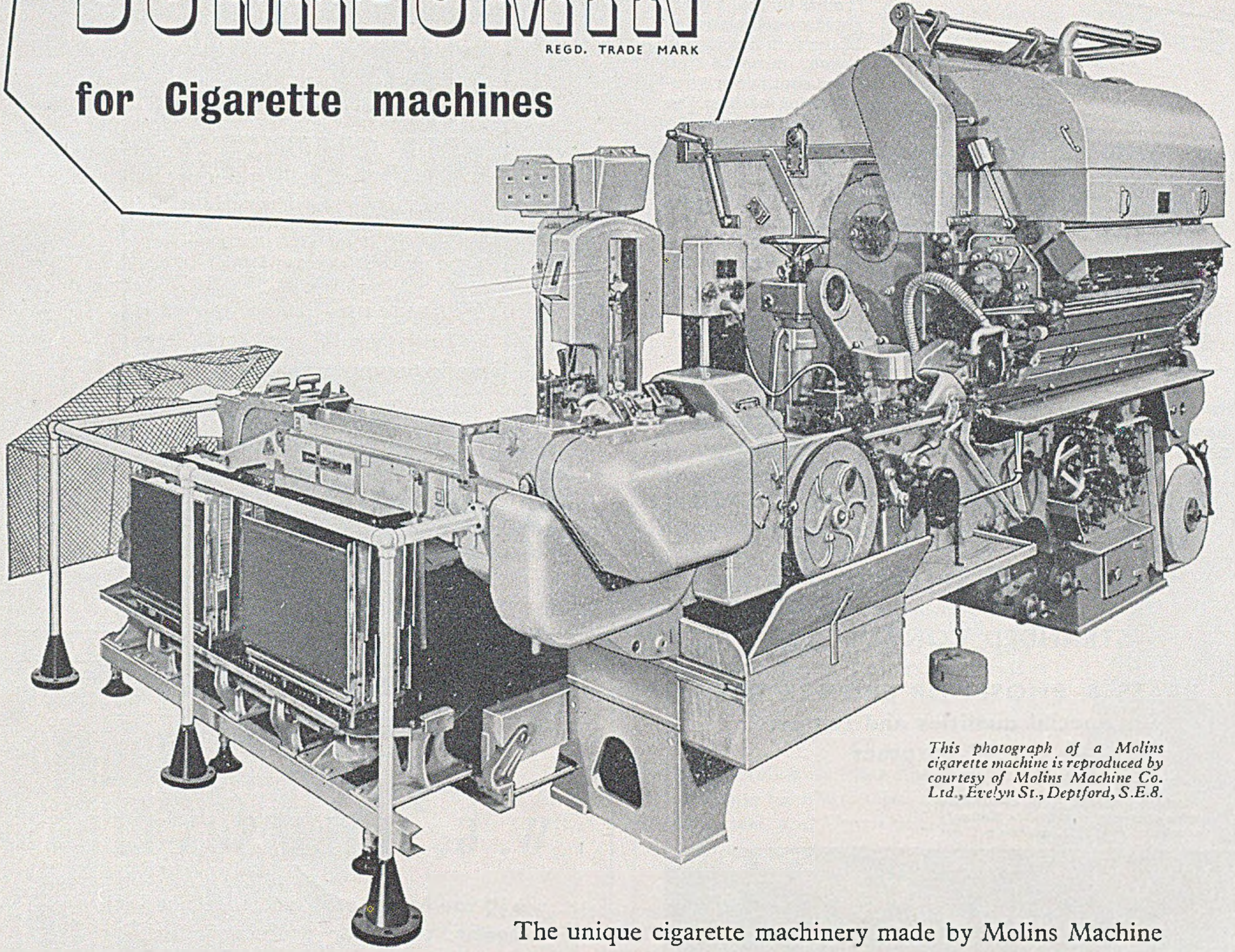

BOLTON'S COPPER
in industrial progress

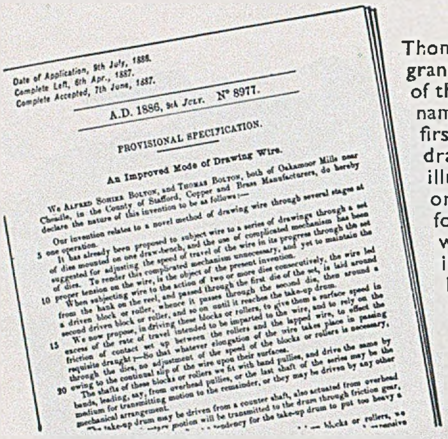

Date of Application, 9th July, 1886.
Complete Left, 6th Apr., 1887.
Complete Accepted, 7th June, 1887.

A.D. 1886, 9th July. N° 8977.

PROVISIONAL SPECIFICATION.

An Improved Mode of Drawing Wire.

We Alfred Sohier Bolton, and Thomas Bolton, both of Oakamoor Mills near Cheadle, in the County of Stafford, Copper and Brass Manufacturers, do hereby declare the nature of this invention to be as follows:—

Our invention relates to a novel method of drawing wire through several stages at one operation.

It has already been proposed to subject wire to a series of drawings through a set of dies mounted on one draw-bench, and the use of complicated mechanism has been suggested for adjusting the speed of travel of the wire in its progress through the set of dies. To render this complicated mechanism unnecessary, and yet to maintain the proper tension on the wire, is the object of the present invention.

When subjecting wire to the action of two or more dies consecutively, the wire led from the hank on the reel, and passed through the first die of the set, is laid around a driven block or roller, whence it passes through the second die, then around a second driven block or roller, and so on until it reaches the take-up drum.

We now propose, in driving these blocks or rollers, to give them a surface speed in excess of the rate of travel intended to be imparted to the wire, and to rely on the friction of contact set up between the rollers and the lapped wire, to effect the requisite draught;—So that whatever elongation of the wire takes place in passing through the dies, no adjustment of the speed of the blocks or rollers is necessary, owing to the continual slip of the wire upon their surfaces.

The shafts of these blocks or rollers we fit with band pullies, and drive the same by bands, leading, say, from overhead pullies, or the last shaft of the series may be the medium for transmitting motion to the remainder, or they may be driven by any other mechanical arrangement.

The take-up drum may be driven from a counter shaft, also actuated from overhead motion will be transmitted to the drum through friction gear, tendency for the take-up drum to put too heavy a blocks or rollers, we excessive

Thomas Bolton, a great grandson of the founder of the firm bearing his name, invented the first continuous wire-drawing machine. The illustration shows the original application for patent rights, which were granted in 1887. Thomas Bolton set the standard for modern wire-drawing practice.

Bolton's Copper Products comply with all relevant British Standard specifications and many other Home, Colonial and Foreign Government requirements.

H.C. COPPER AND CADMIUM COPPER
for Overhead Conductors

TROLLEY AND TELEPHONE WIRE

STRANDED CONDUCTORS

BRASS & PHOSPHOR BRONZE WIRE
in special qualities and tempers
for all purposes

Medium heavy 13 die continuous wire-drawing machines in Bolton's works at Froghall, Stoke-on-Trent

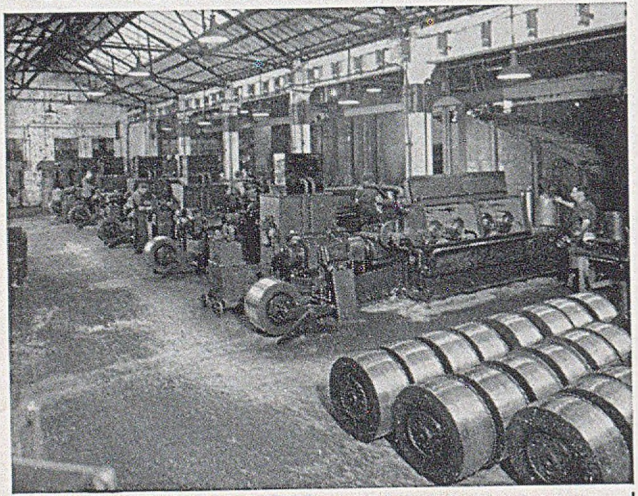

THOMAS BOLTON & SONS LTD
HEAD OFFICE: WIDNES, LANCS. Tel. WIDNES 2022
LONDON OFFICE AND EXPORT SALES DEPARTMENT:
168 Regent Street, W.1 Telephone: Regent 6427/8/9

CVS—163/S3C

FIRE!
PRODUCTION LOST BUT FOR
NU-SWIFT!

A spark...a flash...fire blazing...dial 999! But for at least five minutes that blaze will be YOURS alone! Reliable Nu-Swift is the world's fastest and most certain fire-killer.

NU-SWIFT LTD · ELLAND · YORKS

In Every Ship of the Royal Navy

CHEMICAL PLANT
BY
W. G. JENKINSON LTD

- If you have a problem concerned with storing, piping or processing acids or other corrosive chemicals, our long and varied experience in the provision of chemical plant is at your disposal.
- As Chemical Plumbers and Leadburners we have for many years been associated with high-class fabricated leadwork in sheet and pipe. But we are equally experienced in the use and fabrication of stainless steel, plastics and other corrosion-resisting materials for the manifold purposes demanded by the Chemical Engineering Industry.

All enquiries to:

W. G. JENKINSON, LTD
156-160 ARUNDEL STREET, SHEFFIELD, 1
Telephone: Sheffield 22473

BIGWOOD
EQUIPMENT
for the Steel Industry

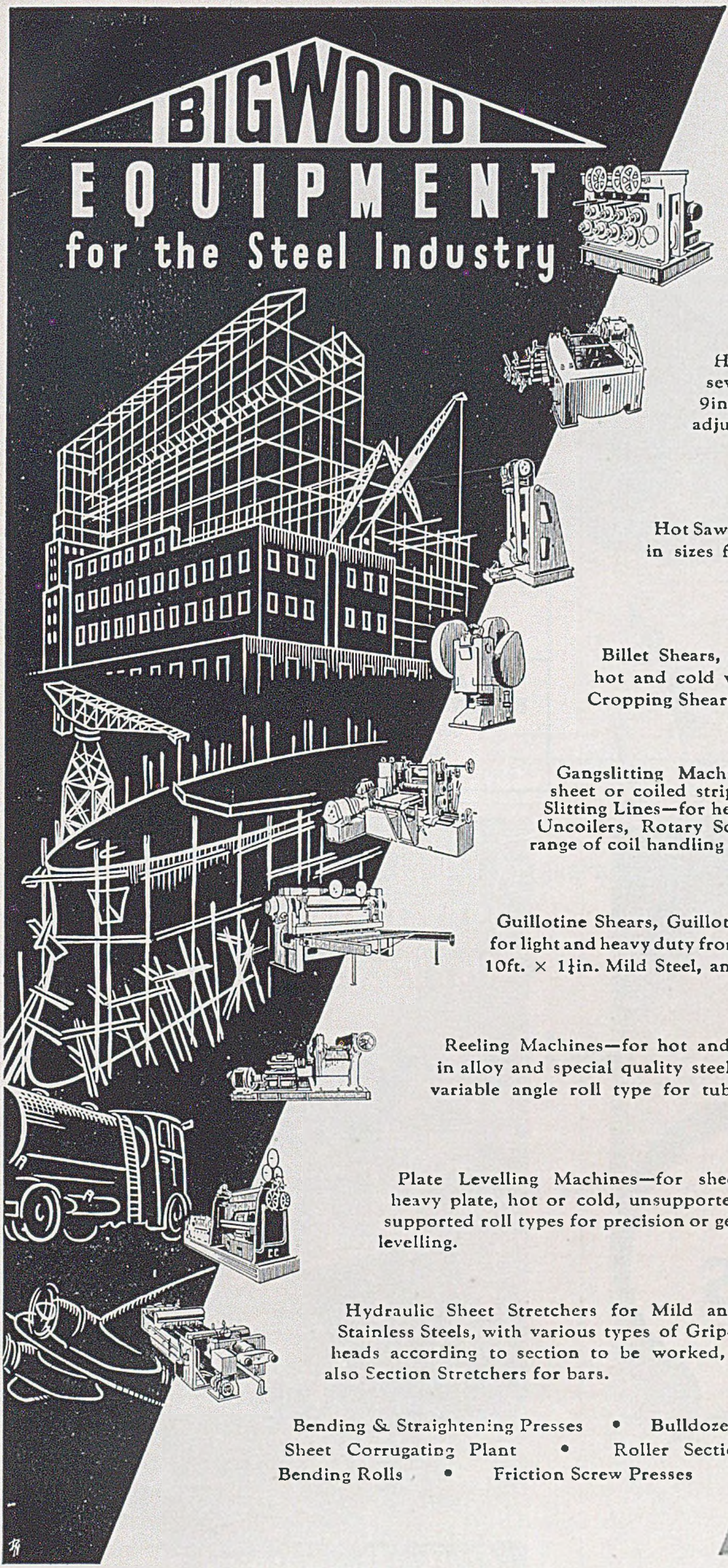

Roller Section Straighteners—full range of high speed Roller Straighteners for bars and sections from 1½in. to 1½in. angles to 24in. × 7½in. joists.

High Speed Tube and Bar Straighteners—in several classes for bar from ¾in. diameter to 9in. diameter, with non-adjustable and adjustable angle driving rolls.

Hot Saws, Pendulum and Horizontal Types—in sizes from 36in. to 60in. Saw diameter.

Billet Shears, Vertical and Horizontal—for hot and cold work. Alligator Shears and Cropping Shears.

Gangslitting Machines,—for slitting from sheet or coiled strip. Complete Mill type Slitting Lines—for heavy coils. Coilers and Uncoilers, Rotary Scrap Cutters, and full range of coil handling equipment.

Guillotine Shears, Guillotine Plate Shears—for light and heavy duty from 4ft. × ⅜in. up to 10ft. × 1¼in. Mild Steel, and Upcut Shears.

Reeling Machines—for hot and cold work, in alloy and special quality steel, fixed and variable angle roll type for tube or bar.

Plate Levelling Machines—for sheet and heavy plate, hot or cold, unsupported and supported roll types for precision or general levelling.

Hydraulic Sheet Stretchers for Mild and Stainless Steels, with various types of Gripheads according to section to be worked, also Section Stretchers for bars.

Bending & Straightening Presses • Bulldozer Forging Machines • Drawbenches Sheet Corrugating Plant • Roller Section Forming Machines • Plate Bending Rolls • Friction Screw Presses • Centreless Bar Turning Machines.

JOSHUA BIGWOOD & SON LIMITED • WOLVERHAMPTON • ENGLAND

B 114

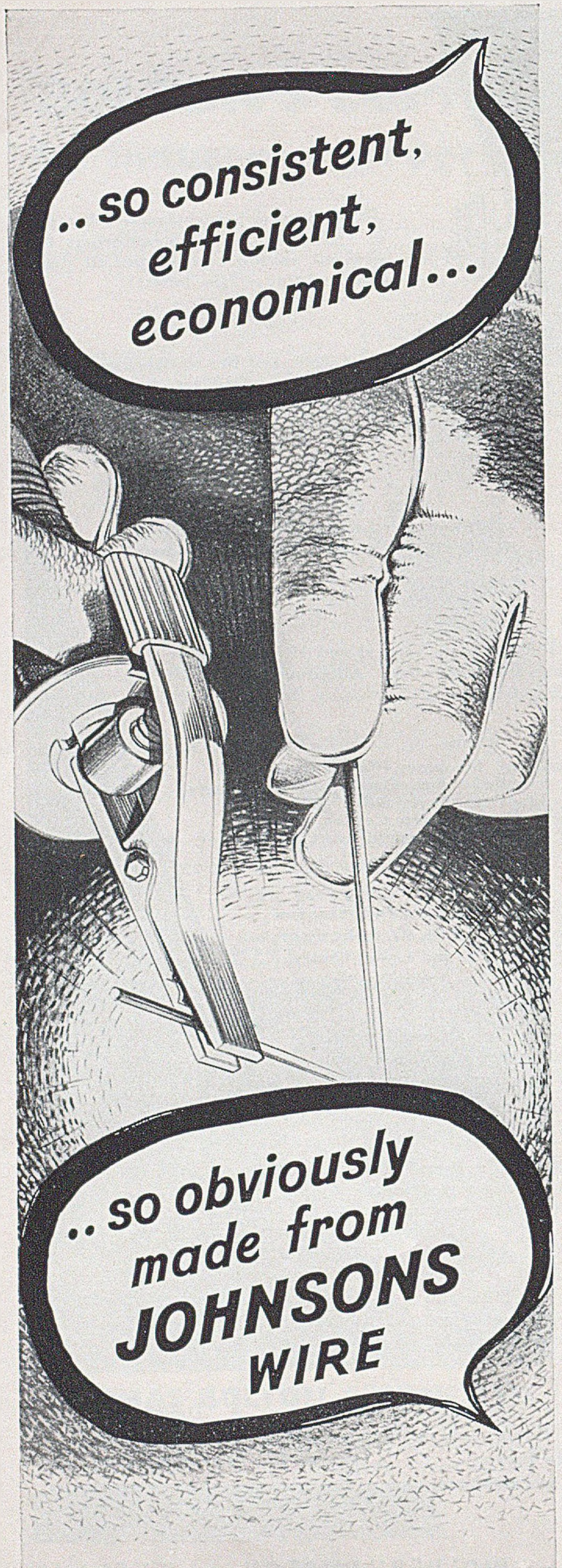

.. so consistent, efficient, economical...
.. so obviously made from JOHNSONS WIRE

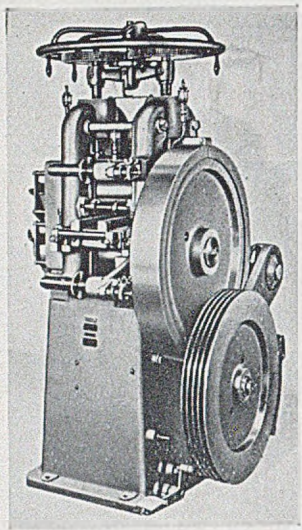

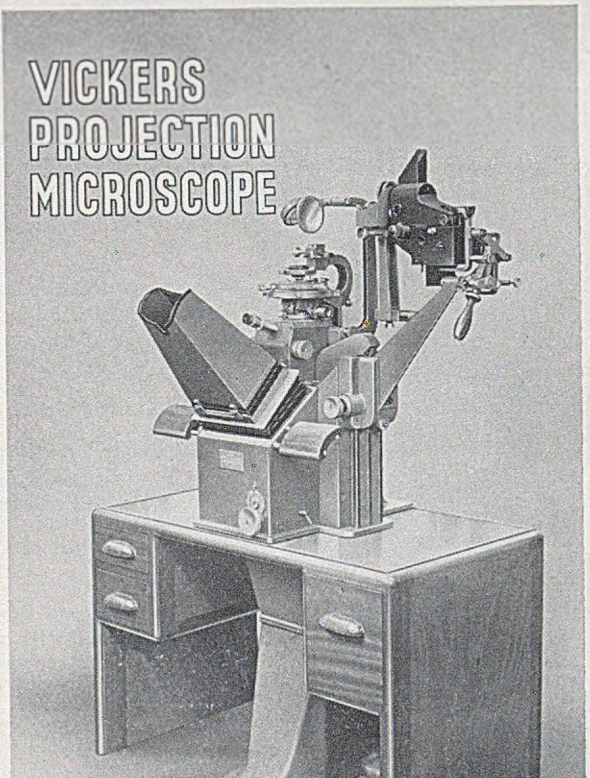

VICKERS PROJECTION MICROSCOPE
Cooke Troughton & Simms LTD
YORK ENGLAND

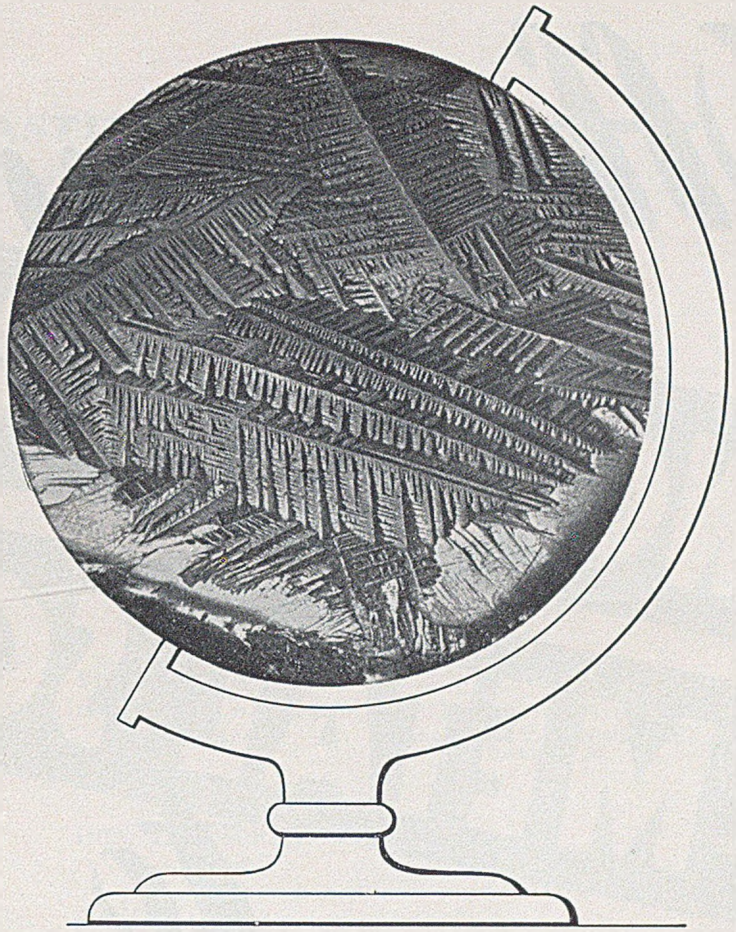

THE INSTITUTE OF METALS

4 Grosvenor Gardens, London, S.W.1

COUNCIL AND OFFICERS

PRESIDENT

Professor F. C. THOMPSON
D.Met., M.Sc.

PAST-PRESIDENTS

Professor A. J. MURPHY, M.Sc.
C. J. SMITHELLS, M.C., D.Sc.
H. S. TASKER, B.A.

VICE-PRESIDENTS

G. L. BAILEY, C.B.E., M.Sc.
Major C. J. P. BALL, D.S.O., M.C.
S. F. DOREY, C.B.E., D.Sc., F.R.S.
A. B. GRAHAM
P. V. HUNTER, C.B.E.
Professor G. V. RAYNOR, M.A., D.Phil., D.Sc.

HON. TREASURER

E. H. JONES

ORDINARY MEMBERS OF COUNCIL

Alfred BAER, B.A.
W. A. BAKER, B.Sc.
N. I. BOND-WILLIAMS, B.Sc.
K. W. CLARKE
J. C. COLQUHOUN, M.B.E.
E. R. GADD
The Hon. John GRIMSTON, M.P.
N. P. INGLIS, Ph.D., M.Eng.
Ivor JENKINS, D.Sc.
L. B. PFEIL, O.B.E., D.Sc., A.R.S.M., F.R.S.
A. G. RAMSAY, Ph.D., B.Sc.
Christopher SMITH
H. SUTTON, C.B.E., D.Sc.
Major P. L. TEED, A.R.S.M.
W. J. THOMAS

EX-OFFICIO MEMBERS OF COUNCIL

E. A. FOWLER, B.Sc., A.R.T.C.
(Scottish Local Section)
C. E. RANSLEY, Ph.D., M.Sc.
(London Local Section)
R. T. PARKER, B.Sc., Ph.D., A.R.S.M.
(Oxford Local Section)
K. M. SPRING
(South Wales Local Section)
W. R. MADDOCKS, Ph.D., B.Sc.
(Sheffield Local Section)
H. H. SYMONDS
(Birmingham Local Section)

REPRESENTATIVES OF OTHER BODIES

The following, in accordance with Article 32, represent Government Departments and allied societies at Council meetings, for purposes of liaison

Admiralty	Capt. (E.) H. J. B. GRYLLS, R.N.
War Office	Major-General S. W. JOSLIN, C.B.E., M.A.
Iron and Steel Institute	JAMES MITCHELL, C.B.E.
Institution of Metallurgists	MAURICE COOK, D.Sc., Ph.D.; E. G. WEST, B.Sc., Ph.D.

SECRETARY

Lieut.-Colonel S. C. GUILLAN, T.D.

ASSISTANT SECRETARY

Major R. E. MOORE

EDITOR OF PUBLICATIONS

N. B. VAUGHAN, M.Sc.

JOURNAL OF THE INSTITUTE OF METALS

WITH THE BULLETIN AND METALLURGICAL ABSTRACTS

SUBSCRIPTIONS
Members: Free

Non-Members: £6 0 0 ($17.25) per annum, post free

Single Copies 10s. 6d. ($2.00) each, post free

Secretary
Lieut.-Colonel S. C. GUILLAN, T.D.

EDITORIAL AND ADVERTISEMENT OFFICES
4 Grosvenor Gardens, London, S.W.1
Telephone and Telegrams: SLOane 5928 & 6233

Editor of Publications
N. B. VAUGHAN, M.Sc., F.I.M.

Manager, Advertisement Department
E. R. MORT, B.Sc., F.I.M.

Entered at Stationers' Hall

1953, PART 11 | PUBLISHED MONTHLY | JULY

CONTENTS

BULLETIN

METALLURGICAL ABSTRACTS

JOURNAL

THE INSTITUTE OF METALS, 4 GROSVENOR GARDENS, LONDON, S.W.1

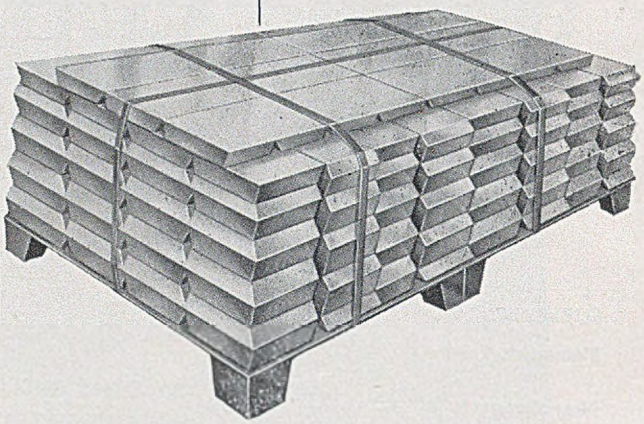

BULLETIN

OF THE INSTITUTE OF METALS

VOLUME I JULY 1953 PART 23

INSTITUTE NEWS

Representatives on Other Bodies

MR. W. S. GIFFORD has been appointed as the Institute's representative on a Committee on the Application of Electricity to Industrial Process Heating, convened by the Institution of Electrical Engineers.

DR. IVOR JENKINS has been appointed as representative of the Institute on the Advisory Council of the City and Guilds of London Institute, *vice* Dr. F. A. Fox.

DR. D. TABOR has been appointed as the Institute's representative on British Standards Institution Panel MEE/37/9/1: Rockwell Hardness Test.

MAJOR P. LITHERLAND TEED has been appointed as one of the Institute's representatives on British Standards Institution Committee NFE/-/-: Non-Ferrous Metals Industry Standards, *vice* Dr. F. A. Fox.

"Metallurgical Abstracts" Volumes Wanted

The Institute will pay £1 each for bound volumes, in good condition, of *Metallurgical Abstracts* 1940 (Vol. 7), 1941 (Vol. 8), 1942 (Vol. 9), 1943 (Vol. 10).

The following monthly parts of the *Journal* and *Metallurgical Abstracts* are also urgently required, and the Institute will pay 7*s.* 6*d.* for each copy in good condition:

1941: July, Aug.
1942: July, Aug., Oct.
1943: May, July, Aug., Sept., Oct.

Copies offered for sale should be addressed to the Secretary.

Election of Members

The following 12 Ordinary Members, 1 Junior Member, and 7 Student Members were elected on 19 May 1953:

As Ordinary Members

BULOW, Carl Lawrence, Corrosion Metallurgist, Bridgeport Brass Company, 30 Grand Street, Bridgeport 2, Conn., U.S.A.

CHANG, Hsing Chien, M.S., Sc.D., D.I.C. Research Staff, Department of Metallurgy, Massachusetts Institute of Technology, Cambridge 39, Mass., U.S.A.

VAN DER GLAS, Bastiaan Gerrit, Chief, Material Testing Laboratory, K.L.M. (Royal Dutch Airlines), Schipol, Netherlands.

HYMAN, Edward David, Met.E., Metallurgical Engineer, National Bearing Division, American Brake Shoe Company, Manchester Avenue, St. Louis, Mo., U.S.A.

McLELLAN, David Smith, B.S., Plant Metallurgist, Reynolds Metals Company, Phoenix, Ariz., U.S.A.

RILEY, Hilary Francis, B.Sc., A.R.S.M., Manager and Metallurgist, Beryllium and Copper Alloys, Ltd., 47 Victoria Street, London, S.W.1.

SEYBOLT, Alan Upson, B.S., Ph.D., Research Associate, Metallurgy Department, Research Laboratory, General Electric Company, Schenectady, N.Y., U.S.A.

TAYLOR, Alan Wright, B.Sc., A.I.M., Divisional Metallurgist, British Electricity Authority, South Wales Division, B.E.A. House, Twyn-Fedwen Road, Gabalfa, Cardiff.

TAYLOR, *Professor* Howard Floyd, M.S., Professor of Mechanical Metallurgy, Massachusetts Institute of Technology, Cambridge 39, Mass., U.S.A.

WESTBROOK, Jack Hall, M.Met.E., Sc.D., Research Associate, Research Laboratory, General Electric Company, Schenectady, N.Y., U.S.A.

ZULLIG, Alfons J., Dipl.-Ing., Director of Operations—Staff, Aluminium, Ltd., Montreal, Que., Canada.

ZUREK, Emil, M.C., Dr.-Ing., M.I.Mech.E., Managing Director and Development Engineer, John Yuille (Metal Works) Ltd., Hillington Estate, Glasgow, S.W.2.

As Junior Member

LENHART, Robert Eugene, B.Met.E., Research Assistant, Metallurgy Department, Research Laboratory, General Electric Company, Schenectady, N.Y., U.S.A.

As Student Members

CUFF, Frank B., Jr., B.Met.E., Postgraduate Student of Metallurgy, Massachusetts Institute of Technology, Cambridge 39, Mass., U.S.A.

EDMONDSON, Bryan, B.Sc., Postgraduate Student of Metallurgy, University of Birmingham.

EVANS, John L., Student of Metallurgy, University of Sheffield.

HOWLETT, Brian Wilfred, B.Sc., Postgraduate Student of Metallurgy, University of Birmingham.

MASSALSKI, Tadeusz Bronislaw, B.Sc., Postgraduate Student of Metallurgy, University of Birmingham.

SHEIKH, A. M., M.Sc., 10 Macoma Terrace, Plumstead Common, London, S.E.18.

WERNER, Fred Eugene, Jr., S.B., Instructor and Graduate Student, Metallurgy Department, Massachusetts Institute of Technology, Cambridge 39, Mass., U.S.A.

PERSONAL NOTES

Mr. J. N. Auld has returned to Australia, where he will be working at the Defence Research Laboratories, Maribyrnong, Victoria.

Mr. J. E. Chard has resigned from the Royal Naval Scientific Service to take up an appointment at the Canadian Armament Research and Development Establishment at Valcartier, Quebec.

Mr. E. S. Cornwall has been appointed General Manager and Chief Engineer of the Southern Electric Authority of Queensland, Brisbane, Australia.

Mr. J. F. Ewing, has taken a post in the Research Department of The Babcock and Wilcox Company, Tubular Products Division, Beaver Falls, Pa., U.S.A.

Dr. P. T. Gilbert has received the 1953 Francis Mills Turner Award of the Electrochemical Society for a paper on "The Nature of Zinc Corrosion Products".

Mr. W. L. Hall has resigned his position as Chief Liaison Officer to the British Non-Ferrous Metals Research Association in order to become General Manager to General Galvanizers, Ltd., Wolverhampton.

Mr. R. D. Hamer, Vice-President and Director of Aluminium Laboratories, Ltd., has been elected President of the Aluminium Development Association for the year 1953–54.

Mr. T. B. V. Hirst has been appointed Chairman and Managing Director of Tekon, Ltd., 17 Broadstone Place, Dorset Street, London, W.1.

Dr. Børge Lunn has been appointed Assistant Technical Director of the Nordiske Kabel- og Traadfabriker (Northern Cable and Wire Works), Copenhagen.

Mr. E. C. Mantle has been appointed Chief Liaison Officer to the British Non-Ferrous Metals Research Association, in succession to Mr. W. L. Hall.

Mr. B. Podezaski has been appointed Managing Director of the steelworks Crisoldinic E.N., Quilmes, Province of Buenos Aires, Argentina.

Mr. M. L. Samways has taken up an appointment as Development Engineer with The Dowsett Engineering and Construction Co., Tallington, Stamford, Lincs.

Mr. B. N. H. Thornely, Chief Engineer to the Northern Aluminium Co., Ltd., has been appointed a Director of the Company.

Deaths

The Editor regrets to announce the deaths of:

Mr. William Waterhouse Gibbins, M.A., Chairman of The Birmingham Battery and Metal Company, Ltd., Selly Oak, Birmingham, on 5 May 1953. He was an Original Member of the Institute.

Sir Thomas Kirke Rose, D.Sc., A.R.S.M., on 10 May 1953. Sir Thomas served as a Member of Council of the Institute from 1914 to 1916, and as a Vice-President from 1916 to 1927. He joined the Royal Mint in 1890, was appointed Chemist and Assayer in 1902, and retired in 1926. He was 87 years of age.

OBITUARY

Mr. G. B. Harris

Geoffrey Bastion Harris, who died on 8 March as the result of a road accident, was educated at Redruth County School. He obtained an Exhibition at St. Catharine's College, Cambridge, and was placed in Class I in Tripos Part I, and Class II in Part II in Physics. On leaving the University in 1946, he was appointed an Experimental Officer in the National Physical Laboratory, and within a year was promoted to the Scientific Officer Grade. He worked in the Metallurgy Division, almost exclusively on the metallography of uranium alloys, and made valuable observations on dimensional changes in relation to orientation textures in uranium. He also worked on preferred orientation in uranium, and published a paper on this subject in 1952. In 1950 he obtained a B.I.S.R.A. Bursary for work at Oxford on the freezing and melting points of iron alloys, and one paper is to appear shortly in the *Journal* of the Iron and Steel Institute.

Mr. Harris was a man of exceptional ability, a brilliant designer of apparatus, and a constant source of help to his colleagues at Oxford. His linguistic powers were considerable, and he could read French, German, and Russian with ease. His work on the thermal analysis of iron alloys is probably the most accurate which has yet been carried out, and his tragic death means the loss of one of the most promising of the younger generation of metal physicists.

W. H.-R.

JOINT ACTIVITIES

Capper Pass Awards

The Capper Pass Awards Adjudicating Committee, on behalf of the Councils of the Institution of Mining and Metallurgy and the Institute of Metals, have made the following awards for papers published in 1952 in the *Transactions of the Institution of Mining and Metallurgy* and the *Journal of the Institute of Metals*.

(i) Fifty Pounds to Mr. Edwin Davis, M.Sc., F.I.M., and Mr. S. G. Temple, M.Sc., A.I.M., for their paper on "Batch and Continuous Annealing of Copper and Copper Alloys" (*J. Inst. Metals*, 1951–52, **80**, 287–296).

(ii) Fifty Pounds to Mr. C. P. Paton, B.Eng., for his paper on "Batch Thermal Treatment of Light Alloys" (*J. Inst. Metals*, 1951–52, **80**, 311–322).

(iii) Fifty Pounds to Dr. E. C. Ellwood, F.I.M., and Mr. T. A. Henderson, B.Sc., for their paper on "Some Exploratory Experiments on the Formation and Control of Magnetite During Copper-Smelting Operations" (*Trans. Inst. Min. Met.*, 1952, **62**, 55–65).

(iv) Fifty Pounds to Mr. P. M. J. Gray, B.Sc., A.R.S.M., for his paper on "The Production of Pure Cerium Metal by Electrolytic and Thermal-Reduction Processes" (*Trans. Inst. Min. Met.*, 1952, **61**, 141–170).

(v) Twenty-Five Pounds to Mr. E. A. Hontoir, B.Sc., A.I.M., for his paper on "Determination of Sulphur in Iron Pyrites" (*Trans. Inst. Min. Met.*, 1952, **62**, 95–107).

Terms of Capper Pass Awards

The Capper Pass Awards, which are made annually from a sum of £200 placed each year at the disposal of the Councils of the Institution of Mining and Metallurgy and of the

Institute of Metals, by the Directors of Capper Pass and Son, Ltd., Bristol, are intended to encourage the publication of papers in the *Transactions of the Institution of Mining and Metallurgy* and in the *Journal of the Institute of Metals* on processes and plant used in extraction metallurgy and on the subject of assaying and of papers on processes and plant used in all branches of the non-ferrous metal industry.

Provided that the Adjudicating Committee is satisfied that the quality and numbers of papers submitted, of the types for which the awards are made, reach a suitable standard:

> (*a*) £100 per annum is available for one or more awards to authors of papers on some aspect of non-ferrous extraction metallurgy, including assaying;
>
> (*b*) £100 per annum is available for one or more awards to the authors of papers relating to some processes or plant used in the extraction or fabrication of non-ferrous metals.

The Adjudicating Committee meets annually to consider, on behalf of the two societies, papers published during the past calendar year in the two journals referred to above. It may, at its discretion, make no award or awards of less than the money available, if, in its opinion, the quality or number of papers submitted in any year fails to reach a suitable standard. Any sums not awarded will be carried forward to future years.

The Councils of the Institution of Mining and Metallurgy and of the Institute of Metals hope that the generous offer made by Messrs. Capper Pass and Son, Ltd., will stimulate the writing of many papers of the types for which the awards are to be made. Papers on extraction metallurgy should preferably be submitted to the Institution of Mining and Metallurgy, while those on processes and plant used in the fabrication of non-ferrous metals should preferably be offered to the Institute of Metals. Both societies are prepared to accept papers from non-members.

Authors should note that applications should not be addressed to the Adjudicating Committee requesting that their papers should be considered for the Award of a Premium. All papers published by both societies will be examined by the Committee annually, and notices of the Awards will be published in the journals of the two societies and in the Press.

NEWS OF KINDRED SOCIETIES

Australian Institute of Metals: Symposium on Wire Drawing

The Physical Metallurgy Division of the Melbourne Branch of the Australian Institute of Metals has arranged for a Symposium on the "Theory and Practice of Wire Drawing" to be held in Melbourne on 13 November this year. Seven papers (listed below) have been contributed by Australian and English authors; the papers include original work as well as reviews. They will be preprinted in booklet form, and the meeting in November devoted to discussion; it is hoped that the preprints will be available in time for copies to be sent by air to anyone outside Australia who is interested in contributing to the discussion, which will be printed subsequently. Copies of the preprints and discussion may be ordered from the Hon. Secretary, R. C. Gifkins, Baillieu Laboratory, University of Melbourne, Carlton, N.3, Victoria, Australia. The provisional price in sterling for the preprints is 15*s*. (including postage by air) or 12*s*. (surface mail); the discussion, which will be available in 1954, will probably cost an extra 2*s*. (stg.). Cheques or money orders should be made payable to "The Australian Institute of Metals".

The titles and authors of the papers are as follows:

> "Core Wire for the Production of Extruded Metal Arc-Welding Electrodes", by Dr. W. I. Pumphrey.
>
> Some Researches on Wire Drawing", by Professor F. C. Thompson.
>
> "Researches Concerning Wire-Drawing Dies", by J. G. Wistreich.
>
> "The Problem of Rod Diameter", by C. Blazey and V. W. Benjamin.
>
> "Temperature-Lubrication Relations for the Surface of Copper During Wire Drawing", by J. S. Hoggart.
>
> "The Effect of the Surface Temperature Attained During Drawing on the Tensile Strength of Copper Wire", by S. Z. M. Kopczynski and J. S. Hoggart.
>
> "Australian Developments in Drawn, Galvanized Rope Wires", by F. W. Welshman and C. James.

OTHER NEWS

Postgraduate School in Physical Metallurgy

In view of the need of the metallurgical industries for more men with advanced scientific training, the University of Sheffield has established a Post-Graduate School in Physical Metallurgy to provide special tuition in this branch of science.

Applications for admission to courses are invited from:

> (*a*) scientists already in industry, holding a degree or equivalent qualification, who have had at least three years' experience and wish to pursue more advanced studies in physical metallurgy:
>
> (*b*) recent graduates in physics, chemistry, or engineering who wish to pursue a metallurgical career.

In certain circumstances applications will also be accepted from recent graduates in metallurgy with little or no industrial experience.

Courses will embrace all aspects of physical metallurgy. Primary consideration will be given to fundamental principles, but every effort will be made to relate these to industrial practice where possible. Courses will be planned to meet the needs of the students enrolled, and will normally be of one or two years' duration. In general, the first-year course will be primarily for non-metallurgists, and lectures, together with courses of practical work, will provide a sound metallurgical background.

The second-year course is intended both for those who have completed the first year and for metallurgists returning from industry. Formal lectures will be largely replaced by study groups and colloquia in which recent developments in physical metallurgy will be critically reviewed. A large part of the time will be devoted to advanced practical work designed to promote further discussion on selected topics.

Preference will be given to men sponsored by their employers, but a number of senior awards are available for independent candidates each year. The fee for a full-time Postgraduate course of study is £50 per annum.

The 1953–54 session will be divided into five courses, each of five weeks' duration, as follows:

Oct. 5–Nov. 7.	Course I—Metallurgical Techniques.
Nov. 9–Dec. 12.	Course II—Deformation of Metals.
Jan. 11–Feb. 13.	Course III—Solidification of Metals.

Feb. 15–March 20. Course IV—Physical Metallurgy of Heat-treatment.

April 26–May 29. Course V—Theory of Alloy Steels.

Enquiries may be addressed to the Professor of Physical Metallurgy, The University, St. George's Square, Sheffield, 1.

APPOINTMENTS VACANT

METALLURGIST. Imperial Chemical Industries, Ltd., Billingham Division, has a vacancy for a research metallurgist. Candidates should be between the ages of 23 and 35, and have a good Honours degree in metallurgy with post-graduate experience in research or productive industry. The work is in the field of physical metallurgy, and the post gives scope for carrying out complete investigations of very varied character. Adequate technical assistance and equipment will be provided. Publication of results will be encouraged. Write, giving full details, to the Staff Manager, Imperial Chemical Industries, Ltd., Billingham Division, Billingham, Co. Durham, quoting ref. no. A.3.

QUALIFIED ANALYTICAL CHEMISTS required for Assay Laboratory of the Northern Rhodesian Copper Mine. Starting basic salary £68 per month plus fluctuating cost of living allowance, now about £7 per month. Life assurance and contributory pension scheme. Cash bonus scheme which at present rate is equal to 65% of basic salary. Outward passage paid. Apply giving full details of age, marital status, qualifications, and experience to Box 196, Dorland Advertising, 18/20 Regent Street, London, S.W.1.

UNIVERSITY OF BIRMINGHAM

Department of Industrial Metallurgy

Applications are invited for the position of Investigator to carry out research on: Elastic Properties of Spring Materials. The salary will be in the range £300 to £600 per annum, depending upon qualifications and experience. Candidates should possess a degree in Metallurgy, Physics, or Engineering or equivalent qualification. The research will be appropriate for a candidate for a higher degree.

Applications should be submitted as soon as possible to: The Registrar, The University, Birmingham, 15.

C. G. BURTON,
Secretary.

UNIVERSITY OF QUEENSLAND

Applications are invited for the position of Lecturer (grade II) in Physical Metallurgy. Salary £A971 10*s*./£A1096 10*s*. p.a.

Applicants must hold a degree, preferably with honours either in science with metallurgy as a major subject or in metallurgical engineering. Some applied or research experience in physical metallurgy is desirable. Further particulars and application forms are obtainable from the Secretary, Association of Universities of the British Commonwealth, 5 Gordon Square, London, W.C.1. Applications should be sent to the undersigned as soon as possible after the appearance of this advertisement.

C. PAGE HANIFY,
Registrar.

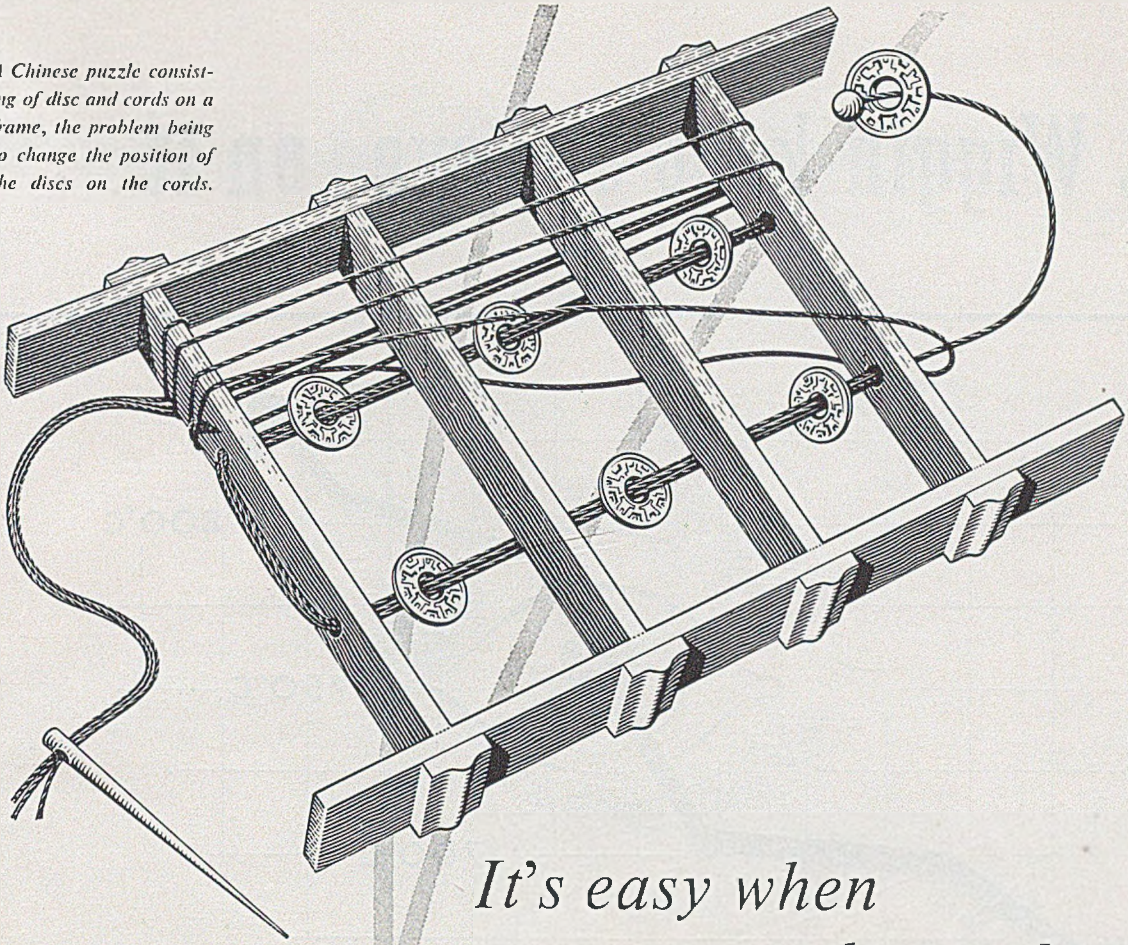

A Chinese puzzle consisting of disc and cords on a frame, the problem being to change the position of the discs on the cords.

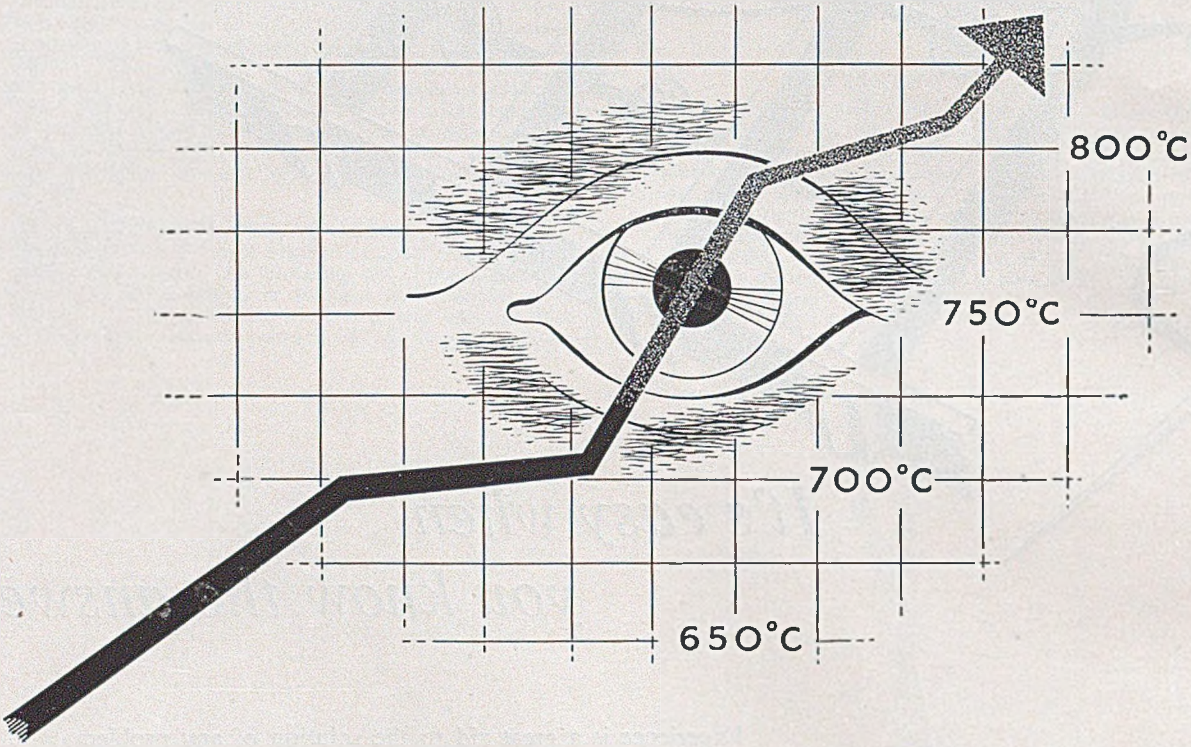
800°C
750°C
700°C
650°C

HYDROGEN BLISTERS IN BRASS SHEET* 1470

By R. EBORALL,† M.A., MEMBER, and A. J. SWAIN,‡ M.A., MEMBER

(Communication from the British Non-Ferrous Metals Research Association.)

SYNOPSIS

Blisters appearing near the centre plane of brass sheet were attributed to hydrogen collecting and persisting in central voids of the cast slab, so that these voids did not weld up during rolling; expansion of the compressed hydrogen on annealing the brass after it had been reduced to thin sheet and so was unable to withstand the stresses produced, caused the appearance of blisters. It was found that hydrogen was lost during annealing, and an effective remedy was developed based on this observation and on a proposed mechanism of blistering. Approximate measurements of the solubility of hydrogen in solid 2 : 1 brass gave values somewhat lower than the published values for copper.

I.—INTRODUCTION

THE work described in the present paper was undertaken to ascertain the causes of a very severe and persistent case of blistering in 2 : 1 and 70 : 30 brass sheet. The sheet was made from chill-cast ingots by breaking down hot and subsequently rolling cold, after surfacing, with intermediate anneals. Considerable amounts of cross-rolling were involved. The blisters first appeared after annealing when the sheets were from about ⅛ in. thick to about 18 gauge, depending on the thickness of the original ingot, and were all on or near the centre plane of the sheet.

Preliminary experiments, in which blisters were drilled *in vacuo* and the released gas measured and analysed, showed the gas to consist entirely of hydrogen. The calculated volume of one blister was approximately 30 mm.^{3}, and the quantity of hydrogen obtained from it was 15·6 mm.^{3} at N.T.P. Thus the hydrogen exerted a pressure of approximately ½ atmosphere in the blister at room temperature, or about 1½ atmospheres at the annealing temperature (550° C.). The surface of the metal inside the blisters was completely clean.

The fact that the gas extracted from the blisters was pure hydrogen indicated that the blisters did not arise from mechanically entrapped bubbles of gas injected into the solidifying ingot during pouring—a generally accepted and well-established cause of surface blistering in cross-rolled brass sheet[1]—and experiments were accordingly planned to determine whether the blisters were formed by another mechanism, which is generally accepted for some other metals. A brief outline of this mechanism is given and the experimental work and remedial measures and their successful application in practice are described.

II.—MECHANISM OF BLISTER FORMATION

The established mechanism of blister formation in metals as a result of the presence of dissolved gas (see, for instance, Edwards[2] on pickling steel) may be summarized briefly as follows. A dissolved gas exists in solution in a metal in the atomic or ionic state, and is frequently present in excess of the equilibrium solid solubility at atmospheric pressure and at the temperature of heat-treatment. This dissolved gas may be present in the ingot as cast, and in some circumstances the quantity may be increased by surface reactions, e.g. during pickling or during heat-treatment in an unsuitable atmosphere. In many cases the dissolved gas atoms are practically immobile at room temperature, but at elevated temperatures they become free to diffuse through the metal; this would be expected in the case of copper-base alloys. When they are sufficiently mobile, the dissolved gas atoms associate to form molecules at the free surface of the metal, these are evolved into the atmosphere, and the concentration of dissolved gas just below the surface tends towards the value in equilibrium with the partial pressure of the particular gas in the atmosphere. At any internal cavity or discontinuity, gas atoms similarly associate and are released into the cavity; here, however, the gas is not free to escape, and so a gas pressure is built up in the cavity, until equilibrium is reached with the dissolved gas which is present around the cavity. Since the solubility of a diatomic gas such as hydrogen is proportional to the square root of the pressure, it is evident that large pressures may be developed in the cavity; for instance, if the gas is present at a concentration of 10 times the equilibrium value at atmospheric pressure (a not unusual occurrence), a pressure of 100 atmospheres may be developed.

---

* Manuscript received 19 February 1953. The work described in this paper was made available to members of the B.N.F.M.R.A. in a confidential Technical Memorandum issued in November 1949.

† Head of the General Metallurgy Section, British Non-Ferrous Metals Research Association, London.

‡ Aluminium Wire and Cable Co., Ltd., Swansea; formerly Investigator, British Non-Ferrous Metals Research Association.

Heating the metal to sufficiently high temperatures will result in diffusion over longer distances, and the concentration of dissolved gas throughout the metal will tend towards the value in equilibrium with the external atmosphere; this value may be greater or less than the original concentration. Although large pressures may frequently be developed, it is unlikely that a blister will form unless either the metal is very weak, e.g. partially molten, or the cavity is particularly suitable. It is evident that an extensive flat discontinuity parallel to the surface and only a short distance below it is the most conducive to blister formation, while a small spherical hole at a great depth can only be enlarged by a very great pressure.

The prerequisites for the formation of gas blisters, therefore, are: (*a*) The presence of gas in the metal in quantities substantially exceeding the solubility at the temperature concerned and at atmospheric pressure. (*b*) The presence of suitable discontinuities, the most favourable to blistering being discontinuities of large length and breadth in a plane parallel to the surface and lying a little below it.

In the present instance the cavities concerned were near the central plane of the sheet, and it can readily be seen that the disposition of the cavities becomes more favourable to blistering as the sheet becomes thinner, for the lateral dimensions of any cavities initially present are progressively enlarged and the distance below the surface is reduced. It is evident, too, that strip rolling should give a product less liable to this type of trouble, for by this method the cavities are simply extended in one direction and the bridge of metal over them is therefore short and well supported.

To understand the blistering occurring in this instance, it is necessary to know (*a*) the source of hydrogen and the way in which the hydrogen content varies in processing, and (*b*) the origin of the cavities.

III.—GAS CONTENT OF CAST AND WROUGHT BRASSES

1. Occurrence of Cavities

The ingots, which were normally about 3 ft. long and 1¼ in. thick, were chill cast in vertical cast-iron moulds which were coated with a mixture of lard oil and resin that volatilized during pouring and burned at the mouth of the mould. Pouring was done through a tundish with a number of holes and was completed in 10–15 sec.

Examination of an ingot showed it to be substantially sound apart from some centre-line shrinkage. It is improbable that a much sounder product could be obtained by altering the casting conditions, unless the thickness of the ingot were increased. The amount of central shrinkage, although not large, appeared to be sufficient to explain the occurrence of centre-line blisters during fabrication, provided that sufficient hydrogen was present.

2. Hydrogen Content of the Metal

The hydrogen present in the metal might have come from one or more of several sources. The most obvious possibilities were:

(i) Raw materials and scrap used for the furnace charge. These might introduce hydrogen into the molten metal.

(ii) Melting furnace atmosphere. Hydrogen might be absorbed from moisture and/or other hydrogen-containing gases, although the high vapour pressure of zinc in the molten brass would minimize such absorption.

(iii) Mould atmosphere. Hydrogen might be introduced during casting from the cracking of hydrocarbons from the volatile dressing or from the decomposition of steam by the zinc.

(iv) Preheating furnace atmosphere. The ingots were preheated for rolling in a coal-fired furnace in which the flue gases formed the furnace atmosphere. There appeared to be a possibility that a reaction of the type

$$(\mathrm{Zn})_{\text{in brass}} + \mathrm{H_2O}_{(\text{vapour})} \longrightarrow \mathrm{H_2} + \mathrm{ZnO}$$

could occur and that some of this hydrogen might be forced into the metal, as it is when the analogous reaction occurs with aluminium–magnesium alloys. It is unlikely that hydrogen itself would be present in the atmosphere in any large quantity.

(v) Annealing furnace atmosphere. Intermediate anneals during cold rolling were done in air in an electric muffle furnace, and it was thought unlikely that gas was absorbed at this stage.

Accordingly, samples were taken from typical products and examined for hydrogen content with the results shown in Table I.

TABLE I.—*Hydrogen Contents of* 2 : 1 *Brass Samples Taken at Random at Various Stages of Production.*

Stage in Production	Hydrogen Content, c.c. at N.T.P./100 g.
Ingot	0·36, 0·34
(*a*) *Normal Hot- and Cold-Rolling Schedule:*	
Hot-rolled plate ($\frac{3}{8}$ or $\frac{7}{32}$ in.) . .	0·24
0·068 in. sheet	0·06 *
0·041 in. sheet	0·06 *
(*b*) *Cold-Rolled from Ingot:*	
$\frac{3}{16}$ in plate (annealed at $\frac{7}{16}$ in.) .	0·12
$\frac{1}{8}$ in. sheet (annealed again at $\frac{3}{16}$ in.)	0·02 †
20 S.W.G. sheet (0·036 in.)	0·04 †
,, ,, ,, (annealed)	0·08 †

* From sound parts of sheets.

† There is a blank error (not allowed for) probably associated with the surface of the sample, and this will be proportionately greater for thin samples. The higher figures obtained on 20-S.W.G. sheet compared with $\frac{1}{8}$-in. sheet may, therefore, not represent a real increase in hydrogen content.

In a further experiment a 2 : 1 brass ingot was cut in half and one half hot rolled. Samples taken from the ingot and from the equivalent position in the hot-rolled plate gave gas contents of 0·29 and 0·14 c.c./100 g., respectively.

A small sample of a 70 : 30 brass melt was poured on to a copper block free from mould coating, and another sample was taken from an ingot cast from this melt in the usual way. The corresponding gas contents were 0·13 and 0·44 c.c./100 g., which may indicate absorption of gas during casting, although some gas may have escaped from the thin sample poured on to the copper block.

The results show that the metal as cast has a considerable hydrogen content, and that hydrogen is lost in both the preheating and the annealing furnaces.

The mechanism postulated for the blistering in this case is, therefore, that during preheating for hot rolling some of the hydrogen present in the ingot diffuses to the shrinkage cavities and develops a large pressure of gaseous hydrogen in them. On hot rolling the cavities are closed up to some extent, but complete welding up is prevented by the compressed hydrogen. These flattened-out cavities remain in existence during the subsequent cold rolling until the sheet becomes thin enough to allow the gas pressure to expand the cavities to a visible extent when the metal softens during annealing.

IV.—REMEDIAL MEASURES AND THEIR PRACTICAL APPLICATION

The foregoing measurements show that hydrogen is removed by annealing. Experiments were done to see how rapidly this removal occurred and to what extent it was limited by atmospheric conditions.

Samples approximately $1 \times \frac{3}{4} \times \frac{1}{4}$ in., from the ingot and hot-rolled plate ((*a*) of Table I) were heated to 800° C. for 1 hr. in a silica-tube furnace in dry air and in a steam/air mixture (very roughly equal quantities of each). The hydrogen contents after treatment were as shown in Table II.

Table II.—*Effect of Annealing Atmosphere on Gas Content of* 2 : 1 *Brass.*

Sample	Hydrogen Content, c.c. at N.T.P./100 g.		
	Initially	After Heating to 800° C. for 1 Hr.	
		In Dry Air	In Steam/Air
Ingot . . .	0·29	0·01	0·01
Hot-rolled plate .	0·14	0·02	0·02

A subsequent test on samples from which the gas had been extracted *in vacuo* showed that the blank was of this order of magnitude, so that the true hydrogen content after treatment was effectively zero.

Samples of the same size, taken from the hot-rolled plate, were given shorter treatments in dry air at 600° and 800° C. and the loss of hydrogen followed, with the results shown in Table III.

The hydrogen content of a ¼-in.-thick piece is thus reduced to a very low value after ¼ hr. at 800° C. or 1 hr. at 600° C. Corresponding times for other thicknesses may be obtained by multiplying by the square of the thickness ratio; thus for x in. thick at 600° C. the time would be $16x^2$ hr., and at 800° C. it would be $4x^2$ hr.

Table III.—*Removal of Hydrogen by Annealing.*

Time, hr.	Hydrogen Content, c.c. at N.T.P./100 g.	
	800° C.	600° C.
¼	0·01	0·12
½	0·01	0·04
1	0·01	0·02
1½	...	0·02

These results suggest a possible remedy for blistering. The hydrogen can be almost completely removed by annealing at such a stage that: (*a*) the cavities are substantially flattened out at the start of annealing, so as not to provide a reservoir for the gas, (*b*) the metal is thick enough to withstand the very large pressures developed in the flattened cavities at the start of annealing, and (*c*) the metal is not so thick that the required combination of time and temperature is impracticable.

On this basis a remedy was proposed, consisting of returning the hot-rolled plates (7/16 in. thick) to the preheating furnace (700°–800° C.) for 2 hr.

Samples were taken of the products at different stages from two ingots of the same batch, one of which was given the normal processing and the other given the extra furnace treatment. The hot-rolled plate had a hydrogen content of 0·39 c.c. at N.T.P./100 g. compared with 0·02 c.c. at N.T.P./100 g. for the similar plate after the extra furnace treatment.

Production trials showed that the remedy was completely effective. A large-scale test was carried out in which a batch of 100 ingots, cast four per melt, was halved, two ingots per melt being in each half-batch. One half-batch was processed by the usual hot- and cold-rolling schedule, and the sheet produced proved to be even more severely blistered than usual, 90% of the sheets being rejected because of this defect. The other half-batch was given the extra heat-treatment of 2 hr. in the preheating furnace at about 800° C., and none of the sheets produced was rejected for blistering.

V.—SOLUBILITY OF HYDROGEN IN 2 : 1 BRASS

1. Experimental Methods

The method used was to soak sound, gas-free metal in hydrogen, quench it, and subsequently measure the gas content in the usual way. The hot-rolled plate (with initially 0·14 c.c. hydrogen at N.T.P./100 g.) described above was used for all experiments. Pieces of the plate were degassed by heating in dry air at 800° C. for ½ hr. The oxide scale was removed by filing. The pieces were then hammered to close any internal discontinuities, the thickness being reduced by about 25% in this operation. Samples of the plate so prepared were heated in dry hydrogen at various temperatures, in most cases for more than one period in order to check the degree of saturation, and were quenched into molten lead and then into iced water. After removal of the zinc-impoverished layer (about 1 mm. was removed from each surface after soaking at the highest temperature), the hydrogen content was estimated by vacuum extraction in the usual way.

2. Results

The results of the solubility measurements are given in Table IV, and values derived from these are plotted logarithmically against the reciprocal of the temperature in Fig. 1. The line drawn represents the best straight line for the points relating to alloys free from β phase (i.e. excluding the highest temperature).

Table IV.—*Results of Solubility Measurements on* 2 : 1 *Brass.*

Temperature, °C.	Duration of H_2 Soak, hr.	H_2 Content, c.c. at N.T.P./100 g.	Mean H_2 Content, c.c. at N.T.P./100 g.
875	2½	0·385	0·347
		0·310	
850	3	0·095	0·088
		0·081	
800	2	0·080	0·087
		0·091	
	4	0·095	
		0·083	
750	3½	0·062	0·063
		0·065	
	4	0·063	
700	5½	0·050	0·049
		0·052	
	6½	0·045	
		0·049	
650	7	0·021	0·019
		0·021	
	8	0·018	
		0·017	
600	4	0·015 *	0·032
	7½	0·025	
		0·040	

* Ignored, since saturation may not have been reached.

Values for the solubility at 100° C. intervals in the range 500°–800° C., obtained from the best straight line of Fig. 1 are given in Table V. No great accuracy is claimed for these values, which are certainly liable to errors of up to ±0·01 c.c./100 g. at the higher temperatures. They suffice, however, to indicate that the explanation of blistering put forward above is not based upon false assumptions. The results are substantially lower than those given by Sieverts and Krumbhaar[3] and by Röntgen and Möller for copper.[4]

Table V.—*Solubility of Hydrogen in* 2 : 1 *Brass.*

Temperature, °C.	Solubility, c.c. at N.T.P./100 g.
800	0·076
700	0·044
600	0·023
500	0·010

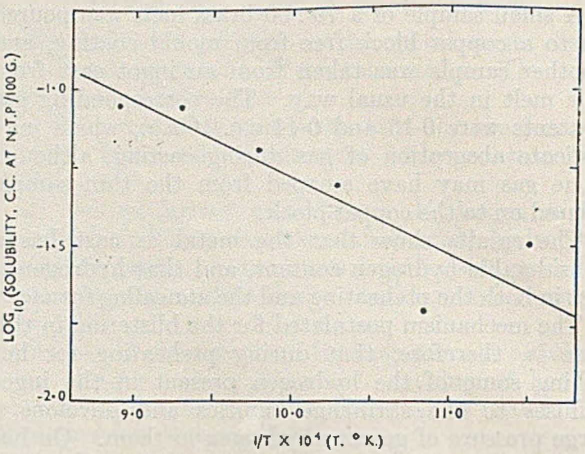

Fig. 1.—Solubility of Hydrogen in 2 : 1 Brass.

The two measurements at 875° C., at which temperature some β phase is present, appear to indicate that the solubility in the β phase may be considerably higher.

VI.—CONCLUSIONS

1. A form of centre-plane blistering in α-brass sheet has been shown to be due to hydrogen.
2. The hydrogen is present in the cast billet and is to some extent reduced at every anneal, even in a burnt-coal atmosphere.
3. The blistering can be eliminated by allowing the hydrogen to diffuse away under suitable conditions.
4. Hydrogen has a fair solubility in α-brass, though it is somewhat less than the published values for copper.
5. Hydrogen diffuses fairly rapidly in α-brass at 600° C. and above.

ACKNOWLEDGEMENTS

The authors are indebted to the Director and Council of The British Non-Ferrous Metals Research Association for permission to publish this paper.

REFERENCES

1. R. Genders and G. L. Bailey, "The Casting of Brass Ingots" (B.N.F.M.R.A. Research Monograph No. 3). London: **1934**.
2. C. A. Edwards, *J. Iron Steel Inst.*, **1924**, **110**, 9.
3. A. Sieverts and W. Krumbhaar, *Z. physikal. Chem.*, **1910**, **74**, 277.
4. P. Röntgen and F. Möller, *Metallwirtschaft*, **1934**, **13**, 81, 97.

CRITICAL-STRAIN EFFECTS IN COLD-WORKED WROUGHT ALUMINIUM AND ITS ALLOYS*

1471

By W. M. WILLIAMS,† B.Sc., and R. EBORALL,‡ M.A., Member

(Communication from the British Non-Ferrous Metals Research Association.)

SYNOPSIS

Straining and annealing treatments have been applied to super-purity and commercial-purity aluminium and to four aluminium alloys, to test their behaviour against a set of empirical rules describing the effects of strain, annealing temperature, and initial grain-size on the critical strains and final grain-sizes. The final grain-size of the recrystallized material was found, for a given composition, to depend strongly on the strain and in most cases comparatively little on the annealing temperature and initial grain-size, although the latter had a definite effect, especially in super-purity aluminium. Owing to the strength of this effect in super-purity aluminium, the maximum grain-size which could be produced by annealing at a given temperature was generally increased by coarsening the initial grain-size, although for other materials the reverse was normally true.

I.—INTRODUCTION

The experiments described in the present paper were designed to test the recrystallization behaviour of aluminium and some of its commercial alloys, with particular reference to critical strains and the coarse grain-sizes associated with them and to the effect of original grain-size. Published literature on this subject indicates that the grain-sizes produced by recrystallization during annealing can be described to a fair approximation in terms of the following general empirical rules :

(*a*) When a metal is cold worked and then annealed, the as-recrystallized grain-size decreases as the amount of deformation before annealing is increased, and is substantially independent of the annealing temperature.

(*b*) With a given annealing treatment, there is a critical strain below which complete recrystallization does not occur. This critical strain gives rise to the largest grains after annealing.

(*c*) The critical strain is higher, the lower the annealing temperature.

(*d*) For a given annealing temperature, the critical strain is higher, the larger the initial grain-size of the material and, because the recrystallized grain-size is mainly dependent on the strain, the maximum grain-size which can be produced by the given annealing treatment is smaller for initially coarse material than for fine-grained material.

The first three rules, and particularly (*b*) and (*c*), have been widely appreciated, and are derived from very early work, especially that of Chappell [1] and of Carpenter and Elam.[2] Rule (*d*) is not so well known, but reference may be made to the work of Matthaes and Schroeder on Duralumin-type alloys [3] and that of Gries and Esser on iron.[4] Anderson and Mehl [5] found that coarse-grained aluminium had both a slower rate of nucleation for new grains and a slower rate of grain growth under given conditions, than had a fine-grained material, and this would lead to a similar result.

The validity of these rules, as applied to aluminium and several of its alloys, has been tested, and the quantitative results are reported in the following sections. The rules take no account of any changes, such as coalescence and secondary recrystallization, which may in some metals take place after recrystallization during prolonged annealing or annealing at a high temperature.

II.—MATERIALS

The materials were all supplied by the courtesy of a member firm in the form of cold-rolled sheet of various tempers, and 0·064 in. thick. The analyses of these materials are given in Table I.

III.—EXPERIMENTAL PROCEDURE

1. Production of Materials with Various Initial Grain-Sizes

For all the materials, except super-purity aluminium, a range of initial grain-sizes was obtained by annealing batches of different tempers at suitable temperatures. In several cases where the as-received materials did not yield a sufficient range of grain-sizes on annealing,

---

* Manuscript received 10 September 1952. The work described in this paper was made available to members of the B.N.F.M.R.A. in a confidential research report issued in January 1951.

† Investigator, British Non-Ferrous Metals Research Association, London.

‡ Head of the General Metallurgy Section, British Non-Ferrous Metals Research Association, London.

TABLE I.—*Analyses of Alloys Examined.*

Material	Fe, %	Si, %	Cu, %	Mn, %	Ti, %	Zn, %	Mg, %	Ni, %	Pb, %
S.p. Al . . .	0·004 *	<0·002 *	<0·001 *	<0·001	<0·002 †	⩽0·01 †	<0·01	<0·01 †	<0·002 †
C.p. Al . . .	0·45	0·16	0·02	0·01	0·01	⩽0·01 †	<0·01	<0·01 †	<0·002 †
2% Mg alloy . .	0·34	0·22	0·02	0·49	~0·01	0·01	2·1 *	<0·01 †	<0·002 †
1% Mg, 1% Si alloy .	0·4	0·98 *	~0·01	~0·02	<0·01	⩽0·01 †	0·90 *	<0·01 †	<0·002 †
Duralumin-type alloy .	0·35	0·73 *	4·78 *	0·73 *	<0·01	⩽0·01 †	0·43 *	<0·01 †	<0·002 †
1¼% Mn alloy . .	0·59	0·21	0·12	1·14 *	<0·01	⩽0·01 †	0·008	<0·01 †	~0·002

* Chemically determined, remainder spectrographically. † Not detected.

they were annealed, rolled to a suitable reduction, or stretched by a suitable amount in a tensile machine, and then re-annealed to obtain the desired grain-size. As far as possible, the same annealing temperature was used throughout for any one alloy. Details of these treatments are given later.

In super-purity aluminium coalescence occurs readily at temperatures above 300° C., and specimens of the as-received material were accordingly annealed at various temperatures from 300° to 500° C. to produce various degrees of coalescence.

Using such methods, fully-annealed specimens of various initial grain-sizes were obtained with each material. For each different working and annealing treatment, an X-ray back-reflection photograph was taken to confirm that recrystallization was complete. This was followed by a metallographic examination of the grain structure. Except in the case of the Duralumin-type alloy (which was hand-polished at the final stage), the micro-specimens were electrolytically polished after a preliminary hand-polish and then anodically or chemically etched.

Grain counts were made with a Vickers projection microscope fitted with a moving stage and two vernier scales. The distance traversed when 50 grains passed the cross-wires was measured and used to give the number of grains/cm. traversed. Between five and ten separate counts were made in random directions on the surface of each specimen, and the reciprocal of the average count was taken as the grain dia. All grain-sizes were measured on the etched surface of the sheet.

2. RECRYSTALLIZATION EXPERIMENTS

The recrystallization behaviour of super-purity aluminium, commercial-purity aluminium, 2% magnesium alloy, and the 1% magnesium, 1% silicon alloy was conveniently studied by using tapered tensile specimens. Specimens were machined from the supplied sheet with their length parallel to the rolling direction, with a gauge-length of 20 cm., and a width decreasing from 1 in. at one end to ½ in. at the other. These gave a suitable range of strains when stretched or broken in tension.

Before being annealed to produce a range of initial grain-sizes, the gauge-length of each specimen was marked out at intervals of approximately 1 cm., the actual intervals being measured to 0·01 mm. with a travelling microscope. Batches of the specimens were then annealed at a temperature appropriate to the particular alloy to produce several different starting grain-sizes. These annealing treatments were carried out in air in a muffle furnace, and details are given later.

The specimens were stretched in an Avery tensile-testing machine and each one remeasured with the travelling microscope to determine the exact strain at each point along the gauge-length. They were introduced into a salt bath to recrystallize as soon after deformation as possible (within a few hours) in order to minimize any effects on the recrystallization characteristics due to prior recovery at room temperature. The temperature of the salt bath was constant to ±1° C., and the annealing time in all cases was 30 min. Several recrystallization temperatures were used for each alloy with each initial grain-size. On removal from the salt bath, the specimens were macro-etched in a solution of one part water, one part conc. HNO_3, one part conc. HCl, and one-sixth part conc. HF by volume.

The grain-size was measured at various points along the recrystallized portion of the gauge-length and related to the strain values before recrystallization. The critical strain was taken to be the strain at the junction between the recrystallized and un-recrystallized parts of the gauge-length, the exact point being that beyond which none of the original structure was retained.

A modification to the above sequence of operations had to be made for the Duralumin-type and the 1¼% manganese alloys. The critical strains were too large to be studied by using tensile specimens, and the specimens were therefore deformed by rolling, as follows. Rectangular strips approximately 8 in. long and 1 in. wide were annealed to obtain the required initial grain-size, and then "wedge-rolled", i.e. the rolls were screwed down more one side than the other and the strip was fed with its length parallel to the axes of the rolls to give a range of deformation along the length of the strip. A micrometer measurement of the reduced thickness at any point gave a direct value of the reduction at that point. The lateral spread (~1%) was negligible. In this way a range of strain of 10–75% could be produced on a single specimen; the typical range necessary was about 15–50%. Subsequent procedure was then similar to that for the tapered tensile specimens, the rolled pieces being recrystallized at various temperatures for ½ hr.

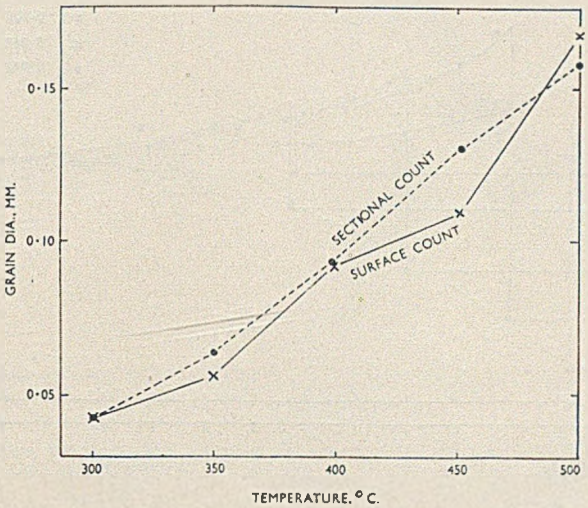

FIG. 1.—Grain-Size/Heat-Treatment Curve for Super-Purity Aluminium Annealed 2½ hr. at 298° C. + 1 hr. at Various Temperatures.

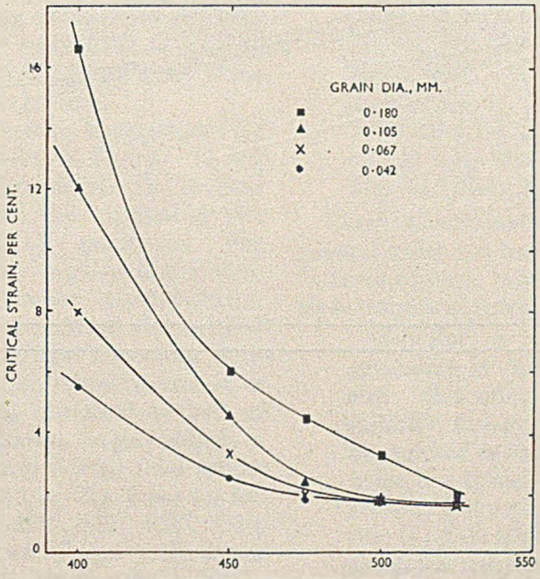

FIG. 2.—Critical-Strain/Recrystallization-Temperature Curves for Super-Purity Aluminium with Various Initial Grain-Sizes. Annealing time 30 min.

The Duralumin-type and 1¼% manganese alloys presented a new difficulty in that a macro-etch in mixed acids was suitable only for the highest temperature of recrystallization used. At other temperatures a micro-etch was necessary in order to reveal the grain-sizes after recrystallization. The boundary between the recrystallized and the unrecrystallized parts of the gauge-length was not readily detected by micro-examination and, to determine the point of critical strain, a series of X-ray back-reflection patterns was taken along the length of the rolled and partly recrystallized specimen. From such a series of pictures it was possible to gauge the point of critical strain with reasonable accuracy (see X-ray patterns Figs. 13 (*a*) and (*b*), Plate LXXIX). The surface of that part of the specimen where the critical strain had occurred was then polished and etched to reveal the grain-size.

IV.—EXPERIMENTAL RESULTS

1. SUPER-PURITY ALUMINIUM

The results obtained with high-purity aluminium are reported in detail, since they are typical of the behaviour of all the materials tested. The results presented later for each individual alloy differ only

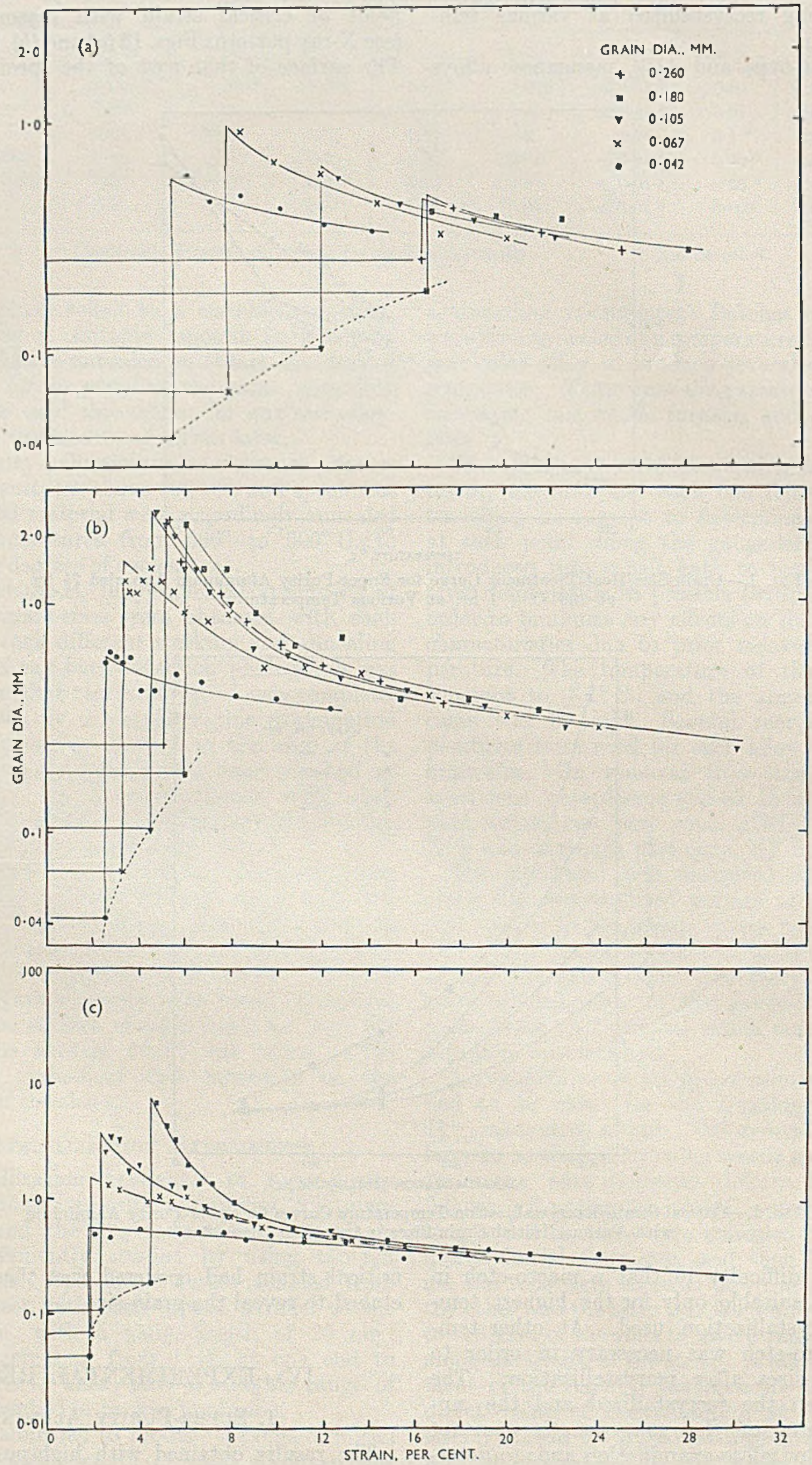

Fig. 3.
(For caption see opposite page.)

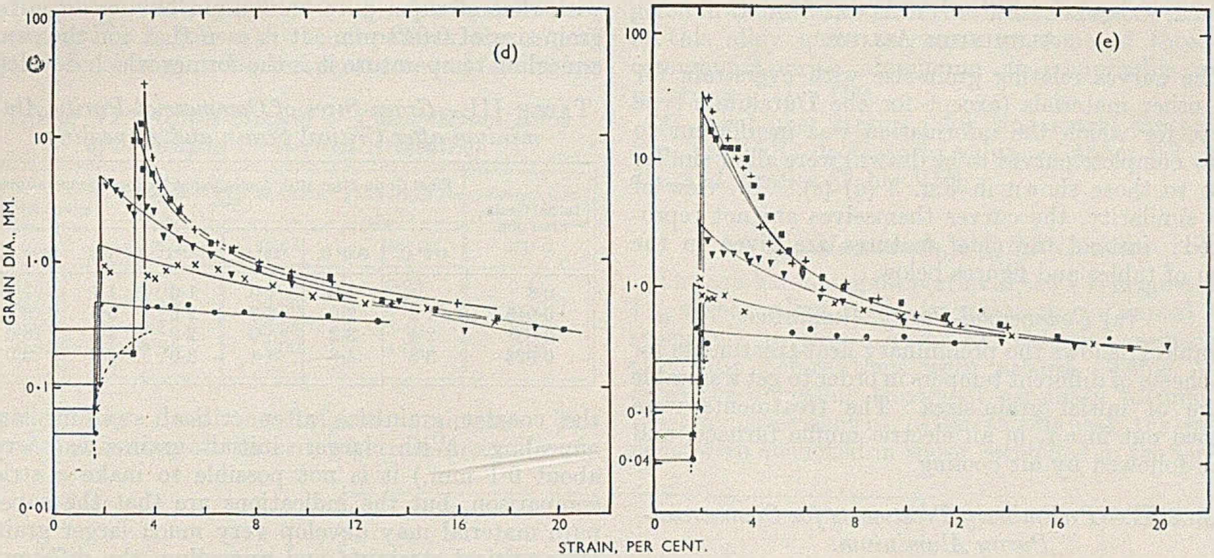

FIG. 3.—Recrystallization Diagrams for Super-Purity Aluminium with Various Grain-Sizes. Heat-treatment was 30 min. at (*a*) 400° C., (*b*) 450° C., (*c*) 475° C., (*d*) 500° C., and (*e*) 525° C.

numerically from those given for super-purity aluminium.

As mentioned previously, various initial grain-sizes were obtained by annealing as-received material in air at temperatures ranging from 298° to 500° C. (Fig. 1). Specimens with initial grain-sizes from 0·042 to 0·26 mm. were used in the tests.

Curves relating critical strain with temperature for various initial grain-sizes are given in Fig. 2. It will be seen that at the lower temperatures the critical strain is greatly dependent on the original grain-size, increasing with increasing grain-size. The dependence on initial grain-size rapidly diminishes, however, at higher recrystallization temperatures. For the initially fine-grained specimens the critical strain is relatively insensitive to the annealing temperature, so that at these higher temperatures it is almost independent both of the temperature and of the initial grain-size for the grain-size range studied.

Curves relating original grain-size with final grain-size for various strains are given in Fig. 3 (*a*)–(*e*) for the five temperatures used, viz. 400°, 450°, 475°, 500°, and 525° C. To gauge the effect of any coalescence occurring after recrystallization on the final grain-sizes initially shown in these curves, a short series of experiments was made. These consisted of measuring the grain-size of specimens with initial grain-sizes of 0·28 and 0·5 mm., before and after heat-treatments of 30 min. at temperatures up to 525° C. The results showed that the effect of coalescence is negligible for the grain-sizes and temperatures occurring in the present experiments, and the results given in Fig. 3 (*a*)–(*e*) should therefore be the true as-recrystallized values.

Each set of curves shows similar characteristics, and the following generalizations can be made :

(i) For a particular initial grain-size and temperature, coarse grain is developed at the critical strain, the grain-size then rapidly decreasing with greater deformations to a less rapidly varying value.

(ii) Comparison of the curves in Fig. 3 (*a*)–(*e*), for specimens with a given initial grain-size shows that the final grain-size is mainly determined by the strain before annealing and is little affected by the temperature of the anneal, except near the points of critical strain (see also Fig. 11, Plate LXXIX).

These observations are in accordance with the general rules set out in Section I. There are other features of note, however, which are not predicted by these empirical rules.

(iii) For a constant strain, the resultant grain-size is finer, the finer the original grain-size; this effect is particularly noticeable with initially fine-grained material at small strains. So marked is this effect in super-pure aluminium when the initial grain-size is small and when the annealing temperature is high, that the empirical rule (*d*) does not in general apply to this material, the grain-size after critical straining and annealing in many conditions being larger, the greater the initial grain-size. However, the rule does apply when the initial grain-size is large and the annealing temperature is low (Fig. 3), and, as will be seen later, it applies to the other materials examined (Fig. 12, Plate LXXIX) in almost all the conditions studied.

(iv) For fine-grained super-pure aluminium (0·042 mm. grain-size), the dependence of the final grain-size on the amount of strain is small, and the grain-size after critical straining and annealing is not very much coarser than the final grain-size resulting from a relatively high deformation, e.g. 12%.

2. Commercial-Purity Aluminium and Aluminium Alloys

The curves relating grain-size with overstrain for the other materials (except for the Duralumin-type alloy, for which the information was insufficient to allow complete curves to be drawn) were all of similar type to those shown in Fig. 3 (*a*)–(*e*). In view of this similarity, the curves themselves are not reproduced; instead the chief features are given in the form of tables and figures below.

(a) *Commercial-Purity Aluminium*

Table II shows the preliminary heat-treatments for the sheets of different tempers in order to get a suitable range of initial grain-sizes. The treatments were carried out in air, in an electric muffle furnace, and were followed by air cooling.

Table II.—*Preliminary Treatments for Commercial-Purity Aluminium.*

Previous Deformation, %	Annealing Treatment	Resultant Grain-Size, mm.
15	24 hr. at 450° C.	0·6
29	1½ hr. at 400° C.	0·045
45		0·031
55		0·023

Fig. 4 shows the curves relating critical overstrain with temperature for commercial-purity aluminium of each of the four initial grain-sizes. Though the form of the curves is approximately the same as that for super-purity aluminium, the critical strains for comparable initial grain-sizes and the same temperature are much higher (cf. Fig. 2, p. 503).

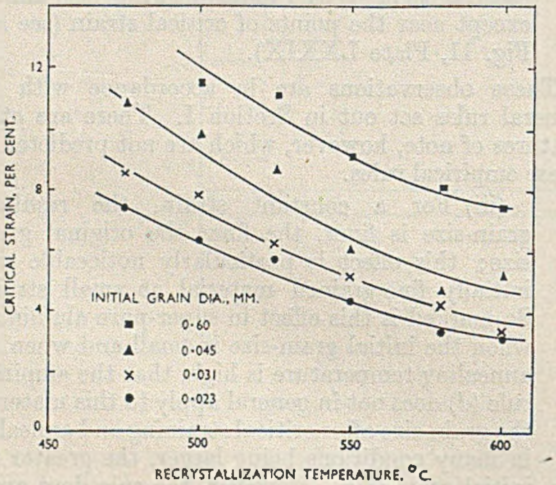

Fig. 4.—Critical-Strain/Recrystallization-Temperature Curves for Commercial-Purity Aluminium with Various Initial Grain-Sizes. Annealing time 30 min.

Table III shows, for material with various initial grain-sizes, the grain-size developed at the critical strain after annealing at different temperatures.

Comparing the behaviour of commercial-purity aluminium having an initial grain-size of 0·045 mm. with that of super-pure aluminium having an initial grain-size of 0·042 mm., it is seen that for the same annealing temperature it is the former which develops the coarser grain-size after critical straining and annealing. With larger initial grain-sizes (over about 0·1 mm.) it is not possible to make a strict comparison, but the indications are that the super-pure material may develop very much larger grains after critical straining and annealing, the difference between the two materials appearing to increase as the initial grain-size increases above this figure.

Table III.—*Grain-Sizes of Commercial-Purity Aluminium after Critical Strain and Annealing.*

Initial Grain-Size, mm.	Final Grain-Sizes after Annealing at Various Temperatures, mm.					
	475° C.	500° C.	525° C.	550° C.	575° C.	600° C.
0·6	...	1·0	1·0	1·0	1·4	1·4
0·045	1·8	2·0	2·3	2·2	5·5	9·4
0·031	2·4	3·2	5·0	2·2	4·8	18·0
0·023	3·8	4·8	4·4	3·0	6·8	6·0

Table IV.—*Grain-Sizes of Commercial-Purity Aluminium Recrystallized after Various Extensions.*

Initial Grain-Size, mm.	Temp., °C.	Grain-Size after Various Extensions, mm.		
		5%	10%	20%
0·6	500	...	...	0·56
	550	...	0·83	0·51
	600	...	0·90	0·52
0·045	500	...	1·8	0·29
	550	...	0·78	0·31
	600	(10)	1·2	0·36
0·031	500	...	1·1	0·29
	550	(2·2)	0·65	0·26
	600	2·0	0·53	0·23
0·023	500	...	0·88	0·24
	550	2·0	0·59	0·23
	600	1·9	0·66	0·31

When the critical strain is exceeded in this material, the grain-size becomes progressively finer, as in super-purity aluminium, falling to about 0·2 mm. at about 25% strain. Some values for various fixed strains are given in Table IV.

(b) 2% *Magnesium Alloy* (*Containing Manganese*)

The preliminary treatments for the production of a range of initial grain-sizes are given in Table V.

Table V.—*Preliminary Treatments for* 2% *Magnesium Alloy.*

Previous Deformation, %	Annealing Treatment *	Resultant Grain-Size, mm.
15	3 hr. at 500° C.	0·30
30	1 hr. at 400° C.	0·042
45		0·024
60		0·018

* In air, as for commercial aluminium.

The curves relating critical strain with temperature, shown in Fig. 5, follow the usual pattern, the critical strain decreasing with temperature and becoming smaller, the finer the original grain-size. The numerical values of the critical strain are not very different from those of commercial-purity aluminium at comparable initial grain-sizes and at the same temperature. Moreover, as is clear from the data given in Table VI, a grain structure can be developed in this alloy quite as coarse as some of those in commercial-purity aluminium at comparable temperatures (Table III).

TABLE VI.—*Grain-Sizes of 2% Magnesium Alloy after Critical Strain and Annealing.*

Initial Grain-Size, mm.	Final Grain-Sizes after Annealing at Various Temperatures, mm.			
	400° C.	450° C.	500° C.	575° C.
0·3	...	...	0·33	0·41
0·042	0·12	0·26	1·20	1·30
0·024	0·27	0·55	2·40	8·00
0·018	0·34	1·00	4·00	5·20

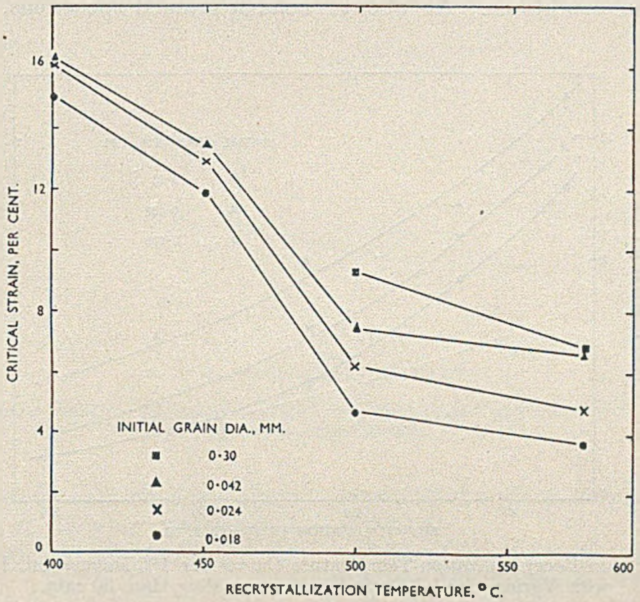

FIG. 5.—Critical-Strain/Recrystallization-Temperature Curves for 2% Magnesium Alloy with Various Initial Grain-Sizes. Annealing time 30 min.

TABLE VII.—*Grain-Sizes of 2% Magnesium Alloy Recrystallized after Various Extensions.*

Initial Grain-Size, mm.	Temp., °C.	Grain-Size after Various Extensions, mm.		
		5%	10%	20%
0·30	500 575	... ...	0·33 0·38	... ...
0·042	500 575	... ...	0·50 0·37	... ...
0·024	500 575	... 5·8	0·53 0·42	... 0·16
0·018	500 575	3·2 1·7	0·31 0·29	... ...

At the higher strains (25% and more) the grain-sizes gradually decrease to values of about 0·1 mm. dia. and smaller (Table VII).

(c) 1% *Magnesium*, 1% *Silicon Alloy*

The age-hardening properties of the 1% magnesium, 1% silicon alloy made it necessary to anneal the specimens, to obtain a variety of initial grain-sizes, only just before they were needed. Table VIII gives the annealing treatment necessary to produce the grain-sizes shown. After this anneal, the specimens were quenched in water, stretched in the tensile machine, measured, and recrystallized for 30 min. at the appropriate temperature as soon as possible. These operations were completed within an hour or two of quenching.

TABLE VIII.—*Preliminary Treatments for* 1% *Magnesium*, 1% *Silicon Alloy.*

Previous Deformation, %	Annealing Treatment *	Resultant Grain-Size, mm.
15 50 70	1 hr. at 420° C.	0·33 0·038 0·028

* In air, as for commercial aluminium, but water-quenched.

The critical-strain/temperature curves for the three initial grain-sizes are given in Fig. 6, and the effects of temperature and initial grain-size follow the usual trend. The critical strains necessary to produce coarse grain are relatively low, lower than for commercial-purity aluminium under comparable conditions. Table IX gives the grain-sizes developed at the critical strains and shows that grain-sizes can be produced as coarse as those developed in super-pure aluminium under the same conditions. At about 25% overstrain the recrystallized grain-sizes are of the order of 0·1 mm. dia. (see Table X).

Table IX.—*Grain-Sizes of 1% Magnesium, 1% Silicon Alloy after Critical Straining and Annealing.*

Initial Grain-Size, mm.	Final Grain-Sizes after Annealing at Various Temperatures, mm.				
	380° C.	415° C.	465° C.	515° C.	550° C.
0·33	0·5	0·68	1·3	2·4	3·0
0·038	0·6	0·82	4·5	9·0	13
0·028	1·2	1·5	10	14	11

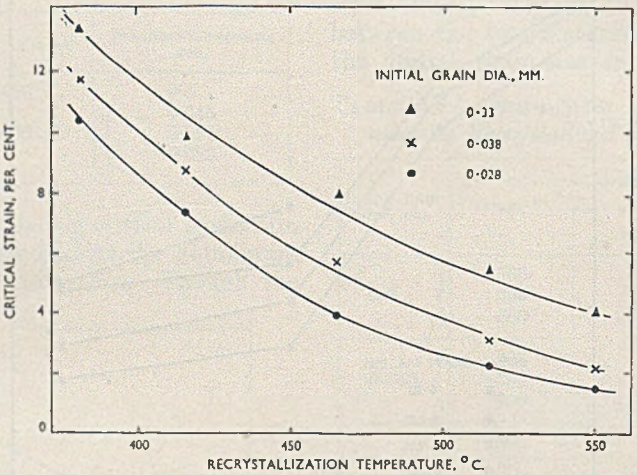

Fig. 6.—Critical-Strain/Recrystallization-Temperature Curves for 1% Magnesium, 1% Silicon Alloy with Various Initial Grain-Sizes. Annealing time 30 min.

Table X.—*Grain-Sizes of 1% Magnesium, 1% Silicon Alloy Recrystallized after Various Extensions.*

Initial Grain-Size, mm.	Temp., °C.	Grain-Size after Various Extensions, mm.		
		5%	10%	20%
0·33	415	...	0·75	...
	465	...	0·58	0·27
	515	...	0·52	0·20
	550	...	0·56	0·26
0·038	415	...	0·50	...
	465	...	0·45	0·15
	515	1·8	0·43	0·14
	550	0·96	0·35	...
0·028	415	...	0·51	...
	465	3·9	0·35	0·14
	515	1·4	0·33	0·13
	550	0·76	0·31	...

(d) *Duralumin-Type Alloy*

As in the 1% magnesium, 1% silicon alloy, the age-hardening characteristics of Duralumin-type alloy necessitated a continuous sequence of annealing for grain-size, quenching in water, rolling (instead of stretching), and recrystallizing with as little delay as possible. To test the effect of different amounts of alloying elements in solution, two batches of specimens were quenched in water from two different temperatures after annealing to obtain suitable initial grain-sizes. Two initial grain-sizes were used, and the annealing treatments for their production are given in Table XI.

The critical-strain/temperature curves for the two initial grain-sizes and for the two quenching treatments are given in Fig. 7. As for the previous materials, the critical strains are higher for the coarser-grained specimens, but the effect of different amounts of alloying elements in solution is a much greater one, especially at the lower temperatures.

The grain-sizes developed after the critical straining and annealing are given in Table XII.

Table XI.—*Preliminary Treatments for Duralumin-Type Alloy.*

Previous Deformation, %	Annealing Treatment	Resultant Grain-Size, mm.
15	(i) 6 hr. at 500° C. and quenched. (ii) 6 hr. at 500° C., furnace-cooled to 425° C., held 1 hr. at temp., and quenched.	0·17
70	(i) 1 hr. at 500° C. and quenched. (ii) 1 hr. at 425° C. and quenched.	0·035

The variation of these grain-sizes with temperature is the usual one, viz. the lower the temperature, the finer the grain-size after critical straining and annealing. In the case of material quenched from 425° C., the effect of initial grain-size on the grain-size after critical straining and annealing is in accordance with rule (*d*) (p. 501). From Table XII (*a*), however, it will be seen that the opposite is the case for material quenched from 500° C. This behaviour is reminiscent of that of super-pure aluminium.

Table XIII.—*Preliminary Treatments for* 1¼% *Manganese Alloy.*

Previous Treatment	Annealing Treatment *	Resultant Grain-Size, mm.
Homogenized, cold rolled 25% .	8 hr. at 500° C.	0·34
Unhomogenized, cold rolled 25%	128 hr. at 500° C.	0·36
Homogenized, cold rolled 85% .	5 hr. at 500° C.	0·026
Unhomogenized, cold rolled 85%	5 hr. at 500° C.	0·027

* In air, as for commercial aluminium (air-cooled).

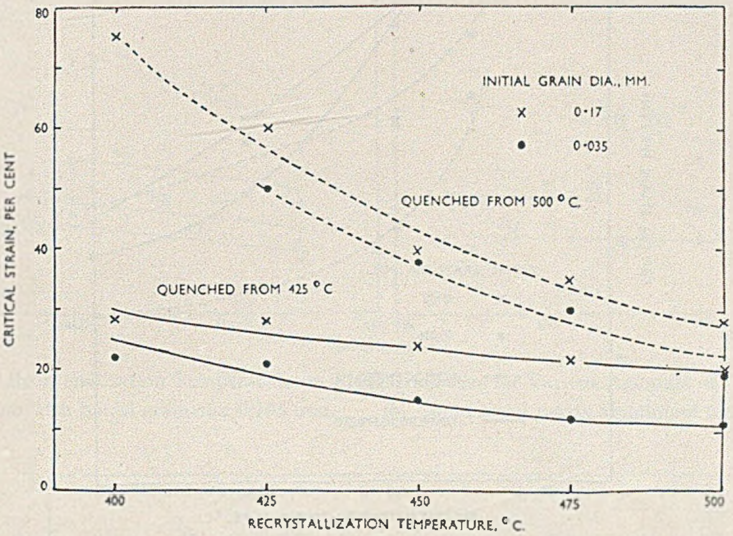

Fig. 7.—Critical-Strain/Recrystallization-Temperature Curves for Duralumin-Type Alloy with Various Initial Grain-Sizes. Annealing time 30 min.

The effect of the quenching treatment on the values of the grain-size after critical straining and annealing is very marked, as would be expected from the substantial difference in the critical-strain values already noted. In short, for Duralumin-type alloys the greater the amounts of alloying elements in solution, the higher is the critical strain, and hence the finer is the largest grain-size which can be obtained by annealing at a given temperature.

Table XII.—*Grain-Sizes of Duralumin-Type Alloy after Critical Straining and Annealing.*

Initial Grain-Size, mm.	Final Grain-Sizes after Annealing at Various Temperatures, mm.				
	400° C.	425° C.	450° C.	475° C.	500° C.
(a) *Material Quenched from* 500° *C.*					
0·035	...	...	0·025	0·028	0·032
0·17	...	0·026	0·030	0·033	0·050
(b) *Material Quenched from* 425° *C.*					
0·035	0·075	0·085	0·2	0·5	0·55
0·17	0·037	0·038	0·05	0·067	0·059

(e) 1¼% *Manganese Alloy*

The 1¼% manganese alloy was supplied in two batches: (i) homogenized before hot rolling and (ii) unhomogenized. The homogenization treatment consisted of a 27-hr. anneal of the cast billet, finishing at 600° C.

Table XIII shows the preliminary heat-treatments for the production of two initial grain-sizes (0·35 and 0·026 mm.) in both homogenized and unhomogenized materials.

Curves are plotted in Fig. 8 of critical strain versus temperature for both homogenized and unhomogenized materials. In either material the critical strain decreases with rise in temperature, and fine-grained material makes for lower critical strains. It will be seen too that the critical strains are lower for material homogenized before hot rolling, though the

Table XIV.—*Grain-Sizes of* 1¼% *Manganese Alloy after Critical Straining and Annealing.*

	Initial Grain-Size, mm.	Final Grain-Sizes after Annealing at Various Temperatures, mm.			
		425° C.	450° C.	500° C.	550° C.
Homogenized {	0·35	0·12	0·15	0·17	0·21
	0·026	0·13	0·17	0·33	1·40
Unhomogenized {	0·35	...	0·038	0·095	0·10
	0·026	0·032	0·034	0·10	0·17

distinction becomes less important at the higher temperatures.

Table XIV gives the value of the recrystallized grain-size after critical straining and annealing. These grain-sizes are finer for the material not homogenized before hot rolling (in accordance with the higher critical strain) and are comparable with those found in the Duralumin-type alloy.

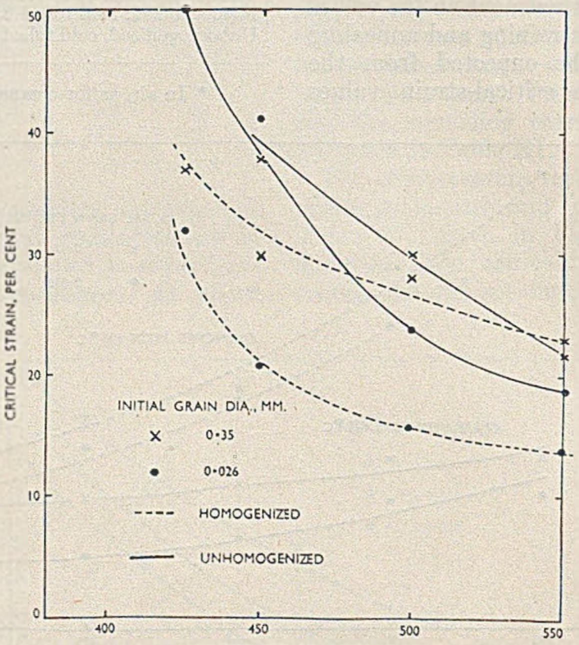

Fig. 8.—Critical-Strain/Recrystallization-Temperature Curves for Homogenized and Unhomogenized 1¼% Manganese Alloy with Various Initial Grain-Sizes. Annealing time 30 min.

V.—DISCUSSION

The experiments reported show the effects of some of the controlling factors, viz. amount of cold deformation, temperature, and original grain-size, on the recrystallization of several alloys; other variables, including time at temperature and rate of heating, have not been investigated. Apart from some additional effects of the initial grain-size, discussed below, the results substantiate the empirical rules set out in the introduction (p. 501). Rule (*a*), that the grain-size in a particular material is primarily determined by deformation before annealing and is substantially independent of the annealing temperature, can be roughly checked by comparison of the recrystallization diagrams for any particular material at different temperatures. The temperature of recrystallization has, however, a slight effect on the final grain-size, the final grain-size being in general finer, the higher the temperature. Fig. 9 gives two examples. Super-purity aluminium (Fig. 9 (*a*)) appears to show the effect most strongly of the materials for which adequate data are available, and in all cases the largest effect is at low strains. These results for super-pure aluminium are qualitatively in agreement with those of Anderson and Mehl.[5]

No departure at all has been found from rules (*b*) and (*c*), but (*d*) now needs some qualification, as it has been found that the recrystallized grain-size may, for a given deformation and annealing temperature, depend more or less strongly on the initial grain-size. This effect is especially noticeable in super-purity aluminium and for small deformations, with the result that for this material at high temperatures the maximum grain-size obtainable by critical strain increases with the initial grain-size, instead of decreasing as predicted. The first part of the rule, however, that the critical strain increases with the initial grain-size (as in Fig. 12, Plate LXXIX), remains true in practically all cases.

The dependence of the final grain-size on the initial grain-size presumably arises from the fact that during recrystallization after low strains nuclei form preferentially at structural discontinuities, especially grain boundaries; in fine-grained material the grain-boundary area is larger and more nuclei will be formed in any given conditions than in coarse-grained. For higher strains, nucleation takes place also within the grains, so that the difference in grain-boundary area has a less-marked effect and the final grain-size becomes progressively less dependent on the initial grain-size as now observed. The strong dependence observed in super-purity aluminium, compared with that in other alloys, is no doubt largely due to the comparatively very low critical strains, for a given grain-size, which make observations possible in a strain range which does not occur in other materials;

but the difference does not appear to be completely accounted for in this way, and there may be other factors operative, such as the possible effect of minor constituents or dissolved elements in promoting nucleation within the grains relative to nucleation at the grain boundary.

There is little in the literature on the effect of alloying on recrystallization. However, experiments of a type similar to those described in the present paper have been reported by Chadwick, Richards, and others [6, 7] both for an alloy of the Duralumin type and for a series of alloys with small quantities of magnesium and manganese. These authors concluded that the critical strain for recrystallization at 500° C. in the Duralumin-type alloy increased with the amount of alloying elements in solution, and that in the aluminium–magnesium–manganese series manganese, but not magnesium, had a large effect in increasing the critical strain. On the other hand, the grain-size on recrystallization after a given large strain (in the range above about 20% extension) was considerably larger for a $1\frac{1}{4}$% manganese alloy than for commercial-purity aluminium or a 1% magnesium alloy, while in ternary alloys magnesium tended to offset the coarsening effect of manganese.

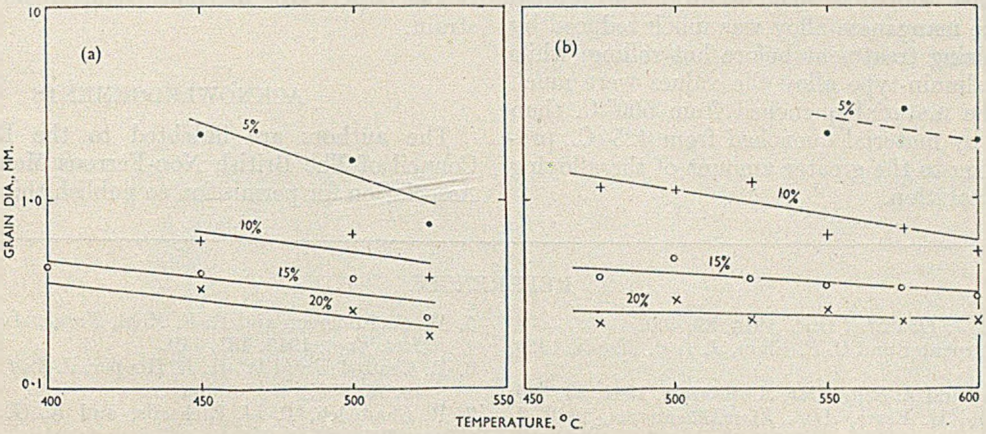

FIG. 9.—Effect of Recrystallization Temperature on Final Grain-Size for Various Amounts of Cold Deformation.

(*a*) Super-purity aluminium with initial grain-size 0·105 mm. (*b*) Commercial-purity aluminium with initial grain-size 0·031 mm.

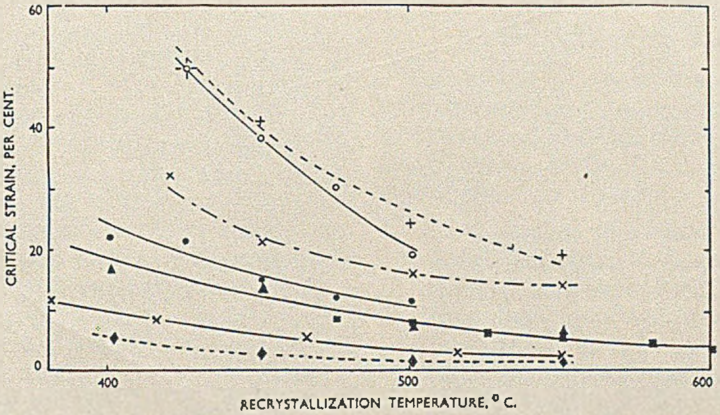

FIG. 10.—Relationship Between Critical Strain and Recrystallization Temperature for All Alloys Tested.

KEY.

- - - - + - - - -	Al–$1\frac{1}{4}$% Mn alloy. Unhomogenized. Initial grain-size 0·026 mm.
— — — × — — —	Al–$1\frac{1}{4}$% Mn alloy. Homogenized. Initial grain-size 0·026 mm.
——— ○ ———	Duralumin-type alloy. Quenched from 500° C. Initial grain-size 0·035 mm.
——— ● ———	Duralumin-type alloy. Quenched from 425° C. Initial grain-size 0·035 mm.
——— ■ ———	Commercial-purity aluminium. Initial grain-size 0·031 mm.
——— ▲ ———	Al–2% Mg alloy. Initial grain-size 0·042 mm.
——— × ———	Al–1% Mg–1% Si alloy. Initial grain-size 0·038 mm.
- - - - ♦ - - - -	Super-purity aluminium. Initial grain-size 0·012 mm.

If the entire results of the present investigation are plotted in the form of a graph of recrystallized grain-size against previous deformation, the points lie within a band, the width of which corresponds to a variation of grain-size of the order of 30 : 1 for any given deformation; but it has not been found possible to generalize in any useful way on the effects of alloying on the grain-size produced on recrystallization.

The most striking effect of composition observed is that on the critical strain. Curves illustrating the variation of critical strain with temperature for materials of comparable grain-size are given in Fig. 10. There are very wide differences, e.g. between 3 and 40% at 450° C. As might be expected, superpure aluminium has the lowest critical strain, and alloying elements and impurities have in general the effect of raising the critical strain. The element most effective in this way appears to be manganese, and the least effective magnesium. The critical strain for the manganese alloy was much reduced by an homogenizing treatment before hot rolling, while for the Duralumin-type alloy the values were much larger for the material quenched from 500° C. than those given by material quenched from 425° C., presumably owing to the greater amount of the alloying elements in solution.

VI.—CONCLUSION

With one exception, the results confirm the empirical rules set out in the Introduction (p. 501). This exception is that, especially in super-purity aluminium recrystallized after given small strains, the final grain-size varies to some extent with the initial grain-size. The effect is not large in most of the materials. The most striking effect of composition is the large effect of some elements on the critical strain.

ACKNOWLEDGEMENTS

The authors are indebted to the Director and Council of The British Non-Ferrous Metals Research Association for permission to publish this paper.

REFERENCES

1. C. Chappell, *J. Iron Steel Inst.*, 1914, **89**, 460.
2. H. C. H. Carpenter and C. F. Elam, *J. Inst. Metals*, 1920, **24**, 83.
3. K. Matthaes and A. Schroeder, *Aluminium*, 1941, **23**, 599.
4. H. Gries and H. Esser, *Arch. Eisenhüttenwesen*, 1929, **2**, 749.
5. W. A. Anderson and R. F. Mehl, *Trans. Amer. Inst. Min. Met. Eng.*, 1945, **161**, 140.
6. R. Chadwick and W. H. L. Hooper, *J. Inst. Metals*, 1948–49, **75**, 609.
7. R. Chadwick, T. Ll. Richards, and K. G. Sumner, *ibid.* p. 627.

THE APPLICATION OF GRAIN REFINEMENT TO CAST COPPER–ALUMINIUM ALLOYS CONTAINING THE BETA PHASE *

1472

By J. P. DENNISON,† B.Sc., Ph.D., JUNIOR MEMBER, and
E. V. TULL,‡ B.Sc., A.I.M., JUNIOR MEMBER

SYNOPSIS

A consideration of previous work pointed to the nucleation method as offering the greatest chance of success in refining the grain-size of cast duplex $(\alpha + \beta)$ copper–aluminium alloys. Accordingly, melts were treated with a range of additions likely to form nucleating compounds. The selection of possible compounds was based on their having a lattice structure and dimensions similar (within certain limits) to those of either the α or the β phase of the copper–aluminium system. Good confirmation of the nucleation theory was obtained, particularly with additions of boron, which is thought to produce nucleation when present as boron carbide. It has been found that in the presence of boron the mechanism of solidification of the 90 : 10 copper–aluminium alloy involves the initial solidification of the β phase. Results obtained on the laboratory scale were entirely confirmed by tests on a commercial scale with 500-lb. billets. With the latter, comparative mechanical tests showed that the tensile strength had increased by 13% and the elongation by 46%, when refinement was at a maximum.

I.—INTRODUCTION

THE literature on the mechanism of grain refinement in castings provides a preponderance of evidence in favour of the nucleation theory. When investigating the possibilities of reducing the as-cast grain-size of copper–aluminium alloys, it was therefore decided to make first an attempt to produce grain-refining nuclei in the molten alloy. As the mode of solidification of the duplex copper–aluminium alloy containing 10% aluminium was in some doubt, the initial work aimed at producing nuclei favourable to the crystallization of either the α or the β phase. It was found that in the presence of certain nuclei, thought to be boron carbide, which would be expected to nucleate the β phase, this alloy solidified with the initial deposition of β crystals. Considerable grain refinement was obtained.

The commercial alloy containing 14% aluminium and 5% iron, which initially deposits β crystals, showed grain refinement of the same order as that of the copper–12% aluminium alloy cast in the laboratory, which consists entirely of the β phase.

The effect was studied of reductions in grain-size on the mechanical properties of the duplex 10% aluminium alloy. Previous work[1] had indicated that little improvement was to be expected for two-phase material, but the present results show considerable increases in both tensile strength and elongation.

II.—PREVIOUS WORK

1. MECHANISM OF GRAIN REFINEMENT

The fact that a reduction in pouring temperature tends to increase the proportion of equi-axial grains in castings of certain alloys has been explained by Genders and Bailey,[2] who outline two methods of formation of such grains :

> (i) *Growth Restriction.*—The growth of the initial columnar crystals sets up such concentration gradients within the still-liquid alloy that there is an excess of the low-melting-point constituent in the immediate vicinity of the columnar crystals, and hence on further cooling, independent crystallization begins in the main bulk of the liquid alloy beyond this low-melting-point region. This process is further aided by the latent heat of solidification of the columnar crystals, which causes a slight increase in the temperature of the liquid alloy in their immediate vicinity. The tendency towards independent crystallization becomes greater with decrease in temperature gradient from the outside of the ingot to the centre, i.e. it increases with decrease in pouring temperature. A similar theory was put forward by Northcott[3,4] to account for the periodic crystallization of steel and certain non-ferrous alloys.

---

* Manuscript received 12 December 1952.

† Lecturer in Metallurgy, University College, Swansea.

‡ Research Student, University College, Swansea.

> (ii) *Nucleation by Solid Particles in the Molten Alloy.*—Solid particles may be present in the liquid zone as a result of the injection by the pouring stream of solid from the ingot top. Similar effects are observed when turbulence is produced in other ways, e.g. by the use of volatile mould dressings.[5]

Subsequent theories have been based on these two main concepts.

An interesting adaptation of the nucleation theory was introduced by Scheil,[6] who found that the grain-size of cast ingots could be refined appreciably by inserting wires of the metal in the mould before casting. The resulting grain-size was a function of the number and diameter of the wires used. It was assumed that the wires acted as artificial nuclei.

In 1936, Iwasé, Asato, and Nasu [7] investigated the grain refinement produced in some binary copper alloys by the addition of iron or cobalt. They concluded that the grain refinement resulted from the break-up of primary crystals during a peritectic reaction caused by these additions, thus providing a large number of nuclei for the formation of secondary crystals.

Mitsche,[8] in the same year, published details of his work on the effect of non-metallic inclusions on the grain-size of aluminium, cast iron, and steel. He considered that two kinds of nuclei existed: "kindred nuclei", which were fragments of metallic lattices and refined the grain-size by inoculation; and "foreign nuclei", which were non-metallic inclusions, and could either refine or coarsen the grain-size depending on their size and concentration in the melt.

Further evidence in support of the concentration-gradient theory was provided in 1937 by the work of Hanemann and Hofmann [9] on the effect of various additions on the grain-size of magnesium alloys.

In 1938, Northcott [4] made a systematic study of the effect of small additions (0·01–2%) of 35 elements on the grain-size of copper. He considered grain-refinement to be due to growth restriction, which could arise from two causes: (*a*) the existence of concentration gradients, as postulated by Genders and Bailey; [2] or (*b*) the adsorption of a very thin layer of the alloying element on the surface of the crystallites, thus preventing further growth. Northcott believed the latter to be the main factor in determining the refinement achieved, and thought that the effect was a periodic one, dependent on the structure of the outer electron shells of the element adsorbed.

This work was extended to cover the effect of larger additions of several of these elements on the grain-size of copper.[10] An attempt was made to correlate the results obtained with constitutional diagrams, and in doing so the effect of an additional, or "second-phase", factor had to be considered. The concentration-gradient effect increased with increase in freezing range, whilst the adsorption effect reached a maximum at a very low percentage of alloying element, and thereafter remained constant or even decreased. The "second-phase" effect could either refine or coarsen grain-size, depending on the nature of the second phase. If the latter was a eutectic, refinement generally occurred, whereas if it was a peritectic the reverse was true, in opposition to the peritectic theory of Iwasé, Asato, and Nasu [7] previously described.

Since 1939, a great deal of work has been done upon the grain refinement of magnesium- [11–18] and aluminium-base [19–24] alloys, resulting in a theory of grain refinement due to Cibula, which is applicable to alloys in general.[22] Cibula states that there are two ways in which grain refinement can be achieved:

> (i) *Concentration Gradients.*—This is a growth-restriction process, and is associated with increased undercooling at the surface of castings, and, more particularly, with the spread of undercooling into the interior of the casting, the latter condition producing an equi-axial structure. This type of grain refinement is relatively slight, until a large proportion of the alloying element is present, and is never very marked.
>
> (ii) *Nucleation.*—The formation of nuclei upon which the alloy crystallizes easily; this effect being associated with the virtual suppression of undercooling. This mechanism in itself will only refine a coarse columnar structure to a much finer but still columnar one, and will not give rise to the equi-axial structures characteristic of marked grain refinement. The combination of these two effects, however, produces grain refinement to a high degree. In cases where the grain-refining element is sufficiently soluble in the parent alloy, it may provide both nuclei and concentration gradients; where the solubility of the grain-refining element in the parent alloy is too small to permit the formation of concentration gradients, the latter must be produced by the addition of another element.

According to Cibula the conditions to be satisfied by a foreign particle to produce nucleation of the alloy are as follows: (1) Attractive forces should exist between the atoms of the solid metal and of the foreign particle; and (2) there should be an absence of strain in the metal lattice at the nucleus/metal interface.

The first condition is also that which results in the formation of stable solutions or intermetallic compounds, i.e. it would lead to solution of the foreign particle. If solution is not to occur, the stability of the compound forming the foreign nuclei must be very high.

The second factor requires a fairly close structural relation between the lattice of the solid metal and that of the foreign particle. In this respect, van der Merwe [25] states that a limiting lattice misfit exists which allows the formation of an oriented nucleus on a substrate. He estimated the limiting difference to be 9%, or somewhat greater if there are strong attractive forces between the deposited atoms and the substrate. Thus Royer[26] has proved that differences in lattice dimensions of up to 16% can be tolerated in the case of halides deposited from solution on to crystals of lead sulphide, potassium chloride, sodium chloride, and mica.

Cibula found that the quantities of the combining elements necessary to produce satisfactory nucleation and refinement are extremely small, of the order of 0·001–0·1%, and that the number of nuclei present was several hundred times the number of grain centres on solidification. Formation of the nucleating compounds within the molten metal was more efficient from the point of view of nucleation than the direct addition of the compounds to the melt, the difference being attributed to the difficulty in obtaining satisfactory wetting in the latter case.

The above theory offers a satisfactory explanation of most of the phenomena associated with grain refinement, and has been used as the basis of the present work. Crossley and Mondolfo[27] have offered an alternative explanation of the grain refinement of aluminium alloys involving a peritectic-reaction theory, but the evidence in support of their theory is inconclusive.

2. GRAIN REFINEMENT OF COPPER-BASE ALLOYS

Apart from the work of Northcott,[4,10] very little has been published on the grain refinement of copper and copper-base alloys. Northcott found that in additions from 0·1 to 2% the most effective grain refiners were lead, thallium, platinum, oxygen, tin, selenium, arsenic, and indium, in that order. He then investigated the grain-size of a series of binary alloys of copper over a wide range of compositions. Copper–aluminium alloys were characterized by very large crystal size, having longer and much wider columnar crystals than those found in the other binary alloys examined. Northcott showed that aluminium is capable of conferring the property of wide columnar growth upon other alloys to which it is added. Curves of crystal length against composition were plotted for these binary alloys. For copper–aluminium alloys of the eutectic composition (8·5% aluminium) the structure is wholly columnar. Further increase in aluminium content results in a slight reduction in columnar crystal length, to a minimum at 10% aluminium and 40% reduction in crystal length, the curve then rising again until at 12% aluminium the structure is again wholly columnar (the all-β region).

Hermann and Sisco[28] in 1931 studied the effect of 1% and 5% additions of iron, nickel, manganese, cobalt, and silicon on the structure and hardness of 8%, 10%, and 12% aluminium bronzes. Iron gave the greatest refinement in grain-size, and manganese also produced some refinement. Nickel and cobalt had no effect, and silicon produced grain coarsening. These results were confirmed by Iwasé, Asato, and Nasu in 1936.[7]

The complex aluminium bronzes containing nickel and iron (e.g. Cu 80, Al 10, Fe 5, Ni 5%) have an equi-axial grain structure throughout the ingot even when relatively high pouring temperatures are employed. Murphy and Callis[29] suggest the possibility that the primary crystals of iron-bearing constituent found in these alloys are the nuclei responsible for grain refinement.

Additions of several other elements to aluminium bronze have been made by various workers, but the effect upon the grain-size has not been considered in most cases. Landolt and Pyne,[30] however, report that lithium additions of the order of 0·005–0·02% produce some grain refinement in high-conductivity copper, gun-metal, and nickel bronze.

Colton and Margolis[31] studied the effect of nickel additions (0–5%) upon the cast macrostructure of an 85 : 5 : 5 : 5 copper–tin–zinc–lead alloy, and concluded that the element responsible for the small grain-size (as compared with that of pure copper) was lead, nickel additions having no effect on grain-size.

3. EFFECT OF GRAIN-SIZE ON THE MECHANICAL PROPERTIES OF CAST ALLOYS

It has long been recognized that the grain-size of cast alloys may have an important influence upon their tensile properties, the precise effect in each case being the resultant of several factors. The most obvious factor is, of course, the resistance offered by grain boundaries to the simple type of deformation undergone by a single crystal, the effect of which is to increase tensile strength as the grain-size decreases.

In cubic alloys, however, other indirect effects of grain-size variation may far outweigh the grain-boundary factor; e.g. Cibula and Ruddle[21] found that in certain aluminium alloys the distribution and shape of the intergranular shrinkage voids, as influenced by grain-size, was the dominant factor in determining the tensile properties. In this case, the type of void associated with small grain-size was the least detrimental, but this is not always the case, as was shown by the work of Ames and Kahn[32] on tin bronzes, in which maximum tensile properties were associated with a coarse-grained structure.

Northcott[1] has studied the influence of crystal size and orientation upon the mechanical properties of several copper-base alloys in the cast condition. He found that single-phase alloy test-pieces composed of columnar crystals disposed longitudinally showed low values for maximum stress but high elongation; transverse columnar crystals exhibited a higher maximum stress but low elongation; and small equi-axial crystal samples showed the highest maximum stress, but low to intermediate elongation. The tensile properties of two-phase alloys were found to be much less affected by crystal size, a fact Northcott attributed to the presence within each crystal of phase boundaries which behaved like ordinary crystal boundaries in their resistance to slip.

III.—SELECTION OF POSSIBLE INOCULANTS

At the beginning of the present work, the mode of solidification of a binary copper-base alloy containing 10% aluminium was in doubt. The constitutional diagram indicates that the β phase is the first to solidify, but Ruddle and Mincher[33] suggest that under non-equilibrium conditions eutectic crystallization may occur, initiated by nuclei of the α phase. Inoculants were therefore selected to cover both possibilities and particulars of these are given in Table I. Lattice misfit up to $\pm16\%$, the highest value at which nucleation has been reported,[26] was tolerated, although the limiting misfit is generally taken as about 9–10%.[25,34]

TABLE I.—*Possible Inoculants for Copper–10% Aluminium Alloy.*

Compound	Structure	Lattice Dimensions, Å.*	Lattice Misfit, % *
		A—*Suitable for α-Phase Nucleation*	
α-Cu–Al (7·5% Al)	F.c.c.	$a_0 = 3\cdot657$ (ref. 35)	...
CaB_6	Cubic	$a_0 = 4\cdot15$	+13·3
CeB_6	„	$a_0 = 4\cdot13$	+12·9
CoB	Orthorhombic	$a_0 = 3\cdot95,^*$ $b_0 = 5\cdot24$, $c_0 = 3\cdot04$	+ 7·9
Co_2B	?	$a_0 = 5\cdot00$, $c_0 = 4\cdot21^*$	+15·0
TiB_2	Hex. c.p.	$a_0 = 3\cdot03$, $c_0 = 3\cdot23^*$	−11·8
ZrB_2	„	$a_0 = 3\cdot15,^*$ $c_0 = 3\cdot53^*$	−14, −3·6
ZrC	Cubic	$a_0 = 3\cdot31$	− 9·6
CeO_2	Tetragonal	$a_0 = 3\cdot87,^*$ $c_0 = 6\cdot48$	+ 5·8
AlB_2	Hex. c.p.	$a_0 = 3\cdot00$, $c_0 = 3\cdot25^*$	−11·3
		B—*Suitable for β-Phase Nucleation*	
β-Cu–Al (10·0% Al)	B.c.c.	$a_0 = 5\cdot887$ (ref. 33)	...
CeO_2	Tetragonal	$a_0 = 3\cdot87$, $c_0 = 6\cdot48^*$	+10·0
CaC_2	„	$a_0 = 5\cdot48,^*$ $c_0 = 6\cdot37^*$	−6·8, +8·1
CaS	Cubic (NaCl-type)	$a_0 = 5\cdot67$	−3·8
Li_2S	Cubic (CaF_2-type)	$a_0 = 5\cdot70$	−3·3
B_4C	Rhombohedral	$a_0 = 5\cdot62,^*$ $c_0 = 12\cdot12$	−4·5

* Where more than one lattice parameter is given, misfit is calculated only for the parameter marked with an asterisk.

IV.—LABORATORY TESTS

1. EXPERIMENTAL PROCEDURE

The melts were prepared from copper–aluminium alloy containing Al 12·27, Fe 0·07, Si 0·04, Zn 0·02%, balance Cu, and high-purity copper (B.S.S. MC3) containing Cu 99·96, Ni 0·01, O 0·019, Bi 0·0003%, and a trace of As. A straight copper–10% aluminium alloy prepared from these materials showed no difference in macrostructure from a similar alloy prepared from the same copper and super-purity aluminium (99·99%). It was therefore assumed that the 0·07% iron in the copper–12% aluminium alloy had no grain-refining effect.

The various elements intended to produce grain refinement were added either in elemental form, or as alloys with copper or aluminium, with the exception of cerium (added as Mischmetall, a 50% alloy with rare earth metals). Additions of the pure metals and the Mischmetall were wrapped in copper foil; in the case of carbon, acetylene was bubbled through the molten metal in the casting-machine reservoir via a thin silica tube. All additions were made to the melt in the furnace, with the exception of the Mischmetall, lithium, and copper sulphide, which were added in the reservoir of the casting machine.

Cerium Mischmetall was used instead of pure cerium for economic reasons. For comparison, a melt was cast using pure cerium. The macrostructure of the two ingots showed no significant difference.

Analyses of the various alloys used are given below:

Boron (as copper-base alloy):
B 4·75, Cu 93·7, Si 0·6, Fe 0·06, Mg 0·20%, traces of Mn and Pb.
Cerium (as Mischmetall):
Typical analysis: Ce 51–53, Nd 15–17, Pr 3–4, La 22–25, Sm 2–3, Y + Tb 3, Fe 5, C approx. 0·054, CaC_2 approx. 0·022, Ca approx. 0·014%, traces of Al and Si.
Cobalt (as copper-base alloy):
Co 12·0, Ni 0·20%, balance Cu.
Titanium (as aluminium-base alloy):
Ti 10·3, Fe 0·47, Si 0·33, Cu 0·08%, balance Al.
Zirconium (as aluminium-base alloy):
Zr 8·2, Ti 0·20, Fe 0·50, Si 0·35, Cu 0·10%, balance Al.
Calcium and Lithium: added as pure metals.
Copper sulphide: added as powder (Analar purity).

All melts were made in a high-frequency electric furnace, employing a Sillimanite crucible, and a proprietary flux was used to clean the metal before casting. The ingots were Durville-cast into steel moulds. The melt temperature was checked by immersing a thermocouple in the reservoir of the casting machine (consisting of a Salamander crucible) immediately before pouring. Exothermic feeding compound was applied to the ingot top to prevent the formation of shrinkage cavities, and a constant pouring temperature (1150° C.) and pouring rate were employed for all casts. This temperature proved sufficiently high to ensure that untreated ingots would have a coarse-grained macrostructure consisting entirely of columnar crystals.

The ingots were cylindrical, 3 in. dia. × 8 in. long. For macro-examination they were sectioned halfway between the bottom of the pipe and the base of the ingot, parallel to the base. The surface so exposed was machined and then etched in a warm saturated solution of ammonium bichromate containing 10% conc. H_2SO_4 and 1% HCl, with continuous swabbing for about 10 min.

2. RESULTS ON GRAIN REFINEMENT

It will be seen from the results given in Table II that marked grain refinement was obtained in all the ingots containing boron. Since boron additions produced refinement when used alone, the part played by calcium, cerium, cobalt, titanium, and zirconium in ingots 2–6 inclusive may not have been important, i.e. the nucleating compound may have been a compound of boron with some other element already present in the copper–aluminium alloy. External addition of carbon was not essential to grain refinement by boron, as shown by ingot 13. This does not, however, rule out the possibility that the nucleating compound was boron carbide, since Cibula[22] has shown that even super-purity aluminium (99·99%) contains enough carbon to combine with added titanium to form the nucleating compound titanium carbide. If the nucleating compound was in fact boron carbide, this would imply that the β phase is the first to solidify, since the boron-carbide lattice is favourable to β-phase nucleation only. On the other hand, the nucleating compound may have been aluminium boride, which is an α-phase nucleator, in which case the α-phase must be the first to solidify.

TABLE II.—*Effect of Various Additions on the Grain-Size of Copper–10% Aluminium Alloy.*

Ingot No.	Desired Compound	Lattice Misfit, %	Addition, % (nominal)	Degree of Grain Refinement	Average Grain-Size of Equi-Axial Crystals, mm.
1	...	Standard ingot		...	Entirely columnar.
		A—Suitable for α-Phase Nucleation			
2	CaB_6	+13·3	0·04 Ca,* 0·01 B	Marked	0·5
3	CeB_6	+12·9	0·04 Ce,* 0·01 B	„	0·5
4	CoB Co_2B	+ 7·9 +15·0	0·01 Co, 0·01 B	„	0·5
5	TiB_2	−11·8	0·01 Ti, 0·01 B	„	0·5
6	ZrB_2	−14, −3·6	0·01 Zr, 0·01 B	„	0·5
7	CeC_2	+ 5·8(α) +10·0(β)	0·04 Ce * + C	Slight	Entirely columnar.
		B—Suitable for β-Phase Nucleation			
9	CaC_2	−6·8, +8·1	0·04 Ca * + C	Moderate	2·0
10	CaS	−3·8	0·04 Ca,* 0·01 S	Nil	Entirely columnar.
11	Li_2S	−3·3	0·04 Li,* 0·01 S	„	„
12	B_4C	−4·5	0·01 B + C	Marked	0·5
13	B_4C	−4·5	0·01 B	„	0·5

* Nominal addition increased to allow for high oxidation loss of these elements during addition.

TABLE III.—*Macrostructure and Grain-Size of Laboratory Ingots.*

Ingot dimensions; 3 in. dia. × 8 in. long.

Ingot No.	Addition, % (nominal)	Average Grain-Size, mm.		Structure
		Columnar (width)	Equi-Axial	
1 *	Standard	2·0	...	Entirely columnar to centre (1·5 in. long).
7	0·04 Ce + C	1·5	...	„ „ „
9	0·04 Ca + C	1·5	2·0	Columnar crystals $\frac{7}{8}$ in. long. Equi-axial central zone.
13 †	0·01 B	1·0	0·5	Columnar crystals $\frac{5}{8}$ in. long. Equi-axial central zone.

* 10 and 11 similar. † 2, 3, 4, 5, 6, and 12 similar.

Calcium additions, in conjunction with acetylene bubbling, also produced some refinement, but this was not nearly so marked as with boron additions, although producing an equi-axed zone. Cerium in conjunction with acetylene gave slight indications of grain refinement by diminishing the width of columnar crystals.

The macrostructure of copper–10% aluminium alloy, without and with boron additions, is illustrated in Figs. 1 and 2 (Plate LXXX), respectively. In the untreated alloy, the structure consists of coarse columnar crystals extending to the centre of the ingot, whereas in the boron-treated alloy these columnar crystals are much smaller, and the whole of the centre of the ingot consists of fine equi-axial crystals.

A more detailed description of the macrostructure and grain-size of the ingots is given in Table III.

3. MODE OF SOLIDIFICATION OF COPPER–10% ALUMINIUM ALLOY.

A means of refining the grain-size of the duplex copper–10% aluminium alloy having been found, the solidifying phase in this alloy was next determined. Three ingots containing 7·5%, 10%, and 12·5% aluminium, respectively, were cast, representing the all-α, duplex (α + β), and all-β structures. A further series of three ingots was then cast of the same aluminium contents, but with 0·01% boron added to each alloy before casting. Comparison of the macrostructures of the six ingots showed that boron additions refined the grain-size of the (α + β) (Figs. 1 and 2) and all-β alloys (Figs. 3 and 4, Plate LXXX), but not that of the all-α alloys. In the presence of boron the solidifying phase in the duplex copper–10% aluminium alloys must therefore be β. This finding does not, however, entirely rule out the theory of Ruddle and Mincher[33] that, under non-equilibrium conditions, the α phase is the first to solidify and initiates eutectic-type solidification, since in the absence of suitable nuclei undercooling may occur to such an extent that this mechanism becomes possible. In the presence of suitable nuclei, such as are provided by boron additions, undercooling is prevented, and solidification conditions approach much more closely to those indicated by the equilibrium diagram, i.e. the β phase is the first to solidify. Further, since the aluminium boride structure is suitable only for nucleating the α-phase, it can be ruled out as an inoculant, thus lending further support to the view that boron carbide is the nucleating compound. Similarly, the nucleating compounds in ingots 2–6 cannot be the metal borides listed in column 2 of Table II, since these compounds are also suitable only for nucleating the α phase.

The macrostructure of the boron-treated copper–12·5% aluminium ingot showed a $\frac{1}{4}$-in.-deep zone of equi-axial crystals round the periphery of the ingot. These crystals were largest at the immediate edge of the ingot, and decreased in size towards the inner edge of the zone, the finest crystals being comparable in size with those in the centre of the ingot. It is difficult to account for the presence of the columnar zone between these two zones of equi-axial crystals. It may represent a form of periodic crystallization, as outlined by Northcott,[3] which would imply that the nucleating compound is partially soluble in the molten alloy. This phenomenon occurs only in the all-β alloy and not in the (α + β) alloy. An all-β alloy cast at a lower pouring temperature (about 50° C. above the solidus) showed a narrow band of squat columnar crystals at the periphery, with very fine equi-axial crystals in the centre of the ingot, indicating that grain refinement increases with decrease in pouring temperature.

It is possible that calcium carbide formation is responsible for the grain refinement observed in ingot No. 9, since this compound is suitable for nucleating the β phase.

4. Remelting Characteristics

To determine the persistence of grain refinement on remelting and casting, a laboratory ingot containing 0·01% boron was remelted and cast as before. Macro-examination showed that no loss of grain refinement had occurred, indicating that boron loss on remelting was negligible. The maximum temperature reached by the melt in the furnace was about 1200° C. A further remelt again showed no loss in grain refinement.

V.—COMMERCIAL APPLICATION OF GRAIN REFINEMENT

1. Tests on Ingots

Laboratory experiments having shown that additions of boron, calcium, and cerium to copper-aluminium alloy produced varying degrees of grain refinement, additions of these elements were made to normal commercial ingots to determine whether this method of refinement was a practical possibility.

These tests were carried out at the works of Messrs. N. C. Ashton, Ltd., Huddersfield, on 500-lb. cylindrical ingots, 7 in. dia. × 45 in. long, cast by a semi-Durville method from rotating oil-fired furnaces. Melts were made up from high-grade copper (99·9%) and aluminium (Al 99·6, Si 0·2, Fe 0·15, Cu 0·02%). A typical analysis of one of these ingots gave Al 9·63, Fe 0·05, Zn 0·01, Si 0·02%, a trace of Ni, Cu 90·3%.

Five such ingots were cast from each melt. The grain-refining additions were made to the metal in the pouring stream as the ingot was being poured, in the case of calcium and cerium, and to the melt in the furnace in the case of boron. The pouring temperature was checked by an optical pyrometer focused on the metal in the pouring stream, and the melt temperature was determined by an immersion pyrometer. The casting temperature varied between 1090° and 1120° C. during the tests; this variation produced no noticeable alteration in the grain-size of standard ingots. An exothermic feeding compound was employed to prevent piping.

Table IV gives details of the tests carried out using varying additions of boron, calcium, and cerium. Carbon was added to the calcium and cerium melts by bubbling acetylene through the feeder stream. The additions were identical with those employed for the laboratory tests.

Table IV.—*Effect of Grain-Refining Additions on Commercial Ingots of Copper*–10% *Aluminium Alloy.*

Desired Compound	Addition, % (nominal)	Degree of Grain Refinement	Average Grain-Size of Equi-Axial Crystals, mm.
B_4C	0·001 0·0025 0·01	Nil Moderate Marked	Entirely columnar 2·2 1·0
CaC_2	0·001 0·0025 0·01 0·04 } + C	Nil ,, ,, Moderate	Entirely columnar ,, ,, ,, ,, 2·0
CeC_2	0·001 0·0025 0·01 } + C	Nil ,, ,,	Entirely columnar ,, ,, ,, ,,

A more detailed description of the macrostructure and grain-size of those of the above ingots showing grain refinement is given in Table V.

These results confirm those obtained with the laboratory ingots. The grain refinement produced by addition of 0·04% calcium and 0·0025% and 0·01% boron is illustrated in Figs. 6, 7, and 8 (Plate LXXX), which should be compared with the standard ingot structure shown in Fig. 5 (Plate LXXX). The grain refinement produced by 0·01% boron in the commercial ingot was even more marked than in the laboratory ingot, an entirely columnar structure being changed to one in which the columnar crystals formed a narrow band about ½ in. deep around a central region of very fine equi-axial grains.

The sections examined were transverse slices taken from near the top of the ingot. Sections taken from the middle and base of certain ingots confirmed that the structure was uniform throughout their length.

Closer examination of the section from the ingot to which 0·04% calcium had been added revealed evidence of porosity, which was confirmed by micro-examination. The porosity was on a micro-scale, and micro-cracking was also observed throughout the section.

2. Effect of Variation in Boron Content on Grain-Size and Mechanical Properties

A series of four commercial ingots (see Section V, 1) was cast, having boron contents of 0·00, 0·01, 0·02, and 0·03%, respectively. Transverse slices were taken from near the top of the ingots for macro-examination, the results of which are given in Table V; immediately below these slices, 9-in. lengths of the ingot were cut off to provide material for transverse and longitudinal tensile test-pieces. The casting temperature varied between 1090° and 1110° C.

The results obtained are given in Table VI. Macro-examination of ingots containing 0·02 and 0·03% boron revealed a completely equi-axial structure, with no outer band of columnar crystals (see Table V). Data on the macrostructure of the 0·0025% boron and 0·04% calcium ingots cast during the previous commercial tests (Section V, 1) are included in Table V.

TABLE V.—*Macrostructure and Grain-Size of Commercial Ingots.*

Ingot dimensions: 7 in. dia. × 45 in. long.

Addition, nominal)	Average Grain-Size, mm.		Structure
	Columnar (width)	Equi-axial	
Standard	2·5	...	Entirely columnar to centre (3·5 in. long).
0·04% Ca	1·2	2·0	Columnar crystals 1·75 in. long. Equi-axial central zone.
0·0025% B	1·5	2·2	Columnar crystals 1·5 in. long. Equi-axial central zone.
0·01% B	4·0	1·0	Columnar crystals 0·5 in. long. Equi-axial central zone.
0·02% B	...	0·7	Entirely equi-axial.
0·03% B	...	0·5	,, ,,

TABLE VI.—*Effect of Varying Boron Additions on the Mechanical Properties of Copper–10% Aluminium Alloy.*

Nominal Boron Content, %	Position of Test-Piece *	Tensile Strength, tons/in.^{2}	Elongation, %, on 1-in. Gauge-Length
0	Transverse (top)	22·0 23·0	12·5 17·0
0		22·9 24·0	14·5 16·0
0·01		25·6	25·0
0·02		26·2	26·0
0·03		25·9 26·9	22·0 22·0
0	Longitudinal	22·4 23·2	18·5 24·0
0		24·3 22·7	22·0 15·0
0·02		26·5 26·4	25·0 24·5
0·03		27·0 26·2	31·5 29·5
0	Transverse (centre) †	24·1 23·2	19·0 20·0
0		24·5 24·3	22·0 20·0
0·02		26·5 26·4	28·0 28·0
0·03		26·4 26·7	26·0 30·5

* The test-pieces were machined according to B.S. No. 18 (1938).

† From the end of the 9-in. length nearest to the centre of the ingot (i.e. the lower end).

Table V indicates that an addition of 0·02% boron to commercial ingots of copper–10% aluminium completely eliminates columnar crystal growth, and that further increase in boron reduces the size of the equi-axial crystal slightly.

Table VI indicates that boron additions increase both the tensile strength and ductility of copper–10% aluminium by virtue of their grain-refining effect.

The average of the results given in Table VI for each individual boron addition, together with the percentage increase in tensile strength and elongation relative to the untreated alloy, are set out in Table VII. Analyses for aluminium content were made on samples from the ingots, and the results are included in the table.

TABLE VII.—*Percentage Increase in Tensile Strength and Elongation Produced by Boron Additions in Copper–10% Aluminium Alloy.*

Nominal Boron Content, %	Aluminium Content, %	Tensile Strength, tons/in.^{2}	Increase in Tensile Strength over Untreated Alloy, %	Elongation, %, on 1-in. Gauge-Length	Increase in Percentage Elongation over Untreated Alloy, %
0	9·50	23·4	...	18·4	...
0·01	9·39	25·6	9·4	25·0	35·9
0·02	9·49	26·4	12·8	26·3	42·9
0·03	9·42	26·5	13·2	26·9	46·2

Micro-examination of specimens from the untreated and boron-treated ingots revealed no differences in constitution. No foreign nuclei were visible, even under a magnification of 1500×, in the boron-treated ingots.

3. OTHER COMMERCIAL APPLICATIONS

Experiments on commercial castings have shown that boron additions may be used to advantage in obtaining grain-refinement of the hard 14% aluminium, 5% iron alloys used in the manufacture of die-blocks, which have an all-β phase structure. A cast hollow cylinder, 14 in. outside dia. × 8 in. inside dia. × 6 in. high, which was normally entirely columnar on solidification, exhibited a completely equi-axial structure when 0·01% boron was added to the melt, other conditions being maintained constant. The average diameter of the equi-axial crystals was 2 mm.

VI.—SUMMARY AND CONCLUSIONS

It has been found that additions of boron of between 0·0025 and 0·03% to molten copper–aluminium alloy containing 10% aluminium produce grain refinement of the alloy on solidification, the degree of refinement increasing with the quantity of boron added up to about 0·02%, when a completely equi-axial structure is obtained in contrast to the entirely columnar structure of the untreated alloy. This grain refinement is associated with increased tensile strength and percentage elongation.

It has been shown that in the presence of these boron additions, the copper–10% aluminium alloy solidifies initially as the β phase, which is nucleated by some compound formed as a result of the boron additions. This compound is thought, from lattice-structure considerations, to be boron carbide, B_4C.

Additions of calcium in conjunction with carbon (as acetylene gas bubbled through the molten alloy) also resulted in grain refinement, but this was associated with micro-porosity and cracking.

The grain refinement produced by boron additions was found to be practically unaffected by repeated remelting and casting, indicating that loss of boron on remelting was negligible.

The use of high pouring temperatures tended to decrease the degree of grain refinement in cases where the boron addition was not sufficient to produce a completely equi-axial structure.

Boron additions also refined the grain-size of the copper–14% aluminium alloys used in the manufacture of die-blocks, which consist entirely of the β phase on solidification.

REFERENCES

1. L. Northcott, *J. Inst. Metals*, 1942, **68**, 189.
2. R. Genders and G. L. Bailey, "The Casting of Brass Ingots" (B.N.F.M.R.A. Research Monograph No. 3), p. 59. London: **1934**.
3. L. Northcott, *J. Iron Steel Inst.*, 1934, **129**, 171.
4. L. Northcott, *J. Inst. Metals*, 1938, **62**, 101.
5. G. L. Bailey and W. A. Baker, *ibid.*, 1948–49, **75**, 285.
6. E. Scheil, *Z. Metallkunde*, 1936, **28**, 228.
7. K. Iwasé, J. Asato, and N. Nasu, *Sci. Rep. Tôhoku Imp. Univ.*, **1936**, [i], (Honda Anniv. Vol.), 652.
8. R. Mitsche, *Carnegie Schol. Mem.*, *Iron Steel Inst.*, 1934, **23**, 65; 1936, **25**, 41.
9. H. Hanemann and W. Hofmann, *Z. Metallkunde*, 1937, **29**, 149.
10. L. Northcott, *J. Inst. Metals*, 1939, **65**, 173.
11. K. Achenbach, H. A. Nipper, and E. Piwowarsky, *Giesserei*, 1939, **26**, 597.
12. F. A. Fox and E. Lardner, *J. Inst. Metals*, 1945, **71**, 1.
13. W. A. Baker and M. D. Smith, *B.N.F.M.R.A. Research Rep.*, 1945, (A.694).
14. J. A. Davis, L. W. Eastwood, and J. De Haven, *Amer. Foundryman*, 1945, **8**, (1), 34.
15. C. H. Mahoney, A. L. Tarr, and P. E. Le Grand, *Trans. Amer. Inst. Min. Met. Eng.*, 1945, **161**, 328.
16. N. Tiner, *ibid.*, 1946, **166**, 242.
17. C. E. Nelson, *Trans. Amer. Found. Soc.*, 1948, **56**, 1.
18. W. A. Baker, M. D. Eborall, and A. Cibula, *J. Inst. Metals*, 1952–53, **81**, (1), 43.
19. A. Dumas, *Rev. Mét.*, 1944, **41**, 273.
20. M. D. Eborall, *J. Inst. Metals*, 1949–50, **76**, 295.
21. A. Cibula and R. W. Ruddle, *ibid.*, 1949–50, **76**, 361.
22. A. Cibula, *ibid.*, 1949–50, **76**, 321.
23. V. Kondic and D. Shutt, *ibid.*, 1950–51, **78**, 105.
24. A. Cibula, *ibid.*, 1951–52, **80**, 1.
25. J. H. van der Merwe, *Discussions Faraday Soc.*, 1949, (5), 201.
26. L. Royer, *Compt. rend.*, 1925, **180**, 2050.
27. F. A. Crossley and L. F. Mondolfo, *Trans. Amer. Inst. Min. Met. Eng.*, 1952, **195**, 1190.
28. S. F. Hermann and F. T. Sisco, *Trans. Amer. Inst. Min. Met. Eng.*, *Inst. Metals Div.*, **1931**, 262.
29. A. J. Murphy and G. T. Callis, *J. Inst. Metals*, 1948–49, **75**, 325.
30. P. E. Landolt and F. R. Pyne, *Foundry*, 1949, **77**, 90, 262.
31. R. A. Colton and M. Margolis, *Trans. Amer. Found. Soc.*, 1951, **59**, 360.
32. B. N. Ames and N. A. Kahn, *ibid.*, 1950, **58**, 229.
33. R. W. Ruddle and A. L. Mincher, *J. Inst. Metals*, 1950–51, **78**, 229.
34. J. A. Reynolds and C. R. Tottle, *ibid.*, 1951–52, **80**, 93.
35. A. J. Bradley and P. Jones, *ibid.*, 1933, **51**, 131.

THE STRUCTURE OF TITANIUM–TIN ALLOYS IN THE RANGE 0–25 AT.-% TIN *

1473

By H. W. WORNER,† M.Sc., MEMBER

SYNOPSIS

Titanium-tin alloys in the range 0–25 at.-% tin have been investigated by metallographic and Debye–Scherrer X-ray-diffraction methods, and a partial phase diagram has been established. Detailed results for two groups of alloys are given; one group was based on a commercial grade of titanium, the other on titanium refined by the iodide process. Tin depresses the freezing point of titanium, and there appears to be a eutectic point in the vicinity of 17 at.-% tin at 1550° C. approximately, the solid constituents involved in the eutectic transformation being a solid solution of tin in β-titanium and a phase, designated γ, based on Ti_3Sn. The solid solubility of tin in α-titanium is just over 10 at.-%, and it varies only slightly in the range 700°–880° C. The solubility of tin in β-titanium increases from 7·5 at.-% at 885° C. to approximately 10 at.-% at 1100° C. Addition of tin to titanium depresses the $\alpha \rightleftharpoons \beta$ transformation region to a minimum of 845° C. at 5 at.-% tin; above 5 at.-% the $(\alpha + \beta)$ range rises to meet a peritectoid horizontal at 885° C. The peritectoid composition is 10·5 at.-% tin, and the peritectoid reaction is: α (10·5 at.-% Sn) $\rightleftharpoons \beta$ (7·5 at.-% Sn) + γ (22 at.-% Sn). The γ phase has an ordered structure (DO_{19}-type) based on the hexagonal close-packed structure. Tin hardens α-titanium considerably, but the hardness of the alloys cannot be appreciably varied by heat-treatment.

I.—INTRODUCTION

THE investigation to be described formed part of a research programme concerned with titanium-base alloy systems in which the alloying elements have atomic sizes similar to that of titanium itself. Very little information about titanium–tin alloys has been published. Craighead, Simmons, and Eastwood [1] have shown that 0·7 at.-% tin can be held in solid solution in both α- and β-titanium. Pietrokowsky and Duwez [2] have determined the crystal structure of Ti_5Sn_3, and Pietrokowsky [3] has reported the structure of Ti_3Sn.

The present work covered the range 0–25 at.-% tin. Alloys made with a commercial grade of titanium were first studied in an exploratory investigation, then alloys based on refined titanium were examined. The exploratory investigation was designed partly to yield results of practical value, but chiefly to provide some general information about the system so that the number of purer alloys made in the subsequent work could be kept to a minimum in the interests of economy. Both stages of the research involved metallographic and X-ray-diffraction studies of heat-treated specimens. Particular attention was paid to the effect of tin on the $\alpha \rightleftharpoons \beta$ transformation in titanium and to the limits of solubility of tin in the two forms of titanium. The freezing ranges of the alloys were estimated only very approximately.

II.—MATERIALS USED

Titanium prepared by the Kroll process was used in the exploratory work. This metal, which was made by the United States Bureau of Mines, will be referred to as commercial titanium. Metal refined by the iodide process in the Philips Laboratories, Holland, was used in more critical experiments aimed at establishing phase boundaries. Impurities found in these two grades of titanium are listed in Table I.

TABLE I.—*Concentrations of Impurities in Commercial and Refined Titanium after Melting in an Argon-Arc Furnace.*

Impurity	Commercial Ti, at.-%	Refined Ti, at.-%
Oxygen	0·6	0·15
Nitrogen	0·2	0·03
Carbon	0·1	...
Iron	0·15	0·02
Magnesium	0·1–0·2	Faint trace *
Silicon	Trace *	Strong trace *
Antimony	Not detected *	Strong trace *
Tin	Trace *	Strong trace *
Copper	Trace *	Trace *
Na, K, Ca, Sr, Ba, Be, Al, Ag, Zn, Cd, Pb, Bi, As, Co, Ni, Cr, Mo, W, V, Nb, Ta, Zr	Not detected *	Not detected *

* Result of spectrographic test.

The oxygen concentrations reported in the table were determined by the chlorination method, as described by Corbett.[4]

The $\alpha \rightleftharpoons \beta$ transformation range for each grade of titanium was determined by observing the microstructures of specimens quenched from various temperatures. For the commercial metal, the range was 870°–960° C. and for the refined grade, 885°–895° C.

---

* Manuscript received 12 January 1953.

† Physical Metallurgy Section, Commonwealth Scientific and Industrial Research Organization, Baillieu Laboratory, University of Melbourne, Australia.

The tin, which was supplied by the Bureau of Analysed Samples, Ltd., England, contained the following impurities: iron, 0·015; antimony, 0·0035; lead, 0·0025; copper, 0·001; and bismuth, 0·0003 at.-%.

III.—EXPERIMENTAL

The alloys were made by melting together weighed amounts of titanium and tin in an argon-arc furnace of the type developed by Kroll.[5] Both metals were initially in lump form. The commercial titanium had been previously melted in the arc furnace; pieces of refined titanium were taken direct from the "as-deposited" bars.

The metals mixed readily during melting, and losses due to spitting and fuming were small. Most of the alloys were analysed, and a comparison of the analytical results with the nominal compositions showed that losses during melting comprised a little tin and practically no titanium. For practical purposes, the composition of an alloy could be calculated from the mass of titanium used and the mass of the final ingot, assuming the difference to be the mass of tin in the ingot. This calculated value will be termed the synthetic composition.

In the text of this paper all alloy compositions will be reported in at.-% tin, and the analytical results rather than synthetic compositions will be used for alloys which were analysed.

The "ingots" were limited in weight to about 2 g. Such small specimens cooled rapidly after the arc was switched off, and the sudden chilling minimized macro-segregation during solidification. After the first melting operation, the ingots were allowed to solidify and were then inverted and remelted. This was repeated two or three times to ensure thorough mixing of the component metals in the liquid state. A cross-section through each ingot was examined to ascertain the as-cast structure and to check its uniformity.

Alloys containing not more than 13·5 at.-% tin could be mechanically worked at about 700°–800° C. They were hammered in this temperature range in order to facilitate the attainment of equilibrium in subsequent heat-treatments. The superficial oxide layer formed during hot working was removed by first grinding the surface and then pickling in a mixture of concentrated nitric acid (80% by volume) and concentrated hydrofluoric acid (20%).

Specimens for heat-treatment were sealed in small, clear silica bulbs in which the pressure had been reduced to approximately 5×10^{-3} mm. mercury. Each bulb had a volume of only 0·1–0·2 c.c., so that residual gases after evacuation would cause little or no contamination of the specimen during subsequent heating. To minimize diffusion of atmospheric gases through the silica envelopes during heat-treatments, the bulbs were placed inside a continuously evacuated silica tube in which the pressure was kept below 10^{-2} mm. mercury. The temperature of the furnace could be maintained within ±2° C. of the required value. For treatments above 950° C. the minimum period of heating necessary to produce a practically stable structure was found to be of the order of 2–3 hr. At temperatures in the range 700°–900° C. the duration of heating had to be increased to at least 5 hr. Most of the heat-treatments consisted in heating the specimens up to the required temperature, maintaining them at that temperature for the necessary time, and then quenching into water. Some of the treatments involved first heating the specimens to 100°–200° C. above the quenching temperature, then cooling to the latter, holding at that temperature, and finally quenching. Quenching was effected by rapidly withdrawing the tube enclosing the specimens from the furnace and tipping the specimen bulbs into a shallow dish of water. After entering the water the bulbs were broken by a light blow from a hammer.

During the heating and subsequent water quenching, slight superficial contamination of the alloys occurred. Care was taken in removing the contaminated layer, especially from specimens intended for Debye–Scherrer X-ray-diffraction experiments. For practically all the X-ray-diffraction work, small, solid specimens were used. These were initially prepared in the form of small prisms, approximately 1·5 mm. square by 8 mm. long. After heat-treatment, the prisms were pickled in the nitric acid–hydrofluoric acid mixture described above until the cross-sectional width was reduced to 0·5–0·8 mm. This ensured removal of the contaminated surface as well as producing specimens with dimensions convenient for Debye–Scherrer experiments. Microscopical examination of two-phase alloys prepared as outlined above revealed no significant evidence of preferential dissolution of one phase.

Cobalt $K\alpha$ radiation was employed in all the X-ray experiments, photographic records being made with an 11·46-cm.-dia. powder camera which had been calibrated by means of 99·986% silver and spectroscopically pure copper. All calculations of lattice parameters were carried out by Cohen's method of least squares.

Specimens for metallographic examination were pickled to remove the contaminated surface layers, roughly polished by means of waterproof carborundum papers, and finally polished by hand on fine linen laps furnished with diamond dust. An aqueous solution containing 2 wt.-% nitric acid and 1 wt.-% hydrofluoric acid was used to etch most of the alloys. A similar etchant, but containing a higher concentration of hydrofluoric acid (up to 3 wt.-%) was used in some cases to reveal more markedly the fine, acicular structure which results from a rapid $\beta \rightarrow \alpha$ transformation occurring during a quench.

The effect of tin on the freezing point of titanium was ascertained by following the cooling of the alloys, after melting in the arc furnace, with the aid of a disappearing-filament optical pyrometer. On account of the rapidity of cooling in the arc furnace, considerable undercooling is likely to occur. Moreover, the effect of tin on the emissivity of titanium is not known. The freezing ranges of the alloys could thus be estimated only very approximately.

IV.—ALLOYS MADE WITH COMMERCIAL TITANIUM

1. Alloys Used

The alloys made in the course of the exploratory investigation are listed in Table II. Losses during the melting of the 15·3 and 17·0 at.-% tin alloys were only very slight, and therefore these alloys were not analysed.

Table II.—*Alloys Made with Commercial Titanium.*

Synthetic Composition, at.-% tin	Analytical Result	
	Tin, at.-%	Tin, wt.-%
3·3	3·4	8·0
5·3	5·4	12·0
7·5	7·7	16·9
10·0	9·9	21·6
11·1	11·2	23·8
11·5	11·4	24·2
15·3	...	...
17·0	...	...
18·6	18·7	36·3
21·9	22·0	41·1
23·2	23·5	43·0

2. Freezing Ranges and As-Cast Structures

Addition of tin lowered the freezing point of titanium, the greatest depression, of the order of 150°–200° C., being noted at 17·0 at.-% tin. There seemed to be comparatively little difference between the freezing ranges of the 18·7, 22·0, and 23·5 at.-% tin alloys; all these alloys appeared to start solidifying only 50°–100° C. below the freezing point of titanium.

In the as-cast condition, alloys containing from 3·4–11·4 at.-% tin exhibited a columnar macrostructure. On a microscopic scale there was a fine, acicular structure, similar to that shown in Fig. 7 (Plate LXXXI), resulting from the β → α transformation during rapid cooling. Hence it would appear that alloys containing up to 11·4 at.-% tin crystallized as columnar grains of β solid solution which subsequently transformed rapidly to α solid solution during cooling to normal temperatures. The alloy with 15·3 at.-% tin consisted partly of a constituent having the fine acicular structure represented in Fig. 7, the remainder being a fine mixture of phases arranged in lamellar form. The 17·0 at.-% tin alloy consisted wholly of this fine, lamellar mixture. As-cast alloys containing 18·7, 22·0, and 23·5 at.-% tin consisted largely of a slightly cored, dendritic constituent surrounded by a matrix with a fine, duplex structure. The dendritic constituent, which had obviously crystallized before the matrix, was found to be an intermediate phase, which will be termed the γ phase.

The evidence presented above suggests that there is probably a eutectic point close to 17 at.-% tin, the solid constituents involved in the eutectic transformation being the γ phase and β solid solution with a tin content between 11·4 and 15·3 at.-% tin.

3. Microstructures of Heat-Treated Alloys

The microstructures of alloys quenched from temperatures in the range 650°–1100° C. are represented graphically in Fig. 1. These results indicate that the solid solubility of tin in the α form of the commercial titanium lies between 7·7 and 9·9 at.-% in the range 650°–860° C. From 1020° to 1100° C. the solubility of tin in the β modification of the metal also appears to lie in the region 7·7–9·9 at.-%. Fine acicular structures like that shown in Fig. 7 (Plate LXXXI) and represented by the symbol • in Fig. 1 are taken as evidence of a rapid β → α transformation having occurred during water-quenching. Hence the area above the boundary *BE* in Fig. 1 is marked β.

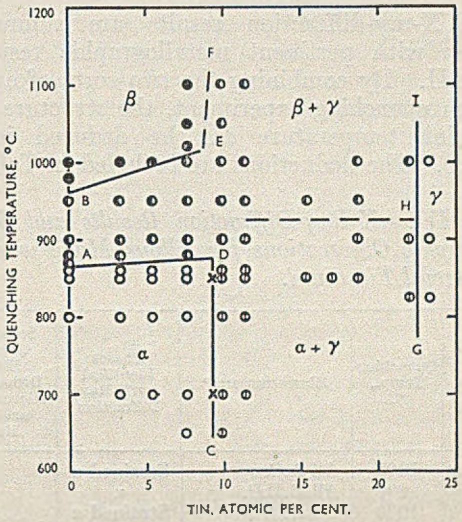

Fig. 1.—Results of Quenching Experiments on Alloys Made with Commercial Titanium.

Key.

● Constituent with fine, acicular structure, as shown in Fig. 7 (Plate LXXXI).
○ Single phase (bright etching).
◐ Mixture of bright-etching phase and constituent with fine, acicular structure.
⦶ Mixture of two bright-etching constituents.
× Determined from X-ray diffraction results.

Only the low-tin boundary (*GHI*) of the γ phase field was determined. It was found that the etching characteristics of the γ phase were similar to those of the 7·7 at.-% tin α solid solution.

The (α + γ) structures were very fine, and all exhibited a Widmanstätten pattern like that shown in Fig. 8 (Plate LXXXI). The microstructures of alloys quenched from the (β + γ) field (*FEDHI* in Fig. 1) were similar to the (α + γ) structures, except that some regions possessed the fine, acicular structure which results from the rapid β → α change. This fine, acicular structure was not well developed in the fine-grained γ + acicular α mixtures, and it could be clearly revealed only by relatively deep etching.

The structures of alloys quenched from the area *ABED* in Fig. 1, i.e. between the α and β fields, were very much coarser than those of alloys quenched from the ($\beta + \gamma$) and ($\alpha + \gamma$) fields (cf. Figs. 8 and 9, Plate LXXXI). Because of the similarity in etching characteristics of the α solid solutions and the γ phase, it was impossible to identify, with certainty, the bright-etching constituents in the alloys quenched from the field *ABED*. Attempts to distinguish between the saturated α solid solutions and the γ phase by microhardness tests were unsuccessful because the microhardnesses of these phases proved to be similar.

4. DEBYE–SCHERRER X-RAY-DIFFRACTION OBSERVATIONS

The X-ray-diffraction results are summarized, together with pertinent metallographic results, in Table III. By combining the two sorts of evidence for each quenching experiment, the structure at the quenching temperature can be deduced in each instance. The deductions are included in Table III.

TABLE III.—*X-Ray-Diffraction Results and Metallographic Observations for Alloys Made with Commercial Titanium.*

Tin Content, at.-%	Quenching Temp., °C.	Microstructure *	Phases Identified by X-Ray Diffraction	Structure at Quenching Temp., Deduced from Microstructure and X-Ray Results
3·4	1000	All A.C.	Strained α	β
	850	All B.E.C.	α	α
5·4	1000	All A.C.	Strained α	β
	950	A.C. + B.E.C.	Strained α	$\alpha + \beta$
	850	All B.E.C.	α	α
7·7	1020	All A.C.	Strained $\boldsymbol{\alpha}$	β
	950	A.C. + B.E.C.	Strained $\boldsymbol{\alpha}$	$\alpha + \beta$
	850	All B.E.C.	α	α
9·9	1050	**A.C.** + B.E.C.	Strained α (+ γ ?)	$\boldsymbol{\beta} + \gamma$
	850	2 B.E.C.'s	α (+ γ ?)	$\boldsymbol{\alpha} + \gamma$
	700	2 B.E.C.'s	α (+ γ ?)	$\boldsymbol{\alpha} + \gamma$
11·2	1000	**A.C.** + B.E.C.	γ	$\boldsymbol{\beta} + \gamma$
	850	2 B.E.C.'s	$\boldsymbol{\alpha} + \gamma$	$\boldsymbol{\alpha} + \gamma$
11·4	1100	**A.C.** + B.E.C.	γ	$\boldsymbol{\beta} + \gamma$
	950	**A.C.** + B.E.C.	γ	$\boldsymbol{\beta} + \gamma$
	850	2 B.E.C.'s	$\boldsymbol{\alpha} + \gamma$	$\boldsymbol{\alpha} + \gamma$
	700	2 B.E.C.'s	$\boldsymbol{\alpha} + \gamma$	$\boldsymbol{\alpha} + \gamma$
18·7	1000	**B.E.C.** + A.C.	γ	$\beta + \boldsymbol{\gamma}$
	850	2 B.E.C.'s	$\alpha + \boldsymbol{\gamma}$	$\alpha + \boldsymbol{\gamma}$
22·0	1000	**B.E.C.** + A.C.	γ	$\boldsymbol{\gamma} + \beta$
	825	2 B.E.C.'s	γ	$\boldsymbol{\gamma} + \alpha$
23·5	1000	All B.E.C.	γ	γ
	825	All B.E.C.	γ	γ

* A.C. = Constituent with fine, acicular structure.
B.E.C. = Bright-etching constituent.
Heavy type denotes the preponderant phase.

It will be noted that the diffraction experiments confirmed the existence of an α solid solution field extending to a limit between 7·7 and 9·9 at.-% tin. Fig. 2 shows the lattice-parameter/tin-concentration relationship for α phase in alloys containing up to 11·4 at.-% tin. These data indicate that the limit of solubility of tin in the α form of the commercial titanium is 9·3 at.-% at both 850° and 700° C.

Alloys consisting entirely of the constituent with the fine, acicular structure (cf. Fig. 7, Plate LXXXI) were shown to possess a strained hexagonal close-packed lattice structure like that found in the commercial titanium after quenching from the β range. Diffraction lines at Bragg angles in excess of 60° were broad and the α_1, α_2 doublets were not resolved in the highest-angle reflections. The broadening of the lines was greater, the higher the tin content. The high-angle reflections from the 7·7 at.-% tin alloy quenched from 1020° C. were so broad that they were not easy to detect.

The patterns from the 23·5 at.-% tin alloy were the same for both quenching temperatures (1000° and 825° C.) and were found to comprise a set of lines practically identical with the spectrum of the high-tin α solid solutions together with a set of weaker lines. All the reflections could be indexed on the basis of a hexagonal lattice with $c/a = 0{\cdot}80$ approximately, and it was apparent that the phase designated γ in Fig. 1 possessed an ordered structure based on the hexagonal close-packed structure. In Table IV are listed the indices assigned to the reflections, together with the observed values of $(1/d)^2$ and line intensities. The calculated values of $(1/d)^2$ included in Table IV were derived from the expression $(1/d)^2 = 0{\cdot}03810(h^2 + hk + k^2) + 0{\cdot}04406\, l^2$. It will be noted that the calculated and observed values of $(1/d)^2$ agree reasonably well. The parameters of the structure cell calculated by the method of least squares from the (40·3), (30·4), (42·1), and (22·4) reflections were: $c = 4{\cdot}768 \pm 0{\cdot}004$ Å., $a = 5{\cdot}922 \pm 0{\cdot}005$ Å., $c/a = 0{\cdot}805$. It will be noted that $(hh\,.\,l)$ reflections were absent when $l \neq 2n$; this indicates space group D^4_{6h}, $C6/mmc$ or a sub-group thereof.

The diffraction data in Table IV were compared with Pietrokowsky's[3] results for the "compound"

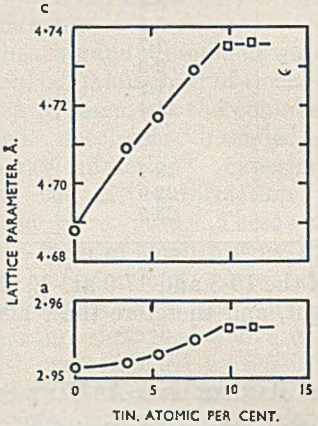

FIG. 2.—Lattice Parameters of α Phase in Alloys Made with Commercial Titanium.

KEY.

○ Single-phase alloys water-quenched from 850° C.
☐ Duplex alloys water-quenched from 850° and 700° C.

Ti_3Sn, and it becomes apparent that the lattice structure of the 23·5 at.-% tin alloy was practically identical with that of Ti_3Sn. Hence it can be considered that the γ phase is based on Ti_3Sn, which, as reported by Pietrokowsky, possesses the DO_{19}-type structure.

TABLE IV.—*X-Ray Diffraction (Debye–Scherrer) Data for 23·5 at.-% Tin Alloy, Water-Quenched from 825° C. (γ phase).*

hk.l.	Relative Intensity Observed	$(1/d)^2$, Å.$^{-2}$	
		Observed	Calculated
10·1	M	0·0829	0·0822
11·0	W	0·1146	0·1143
20·0	M	0·1529	0·1524
00·2	S	0·1764	0·1763
20·1	VS	0·1968	0·1965
10·2	VW	0·2140	0·2144
11·2	W	0·2912	0·2906
21·1	W	0·3112	0·3108
20·2	M	0·3289	0·3287
22·0	M	0·4579	0·4572
20·3	S	0·5493	0·5490
22·2	M	0·6336	0·6334
40·1	M	0·6544	0·6536
00·4	M	0·7045	0·7050
40·2	W	0·7867	0·7858
11·4	VW	0·8190	0·8193
20·4	M	0·8575	0·8574
32·2	W	0·8982	0·9001
21·4	W	0·9758	0·9717
41·2			0·9763
50·1	VW	0·9971	0·9965
40·3	M	1·0070	1·0061
30·4	W	1·0500	1·0479
42·0	W	1·0668	1·0667
00·5	W	1·1006	1·1015
42·1	M	1·1101	1·1108
10·5	W	1·1403	1·1396
22·4	S	1·1614	1·1622

V.S = Very strong. S = Strong. M = Medium. W = Weak. VW = Very weak.

Examination of the diffraction patterns for the 11·2, 11·4, and 18·7 at.-% tin alloys quenched from the $(\alpha + \gamma)$ field in Fig. 1 (p. 523) revealed that almost the whole spectrum of the γ phase was present. The only definite evidence of the presence of α phase was the (11·4) reflection which was sufficiently distant from the (22·4) reflection of the γ phase to be distinguished and measured accurately. All the other reflections from the α phase were apparently so close to the corresponding reflections from the γ phase as to be indistinguishable therefrom. This introduced some uncertainty into the calculation of lattice parameters for the phases in $(\alpha + \gamma)$ mixtures. However, since there was a preponderance of α phase in the 9·9, 11·2, and 11·4 at.-% tin alloys quenched from 860° C. or lower, diffraction patterns from these could be used to estimate the lattice parameters of α solutions saturated with tin.

The 22·0 at.-% tin alloy quenched from the $(\alpha + \gamma)$ range contained such a high proportion of γ phase that the (11·4) reflection from the α constituent could not be detected. Therefore the lattice parameters of γ phase saturated with titanium could be calculated from the diffraction patterns for the 22·0 at.-% tin specimens. The actual values were: $c = 4{\cdot}762 \pm 0{\cdot}004$ Å., $a = 5{\cdot}916 \pm 0{\cdot}005$ Å., $c/a = 0{\cdot}805$. These values pertain to a specimen quenched from 825° C.

Diffraction patterns for the 11·2, 11·4, and 18·7 at.-% tin alloys quenched from the $(\beta + \gamma)$ field in Fig. 1 (p. 523) all showed evidence of the presence of the γ phase. The patterns from the 9·9, 11·2, and 11·4 at.-% tin specimens seemed to contain weak, broad (11·4) reflections from strained α phase, but in this respect the evidence was not conclusive, except perhaps for the 9·9 at.-% alloy.

The diffraction patterns of alloys quenched from the field *ABED* in Fig. 1 (p. 523) were all rather similar to those of alloys quenched from the β field. There were no indications of the presence of γ phase. These results suggest that the area *ABED* can be correctly described as the $(\alpha + \beta)$ field. An alloy quenched after being brought to equilibrium as an $(\alpha + \beta)$ mixture would contain strained α phase, formed from β during quenching, together with comparatively strain-free α. Broad reflections from the strained α would naturally tend to mask sharp reflections from strain-free α.

5. SUMMARY

The exploratory investigation has shown that tin depresses the freezing point of titanium. There seems to be a eutectic point at about 17 at.-% tin, the temperature being of the order of 200° C. below the freezing point of the commercial titanium. Constituents of the eutectic mixture are a solid solution of tin in β-titanium and an intermediate phase designated γ.

It has been revealed that tin dissolves to the extent of approximately 9 at.-% in both forms of the commercial titanium. It has also been shown that tin causes a slight elevation of the $\alpha \rightleftharpoons \beta$ transformation range in the titanium. This suggests a peritectoid system. However, the experiments on the commercial-purity alloys did not yield any conclusive evidence of an $\alpha \rightleftharpoons \beta + \gamma$ reaction. Probably the chief reason for this is the broad transformation range (870°–960° C.) in the commercial titanium. The impurities which produce this effect would almost certainly cause a peritectoid type of transformation to occur over a considerable temperature range.

The effect of tin on the lattice parameters of α-titanium is worthy of note; the c parameter is appreciably increased by addition of tin, whereas a is only slightly expanded. The c/a ratio for the saturated α solid solution is 1·600 as compared with 1·588 for the commercial titanium.

Quenching in water does not cause solid solutions of tin in the β-form of the commercial titanium to be retained with their high-temperature crystal structure. During the quench, a rapid $\beta \rightarrow \alpha$ change occurs with the production of a constituent which, on etching, exhibits a characteristic, fine acicular microstructure.

The intermediate phase γ has an ordered hexagonal crystal structure. It can be considered as based on Ti_3Sn, which, as shown by Pietrokowsky,[3] has the DO_{19}-type structure. The interatomic distances in the γ phase are close to those of tin-saturated α solutions.

V.—ALLOYS MADE WITH REFINED TITANIUM

1. Alloys Used

Compositions of alloys used are listed in Table V. There was satisfactory agreement between the analytical results and the synthetic compositions up to 13·3 at.-% tin. The 21·2 and 24·0 at.-% tin alloys were not analysed, because the losses during the melting of these alloys were very slight and it was considered safe to use the synthetic compositions.

Table V.—*Alloys Made with Refined Titanium.*

Synthetic Composition, at.-% tin	Analytical Results	
	Tin, at.-%	Tin, wt.-%
3·4	3·5	8·2
6·35	6·5	14·4
8·5	8·5	18·9
11·1	11·0	23·6
13·15	13·3	27·6
21·2	...	...
24·0	...	...

2. Freezing Ranges and As-Cast Structures

In general, the observations were in agreement with those reported for the commercial-purity alloys. Addition of tin up to 13·3 at.-% tin depressed the freezing point of the refined titanium. The depression was of the order of 150° C. at 13·3 at.-% tin. The 21·2 and 24·0 at.-% tin alloys started to solidify at temperatures only about 50° C. below the freezing point of the titanium.

The structures of as-cast alloys containing 3·5–13·3 at.-% tin were very similar to those already reported for the commercial-purity alloys with 3·4–11·4 at.-% tin. The structure of the 21·2 at.-% tin alloy as cast resembled that of the 18·7, 22·0, and 23·5 at.-% tin commercial-purity alloys in the same condition, and the 24·0 at.-% tin alloy consisted entirely of slightly cored, dendritic grains of γ phase.

3. Microstructures of Heat-Treated Alloys

The results of experiments covering the range 600°–1120° C. are set out in Fig. 3. There is a general similarity between these results and those presented in Fig. 1 (p. 523) for alloys made with the commercial titanium. However, the quenching experiments on the purer alloys have given a much clearer picture of the phase relationships in the range 850°–900° C., especially in respect to the α ⇌ β transformation range. Results for this range are presented in greater detail in Fig. 4, from which it is apparent that the boundaries of the (α + β) field are depressed by the addition of 3·5 at.-% tin; with further additions of tin, the (α + β) range is elevated up to about 880° C.

Two types of heat-treatment were used to locate the boundaries of the (α + β) field: (*a*) Simply heating the specimen to the quenching temperature and maintaining it at that temperature for at least 5 hr. before quenching (see Fig. 4 (*a*)). (*b*) First heating the specimen at 1000° C., i.e. in the β field, for 1–2 hr., then cooling it in the furnace to the desired temperature, at which it is maintained for at least 5 hr. and finally quenching it (see Fig. 4 (*b*)).

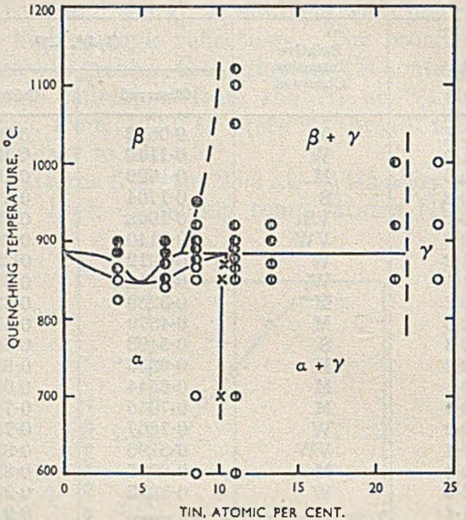

Fig. 3.—Results of Quenching Experiments on Alloys Made with Refined Titanium. Key as in Fig. 1 (p. 523).

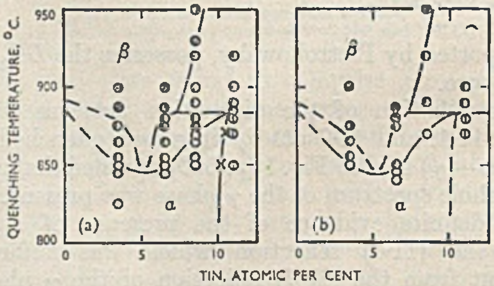

Fig. 4.—Results of Quenching Experiments on Alloys Made with Refined Titanium. (*a*) Alloys heated to desired temperature and water-quenched. (*b*) Alloys heated to 1000° C., cooled to desired temperature, and quenched. Key as in Fig. 1 (p. 523).

There was good agreement between the results in respect of the α/(α + β) boundary, but the β/(α + β) boundary determined by heat-treatments of type (*a*) was a little higher than that deduced from experiments of type (*b*). This discrepancy indicates that the times of heating at the quenching temperatures were not quite sufficient to permit equilibrium to be attained. However, it can be assumed that the equilibrium $\beta/(\alpha + \beta)$ boundary lies between the two $\beta/(\alpha + \beta)$ boundaries shown in Fig. 4.

The results presented in Figs. 3 and 4 indicate that there is a peritectoid horizontal at about 885° C. The most interesting metallographic evidence relating to the peritectoid transformation is shown in Figs. 10 and 11 (Plate LXXXI), which represent the structures found in the 11·0 at.-% tin alloy after quenching from 880° and 890° C., respectively. Heating from 880° to 890° C. caused a change from a relatively coarse-grained, almost single-phase (α) structure to a very fine, duplex structure. This fine structure was observed even when the rate of heating through the range 880°–890° C. had been as low as 0·2° C./min. Further, the structure could be coarsened only slightly by heating at temperatures in the range 1000°–1100° C. for 2 hr. As shown in Fig. 11, the quenched peritectoid mixture consisted of roughly equiaxed particles in a matrix with an acicular structure. Apparently the continuous phase had been β solid solution which had transformed to α during the quench. X-ray-diffraction experiments, the results of which will be discussed in the next section, proved the existence of γ phase in the 11·0 at.-% tin alloy quenched from 900° C. or higher; hence it can be taken that the fine particles in the peritectoid mixture were γ constituent.

4. DEBYE–SCHERRER X-RAY-DIFFRACTION OBSERVATIONS

The X-ray-diffraction results for the purer alloys are presented, together with the corresponding metallographic results, in Table VI. The table also includes deductions based on the results. These deductions are in general concordance with those given in Table III (p. 524) for alloys based on the commercial titanium.

TABLE VI.—*X-Ray-Diffraction Results and Metallographic Observations for Alloys Made with Refined Titanium.*

Tin Content, at.-%	Quenching Temp., °C.	Microstructure *	Phases Identified by X-Ray Diffraction	Structure at Quenching Temp., Deduced from Microstructure and X-Ray Results
3·5	887	All A.C.	Strained α	β
	850	All B.E.C.	α	α
6·5	887	All A.C.	Strained α	β
	865	A.C. + B.E.C.	Strained α	$\alpha + \beta$
	845	All B.E.C.	α	α
8·5	950	All A.C.	Strained α	β
	890	**A.C.** + B.E.C.	γ	$\boldsymbol{\beta} + \gamma$
	875	A.C. + B.E.C.	Strained α	$\alpha + \beta$
	865	All B.E.C.	α	α
11·0	1120	**A.C.** + B.E.C.	γ	$\boldsymbol{\beta} + \gamma$
	900	**A.C.** + B.E.C.	γ	$\boldsymbol{\beta} + \gamma$
	870	2 B.E.C.'s	α	$\boldsymbol{\alpha} + \gamma$
	850	2 B.E.C.'s	α	$\boldsymbol{\alpha} + \gamma$
	700	2 B.E.C.'s	α	$\boldsymbol{\alpha} + \gamma$
13·3	900	A.C. + B.E.C.	γ	$\beta + \gamma$
	875	2 B.E.C.'s	$\alpha + \gamma$	$\alpha + \gamma$
21·2	1000	**B.E.C.** + A.C.	γ	$\boldsymbol{\gamma} + \beta$
	850	2 B.E.C.'s	γ	$\boldsymbol{\gamma} + \alpha$
24·0	1000	All B.E.C.	γ	γ
	850	All B.E.C.	γ	γ

* A.C. = Constituent with fine, acicular structure.
B.E.C. = Bright-etching constituent.
Heavy type denotes the preponderant phase.

The lattice-parameter/composition relationship for the α phase (Fig. 5) revealed that the limit of solubility of tin in the α-form of the refined titanium was 10·5 at.-% at 870° C. and just over 10 at.-% at 850° and 700° C. These values are higher than those already reported for alloys based on the commercial-purity titanium, viz. 9·3 at.-% tin at 850° and 700° C.

The lattice parameters of the titanium-saturated γ phase were determined by experiments on 21·2 at.-% tin specimens quenched from 850° and 1000° C. For both quenching temperatures, the cell dimensions were: $c = 4{\cdot}758 \pm 0{\cdot}004$ Å., $a = 5{\cdot}915 \pm 0{\cdot}005$ Å., $c/a = 0{\cdot}805$. The parameters of the 24·0 at.-% tin alloy quenched from 850° C. were $c = 4{\cdot}766 \pm 0{\cdot}004$ Å., $a = 5{\cdot}920 \pm 0{\cdot}005$ Å., $c/a = 0{\cdot}805$. These data may be compared with the values reported by Pietrokowsky [3] for Ti_3Sn made with refined titanium, viz., $c = 4{\cdot}764 \pm 0{\cdot}004$ Å., $a = 5{\cdot}916 \pm 0{\cdot}004$ Å., $c/a = 0{\cdot}805$.

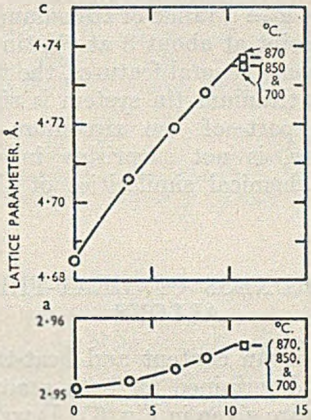

FIG. 5.—Lattice Parameters of α Phase in Alloys Made with Refined Titanium.

KEY.

○ Single-phase alloys water-quenched from 840°–850° C.
☐ Duplex alloys water-quenched from temperatures shown.

X-ray reflections for the γ constituent of quenched peritectoid mixtures in the 11·0 at.-% tin alloy were broad, and this was attributed partly to the fineness of the γ phase in these mixtures. The breadth of the diffraction lines could be reduced only a little by heating the peritectoid mixture for 1 hr. at 1120° C. This result is in conformity with the metallographic observation, already mentioned, that the peritectoid structures could be coarsened only slightly by heating to temperatures as high as 1100° C.

5. DISCUSSION

Perhaps the most interesting feature of the system is the comparatively small effect of tin on the temperature of the $\alpha \rightleftharpoons \beta$ transformation in titanium. All the $\alpha \rightleftharpoons \beta$ changes occur in the range 845°–890° C.

Another point of interest is that the solid solubility of tin in α titanium at 700° C. is only a little less than it is at 870° C.

Most of the metals which have atomic sizes close to that of titanium form more or less extensive β solid-solution series, but only very restricted α solution ranges. However, tin must be classed as a member of a very small group of metals which have atomic sizes similar to that of titanium and which dissolve to an appreciable extent in both forms of titanium. The other metals in this group are zirconium and aluminium. Unfortunately, it does not seem possible at present to offer any satisfactory theoretical explanation of these facts.

Recently McPherson and Hansen[6] reported that tin elevates the $\alpha \rightleftharpoons \beta$ range of zirconium, there being a peritectoid point at about 8 at.-% tin and 980° C. In respect to some general features, the titanium-rich portion of the titanium–tin system is similar to the corresponding part of the zirconium–tin system. This, of course, is not surprising in view of the physical and chemical similarities of titanium and zirconium.

VI.—HARDNESS OF HEAT-TREATED ALLOYS

The effects of tin content and heat-treatment on hardness were determined for both groups of alloys, and the results are given in Fig. 6. It was found that tin hardened α-titanium appreciably, the effect being greater in alloys in which the α phase had the acicular structure produced by quenching from the β field. However, the effects of heat-treatment were small, except perhaps for the 7·7 at.-% tin alloy made with commercial titanium.

The hardness of the γ phase was about 100 D.P.N. lower than that of the high-tin α solid solutions. This explains why the maxima in the hardness/composition curves occur at, or near to, the α solid-solution limits.

Despite its comparatively low hardness, the γ phase could not be forged either at normal temperature or in the range 600°–800° C. The brittleness of this constituent was in marked contrast to the ductility of the harder, high-tin α solid solutions. The latter could be distorted to a very considerable extent at about 700° C., and they would withstand an appreciable amount of cold forging before starting to crack.

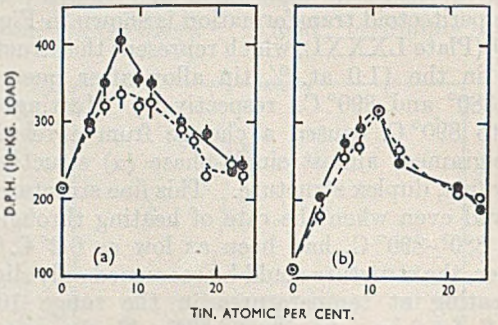

Fig. 6.—Diamond Pyramid Hardness of Heat-Treated Alloys Made with (*a*) Commercial Titanium and (*b*) Refined Titanium.

KEY.

● Water-quenched from β and (β + γ) fields. (*a*) 950°–1000° C., (*b*) 900°–950° C.

○ Water-quenched from α and (α + γ) fields. (*a*) 850° C., (*b*) 815°–870° C.

ACKNOWLEDGEMENTS

The investigation formed part of the programme of the Physical Metallurgy Section of the Commonwealth Scientific and Industrial Research Organization, Australia. The work was carried out in the Baillieu Laboratory, University of Melbourne, under the general direction of Professor J. Neill Greenwood, to whom the author expresses his thanks. Other members of staff of the Baillieu Laboratory are also thanked for their assistance. Mr. J. A. Corbett performed all the chemical analyses required, and Mr. A. White helped in the preparation of specimens.

Spectrographic analyses were done by the Defence Research Laboratories, Maribyrnong.

The United States Bureau of Mines kindly supplied the commercial titanium used in making the alloys.

REFERENCES

1. C. M. Craighead, O. W. Simmons, and L. W. Eastwood, *Trans. Amer. Inst. Min. Met. Eng.*, 1950, **188**, 485.
2. P. Pietrokowsky and P. Duwez, *ibid.*, 1951, **191**, 772.
3. P. Pietrokowsky, *ibid.*, 1952, **194**, 211.
4. J. A. Corbett, *Analyst*, 1951, **76**, 652.
5. W. J. Kroll, *Trans. Electrochem. Soc.*, 1940, **78**, 35.
6. D. J. McPherson and M. Hansen, *Trans. Amer. Soc. Metals*, 1953, **45**, 915.

SOME OBSERVATIONS ON CREEP AND FRACTURE FROM INVESTIGATIONS ON LEAD CABLE-SHEATH ALLOYS *

1474

By A. LATIN,† Ph.D., M.Eng., F.I.M., MEMBER

SYNOPSIS

Tests have been conducted, both at constant internal pressure and at constant hoop stress, on lead and lead alloys chiefly in the form of pipe as extruded for cable sheathing. The results have given some indication of the effects of alloy additions, of grain-size, and of prior deformation (coiling over a drum) upon fracture and general ductility under creep. Some alloy additions, notably antimony (e.g. 0·35%) and tellurium (0·01%), appear to promote considerable embrittlement at slow creep rates, and to some extent their effects have been related to time-dependent (ageing) changes. In several cases, however, poor ductility at slow creep rates does not appear to have any connection with such ageing changes.

Some theoretical concepts are offered, based on the view that intercrystalline cracking in creep results from the occurrence of elastic strain fields at certain grain-boundary localities, as a result of structural and flow heterogeneities. Particularly poor ductility, it is considered, arises from augmentation of such elastic strains by effects due to the alloy additions concerned and to other factors.

I.—INTRODUCTION

THE fractures resulting from the creep of lead and lead alloys as extruded for cable sheathing change from ductile types at moderate creep rates, or more rapid strain rates, to intercrystalline forms at slow creep rates. This has also been observed in other metals and alloys. The ductility, as measured by the general extensions reached at the time of fracture, can also vary notably with the creep conditions. For some alloys at least, very low ductility values are obtained at small creep rates. The chief object of the present paper is to record some observations and views on these matters, based on investigations connected with the development of sound sheathing for types of electricity-supply cables operating under pressure of gas or oil.

II.—METHODS OF INVESTIGATION

Investigations were carried out chiefly on materials extruded in the form of pipe (approximate range of sizes 2–3 in. dia., 0·1–0·13 in. wall thickness) on cable-sheathing presses of both the ram type (including an experimental press and a factory press fitted with liquid-lead seal [1]) and the Pirelli continuous (screw) type.[2] The lead used was of Tadanac or Broken Hill grades of high purity (better than 99·95%) and lead of similar quality was used for the alloys.

Samples (each of 3 or 4 yards length) of the extruded pipe were submitted to internal pressures calculated to give a suitable range of fracture times from a few hours to several thousand hours. Details of procedure have been described previously.[3, 4] In one series of tests the pressure was maintained constant in each sample; in another series the hoop (circumferential) stress in the pipe wall was kept constant by suitably decreasing the pressure as creep progressed. The majority of these latter tests were conducted at a temperature thermostatically controlled at 27° C. (±2° C. maximum variation); the former tests were conducted at room temperature. The constant-stress tests were carried out on samples kept straight during and after extrusion so as to be as strain-free as possible initially. The constant-pressure tests were carried out both on similar samples and on samples taken from coils on cable drums. These will be referred to as "straight lengths" and "drum lengths", respectively. Samples of pipe were also tested for changes resulting from prolonged standing ("ageing") for times up to several thousand hours after extrusion, the creep and fracture characteristics being compared with those of samples tested shortly after extrusion.

Some creep tests at constant uniaxial stress were conducted on samples of strip (4 in. gauge-length, ½ in. width) taken from pipe or extruded as strip. A "hyperbolic pulley" method due to Pearson [5] was used, constancy of stress being achieved within 2% maximum error, as judged by calibration. Tests have also been made with a new apparatus [6] designed to eliminate friction. The temperature was thermostatically controlled at 28° ± 1° C.

---

* Manuscript received 22 April 1952; in revised form 5 November 1952.

† Head of the Department of Metallurgy and Chemistry, National Coal Board, Central Research Department II, Isleworth, Middlesex; formerly at the Research Department, British Insulated Callender's Cables, Ltd., London.

TABLE I.—*Results of Tests of Pipe Samples at Constant Pressure.*

Nominal Composition	Type of Press	Mean Grain Dia., mm.	Initial Hoop Stress, lb./in.^{2}	Time to Failure, hr.	General Diametral Expansion, %	Mean Creep Rate, %/hr.	Type of Fracture *	Remarks
Pure Lead	Ram	0·75	830	27·5	11·7	0·43	KE	Wide scatter of extension (6 to 12%). Straight lengths.
			600	518	11·3	0·022	KE	
			450	11,600	9·6	0·0008	IC	
0·2% Sn	Ram	0·35	800	491	13·0	0·027	KE	Analysis gave 0·21% Sn. Straight lengths.
			600	3,338	14·8	0·0044	KE	
			500	11,384	15·8	0·0014	SI	
	Screw	0·5	800	213	10·1	0·048	KE	Analysis gave 0·21% Sn. Straight lengths.
			600	1,518	12·6	0·0084	KE	
			500	9,381	13·4	0·0014	IC	
0·075% Cd	Ram	0·25	800	479	14·1	0·03	KE	Analysis gave 0·06% Cd. Straight lengths.
			700	1,455	18·3	0·013	KE	
			600	4,235	17·9	0·004	KE	
	Screw	0·45	800	946	20·5	0·021	KE	Analysis gave 0·05% Cd. Straight lengths.
			700	1,903	17·0	0·0089	IC	
			600	7,697	12·6	0·0016	IC	
0·2% Sn, 0·075% Cd	Ram	0·25	1,180	297	15·5	0·063	KE	Analysis gave 0·23% Sn, 0·066% Cd. Straight lengths.
			800	3,860	16·5	0·0045	IC	
			650	5,380	11·6	0·0022	IC	
	Screw	0·5	1,250	39	14·0	0·36	KE	Analysis gave 0·18% Sn, 0·064% Cd. Straight lengths.
			800	2,500	5·8	0·002	IC	
0·4% Sn, 0·15% Cd	Ram	0·2	1,300	180	19·4	0·108	KE	Alloy C to B.S. 801. Straight lengths.
			1,200	263	23	0·087	SI	
			1,000	1,490	19·9	0·013	IC	
			800	3,466	12·9	0·0038	IC	
	Screw	0·4	1,400	94	12·1	0·128	KE	Straight lengths.
			1,300	120	13·2	0·11	SI	
			1,200	489	10·2	0·021	IC	
			800	3,283	3·2	0·00096	IC	
	Screw	0·4	1,400	361	8·3	0·023	IC	Drum lengths.
			1,300	542	6·8	0·013	IC	
			800	5,583	1·7	0·00029	IC	
0·4% Sn, 0·2% Sb	Ram	0·25	1,400	89	18·5	0·21	IC	Alloy E to B.S. 801. Analysis gave 0·34% Sn, 0·21% Sb. Straight lengths.
			1,000	3,990	9·3	0·0023	IC	
			800	6,318	5·4	0·0008	IC	
Pure Lead	Screw	0·7	650	1,065	7·7	0·0072	KE	Drum lengths.
			550	2,882	9·9	0·0034	KE	
			460	31,106	12·1	0·00032	IC	
0·4% Sn, 0·2% Sb	Screw	0·3	1,400	66	16·0	0·24	IC	Knife-edge fracture at higher strain rates. Drum lengths.
			1,000	1,129	7·5	0·0066	IC	
			800	8,280	4·0	0·00048	IC	
			500	44,600	1·95	0·000044	IC	
0·35% Sb	Screw	0·3	1,400	21	17·3	0·82	SI	Knife-edge fracture at higher strain rates. Drum lengths.
			1,100	728	9·1	0·048	IC	
			500	31,530	3·7	0·00012	IC	
0·009% Te	Screw	0·5	1,125	43	21·1	0·49	SI	Knife-edge fracture at higher strain rates. Drum lengths.
			1,000	238	16·0	0·011	IC	
			500	37,188	2·3	0·000062	IC	
0·015% Te	Screw	0·7	1,100	52	16·3	0·31	IC	Knife-edge fracture at higher strain rates. Drum lengths.
			1,000	186	10·3	0·055	IC	
			500	26,400	2·2	0·000083	IC	
0·1% Sn, 0·005% Ag	Screw	0·5	1,250	87	9·4	0·11	IC	Knife-edge fracture at higher strain rates. Drum lengths.
			1,100	288	6·1	0·021	IC	
			650	3,120	1·5	0·00049	IC	

* KE represents knife-edge splits, IC represents intercrystalline fracture, and SI (semi-intercrystalline) represents intermediate types.

III.—RESULTS OF TESTS ON PIPE SAMPLES AT CONSTANT PRESSURE

Several results have been published previously.[3, 4] Some further results are summarized in Table I. In this table the third column represents mean values of the grain diameter as obtained from counts taken radially across the pipe wall, the sixth column represents the mean percentage increase in diameter away from the fracture location at time of fracture, and the next column shows the value obtained by dividing this percentage extension by the number of hours before failure occurred.

The chief results of significance as regards fracture, from these and the previous tests, can be summarized as follows:

(1) The change in type of fracture, from knife-edge splits to intercrystalline cracks occurred roughly at a hoop stress of 500 lb./in.^{2} and a mean creep rate of about 0·001%/hr. for the lead, and most of the alloy additions increased this value. In general, the change in type of fracture took place over a range of conditions rather than at a single well-defined hoop stress or mean creep rate, intermediate forms of fracture being observed in several tests.

(2) The materials tested fell broadly into two groups as regards ductility (as measured by diametral extension) at long times to fracture. (*a*) There was no marked extension decrease (although there was usually considerable scatter of values) even if intercrystalline fracture occurred. The unalloyed lead and some dilute solid-solution alloys, e.g. those containing 0·1% tin or 0·1% antimony, appeared to belong to this group. Addition of copper (up to about 0·06%) also appeared to have no deleterious effects upon ductility at slow creep in pipe free from undesirable extrusion defects which sometimes result from copper additions. (*b*) Alloys containing higher percentages of antimony, in particular those above the equilibrium solid-solubility limit (e.g. one containing 0·35% antimony), alloy E (0·4% tin and 0·2% antimony, conforming to B.S. 801), alloys containing small percentages of tellurium (about 0·01%), and some alloys containing silver (e.g. 0·1% tin and 0·005% silver, tested in drum lengths only) exhibited a marked decrease in ductility (extensibility) at slow creep rates. All the alloys tested gave knife-edge fractures when tested at sufficiently large rates of strain.

(3) In general, ductility at slow creep rates of a given alloy improved with decrease of grain-size. This can be seen from the results on some of the alloys containing tin and cadmium extruded on the ram press. Similar alloys extruded on the screw press had a larger grain-size as a result of the use of higher die temperatures. The effect of grain-size has been confirmed by some tests on extruded strip of fine grain-size (e.g. alloy E of 0·05 mm. grain dia.), which exhibited particularly good ductility at slow creep rates.

(4) Tests on drum lengths showed that the "prestrain" involved in coiling had very complex effects which appeared usually to result in a decrease of extensibility and in some cases to promote intercrystalline fracture. In the case of some alloys, only drum lengths were available for test, and the precise behaviour of these alloys when free from prestrain is not known. There can be little doubt, however, that alloy additions had a marked influence *per se* (see, e.g., the results in Table I for straight lengths of alloy E).

IV.—RESULTS OF TESTS AT CONSTANT STRESS

The well-known equation of Andrade[7] for creep at constant applied stress can be expressed sufficiently accurately for application to the tests here described, in the approximate form:

$$\epsilon - \epsilon_0 = \beta t^{\frac{1}{3}} + \kappa t,$$

where ϵ = strain at time t and ϵ_0, β, and κ are constants. Considerable significance is usually attached to the values of β and κ, the former corresponding to a "transient" creep term, the rate of which decreases with time, and the latter to a steady creep of constant rate or, more exactly, of constant "logarithmic strain" rate.

The equation can also be written:

$$(\epsilon - \epsilon_0)t^{-\frac{1}{3}} = \beta + \kappa t^{\frac{2}{3}}.$$

A straight line should be obtained on plotting corresponding values of the left-hand side against $t^{\frac{2}{3}}$ if the approximate form of the Andrade equation is obeyed. The slope of this line gives κ, and the value of β is given by the intercept at $t = 0$ on the strain co-ordinate axis. A suitable value of ϵ_0 (a type of "adjustment" constant) must be chosen; it was usually small for the tests here described, and could be identified more or less with a small initial "instantaneous" extension. This method of analysis is a slightly modified version of that due to Nabarro.[8]

Constancy of stress in the tests on pipe specimens was checked by measurements of the final wall thickness away from the actual fracture locality. Some results are shown in Table II.

Table II.—*Original and Final Calculated Hoop Stresses in Pipe Samples Tested at Constant Stress.*

Material	Original		Final		Original Hoop Stress, lb./in.^{2}	Final Hoop Stress, lb./in.^{2}
	Outside Dia., in.	Wall, in.	Outside Dia., in.	Wall, in.		
Pure Lead.	2·713	0·107	2·985	0·098	450	445
0·1% Sn .	3·307	0·130	3·582	0·119	550	551·5
0·1% Sb .	2·724	0·109	3·100	0·097	650	640
0·06% Cu .	3·270	0·131	3·670	0·119	950	957

The results of some tests at constant stress on unalloyed lead and on alloy E have been published previously.[3] Creep curves for times up to 800 hr., obtained for the dilute solid-solution alloys containing

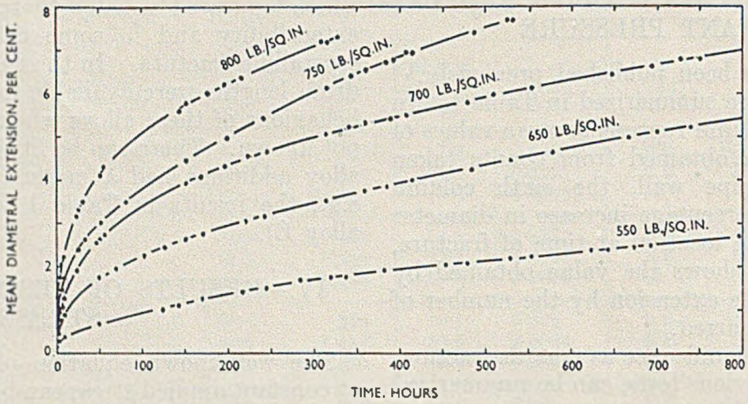

FIG. 1.—Constant-Stress Creep Curves for 0·1% Tin Alloy Pipe (20° C.).

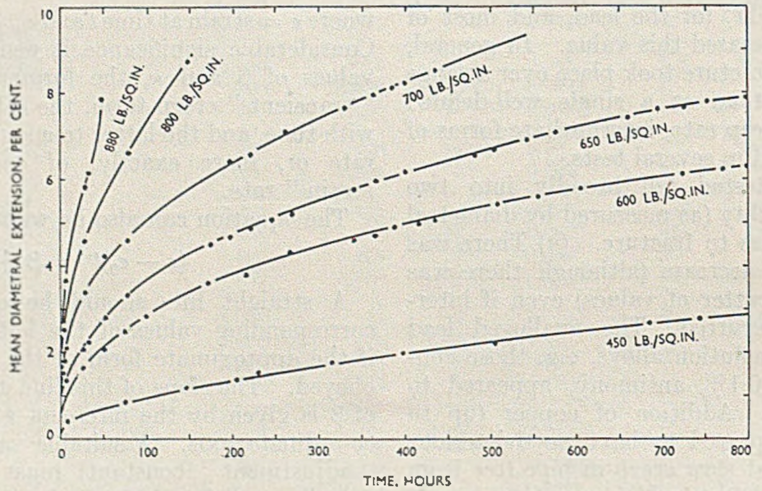

FIG. 2.—Constant-Stress Creep Curves for 0·1% Antimony Alloy Pipe (28° C.).

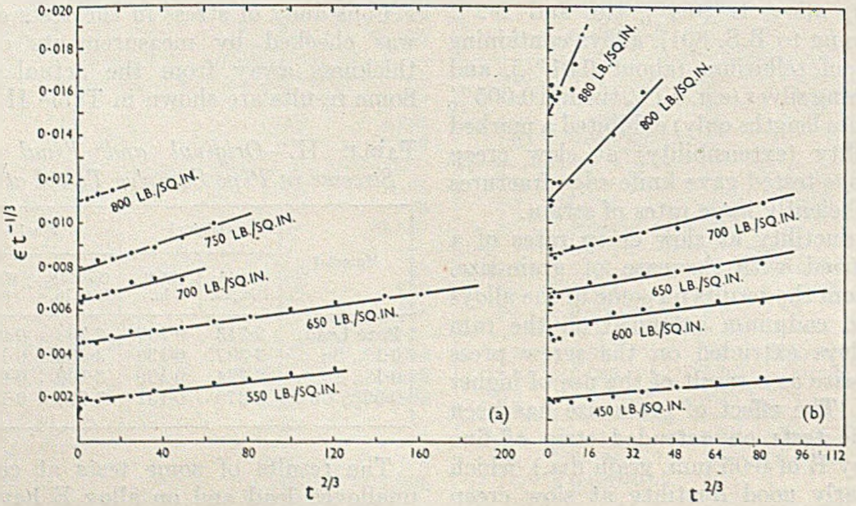

FIG. 3.—Nabarro Analysis Graphs for (*a*) 0·1% Tin Alloy Pipe, and (*b*) 0·1% Antimony Alloy Pipe.

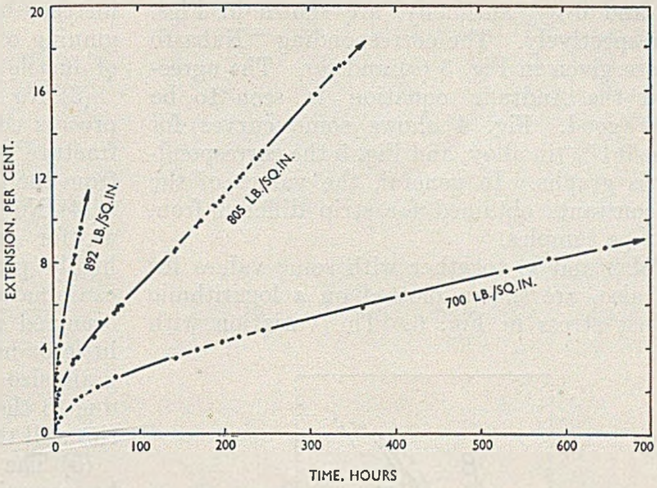

FIG. 4.—Constant-Stress Creep Curves for 0·1% Tin Alloy Strip.

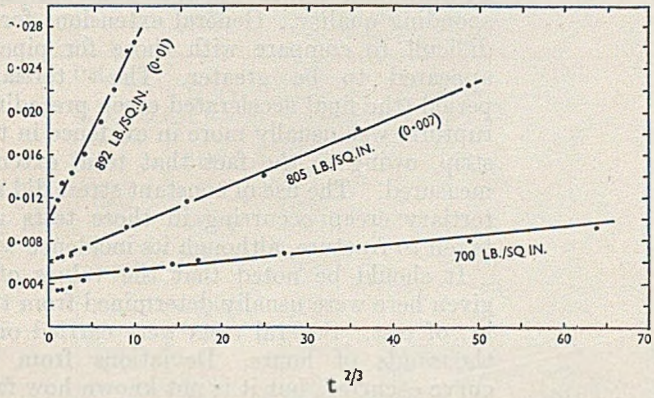

FIG. 5.—Nabarro Analysis Graphs of 0·1% Tin Alloy Strip.

TABLE III.—*Results of Constant-Stress Tests (Pipe Samples) Taken to Fracture.*

Composition	Type of Press	Stress, lb./in.²	β, hr.$^{-1/3}$	$\kappa \times 10^3$, hr.$^{-1}$	Time to Fracture, hr.	Mean General Extension, %	Type of Fracture *
Unalloyed Lead	Ram	725	0·0108	0·204	82·5	7·2	KE
		650	0·0089	0·0066(?)	1,080	10·0	KE
		450	0·002	0·0050	11,600	9·7	IC
0·06% Cu	Ram	750	0·006	0·134	2,025	16·6	KE
		550	0·007	0·0154	20,000	…	Not failed
		450	0·0002	0·0028	Over 20,000	…	,, ,,
0·21% Sn	Ram	1,000	0·0057	0·056	278	13·5	KE
		600	0·0018	0·025	11,560	22·1	IC
0·06% Cd	Ram	1,000	0·012	0·19(?)	281	14·75	KE
		600	0·0016	0·039	Over 10,000	…	Not failed
0·05% Cd	Screw	1,000	0·017	0·035	784	19·4	SI
		600	0·0012	0·021	Over 10,000	…	Not failed
0·23% Sn, 0·07% Cd	Ram	1,250	0·021	0·074	425	20·7	KE
		1,000	0·012	0·039	1,016	17·1	IC
		760	0·0035	0·04(?)	4,903	17·0	IC
0·18% Sn, 0·06% Cd	Screw	1,250	0·027	0·10	87	13·9	SI
		1,000	0·013	0·046	417	11·6	IC
		750	0·004	0·020	2,173	8·0	IC
0·4% Sn, 0·15% Cd	Ram	1,200	0·0057	0·048	1,504	13·7	IC
		1,000	0·0033	0·060	2,630	10·8	IC
	Screw	1,200	0·0050	0·045	616	7·0	IC
0·004% Ag	Ram	975	0·016	0·045	600	17·4	KE
		875	0·012	0·011	1,280	16·0	IC

* Key as in Table I.

0·1% tin and 0·1% antimony, are shown in Figs. 1 and 2, respectively. The corresponding " Nabarro graphs " are given in Fig. 3 (*a*) and (*b*). The agreement with the Andrade equation is seen to be moderately good. Fig. 4 shows some curves for strip of the 0·1% tin alloy, and Fig. 5 the corresponding analysis graphs. In general, the values of the Andrade constants obtained for strip differed from those for pipe samples.

Values of β and κ, together with some values for pure lead also, are shown plotted on a logarithmic scale against stress in Fig. 6. The variation with stress within the range here concerned is seen to be approximately of the exponential form found, more particularly for the κ value, by Andrade and other investigators.[9]

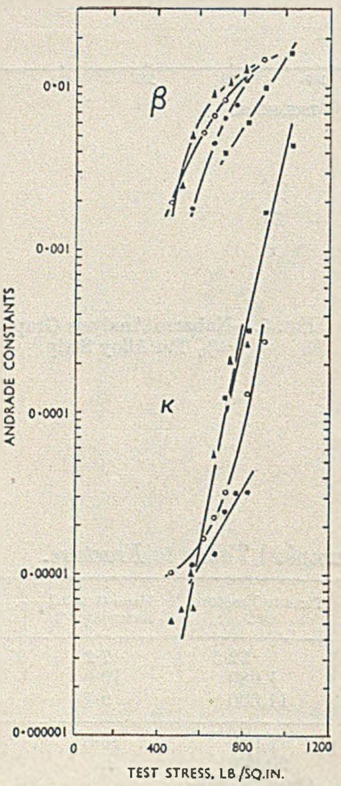

Fig. 6.—Variation of Andrade Constants with Stress for Lead Alloy Pipe and Strip Samples.

Key.

▲ Pure Lead Pipe.
○ 0·1% Antimony Alloy Pipe.
● 0·1% Tin Alloy Pipe.
■ 0·1% Tin Alloy Strip.

In Table III are collected some further results, with data concerning fracture.

The results of principal significance can be summarized as follows :

(1) The value of κ corresponding to change of fracture type (about $0{\cdot}005 \times 10^{-3}$ hr.$^{-1}$ for unalloyed lead) was in general increased by addition of alloying elements; the corresponding β values were less affected.

(2) Increase of grain-size appeared to result in an increase of the value of κ corresponding to the beginning of intercrystalline types of fracture in place of ductile (knife-edge split) types.

(3) No obvious fundamental difference in the creep process corresponding to the two different types of fracture could be observed, as judged in particular from the form of the creep curves.

(4) No clear effects due to recrystallization, such as, for example, that observed by Andrade with highly pure lead,[10] were apparent. Metallographic examination confirmed that recrystallization had not occurred as readily as might have been expected, little or no change being observed usually in general grain-size during test. This may in part have been due to the somewhat large grain-size compared with the wall thickness of the specimens.

(5) The values of κ at a given stress appeared to be somewhat greater for strip than for pipe of corresponding quality. General extensions for strip were difficult to compare with those for pipe, but they appeared to be greater. The " tertiary creep " period (the final accelerated creep preceding ultimate rupture) was usually more in evidence in the tests on strip, owing to the fact that total extensions were measured. The use of constant stress did not prevent tertiary creep occurring in those tests which were taken to fracture, although its incidence was delayed.

It should be noted that the values of constants given here were usually determined from the first 800 hr. of test. Several tests were carried on for many thousands of hours. Deviations from the initial curve occurred, but it is not known how far this may have been due to cumulative error.

V.—INFLUENCE OF STANDING (" AGEING") BEFORE TEST

Various results on samples of pipe are shown in Table IV. Comparisons of tests to fracture at moderately rapid rates of extension (short-time tests) with similar tests on the freshly extruded material are given, and also with some results from the slow creep tests (long-time tests).

From these results it would appear to be possible to group the materials tested as follows :

(1) Those in which no decrease of ductility resulted from prolonged standing, the substances concerned showing also no marked decrease at slow creep rates. Pure lead, the dilute solid-solution alloys mentioned above, and the alloy containing 0·06% copper belonged to this group.

(2) Those in which a marked decrease of ductility (diametral extension at time of fracture) was observed for the short-time test after prolonged standing, of a similar order to that observed in long-time creep tests. An example is the alloy containing 0·35% antimony. The marked decrease of creep rate at the test stress as a result of ageing will also be noted.

(3) Those in which ageing resulted in a considerable decrease of ductility, though of a smaller order than

that observed in the slow creep tests. Alloy E and the tellurium lead behaved in this manner.

(4) Those in which no decrease of ductility was observed as a result of prolonged standing before the short-time test, though the ordinary long-time creep test showed a marked decrease of extension at fracture. The alloy containing 0·005% silver and 0·1% tin is an example. The series of alloys containing both tin and cadmium also showed little or no signs of the "simple ageing" effect.

The effect of ageing upon the ductility of the alloys containing antimony and tellurium appears to be connected with the precipitation of antimony and of a tellurium-rich phase, respectively, at the grain boundaries and within the grains, some degree of precipitation-hardening resulting.[4, 11]

TABLE IV.—*Effect of Standing Upon the Ductility of Pipe Samples Under Creep.*

Composition of Alloy	Type of Press	Time of Ageing, hr.	Rapid Creep Test Hoop Stress, lb./in.^{2}	Slow Creep Test		Mean Creep Rate, %/hr.	General Diametral Expansion, %	Type of Fracture*	Remarks
				Hoop Stress, lb./in.^{2}	Time to Failure, hr.				
Unalloyed Lead	Ram	...	1,100	...	...	0·22	6·0	KE	Initial short-time test.
		24,800	1,040	...	...	1·0	7·0	KE	Similar test after straining.
	Screw	...	1,010	...	...	0·16	6·2	KE	
		24,600	1,010	...	...	0·67	7·5	KE	
0·4% Sn, 0·2% Sb (Alloy E)	Ram	...	1,448	...	...	0·45	11·9	SI	
		50,000	1,448	...	...	0·014	3·1	IC	
	Screw	...	1,400	...	...	0·32	16·7	IC	Rapid creep test on original pipe.
		...	...	800	4,896	0·0007	2·8	IC	Slow creep test on original pipe.
		7,100	1,400	...	...	0·034	9·2	IC	
0·35% Sb	Screw	...	1,280	...	...	0·28	17·0	SI	
		...	...	600	25,000	0·0001	2·5	IC	
		19,000	1,280	...	...	0·0016	1·6	IC	
		28,600	1,280	...	...	0·0014	1·0	IC	
0·23% Sn, 0·06% Cd	Ram	...	1,245	...	...	0·12	15·7	KE	
		17,800	1,250	...	...	0·11	18·2	KE	
0·18% Sn, 0·06% Cd	Screw	...	1,250	...	...	0·36	14·1	KE	
		17,800	1,250	...	...	0·39	16·4	KE	
0·009% Te	Screw	...	1,125	...	...	0·46	17·9	SI	
		...	...	650	19,200	0·0007	1·4	IC	
		23,000	1,125	...	...	0·068	7·8	IC	
0·1% Sn, 0·005% Ag	Screw	...	1,250	...	...	0·52	9·7	KE	Samples from different pipe from that shown in Table I.
		...	...	500	14,000	0·00025	3·4	IC	
		10,150	1,250	...	...	0·61	9·2	KE	

* Key as in Table I.

That such changes need not in themselves lead to intercrystalline fracture in creep was indicated for some results on the alloy E of fine grain mentioned above. As illustrated by Fig. 7 (Plate LXXXII), extensive changes could occur at grain boundaries during creep deformation, but these did not lead to intercrystalline fracture.

In general, it can be concluded that effects due to creep *per se* were for several alloys of more moment than any due to purely time-dependent ageing changes upon the fracture characteristics in prolonged creep tests. There is much evidence from the fracture characteristics of other metals [12–14] in creep to support this view. It remains possible that deformation during creep could affect, for example, the distribution of alloying elements or impurities as between grains and grain boundaries, and this could in turn affect the fracture characteristics; strain-induced changes of other kinds might also occur.

VI.—THEORETICAL CONSIDERATIONS

Although it is not proposed to deal here with all the factors concerned with fracture behaviour in creep, but rather to offer more general theoretical considerations, it may be of value to summarize some of the chief factors concerned.

(1) The mechanism of flow or deformation with particular regard to differences between grain interiors and grain-boundary regions. Associated with this is the relationship between the imposed stresses and the stress/strain system at any point within the substance.

(2) The effect of impurities or addition elements and their distribution between grain interiors and grain-boundary regions; atomic size-factors, &c.

(3) Grain-boundary structure in relation to the presence or development of defects or discontinuities which could aid micro-crack formation.

(4) The effects of addition elements upon cohesive bond strengths or upon the free energy of crack surfaces resulting from bond disruption.

(5) The effects of grain-size and other structural factors such as second phases or precipitates.

(6) The possibility of purely time-dependent changes (ageing) and the effects of stress and strain upon such changes.

(7) The previous history (prestrain, work-hardness, &c.) of the substance.

(8) Factors influencing crack propagation rate.

(9) Surface and environmental conditions.

(10) The effect of temperature.

It is usually accepted, particularly for local fractures of brittle nature, that disruption must be preceded by the development of elastic strains sufficiently large to break interatomic bonds in at least some small region of the material. It is probable also that a minimal size of elastically strained region is usually necessary for the inception of fracture, i.e. there is a "nucleation effect".

Various criteria for the incidence of the different types of fracture have been proposed; on general theoretical grounds that most applicable to the present case would seem to be one of a critical elastic strain energy. Freudenthal,[15] for example, has advanced a general mathematical analysis of fracture inception based on this criterion, his treatment including consideration of the energy of volumetric expansion as an important contribution. It would seem acceptable also that the effect of inelastic strain components as such can either be inhibitory to fracture, for example by superseding local elastic strains, or contributory to fracture, by intensification of strains on adjacent maintained interatomic bonds (i.e. bonds between atoms not taking active part in the inelastic strain processes).

The mechanism of creep in metals is complex in nature. Many theories are extant (see, e.g., Sully [12]) and there have been considerable recent developments both in theoretical concepts and in experimental studies of the mechanism. Questions particularly appropriate to the problems discussed in the present paper are: (i) to what extent glide-plane slip processes occur, such as are involved in ordinary plastic deformation; (ii) to what extent motion of dislocations, now widely accepted as being involved in glide-plane slip, occurs both along and, possibly, out of glide planes; (iii) to what extent, if any, motion of lattice vacancies (Schottky defects) may occur; and (iv) to what extent grain-boundary slip and other possible occurrences at grain boundaries take place.

(i) Dislocation-slip theory has been applied with some success to transient creep and more particularly to "exhaustion creep," [16] but with less success to explanations of the mechanism of steady creep, which plays a major part in tests such as those concerned in the present work. It is common observation that glide-plane slip is not so readily discernible in steady creep as in other types of deformation, and it would seem therefore that such creep involves mechanisms dissimilar from those involved in ordinary plastic deformation.

(ii) A possible clue to the mechanism of steady creep would appear to have been obtained from studies (by Wood and Scrutton [17 &c.]) of the cellular "substructures" which develop during the creep of some metals. These suggest, apart from other possible explanations, motion of or collection of dislocations outside the ordinary slip systems, and would in fact appear to be allied, in some respects at least, to the effect known as "polygonization".[18]

(iii) Nabarro [19] has pointed out that, in theory, creep could result from motion of lattice vacancies (self-diffusion), though his calculations indicated the unlikelihood of such action contributing in practicable measure to creep deformation. Mott,[20] however, has since shown that glide-plane motion of dislocations combined with effects due to associated lattice vacancies, allowing dislocations to move out of their glide-planes as a result also of stress concentrations, would appear to involve activation energies of the right order for steady creep.

(iv) Many investigations have indicated relative movements of adjacent grains during steady creep. In connection with "anelastic" effects in general, Zener [21] has proposed the possibility of viscous movements at grain boundaries, resulting in local stress relaxations, and his theories would appear to be supported by several experimental studies of Kê.[22, 23] King *et al.*[24] have confirmed the occurrence of Zener-type slip at grain boundaries under shear stress. Such slip would appear to involve Newtonian flow when of small amount. Some results of Kê [23] suggest that the mechanism is one of self-diffusion. This is in agreement with theoretical calculations of Read and Shockley [25] based on a "dislocation-array" model of grain boundaries. When the orientation difference between adjacent grains is not small, this model amounts to the more readily acceptable one of a "transition zone" between the lattices. Aust and Chalmers [26] have obtained experimental evidence supporting this transition zone concept.

Since movements of dislocations and, for edge-dislocations,[20] probably also associated lattice vacancies are likely to be concerned in creep, the mechanism of intercrystalline cracking may well include the collection or agglomeration of such discontinuities at grain boundaries. The basic mechanism of fracture, however, still involves the presence of elastic strain fields of sufficient magnitude for the development of, or propagation of, any micro-cracks concerned.

Zener [21] (pp. 126 *et seq.*, 158) has proposed a mechanism of intercrystalline cracking in creep based upon effects resulting from viscous slip at grain boundaries. Fracture stresses are postulated as produced where a boundary on which slip occurs meets another across which stress relaxation does not occur, i.e. on which there is absence of shear components. A somewhat similar mechanism has been propounded by Mott,[27] involving mutual blockage at grain-boundary junctions (triple points). Mott has also explained poor ductility under conditions of slow creep as being the result of relative ease of viscous slip at grain boundaries as compared with resistance to deformation of the grains themselves at small stresses. Difficulties arise, however, in any attempt at quantitative development of such theories. This is because intercrystalline cracking may be associated with strains of some magnitude, and initial grain-boundary slip is presumably blocked at very small strains if it is to be blocked at all. It would seem, therefore, that the development of elastic strain energies of critical magnitude must involve processes not dependent upon such slip alone. An application of Mott's theories of creep to the problem of fracture mechanism has been made by Servi and Grant.[13, 28] Mott's theories[29] have indicated that (at a given stress) grain-boundary slip does not occur below a certain "critical" temperature. The type of creep which then takes place is that which he has called "exhaustion creep", in which the strain produced remains limited. Servi and Grant have connected this with change of fracture characteristics in aluminium. However, the prolonged period of definite steady creep in the tests on lead with which the present paper is concerned, do not indicate that exhaustion creep as such, or for that matter any radical change in creep type, is concerned.

A concept leading to a visualization of the intercrystalline fracture process of attractive simplicity, is that of creep as a flow process which can be represented for an ideally homogeneous substance by a vector point function $\mathbf{u}$, the velocity of flow of each elementary particle. It is usually accepted that density changes do not occur in creep, though actually slight decreases have been noted (e.g. by Hanson and Wheeler[30]). For the "ideal" substance, however, it can be stated that at every point $\operatorname{div} \mathbf{u} = 0$. This statement is based on the "equation of continuity" which connects volume changes (divergence of $\mathbf{u}$) with density changes:

$$\operatorname{div} \mathbf{u} = -\dot{\rho}/\rho$$

where ρ = density at the locality concerned and $\dot{\rho}$ = the "substantial" time rate of density change (see e.g. Brand[31] p. 259).

Real substances are not ideally homogeneous, nor is creep flow ideally uniform, certainly not on the atomic or even microscopic scale. In particular, in polycrystalline materials structural inhomogeneities and flow complications occur at grain boundaries. The hypothesis is offered that, as a result, at certain localities at grain boundaries in a substance undergoing creep, $\operatorname{div} \mathbf{u}$ is positive, i.e. $\dot{\rho}$ is negative and dilatation occurs; associated with such volumetric expansion there must be elastic strains. It is arguable that at localities of structural discontinuity, such as grain boundaries, the equation of continuity cannot be applied rigorously. The transition-zone theory indicates, however, that, as an approximation at least, the function $\mathbf{u}$ and its derivatives can be regarded as continuous at grain boundaries, although possibly changing suddenly with both position and time.

The relationship between $\mathbf{u}$ and the externally imposed constraints on a specimen undergoing creep is obviously not susceptible to exact determination in general. The relationship between $\operatorname{div} \mathbf{u}$ and the local extensile components of the rate of strain tensor can, however, be expressed very simply:

$$\operatorname{div} \mathbf{u} = e_{11} + e_{22} + e_{33}$$

e_{11}, &c., being the three (orthogonal) strain rates concerned.

In applying the equation of continuity, consideration is given to volumetric expansion alone, and it remains possible that other elastic distortion terms (e.g. elastic shear components) may contribute to the total local elastic strain energy. However, the tensors of stress, strain, and strain-rate can always be expressed in terms of the three "principal" components which do not contain shears. Furthermore, combination of the concepts offered here with the Zener theory of fracture, described above, indicates the probable absence of shear components along the actual surface of fracture inception at a suitable grain boundary.

Some further justification for this simplification arises from the observation that intercrystalline fracture often begins in boundaries more or less transverse to the applied stress (or hoop stress in pipe samples). This suggests that the maximum local elastic strain is approximately parallel to the principal stress direction. In addition, it seems likely that in the most probable region of fracture inception there is complete restriction of transverse flow, i.e. taking e_{11} as the rate parallel to the stress axis, fracture has maximum likelihood where $e_{22} = e_{33} = 0$. This corresponds to local triaxial tension, the region concerned expanding elastically in a direction parallel to the stress and not contracting in the orthogonal directions. No dilatation or elastic strain occurs, it should be noted, where $e_{22} = e_{33} = -\frac{1}{2}e_{11}$; this expresses the general conditions of inelastic strain away from the actual locality of fracture inception.

If λ represents the current length, parallel to the stress axis, of the elastically expanding region of fracture initiation visualized, then:

$$-\dot{\rho}/\rho = \operatorname{div} \mathbf{u} = e_{11} = \dot{\lambda}/\lambda$$

In such a region, the critical strain energy for fracture corresponds to a critical value of the local elastic strain. It follows that the general extension of the specimen reached at the time of fracture depends upon the relationship between $\dot{\lambda}/\lambda$ and the general creep rate of the specimen. Simple proportionality of the one to the other leads to an independence of the general extension (reached at beginning of fracture) from the creep rate, and this could at once explain the results for unalloyed lead and for some of the alloys. It is of interest to note further that, as Orowan[32] has pointed out, the order of theoretical strain for the breakage of atom-pair bonds is about 10–20%. This is of the same order as the general extensions reached for the substances here concerned, and suggests that the local elastic strain eventually responsible for fracture may be commensurate with the general inelastic creep strain. Logical interpretation of this would lead to the conclusion that the local stress concentration involved (at least on the atomic scale) would result in a maximum stress of the same order as the theoretical strength of the substance. This is not impossible, but it is arguable that it is improbable, and that the maximum value of the local stress likely to be attained is that corresponding to the so-called "brittle-fracture" stress. However, this must be of quite large value (since the substances concerned do not show notch-brittleness) and furthermore the fracture conditions in creep probably differ considerably from those concerned in ordinary brittle fracture or in notch sensitivity. In any case there is some support for the proposal of a simple relationship between the local elastic strain and the general creep strain for approximate calculation.

On the other hand, it must be quite clearly realized that the simplifications involved in such a calculation are extreme. Elastic distortion terms, or at least the effects of local elastic shear components, in all probability cannot be neglected. The final values of extension experimentally determined must be affected also by the rate of fracture propagation, and this in itself probably depends on quite complex factors. The "tertiary creep" period appeared to follow actual fracture inception in the tests above described, and, in those on pipe, appeared also to be very local. The difference between the total extension at the fracture locality and the general extension of the specimen was sometimes quite large, but usually smaller at slow creep rates than for the more rapid tests.

Notwithstanding possible complications, the simplified concepts above are suggested as being acceptable as first approximations, or as in a sense representing "semi-ideal" but possible conditions. An important consequence is the recognition of the good ductility (extensibility) of lead, even under conditions of creep leading to intercrystalline fracture, as the possible outcome of an expected independence of the extension at fracture from the creep rate.

On the basis of this theory the poor ductility at slow creep of various alloys can be explained as the result of occurrences leading to augmentations of the elastic strain fields at grain boundaries. Elastic strains around foreign atoms could be concerned, or strains resulting from precipitation of antimonial or tellurium-rich constituents, for example, in the lead alloys described above. Work-hardening by deformation before, or even during, primary creep could be another cause of elastic strain augmentation. Stress concentration at discontinuities (or microcracks) could also be concerned.

The marked increase of ductility, at slow creep, resulting from decrease of grain-size for a given alloy must, on the same basis, result from a decrease in the intensity or likelihood of elastic strains in boundary localities. The simplest explanation is that this is due to increased ease of recrystallization or grain-boundary migration; this view is supported by some results on the fine-grained samples of alloy E mentioned above, which recrystallized at large strains. Recrystallization was, however, less obvious in some of the other alloys and cannot afford a complete explanation. Increased ease of grain-boundary slip without stoppage can be suggested as one possible contributory cause of good ductility in fine-grained alloys.

The change in type of fracture with the creep conditions must result basically from differences in the mechanism of creep and ordinary plastic deformation. There is much evidence that the detailed mechanism of creep alters notably with applied stress and with temperature.[17, 28, 33, 34] The change in type of fracture for the substance studied must result from the absence of processes (multiple slip, localized deformations at boundaries, &c.) which limit the development of elastic strains at grain boundaries in ordinary plastic deformation. It would seem quite possible that there is a difference in distribution of associated elastic strains in slow creep and in plastic deformation. At slow creep rates such elastic strains, it is suggested, can become concentrated at localities of structural heterogeneity (providing these are suitably orientated with respect to the imposed stress system) and in plastic deformation they are more uniformly spread. The difference in behaviour in this respect is, it is further suggested, greater the slower the creep rate and the less the finer the grain-size.

VII.—SUMMARY AND CONCLUSIONS

(1) Creep tests to fracture have been conducted on samples of lead and lead alloys as used for cable sheathing, the samples being chiefly in the form of pipe extruded under similar conditions to those used for cable sheathing. The diametral extension produced by internal pressure has been found to be more or less independent of the time to fracture, within wide limits, for pure lead, some dilute solid-solution lead alloys, and some other lead alloys not of the solid-solution type, e.g. one containing 0·06% copper as an alloying addition. Alloys containing antimony in excess of the solid solubility limit (e.g. 0·35% antimony), alloy E (0·4% tin and 0·2% antimony), and some leads containing very small amounts of tellurium (about 0·01%) showed very poor ductility at slow creep rates.

All the substances tested were ductile at sufficiently rapid rates of strain (pipe samples under internal pressure failing with knife-edge longitudinal splits), but showed increasing liability to fracture of the intercrystalline type at slow creep rates.

(2) Tests on samples of pipe with the hoop stress

maintained constant indicated that the Andrade equation was at least approximately obeyed. The value of κ (the steady creep constant) corresponding to supervention of intercrystalline fracture was greater for the alloys than for unalloyed lead; the value of β (the transient creep constant) was less affected. Tests on samples in strip form at constant stress have also shown fair agreement with the Andrade equation. The value of κ at given stress was in general greater for strip than for pipe of the same alloy of similar grain-size.

(3) The creep conditions corresponding to change in type of fracture were notably affected by grain-size, decrease of which, for a given alloy, resulted in improvement in ductility. The results were also affected by degree of deformation of the samples before test, samples taken from coils on drums being in general less ductile under creep than those kept straight before testing.

(4) Some of the alloys, notably those containing antimony and those containing tellurium, showed marked influence of ageing upon the behaviour under subsequent creep; the ductility being greatly decreased. Other alloys having poor ductility under slow creep conditions did not appear to exhibit any purely time-dependent effects due to ageing.

(5) Some theoretical concepts have been advanced in connection with the fracture behaviour observed. It is indicated that under slow creep, elastic strain fields are likely to occur at grain boundaries as a result of structural and flow heterogeneities. Application of the " equation of continuity ", together with some simplifying assumptions, has led to an explanation of the difference in behaviour of unalloyed lead and the dilute solid-solution alloys studied, from the alloys exhibiting very poor ductility at slow creep. Elastic strain " augmenting " effects, it is considered, must account for the behaviour of the latter group of alloys.

ACKNOWLEDGEMENT

Acknowledgement is due to Dr. L. G. Brazier, Director of Research, British Insulated Callender's Cables, Ltd., for permission to publish these results.

REFERENCES

1. C. J. Beaver, *Elect. Rev.*, 1945, **136**, 468.
2. —, *Engineering*, 1949, **167**, 319.
3. A. Latin, *J. Inst. Metals*, 1948, **74**, 259.
4. A. Latin, *Engineering*, 1950, **170**, 121.
5. C. E. Pearson, *J. Inst. Metals*, 1934, **54**, 111.
6. A. Latin, *J. Sci. Instruments*, 1952, **29**, (3), 98.
7. E. N. da C. Andrade, *Proc. Roy. Soc.*, 1911, [A], **84**, 1; 1914, [A], **90**, 329.
8. F. R. N. Nabarro, *J. Inst. Metals*, 1948, **74**, 678 (discussion).
9. A. H. Cottrell and V. Aytekin, *ibid.*, 1950, **77**, 389.
10. E. N. da C. Andrade, *Nature*, 1948, **162**, 410.
11. J. McKeown and L. M. T. Hopkin, *Metallurgia*, 1950, **41**, 135, 219.
12. A. H. Sully, " Metallic Creep and Creep-Resistant Alloys ". London: **1949** (Butterworths Scientific Publications).
13. I. S. Servi and N. J. Grant, *Trans. Amer. Inst. Min. Met. Eng.*, 1951, **191**, 909.
14. W. D. Jenkins and T. G. Digges, *J. Research Nat. Bur. Stand.*, 1950, **45**, 153.
15. A. M. Freudenthal, " Inelastic Behaviour of Engineering Materials ", pp. 156 *et seq.* New York: **1950** (John Wiley and Sons, Inc.).
16. N. F. Mott and F. R. N. Nabarro, *Phys. Soc.: Rep. Conf. on Strength of Solids, Bristol*, **1948**, 1.
17. W. A. Wood and R. F. Scrutton, *J. Inst. Metals*, 1950, **77**, 423.
18. R. W. Cahn, "Progress in Metal Physics" (Edited by B. Chalmers), Vol. 2, pp. 151 *et seq.* London: **1950** (Butterworths Scientific Publications).
19. F. R. N. Nabarro, *Phys. Soc.: Rep. Conf. on Strength of Solids, Bristol*, **1948**, 75.
20. N. F. Mott, *Proc. Phys. Soc.*, 1951, [B], **64**, 729.
21. C. Zener, " Elasticity and Anelasticity of Metals ", pp. 147 *et seq.* Chicago: **1948** (University of Chicago Press).
22. T. S. Kê, *Phys. Rev.*, 1947, [ii], **71**, 533.
23. T. S. Kê, *J. Appl. Physics*, 1949, **20**, 274.
24. R. King, R. W. Cahn, and B. Chalmers, *Nature*, 1948, **161**. 682.
25. W. T. Read, Jr., and W. Shockley, *Symposium on Plastic Deformation of Crystalline Solids* (*Pittsburgh*), **1950**, 124.
26. K. T. Aust and B. Chalmers, *Proc. Roy. Soc.*, 1950, [A], **201**, 210.
27. N. F. Mott, *Research*, 1949, **2**, 162.
28. I. S. Servi and N. J. Grant, *J. Inst. Metals*, 1951–52, **80**, 33.
29. N. F. Mott, *Proc. Phys. Soc.*, 1948, **60**, 391.
30. D. Hanson and M. A. Wheeler, *J. Inst. Metals*, 1931, **45**. 229.
31. L. Brand, " Vector and Tensor Analysis ". New York: **1947** (John Wiley and Sons, Inc.).
32. E. Orowan, *Trans. Inst. Eng. Ship. Scotland*, 1946, **89**, 165.
33. D. McLean, *J. Inst. Metals*, 1951–52, **80**, 507.
34. W. A. Rachinger, *ibid.*, 1952–53, **81**, (1), 33.

NOTICE TO AUTHORS OF PAPERS FOR THE "JOURNAL"
AND CONTRIBUTORS TO DISCUSSIONS

1. **Papers will be considered for publication from non-members as well as members of the Institute.** They are accepted for publication in the *Journal* and not necessarily for presentation at any meeting of the Institute. MSS. should be addressed to The Editor of Publications, The Institute of Metals, 4 Grosvenor Gardens, London, S.W.1.

2. **Papers suitable for publication** may be classified as:

(*a*) Papers recording the results of original research.

(*b*) First-class reviews of, or accounts of progress in, a particular field.

(*c*) Papers descriptive of works methods, or recent developments in metallurgical plant and practice.

(*d*) Papers in classes (*a*), (*b*), and (*c*) above, previously published in languages other than English, French, German, or Italian, if of sufficient merit.

3. **Manuscripts and illustrations** should be submitted in duplicate. MSS. must be typewritten (*double-line spacing*) on one side of the paper only, and authors are requested to sign a declaration that neither the paper nor a substantial part thereof has been published elsewhere. Exceptions may be made in certain cases where a paper has been published in a language other than English, French, German, or Italian (see 2(*d*) above). MSS. not accepted are normally returned within 6 months of receipt.

In the interests of economy, all papers must be written as concisely as possible; in general, internal research reports are not in suitable form for publication as papers in the *Journal*. All but the simplest mathematical expressions should be written by hand, with capital and small letters clearly distinguished. Superscript and subscript letters should also be plainly indicated. Greek letters and special signs should be identified in the margin. For style, spelling, and abbreviations used, any recent issue of the *Journal* may be consulted.

4. **Synopsis.** Every paper must have a synopsis (not exceeding 250 words in length) which, in the case of a paper reporting original research, should state its objects, the ground covered, and the nature of the results. The synopsis will appear at the beginning of the paper, and should be in a form suitable for use by abstracting organizations. Extracts from a "Guide for the Preparation of Synopses" drawn up by the Abstracting Services Consultative Committee are reproduced below.

5. **References** must be collected at the end of the paper and must be numbered in the order in which they occur in the MS. Initials of authors must be given, and the Institute's official abbreviations for periodical titles (as used in *Metallurgical Abstracts*) should be employed, where known. References to papers should be set out in the style:

A. L. Dighton and H. A. Miley, *Trans. Electrochem. Soc.*, 1942, **81**, 321 (i.e. year, volume, page).

References to books should be in the following style:

C. Zener, "Elasticity and Anelasticity of Metals". Chicago: 1948 (University of Chicago Press).

6. **Illustrations.** Each illustration must have a number and description; only one set of numbers must be used in one paper, and it is desirable to number the half-tone illustrations consecutively, rather than to intersperse them with the line figures. The captions should be typed on a separate sheet.

The set of **line figures** sent for reproduction must be drawn (about twice the size to appear in the *Journal*) in Indian ink on smooth white Bristol board, good-quality drawing paper, co-ordinate paper, or tracing *cloth*, which are preferred in the order given. Co-ordinate paper, if used, must be blue-lined, with the co-ordinates to be reproduced finely drawn in Indian ink. Curves should be drawn boldly (i.e. at least twice the thickness of the frame). Experimental points should be indicated by open or closed circles, triangles, squares, &c. (preferably not crosses). Curves should be broken on each side of such symbols and plenty of allowance should be made for closing up in blockmaking. All lettering and numerals, &c., should preferably be in *pencil*, so that the Institute's standard lettering may be affixed, and ample margins must be left outside the framework of the figures to enable this to be done. The second set of line illustrations may be photostat copies.

Photographs must be restricted in number, owing to the expense of reproduction, and photomicrographs should be trimmed to the smallest possible of the following sizes consistent with adequate representation of the subject: 4 in. deep by 3 in. wide: 2 in. deep by 3 in. wide: 2 in. square. Magnifications of photomicrographs must be given in each case. Photographs for reproduction should be loose, not pasted down (and not fastened together with a clip, which damages them), and the figure number and author's name should be written on the back of each. Captions should be given to the photomicrographs, but these should be kept as brief as possible.

Because of the present high cost of printing and paper it is imperative that authors restrict illustrations (particularly photographs) to the absolute minimum deemed necessary to support their argument. Only in exceptional cases will illustrations be reproduced if already printed and readily available elsewhere.

7. **Tables or Diagrams.** Results of experiments, &c., may be given in the form of tables *or* figures, *but* (unless there are exceptional reasons) *not both*. Tables should bear Roman numbers, and each should have a heading that will make the data intelligible without reference to the text.

8. **Corrections.** A certain number of corrections in proof are inevitable, but any modification of the original text is to be avoided. Since corrections are very expensive, the Institute reserves the right to require authors to contribute towards their cost if the Editor deems them to be excessive. The Institute also reserves the right to require a contribution to the cost of remaking any block where this is necessitated by an error on the author's part.

9. **Reprints.** Individual authors are presented with a maximum of 25, and two or more authors with a maximum of 50 reprints from the *Journal*, without covers. Limited numbers of additional reprints can be supplied at the author's expense, if ordered before proofs are passed for press. (Orders should preferably be placed when submitting MSS.)

10. **Discussion.** Except in the case of special symposia, shorthand records of discussions are not taken at meetings. Written discussion may be submitted on any paper, preferably typewritten (*double-line spacing*). References should be given in the form of footnotes. Paragraphs 6 and 7 above are also applicable to such contributions. Reprints of discussion cannot be supplied to contributors.

GUIDE FOR THE PREPARATION OF SYNOPSES

(*As recommended by the Abstracting Services Consultative Committee*)

1. **Purpose.** The synopsis is not part of the paper; it is intended to convey briefly the content of the paper, to draw attention to all new information, and to the main conclusions. It should be factual.

2. **Style of writing.** The synopsis should be written concisely and in normal rather than abbreviated English. It is preferable to use the third person. Where possible use standard rather than proprietary terms, and avoid unnecessary contracting.

It should be presumed that the reader has some knowledge of the subject, but has not read the paper. The synopsis should therefore be intelligible in itself without reference to the paper; for example, it should not cite sections or illustrations by their numerical references in the text.

3. **Content.** The title of the paper is usually read as part of the synopsis. The opening sentence should be framed accordingly and repetition of the title avoided. If the title is insufficiently comprehensive, the opening should indicate the subjects covered. Usually the beginning of a synopsis should state the objective of the investigation.

It is sometimes valuable to indicate the treatment of the subject by such words as: brief, exhaustive, theoretical, &c.

The synopsis should indicate newly observed facts, conclusions of an experiment or argument and, if possible, the essential parts of any new theory, treatment, apparatus, technique, &c.

It should contain the names of any new compound, mineral species, &c., and any new numerical data, such as physical constants; if this is not possible, it should draw attention to them. It is important to refer to new items and observations, even though some are incidental to the main purpose of the paper; such information may otherwise be hidden, though it is often very useful.

When giving experimental results the synopsis should indicate the methods used; for new methods the basic principle, range of operation, and degree of accuracy should be given.

4. **References.** If it is necessary to refer to earlier work in the summary, the reference should always be given in full and not by number. Otherwise references should be left out.

When a synopsis is completed, the author is urged to revise it carefully, removing redundant words, clarifying obscurities, and rectifying errors in copying from the paper. Particular attention should be paid by him to scientific and proper names, numerical data, and chemical and mathematical formulæ.

SIMULTANEOUS DETERMINATION OF THE SURFACE TENSION OF TIN AND ITS CONTACT ANGLE WITH SILICA BY THE USE OF CONICAL CAPILLARIES *

By D. V. ATTERTON,† M.A., Ph.D., Junior Member, and
T. P. HOAR,‡ M.A., Ph.D., F.I.M., Member

SYNOPSIS

The surface tension of a liquid and its contact angle with a solid that it does not wet may be determined by measuring the pressures required to force the liquid into two capillaries of the solid, at least one of which is conical. Experimental and mathematical details of the method, especially as applied to molten metals, are described.

The surface tension of molten tin between 400° and 800° C. in a hydrogen atmosphere, determined by the method, is $(700 \pm 25) - (0{\cdot}17 \mp 0{\cdot}015)T$ dynes/cm., where T is the temperature in °K. The contact angle of tin with fused or polished silica surfaces, determined by the same experiments, is 145° ± 10°, independent of temperature but sensitive to the degree of roughness of the surface.

I.—INTRODUCTION

The reliable determination of surface tension and contact angles of molten metals and alloys has both fundamental and practical interest. Considerable insight into fundamental matters such as the mechanism of solidification, the adsorption of solutes or of gas molecules at molten metal surfaces, and the theory of metallic binding forces could be obtained from appropriate surface-tension measurements. In practical matters such as joining with molten metals, the production by "atomizing" of metal powders, the many kinds of metal casting, and the holding of molten metals in porous refractories, surface-tension phenomena play a critical part: we have previously shown [1] how the penetration of a range of metals into compacted moulding sands is governed by metallostatic pressure, surface tension, and contact angle, and we have indicated [2] the similar state of affairs prevailing in blast-furnace hearths carrying molten iron. All these studies will be greatly facilitated when more reliable values of surface tension, for a range of metals and alloys and for a range of temperatures, become available.

The experimental determination of the surface tension of molten metals and alloys presents several difficulties: the relatively high temperatures involved, the high contact angles between molten metals and refractory solids, and the ease with which metals become contaminated owing to oxidation or adsorption. These difficulties are emphasized by the large discrepancy between the published values of surface tension of molten metals; Fig. 1 shows the more reliable results that have been obtained for tin. The highest precision has been attempted in these determinations, and the scatter of each observer's results is only a few dynes/cm.; yet the differences between the various sets of results are as high as 30%. Unfortunately, full details of experimental technique have not always been published, so that assessment of the results is difficult.

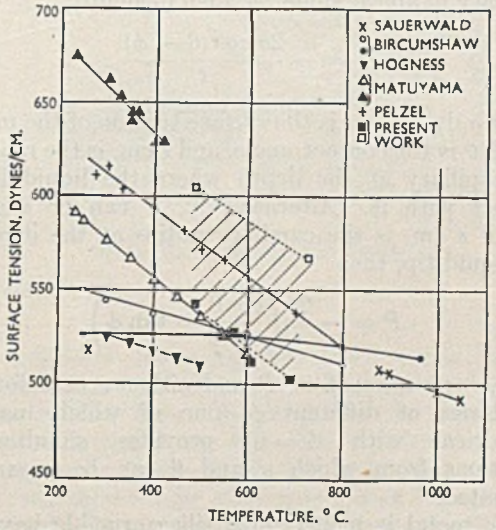

Fig. 1.—The Surface Tension of Molten Tin Between 232° and 1000° C., According to Several Authors.

Most determinations of metal surface tension have

---

* Manuscript received 4 December 1952.

† Formerly, Research Student, Department of Metallurgy, Cambridge University; now Research and Development Manager, Foundry Services, Ltd., Birmingham.

‡ Lecturer, Department of Metallurgy, Cambridge University.

been made using the method of maximum bubble pressure,[3–6] but the drop-weight,[7, 8] sessile-drop,[9–12] sessile-bubble,[13] hanging-drop,[14] and capillary-height [15] methods have also been used. Such quantitative determinations of the contact angles of molten metals with solids as have been made have usually been incidental to the determination of surface tension by the sessile-drop or capillary-height [16] methods; large values, 130°–180°, have been estimated. In previous work,[1] we have observed contact angles of *c.* 130° for sessile drops of several molten metals on silica.

The present paper gives details of a new method [17] for the simultaneous determination of surface tension of molten metals and their contact angles with silica or other refractory solids up to at least 1200° C., under conditions whereby surface contamination can be minimized. The method has so far been used to determine the surface tension of molten tin and its contact angle with silica between 400° and 800° C. Although the method is not at present capable of extreme precision, we believe that the results are reliable.

The principle of the method [17] is to force molten metal into *conical* silica capillaries to predetermined depths and to measure the pressure differences across the resulting molten metal surfaces. If the metal is forced by a pressure, P dynes/cm.^{2}, into a conical capillary of apical angle 2ϕ, then evidently

$$P = -\frac{2\sigma \cos(\theta - \phi)}{r} \quad . \quad . \quad . \quad (1)$$

where σ dynes/cm. is the surface tension of the molten metal, θ is the contact angle, and r cm. is the radius of the capillary at the depth where the liquid leaves contact with it. Alternatively, it can be shown * that if s cm. is the capillary radius at the depth of the liquid tip, then

$$P = -\frac{2\sigma}{s}\left(\frac{\cos\theta}{\cos\phi} + \tan\phi\right) \quad . \quad . \quad (2)$$

Thus, measurement of P and either r or s for two capillaries of different ϕ (one of which may be cylindrical with $\phi = 0$) provides simultaneous equations from which σ and θ can be separately evaluated.

The metal is melted in a silica crucible having a silica tube carrying several capillary bores, at least one of them conical, fused into its bottom. The gas pressure required to force the molten metal to a depth predetermined by means of a metal contacting wire is then measured for each conical capillary, and that required to effect metal entry into each cylindrical capillary is similarly found. The total pressure across the metal surface in a capillary is the sum of the applied gas pressure and the metallostatic pressure of the molten metal in the crucible. The metallostatic pressure cannot be measured directly with any degree of accuracy; consequently, for a single determination of surface tension and contact angle, measurements are made simultaneously on three capillaries, at least one of which is conical, so that three equations containing the three unknowns σ, θ, and the metallostatic pressure are available for their determination.

Several determinations of $\sigma \cos\theta$ for tin and silica, made with cylindrical capillaries only, are also described below. Measurement of the pressure required to force molten metal into a cylindrical capillary of radius r' cm. enables the product $\sigma \cos\theta$ to be determined by means of the usual formula

$$P = -\frac{2\sigma \cos\theta}{r'} \quad . \quad . \quad . \quad . \quad (3)$$

II.—EXPERIMENTAL TECHNIQUE

1. Materials and Apparatus

(a) *Tin*

The tin was of 99·998% purity, the only detectable impurity being 0·002% lead.

(b) *Silica Capillaries*

Conical capillaries were prepared by grinding and polishing from quadruple-bore transparent silica capillary tubing supplied by The Thermal Syndicate, Ltd. Five-cm. lengths of the tubing having one bore of which the major and minor axes differed by less than 0·5% were selected microscopically; such a capillary was used as the cylindrical in those determinations in which two conical and one cylindrical capillaries were used. Grinding tools were prepared by grinding cones, *c.* 2 cm. long, on the ends of 0·3–0·4-cm.-dia. silver-steel rods. A grinding tool, coated with a water slurry of 600-mesh carborundum, was inserted in the capillary and steadily rotated by hand; a conical shape, *c.* 0·4–0·5 cm. long, could be produced in about 1 hr. The final stages of the grinding were followed on a projection microscope to ensure that there was good radial symmetry of the conical portion about the longitudinal axis of the capillary. After grinding, the capillary was thoroughly

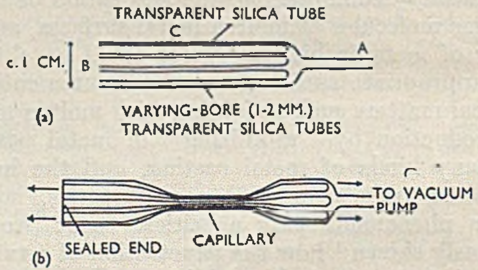

Fig. 2.—Preparation of Multibore Cylindrical Capillary Silica Tubing.

---

* See Appendix I (p. 548).

cleaned with water. A polishing tool was prepared by coating the tip of the grinding tool with molten picien wax, softened by the addition of a little white spirit; while the wax was still soft, it was pressed into the ground portion of the capillary, which had been moistened with water. This produced a sharp wax replica of the ground cone. When the wax had set hard, it was coated with a slurry of very fine rouge and the tool was steadily rotated in the conical portion, the slurry being renewed at intervals. One conical capillary could be polished in *c.* 4–8 hr. to complete transparency. After polishing, the capillaries were thoroughly cleaned by boiling successively in hydrochloric and nitric acids.

Multibore cylindrical capillaries for the determination of $\sigma \cos \theta$ were prepared as follows. Silica tubes were drawn down to have similar external diameter but varying bore (0·1–0·2 cm.); several of such tubes, sealed at one end, were then packed into a larger transparent silica tube (Fig. 2 (*a*)). The outer tube was heated for *c.* 5 min. and then end *B* was sealed, the open ends of the smaller tubes being sealed by allowing them to touch the viscous silica at *B*. The end *A* was connected to a vacuum pump and the outer tube was vigorously heated, whereupon it collapsed on to the smaller tubes and the interstices between them sealed up; collapse of the smaller tubes was prevented by the gas pressure inside them. The tube was then strongly heated at point *C* and steadily rotated, until the silica became sufficiently plastic for the gas pressure in the capillaries to make them become cylindrical. The fabricated tube was then drawn down to an external diameter of *c.* 0·4 cm. (Fig. 2 (*b*)).

(c) *General*

The apparatus (Fig. 3) consisted of a vertical tube furnace suitable for melting small amounts of metal in vacuum or in purified gas atmospheres, by means of high-frequency current obtained from a 35-kVA. spark-gap generator. The vacuum pump was a Speedivac capable of producing a vacuum of 10^{-5} cm. of mercury.

The silica crucible for holding molten metal had the multibore silica capillary fused vertically into a point approximately one-third along the diameter of the crucible base; the length of the capillary in the crucible was 1–1·5 cm. The crucible was fused into the end of a silica tube (Figs. 3 and 4) and the tube was then sealed with picien wax into a recess machined into the bottom brass furnace end (Fig. 3). Temperature gradients in the metal were minimized by surrounding the crucible with an auxiliary heater prepared by close-winding 0·04-cm.-dia. molybdenum wire on a former covered with paper, coating the wire with a thin layer of alumina cement, drying out the coil packed in charcoal at 600° C. in a muffle furnace, and baking it at 1000° C. in vacuum in the high-frequency furnace. The temperature of the molten metal was measured by means of a Chromel/Alumel thermocouple, of which the hot junction was carried in a silica sheath fixed in a brass tube with picien wax. The brass tube passed through a Tufnol taper, fitted into the top furnace end, with a push fit,

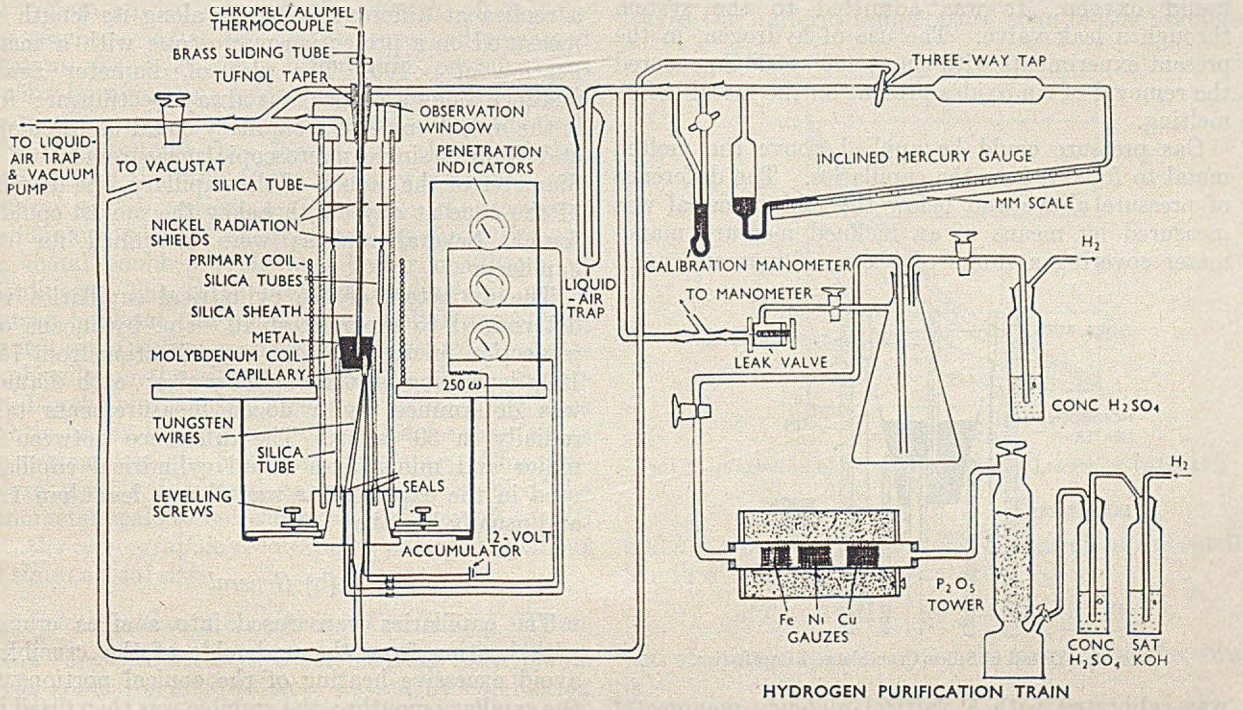

Fig. 3.—General Arrangement of Apparatus.

so that the position of the hot junction could be adjusted. The e.m.f. of the thermocouple was measured with a millivoltmeter calibrated against standard metals up to 1100° C.; readings were accurate to ±1° C., spatial and temporal fluctuations were probably ±3° C., and thus estimated temperatures are probably accurate to ±4° C.

The furnace atmosphere and the gas used for pressure application was hydrogen, purified by passing through saturated potassium hydroxide solution, concentrated sulphuric acid, phosphorus pentoxide, copper, nickel, and iron gauzes (these metals being heated to 650° C.), and a trap cooled in liquid oxygen. It was admitted to the system through a leak valve. The use of hydrogen, in the present experiments with tin at 400°–800° C., ensured the removal of tin oxides present on the metal before melting.

Gas pressure could be applied above the molten metal to force it into the capillaries. The difference of pressure above and below the molten metal was measured by means of an inclined mercury manometer covering a range of 4 cm. of mercury; this was calibrated with a vertical mercury manometer on which pressure differences were measured cathetometrically, so that measurements could be made to ±0·0005 cm. of mercury. To minimize sticking of the mercury in the inclined manometer, its stand was continually tapped with an electric buzzer during calibration and use. Rectilinear calibration curves were obtained for two inclined manometers A and B. A was used for vacuum determinations of $\sigma \cos \theta$ and B for all other determinations. In A, the space above the mercury in the inclined arm was evacuated to *c.* 10^{-4} cm. of mercury and was then sealed; consequently, the manometer was suitable for use only for pressures between 0 and 4 cm. of mercury. In B, the space above the mercury in the inclined arm was connected directly to the underside of the capillaries, and thus this manometer was suitable for measuring any pressure difference of up to 4 cm. of mercury.

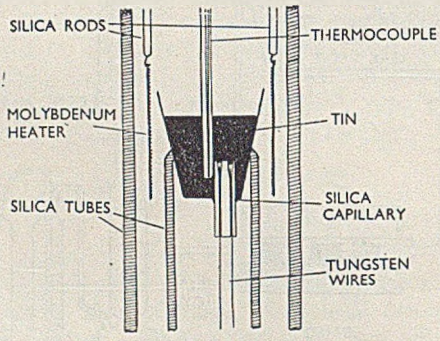

Fig. 4.—Detail of Silica Crucible and Capillaries.

A fixed point in each capillary was located by means of a tungsten wire. As the molten metal penetrated into the capillary, the instant of contact with the tungsten wire tip was indicated by means of an electrical circuit. The manometer reading at the time of contact was recorded photographically.

2. Procedure

(a) *Determination of Capillary Dimensions*

Before fusion of the capillaries into the silica crucible, the diameters at various depths in the conical capillaries were measured. Wax replicas of the conical portions were prepared in the same way as for the polishing tools; the wax was allowed to cool completely in the conical portion under the continuous application of pressure. The diameter of a replica at different distances along its length was measured on a projection microscope with a magnification of ×100. The plot of diameter against distance along a replica was always rectilinear; from it the apical angle of a capillary could be calculated, and from a single microscopic measurement of the diameter of the mouth of the capillary, the diameter of the cone at any depth below the mouth could be found. Several replicas were examined for each capillary.

The diameters of the cylindrical capillaries were determined to the nearest 10^{-4} cm. by means of a projection microscope with magnification from 75 to 150, depending on the capillary size; each diameter was determined by a dozen measurements taken radially in 30° steps. The difference between the major and minor axes of all cylindrical capillaries used in the experiments was always less than 1·0% and usually less than 0·5%.

(b) *General*

The capillaries were fused into a silica crucible, with heating from the underside of the crucible to avoid excessive heating of the conical portions and the capillary mouths; the crucible was then fused into a silica tube. Tungsten wires, *c.* 0·025 cm. in dia., for electrical contacts in the capillaries were heated in air to redness in order to coat the surface of the wire with oxide; this oxide is not wetted by molten metal and thus acts as a barrier to further molten-metal penetration into a capillary after contact has been made with the wire. The tips of the oxidized wires were then snipped off and the wires adjusted until their tips were at approximately the desired depths below the capillary mouths; the wires were then sealed through silica tubes in the bottom end of the furnace with picien wax. The depths of the wire tips below the capillary mouths were measured with a travelling microscope; six separate determinations of each depth were made.

Locating wires were arranged in each conical capillary; a contact wire was also put into the cylindrical capillaries, when these were used, and a further wire in a larger " dummy " capillary provided the necessary first contact with the molten metal.

Small pellets of tin were packed in the crucible, and the apparatus was assembled as shown in Fig. 3.

It was evacuated to a pressure of 1–2 × 10^{-4} cm. of mercury; purified hydrogen was then passed in and the apparatus re-evacuated. This cycle was repeated several times. Power was switched on to the furnace and, when a temperature of 350° C. was reached, the thermocouple junction was pushed into the melt to a depth calculated so that it was adjacent to the capillary mouths. By running the high-frequency generator at fixed values between 3 and 7 kVA., it was found that the temperature reached a constant value after 5–10 min. and remained constant to within ±1–2° C. over a period of several minutes. At *c.* 400° C., purified hydrogen was admitted into the system until a pressure of *c.* 40 cm. of mercury was reached. After the temperature had remained constant for 1–2 min., differential pressure was applied by admitting hydrogen to the upper part of the system only, at a rate controlled by the leak valve. The metal thus forced into the capillaries, coming from the bulk of the metal, was as free from surface contamination as possible; if necessary, preliminary passage of hydrogen upwards through the metal could provide still better conditions of cleanliness. The three pressure readings at which contact between the penetrating molten metal and the tungsten wires occurred were recorded photographically on the same photographic plate. Super-speed ortho-chromatic plates were used; they were slightly under-exposed, and developed for three times the normal time in fine-grain developer. This procedure greatly increased contrast and enabled the manometer scale to be read to an accuracy of ±0·005 cm., the photographic record being enlarged to about 2·5 times actual size.

(c) *Determination of Expansion of Indicating Wires*

The tungsten wires used for locating fixed points in the conical capillaries were heated by conduction through the silica, by conduction along the wire, and by radiation from the crucible. Consequently, the wires expanded and their tips were nearer to the mouths of the capillaries than had been determined in the cold with the travelling microscope. The expansion of the wire consists of two parts: y_1 cm., the expansion of the small length, l_1 cm., in the capillary surrounded by molten tin at a temperature T_m° C., and y_2 cm., the expansion of the length, l_2 cm., between the point where the capillary leaves the constant temperature zone and the point where the wire is fixed at the bottom end of the furnace, which is substantially at room temperature.

y_1 is equal to $l_1\alpha(T_m - T_r)$, where α is the coefficient of expansion of tungsten, 5 × 10^{-6} cm./cm./°C., and T_r° C. is room temperature.

y_2 may be determined from the temperature variation along the length l_2 of the wire. This variation was determined experimentally for a tungsten wire having molybdenum wires spot-welded at various points along its length, so as to make a series of tungsten/molybdenum thermocouples. This wire was inserted as usual into a capillary crucible in which the normally used weight of tin was melted and allowed to reach a constant temperature. During this period, the e.m.f.s of the series of tungsten/molybdenum thermocouples were measured at intervals. Fig. 5 shows the variation of temperature down the length of the wire. After 10 min., a logarithmic relation between temperature and distance was experimentally found,

$$\log_e (T - T_r) = \log_e (T_m - T_r) - bl$$

or

$$T - T_r = (T_m - T_r)e^{-bl},$$

where T° C. is the temperature of the wire at a distance l cm. from the point where the capillary leaves the uniform temperature zone of the crucible and b is a constant. Thus the expansion of the small length of wire dl at temperature T is

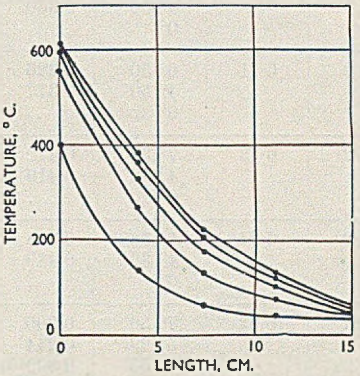

Fig. 5.—Variation of Temperature Along Length of Indicating Wire.

$$\alpha(T - T_r)dl = \alpha(T_m - T_r)e^{-bl} . dl,$$

and the total expansion y_2 of the length l_2 of the wire is

$$\alpha\int_0^{l_2}(T_m - T_r)e^{-bl} . dl$$

$$= -\frac{\alpha}{b}\left[(T_m - T_r)e^{-bl}\right]_0^{l_2}$$

$$= -\frac{\alpha}{b}\left[T - T_r\right]_0^{l_2}.$$

Taking $T = T_m$ when $l = 0$ and $T = T_r$ when $l = l_2$ (the latter a near approximation), we have:

$$y_2 = \frac{\alpha}{b}(T_m - T_r).$$

Thus, the experimental determination of b by the above method enables us to estimate y_2 for any values of T_m and T_r.

III.—RESULTS AND INTERPRETATION

1. Surface-Tension Determination

The relevant data of these determinations are given in Table I. An atmosphere of carefully purified hydrogen was used for these experiments, since preliminary work (described later in this Section) had shown that results obtained for $\sigma \cos \theta$ in hydrogen had better reproducibility than those obtained in vacuum. Fig. 1 shows the surface-tension results obtained over a temperature range of 400°–800° C. The solid squares in the figure represent the variation of surface tension with temperature as determined with two conical and one cylindrical capillary experiments. The two open squares represent results obtained by the use of three conical capillaries; they are significantly higher than the other values, a matter discussed later in this Section. The results of experiment 2 (Table I), evidently due to experimental error, have been ignored; they serve to illustrate that any small error in the experimental measurements may produce a large error in σ, as discussed in Appendix II (p. 550).

TABLE I.—*Data and Results of σ and θ Determinations with Conical Capillaries.*

Expt. No.	Temp., °C.	Density of Tin, g./c.c.	Angle, ϕ	Depth of Wires below Capillary Mouths, cm.	Expansion Correction, $(l_1 + l_2)$, cm.	Radius, s, cm.	Applied Gas Pressure, p_g, cm. Hg.	Pressure Correction for Depths of Wires and for Menisci, p_c cm. Hg.	σ, dynes/cm.	θ, deg.	$\sigma \cos \theta$, dynes/cm.
1	489	6·77	7° 36′ 4° 30′ 0°	0·176(5) 0·337(5) …	0·016(0) 0·015(7) …	0·0610 0·0403 0·0246(5)	0·482 1·038 2·512	0·068 0·151 …	543	155	492
2	408	6·83	6° 50′ 4° 50′ 0°	0·438 0·350 …	0·013(2) 0·013(4) …	0·0628(3) 0·0532 0·0255	0·418 0·716 2·629	0·205 0·162 …	768	132	514
3	609	6·71	6° 50′ 4° 50′ 0°	0·426 0·377 …	0·017(2) 0·017(4) …	0·0647(5) 0·0510(8) 0·0255	0·348 0·680 2·377	0·187 0·164 …	512	159	478
4	572	6·73	7° 38′ 4° 32′ 0°	0·410 0·419 …	0·018(1) 0·018(1) …	0·0592 0·0436 0·0248	0·307 0·755 2·302	0·181 0·188 …	528	152	466
5	692	6·64	7° 38′ 4° 32′ 0°	0·398 0·439 …	0·020(1) 0·020(0) …	0·0610 0·0420 0·0248	0·197 0·669 2·061	0·174 0·196 …	503	148	426
6	727	6·63	7° 50′ 5° 29′ 4° 55′	0·200 0·244 0·309(5)	0·022(1) 0·021(9) 0·021(7)	0·0653(3) 0·0467(5) 0·0398(7)	0·490 0·880 1·090	… 0·023 0·055	567	142	448
7	489	6·77	7° 50′ 5° 29′ 4° 55′	0·215 0·196 0·299	0·016(0) 0·016(0) 0·015(7)	0·0623 0·0507 0·0401	0·664 0·962 1·265	0·008 … 0·052	604	143	482

TABLE II.—*Data and Results of $\sigma \cos \theta$ Determinations with Cylindrical Capillaries.*

Expt. No.	Atmosphere	Temperature, °C.	Radii, cm.			Pressures, cm. Hg.			$\sigma \cos \theta$, dynes/cm.
			r_1	r_2	r_3	p_1	p_2	p_3	
1	Vacuum *	723	0·0528	0·456	…	0·590	0·750	…	354
2	,,	468	0·0674	0·0482	…	0·695	1·074	…	423
3	,,	525	0·0674	0·0482	…	0·657	1·008	…	392
4	,,	567	0·0674	0·0482	…	0·520	0·902	…	426
5	,,	629	0·0674	0·0580	0·0482	0·583	0·725	0·926	384 †
6	,,	580	0·0528	0·0456	…	0·530	0·710	…	398
7	Hydrogen ‡	460	0·0528	0·0456	…	0·645	0·834	…	418
8	,,	608	0·0674	0·0580	0·0482	0·592	0·735	0·938	387 †
9	,,	539	0·0652	0·0416	…	0·683	1·201	…	393
10	,,	672	0·0652	0·0416	…	0·640	1·153	…	389
11	,,	756	0·0652	0·0416	…	0·572	1·055	…	366
12	,,	789	0·0547	0·0412	…	0·523	0·847	…	356

* Hydrogen at 1–5 × 10^{-4} cm. Hg.
† Mean of three values (calculated from the radius and pressure results taken in pairs), all within ±2% of the mean.
‡ At 40–50 cm. Hg.

2. CONTACT-ANGLE DETERMINATION

The relevant data and results are given in Table I. With the exception of the value from experiment 2, the contact-angle values from experiments with two conical and one cylindrical capillaries are all substantially the same. The two experiments with three conical capillaries gave a somewhat lower result.

3. $\sigma \cos \theta$ DETERMINATION

Preliminary experiments were made with cylindrical capillaries to determine values of $\sigma \cos \theta$ for tin and silica in a vacuum (hydrogen at 1–5×10^{-4} cm. of mercury). The relevant data are given in Table II, and the results are shown in Fig. 6. The reproducibility was not very good, possibly on account of a slow rate of approach of the contact angle to its equilibrium value, or on account of surface contamination. To minimize contamination, further experiments were carried out in purified hydrogen at 40–50 cm. of mercury; the results, also shown in Fig. 6, were more reproducible. The regression curves for $\sigma \cos \theta$ on temperature for vacuum and hydrogen conditions are not significantly different, and the straight line of best fit for the joint data is given.

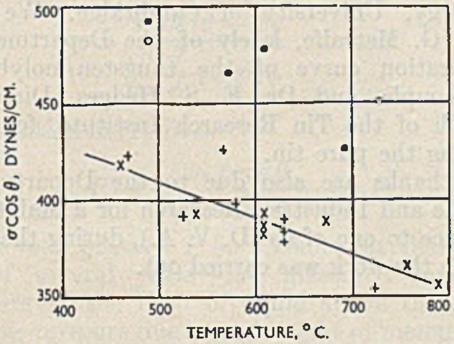

FIG. 6.—$\sigma \cos \theta$ Determinations for Molten Tin Between 400° and 800° C.

KEY.

\+ Vacuum : $\sigma \cos \theta$.
× Hydrogen : $\sigma \cos \theta$.
● Two conical, one cylindrical capillaries : $\sigma \times \cos \theta$.
○ Three conical capillaries : $\sigma \times \cos \theta$.

When the products of the surface tension and cosines of contact angles, obtained from the conical-capillary experiments, are plotted against temperature (Fig. 6), the results are significantly higher (by about 50–80 dynes/cm.) than the $\sigma \cos \theta$ values obtained using cylindrical capillaries. These higher values can only be explained by a different contact angle of tin on the two different silica surfaces, the conical capillaries having a ground and polished surface and the cylindrical having a fused surface. Consequently, since the silica surfaces of the three conical capillaries are essentially the same, we think that the values of surface tension and contact angle obtained with these may be more reliable than the other values. From these surface tension values and the data of the cylindrical capillary experiments, the contact angle of tin with the fused-surface cylindrical capillaries prepared in the laboratory may be calculated as c. 132° at 489° and 727° C.

When the contact angle determined in the experiments with three conical capillaries, viz. 142°, is used for a re-calculation of the experiments with two (polished) conical and one (fused, Thermal Syndicate) cylindrical capillaries, the contact angle for the cylindrical capillary may be calculated to be very close to the same figure. This arises from the form and parameters of the simultaneous equations, which, although they allow a perfect separation of σ and $\cos \theta$ in principle, are very sensitive to small errors. Further mathematical investigation is required to determine the best values of capillary angles and radii for providing the most significant separation of σ and $\cos \theta$ by solution of the simultaneous equations, and further experimental work is necessary to determine the precise influence of surface preparation on contact angle. Meanwhile, the present experimental results are consistent with the following expressions for the surface tension of tin, σ_{Sn}, and its contact angle, $\sigma_{\text{Sn-SiO}_2}$, with fused or polished silica in the range 400°–800° C. :

$$\sigma_{\text{Sn}} = (700 \pm 25) - (0{\cdot}17 \mp 0{\cdot}015)T \text{ dynes/cm.}$$

$$\theta_{\text{Sn-SiO}_2} = 145° \pm 10°, \text{ independent of temperature.}$$

The limits of the expression for σ_{Sn}, in which T is the temperature in °K., are indicated in Fig. 1. The expression leads, by extrapolation, to a value of 614 dynes/cm. for the surface tension of tin at the melting point (232° C.), in close agreement with the value of 610 dynes/cm. recently reported for this temperature by Smirnova and Ormont,[14] who used an improved hanging-drop technique.

IV.—DISCUSSION

The values obtained for the surface tension of tin are of the same order of magnitude as previous results (Fig. 1), although the scatter is somewhat greater. The large discrepancy between the results of various workers may be due partly to contamination of the tin caused by insufficient degassing of the apparatus and by incomplete purification of furnace atmosphere, and partly to differing degrees of purity of the tin. That used in the present experiments was of high purity, which may possibly explain the slightly higher values of surface tension obtained as compared with those of the majority of previous workers. A small percentage of impurity, e.g. lead, in the tin probably has a considerable influence on the surface tension; lead is selectively absorbed at the surface of the tin with consequent reduction of surface energy, as shown experimentally by Bircumshaw.[3] Another possible source of discrepancy is that the theory underlying most methods is insufficiently exact and leads to errors in calculation as well as in experiment.

The variation of surface tension with temperature is similar to that obtained by several other workers, notably Pelzel,[6] Matuyama,[8] and, to a lesser degree, Sauerwald and Drath.[4] Substitution of the best results from the present work in the thermodynamic relation $E_s = \sigma - T\frac{d\sigma}{dT}$, where E_s is the total surface energy necessary to form 1 cm.^{2} of new surface, σ is the surface tension, equivalent to the work done in forming 1 cm.^{2} of surface, and T is the temperature in °K., gives a value of *c.* 700 ergs/cm.^{2} for the total surface energy of liquid tin, independent of temperature, and *c.* 0·17 erg/cm.^{2}/°K. for the surface entropy. If we make the common assumption that surface energy and entropy concern the first atomic layer only, these values correspond to a total surface energy of 9400 cal./g.-atom and a surface entropy of 2·3 cal./g.-atom/°K. These values may be compared with the approximately known latent heat of evaporation, 79,000 cal./g.-atom, and the standard entropy of evaporation, 29·5 cal./g.-atom/°K.; it may be noted that the transfer of a tin atom from the bulk to the surface of liquid tin is associated with only small fractions of the energy and entropy changes occurring during the transfer of an atom from the bulk of the liquid to the vapour phase.

The high values of contact angle between tin and silica are not unexpected, being due to the high cohesion of the metal and its relatively low adhesion to the non-metal, a matter readily understood in terms of the accepted theories of metallic and non-metallic bonding.

The lower values of contact angle found on the surface of the fused capillaries as compared with the values obtained on the ground and polished capillaries may well be due to the greater smoothness of the fused silica surface. Since the true contact angle of tin on perfectly smooth silica is certainly greater than 90°, the tin does not penetrate into micro-crevices on a rough silica surface and there is no adhesion over these crevices; consequently, the average work of adhesion is less than on a smooth surface, which results in a higher contact angle.

In the early work of Smith [15] on liquid-metal surface tensions, calculations were based upon a contact angle of 180° between the metals and graphite; later, Libmann [16] observed very high contact angles between metals and alumina, and, in some cases, calculations were based upon $\cos\theta = -1$. Although a contact angle of 180° cannot be physically possible, it is quite likely that the relatively rough graphite and alumina surfaces used by Smith and by Libmann led to contact angles of greater than 170°, so that the error in taking $\cos\theta = -1$ may well have been small. Extension of the present work using deliberately roughened conical and cylindrical capillary surfaces might well show that, for many metals in contact with roughened silica, $\cos\theta = -1$ is a near approximation, and that consequently surface tensions could conveniently be measured by determinations of $\sigma\cos\theta$ with roughened cylindrical capillaries only. Such a method would greatly simplify both experiment and calculation, as well as minimizing errors in both.

V.—SUMMARY

(1) A method for the simultaneous determination of the surface tension of a molten metal and its contact angle with a refractory solid by the use of conical capillaries is described in experimental and theoretical detail.

(2) The surface tension of tin between 400° and 800° C. in a hydrogen atmosphere, determined by the method, is $(700 \pm 25) - (0{\cdot}17 \mp 0{\cdot}015)T$ dynes/cm., where T is the temperature in °K. The contact angle of tin with fused or polished silica over the same temperature range is $145° \pm 10°$, independent of temperature.

(3) Theoretical and practical implications of the method and of the results are discussed.

ACKNOWLEDGEMENTS

This work was carried out in the Department of Metallurgy, University of Cambridge. We thank Dr. A. G. Metcalfe, lately of the Department, for a calibration curve of the tungsten/molybdenum thermocouple, and Dr. E. S. Hedges, Director of Research of the Tin Research Institute, for kindly providing the pure tin.

Our thanks are also due to the Department of Scientific and Industrial Research for a Maintenance Allowance to one of us (D. V. A.), during the tenure of which the work was carried out.

APPENDIX I

Theory of Conical Capillaries

Fig. 7 represents the meniscus zone of a liquid, e.g. a molten metal, in a capillary of a solid that it does not wet. O is the point located by means of a central contacting wire.

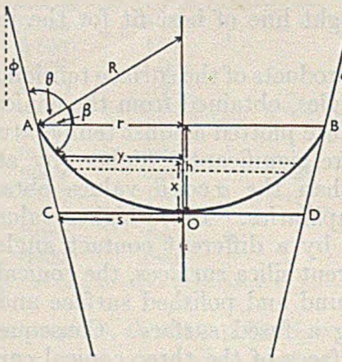

FIG. 7.—Geometry of Non-Wetting Liquid in Conical Capillary.

If P dynes is the total pressure difference across the liquid surface, r cm. the radius of the capillary at the level AB where the liquid leaves the surface, σ dynes/cm. the surface tension of the liquid, θ the contact angle, and 2ϕ the apical angle of the capillary, then by resolving forces vertically

$$P\,.\,\pi r^2 = \sigma\,.\,2\pi r \cos\{180 - (\theta - \phi)\}$$

and

$$P = -\frac{2\sigma\cos(\theta - \phi)}{r} \quad . \quad . \quad (1)$$

The experimental location of the point O enables the radius s cm. of the capillary in the plane CD to be determined. Thus if R cm. is the radius of curvature of the liquid meniscus, assumed spherical, then from Fig. 7

$$\begin{aligned} r &= s + h\tan\phi \\ &= s + R(1 - \sin\beta)\tan\phi \\ &= s + \frac{r}{\cos\beta}(1 - \sin\beta)\tan\phi \end{aligned}$$

or $$r = \frac{s\cos\beta}{\cos\beta - (1 - \sin\beta)\tan\phi};$$

and since $\beta = 180 - (\theta - \phi)$,

$$r = \frac{s\cos(\theta - \phi)}{\dfrac{\cos\theta}{\cos\phi} + \tan\phi} \quad . \quad . \quad . \quad . \quad . \quad (4)$$

Substitution in (1) gives

$$P = -\frac{2\sigma}{s}\left(\frac{\cos\theta}{\cos\phi} + \tan\phi\right) \quad . \quad . \quad (2)$$

The total pressure P for a conical capillary is made up of several parts—the measured applied gas pressure p_g, the head of liquid above the capillary, and the pressure due to the weight of mercury within the capillary. The head of liquid above the capillary is treated as an unknown and is determined by the use of an extra capillary; the correction for the liquid in the capillary is calculated from the experimentally determined dimensions of the capillary.

When determinations are made with two conical and one cylindrical capillaries, it is convenient to define as p_m the depth of liquid from the surface to the level of the capillary mouths, plus that due to the weight of liquid in the cylindrical capillary when its meniscus is just about to enter and run down to its contacting wire. p_m thus includes the meniscus correction H_1 for the cylindrical capillary (Fig. 8), H_1 being the height of a cylinder of liquid of radius equal to that of the capillary and weight equal to that of the liquid meniscus. The meniscus corrections for conical capillaries are H_2, &c. The correction to be added to $p_g + p_m$ for a conical capillary to take account of the depth of liquid in it below the level XY is thus (Fig. 8)

$$\begin{aligned} p_c &= l\,\frac{\rho_{\mathrm{Sn}}}{\rho_{\mathrm{Hg}}} \\ &= \{k - H_1 - (h - H_2)\}\,\frac{\rho_{\mathrm{Sn}}}{\rho_{\mathrm{Hg}}} \text{ cm. of mercury} \quad (5) \end{aligned}$$

where k is the depth of the contacting wire below the capillary mouth, and the ρ's are the metal densities.

The values of h and H for various capillary apical angles and values of the radius s are found as follows. From Fig. 7,

$$\begin{aligned} h &= \frac{r}{\cos\beta}(1 - \sin\beta) \quad . \quad . \quad . \quad . \quad . \quad (6) \\ &= \frac{r(1 - \sin\{180 - (\theta - \phi)\})}{\cos\{180 - (\theta - \phi)\}}, \end{aligned}$$

and substituting for r by means of (4) and simplifying, we have

$$\frac{h}{s} = \frac{\sin(\theta - \phi) - 1}{\dfrac{\cos\phi}{\cos\theta} + \tan\phi} \quad . \quad . \quad . \quad (7)$$

Consider now a circular section of the meniscus shown in Fig. 7, with radius y cm., height x cm.

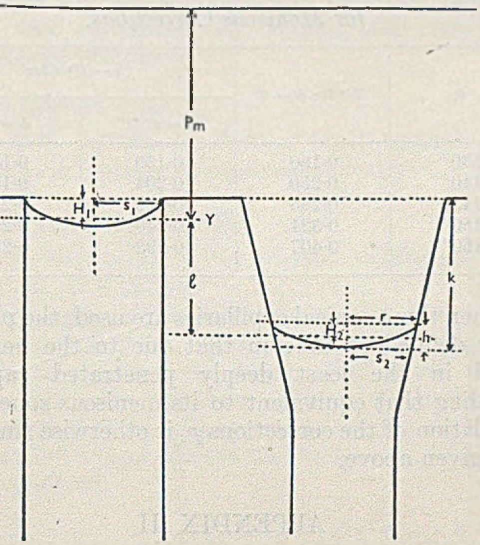

FIG. 8.—Corrections for Head of Metal, Metal in Capillaries, and Menisci.

above the point O and thickness dx cm. Its volume is $\pi y^2 dx$, and hence the total volume of the meniscus is

$$\begin{aligned} \int_0^h \pi y^2 dx &= \pi\int_0^h \{R^2 - (R - x)^2\}dx \\ &= \pi\left(Rh^2 - \frac{h^3}{3}\right) \end{aligned}$$

Thus the height of the cylinder radius r having the same volume is

$$\begin{aligned} H &= \frac{\pi\left(Rh^2 - \dfrac{h^3}{3}\right)}{\pi r^2} \\ &= \frac{h^2}{r^2}\left(R - \frac{h}{3}\right) \end{aligned}$$

Substituting $R = r/\cos\beta$ and for h by means of (6) we obtain

$$H = \frac{r(1 - \sin\beta)^2(2 + \sin\beta)}{3\cos^3\beta},$$

and finally substituting for r by means of (4)

$$\frac{H}{s} = \frac{(1 - \sin \beta)(2 + \sin \beta)}{3(1 + \sin \beta)\{\cos \beta - (1 - \sin \beta) \tan \phi\}}$$

$$= - \frac{\{1 - \sin (\theta - \phi)\}\{2 + \sin (\theta - \phi)\}}{3(1 + \sin (\theta - \phi))\left\{\dfrac{\cos \theta}{\cos \phi} + \tan \phi\right\}} \quad . \quad (8)$$

Table III gives values for $\frac{H}{s}$ and $\frac{(h - H)}{s}$ computed by means of (7) and (8) for different values of θ and ϕ. By its use (with suitable interpolation), the heights H_1 for a cylindrical capillary ($\phi = 0$) and $(h - H_2)$ for a conical may be found for any measured values of the radii s_1, s_2, and substitution of these values in (5) gives the correction p_c for the conical capillary.

TABLE III.—*Computed Values of H/s and $(h - H)/s$ for Meniscus Corrections.*

θ	H/s for $\phi = 0°$	$(h - H)/s$ for	
		$\phi = 4° 30'$	$\phi = 8°$
130°	0·190	0·159	0·145
140°	0·250	0·204	0·193
145°	0·285	0·226	0·217
150°	0·321	0·249	0·241
160°	0·407	0·292	0·289

When three conical capillaries are used, the pressure p_m is defined to take in that due to the height of metal in the least deeply penetrated capillary, including that equivalent to its meniscus zone. The calculation of the corrections p_c is otherwise similar to that given above.

APPENDIX II

Typical Calculation of σ and θ from Experimental Data

Experiment 1.—For data see Table I.

$$- \frac{2\sigma}{13{\cdot}56 \times 981}\left\{\frac{\cos \theta}{0{\cdot}0610 \cos 7° 36'} + \frac{\tan 7° 36'}{0{\cdot}0610}\right\}$$
$$= 0{\cdot}482 + p_m + p_{c_1} \quad . \quad (9)$$

$$- \frac{2\sigma}{13{\cdot}56 \times 981}\left\{\frac{\cos \theta}{0{\cdot}0403 \cos 4° 30'} + \frac{\tan 4° 30'}{0{\cdot}0403}\right\}$$
$$= 1{\cdot}038 + p_m + p_{c_2} \quad . \quad (10)$$

$$- \frac{2\sigma}{13{\cdot}56 \times 981}\left\{\frac{\cos \theta}{0{\cdot}0246(5)}\right\} = 2{\cdot}512 + p_m \quad . \quad (11)$$

p_m and p_{c_1}, p_{c_2} are the pressure corrections for the head of metal in the crucible and for the metal in the conical capillaries (as shown in Appendix I).

Assume $\theta = 150°$; then from (5) and Table III (Appendix I):

$$p_{c_1} = 0{\cdot}176(5) - 0{\cdot}016 - 0{\cdot}008 - 0{\cdot}015$$
$$= 0{\cdot}137(5) \text{ cm. Sn} = 0{\cdot}069 \text{ cm. Hg.}$$

$$p_{c_2} = 0{\cdot}337(5) - 0{\cdot}016 - 0{\cdot}008 - 0{\cdot}010$$
$$= 0{\cdot}303(5) \text{ cm. Sn} = 0{\cdot}152 \text{ cm. Hg.}$$

Subtracting (9) from (11), we have

$$- \frac{2\sigma}{13{\cdot}56 \times 981}\{40{\cdot}56795 \cos \theta - 16{\cdot}53865 \cos \theta$$
$$- 2{\cdot}18738\} = 2{\cdot}512 - 0{\cdot}482 - 0{\cdot}069 \quad . \quad (12)$$

and subtracting (10) from (11)

$$- \frac{2\sigma}{13{\cdot}56 \times 981}\{40{\cdot}56795 \cos \theta - 24{\cdot}89055 \cos \theta$$
$$- 1{\cdot}95285\} = 2{\cdot}512 - 1{\cdot}038 - 0{\cdot}152 \quad . \quad (13)$$

Dividing (12) by (13), we have

$$\frac{24{\cdot}02930 \cos \theta - 2{\cdot}18738}{15{\cdot}67740 \cos \theta - 1{\cdot}95285} = \frac{1{\cdot}961}{1{\cdot}322} = 1{\cdot}4833585$$
$$24{\cdot}0293 \cos \theta - 2{\cdot}18738 = 23{\cdot}2552 \cos \theta - 2{\cdot}89678$$
$$0{\cdot}7741 \cos \theta = - 0{\cdot}70940$$
$$\cos \theta = - 0{\cdot}9164$$
$$\therefore \theta = 156° 30'.$$

We now recalculate p_{c_1} and p_{c_2} for the contact angle of 156° 30′, obtaining as before from (5) and Table III in Appendix I:

$$p_{c_1} = 0{\cdot}176(5) - 0{\cdot}016 - 0{\cdot}009 - 0{\cdot}016$$
$$= 0{\cdot}135(5) \text{ cm. Sn} = 0{\cdot}068 \text{ cm. Hg.}$$

$$p_{c_2} = 0{\cdot}337(5) - 0{\cdot}016 - 0{\cdot}009 - 0{\cdot}011$$
$$= 0{\cdot}301(5) \text{ cm. Sn} = 0{\cdot}151 \text{ cm. Hg.}$$

Whence

$$\frac{24{\cdot}0293 \cos \theta - 2{\cdot}18738}{15{\cdot}6774 \cos \theta - 1{\cdot}95285}$$
$$= \frac{2{\cdot}512 - 0{\cdot}482 - 0{\cdot}068}{2{\cdot}512 - 1{\cdot}038 - 0{\cdot}151} = \frac{1{\cdot}962}{1{\cdot}323}$$
$$24{\cdot}0293 \cos \theta - 2{\cdot}18738 = 23{\cdot}2495 \cos \theta - 2{\cdot}89607$$
$$0{\cdot}7798 \cos \theta = - 0{\cdot}70869$$
$$\cos \theta = - 0{\cdot}90881$$
$$\theta = 155°$$

and from (12)

$$-2\sigma(24{\cdot}0293 \cos \theta - 2{\cdot}18738) = 1{\cdot}962 \times 13{\cdot}56 \times 981$$
$$2\sigma(24{\cdot}02547) = 26099{\cdot}23$$
$$\sigma = 543 \text{ dynes/cm.}$$

APPENDIX III

ESTIMATION OF ERRORS

(1) *Determination of Surface Tension and Contact Angle*

The errors in the values of σ and θ obtained depend on the experimental errors in ϕ, s, and p_g. Although the fundamental equation (2) is an approximation, the error involved is considerably less than these experimental errors.

Error in Capillary Angle, ϕ.

The semi-apical angle of the conical capillary was determined from a plot of diameter of a wax replica against its length. It may be estimated from the graphs obtained that the error is probably only ±1′.

Error in Radius, s cm.

(*a*) The travelling microscope, used for determining the depth of a wire tip below a capillary tip, had a depth of focus of just less than 0·001 cm. It was found experimentally that the readings, on the wire tip and on the capillary tip, could be obtained consistent to 0·001 cm., i.e. the depth could be estimated to ±0·0005 cm. An error of ±0·0005 cm. in the depth corresponds to an error of ±0·0005 tan ϕ cm. in the radius; thus, since tan ϕ is *c.* 0·1, the error in the radius is *c.* ± 0·00005 cm.

(*b*) There is an additional error in the radius associated with the error in the estimation of the expansion of the indicating tungsten wire. The magnitude of this second-order error is not known, but the reproducibility of surface tension and contact angle values suggest that it is small.

(*c*) An error due to the expansion of silica is also present, but it is so small that it may be ignored.

Error in Pressure, p_g cm. Hg

The solution of the simultaneous equations for σ and θ involves pressure differences and not absolute pressures; consequently, any possible errors in gauge calibration, or any systematic errors in reading the gauge, are largely eliminated. The photograph of the gauge, enlarged approximately to 2·5 times the actual gauge size, enabled the readings to be obtained to ±0·005 cm.; thus, since the gauge had a magnification factor of over 5, the error in the absolute pressure is probably less than ±0·001 cm. of mercury.

Table IV records the influence of these errors on the values of surface tension and contact angle, as calculated by the use of equation (2).

TABLE IV.

Error in	Error in θ	Error in σ
Capillary angle : ±1′. .	±0·6%	∓0·75%
Radius : ±0·00005 cm. .	±1·0%	∓1·25%
Pressure : ±0·001 cm. Hg. .	±1·25%	∓1·45%
Total error :	±3·0%	∓3·5%

(2) *Determination of $\sigma\cos\theta$*

For a single determination of $\sigma\cos\theta$, the gas pressure, p_g, needed to force the molten metal into a cylindrical capillary of known radius, r' cm., was measured for two capillaries. The values obtained were substituted in equation (3), and the value of $\sigma\cos\theta$ was calculated by solving the resultant simultaneous equations.

Error in Radius, r' cm.

The radii of the capillaries were measured to ±0·00005 cm., using a projection technique.

Error in Pressure, p_g cm. Hg

This is the same as for conical capillaries, viz. ±0·001 cm. of mercury.

Consideration of these errors in the radius and pressure shows that the $\sigma\cos\theta$ values should be accurate to ±1·2%. However, this is an underestimate, since the difference between the major and minor axes of the capillary bores (usually, however, less than 0·5% and always less than 1·0%) has not been considered.

REFERENCES

1. T. P. Hoar and D. V. Atterton, *J. Iron Steel Inst.*, 1950, **166**, 1.
2. T. P. Hoar and D. V. Atterton, *ibid.*, 1952, **170**, 145.
3. L. L. Bircumshaw, *Phil. Mag.*, 1926, [vii], **2**, 341.
4. F. Sauerwald and G. Drath, *Z. anorg. Chem.*, 1926, **154**, 79; 1927, **162**, 301.
5. T. R. Hogness, *J. Amer. Chem. Soc.*, 1921, **43**, 1621.
6. E. Pelzel, *Berg- u. hüttenmänn. Monatsh. montan. Hochschule Leoben*, 1948, **93**, 248.
7. P. Quincke, *Ann. Chem.*, 1859, **55**, 227.
8. Y. Matuyama, *Sci. Rep. Tôhoku Imp. Univ.*, 1927, [i], **16**, 555.
9. H. Siedentopf, *Ann. Physik u. Chem.*, 1897, **61**, 235.
10. R. Herzfeld, *ibid.*, 1897, **62**, 450.
11. C. Kemball, *Trans. Faraday Soc.*, 1946, **42**, 246.
12. H. H. Kellogg, private communication, 1951.
13. A. Portevin and P. Bastien, *Proc. Inst. Brit. Found.*, 1935–36, **29**, 88; and *Found. Trade J.*, 1936, **55**, 28.
14. Y. I. Smirnova and B. F. Ormont, *Doklady Akad. Nauk S.S.S.R.*, 1952, **82**, 751.
15. S. W. Smith, *J. Inst. Metals*, 1914, **12**, 168.
16. E. E. Libmann, *Univ. Illinois Eng. Exper. Sta. Bull.*, 1928, (**173**).
17. T. P. Hoar and D. V. Atterton, *Research*, 1951, **4**, 42.

1476

A THEORETICAL INVESTIGATION OF THE DEFORMATION TEXTURES OF TITANIUM *

By D. N. WILLIAMS,† Ph.D., Member, and Professor D. S. EPPELSHEIMER,‡ D.Sc., Member

SYNOPSIS

The deformation process in titanium was examined by applying the Calnan and Clews method of texture analysis (*Phil. Mag.*, 1950, [vii], **41**, 1085; 1951, [vii], **42**, 616, 919; 1952, [vii], **43**, 93) to the experimentally determined textures. It proved possible to develop a theoretical deformation process which would result in the formation of the observed deformation textures. This deformation process required the interaction of three slip systems, $\{0001\}\langle 11\bar{2}0\rangle$, $\{10\bar{1}1\}\langle 11\bar{2}0\rangle$, and $\{10\bar{1}0\}\langle 11\bar{2}0\rangle$, and two types of twinning, $\{10\bar{1}2\}$ and $\{11\bar{2}2\}$. Each of these modes of deformation was examined separately, and then they were combined to give the observed deformation textures. The critical shear stresses for slip (C_s) and for twinning (C_t) were found to be related in the following manner: $C_{s0001} = 1\cdot 1\, C_{s10\bar{1}1} = 1\cdot 02\, C_{s10\bar{1}0} = C_{t10\bar{1}2} = C_{t11\bar{2}2}$.

I.—INTRODUCTION

The cold-rolled textures of several hexagonal metals have been found to be predominantly $(0001)[11\bar{2}0]$. This texture is the result of $\{0001\}\langle 11\bar{2}0\rangle$ slip and $\{10\bar{1}2\}$ twinning.[1] Recent investigations of the metals titanium,[2] zirconium,[3] and beryllium [4] have indicated that these hexagonal metals do not deform by this simple mechanism, since their cold-rolled textures deviate considerably from the ideal $(0001)[11\bar{2}0]$ texture.

Titanium showed the greatest deviation from the ideal hexagonal texture; it showed a $(0001)[10\bar{1}0]$ texture rotated 30° toward the transverse direction. The textures of titanium after compression [5] and cold rolling [6] were re-determined, using a semi-quantitative Geiger-counter pole-figure technique. The results of these experimental texture studies were examined by the method of texture analysis developed by Calnan and Clews,[7-10] which had been successful in predicting the texture of both zinc and magnesium.

By use of the Calnan and Clews method of texture analysis, it was possible to postulate a theoretical deformation process which would result in the formation of the experimentally observed deformation textures of titanium.

II.—THE DEFORMATION TEXTURES OF TITANIUM

No texture studies of the tension texture of titanium have been reported in the literature. The wire texture has been examined by Yen [11] and found to be $[10\bar{1}0]$. The tension texture is generally similar to the wire texture in hexagonal metals. The tension texture of titanium has therefore been assumed to be $[10\bar{1}0]$ in the following discussions.

The compression texture of iodide titanium has been described as a rotated [0001] texture.[5] As the amount of reduction in compression increased, the angle of rotation of the [0001] texture decreased, varying from 32·5° at low reductions to 17·5° at 98·9% reduction. The relative intensity of the 0001 maximum was practically constant regardless of the amount of reduction, suggesting that the compression texture was an equilibrium texture existing between two opposing end textures. A slight indication that the [0001] rotation occurred about a $\langle 10\bar{1}0\rangle$ axis was noticed in the $10\bar{1}0$ and $10\bar{1}1$ pole figures.

The texture of cold-rolled iodide titanium was found to be $(0001)[10\bar{1}0]$, rotated 30° in the transverse direction [6] as previously reported. A very strong maximum was found in the rolling direction of the $10\bar{1}0$ pole figure. This maximum was seven times stronger than the second maximum in the $10\bar{1}0$ pole figure. The 0001 pole figure showed a spread of orientations from the transverse direction to the rolling plane normal along the transverse axis. An 0001 maximum was measured at an angle of 30° from the rolling plane normal with a minimum occurring at the rolling plane normal. At lower reductions a weak 0001 maximum was noticed in the transverse direction. This maximum disappeared as the reduction increased.

III.—THE CALNAN AND CLEWS METHOD OF TEXTURE ANALYSIS

The Calnan and Clews method of texture analysis, referred to below as the Calnan and Clews method, is

---

* Manuscript received 28 November 1952.

† Research Engineer, Kaiser Aluminium and Chemical Corporation, Spokane, Washington; formerly National Lead Research Fellow, Missouri School of Mines and Metallurgy, Rolla, Missouri, U.S.A.

‡ Professor of Metallurgical Engineering, Missouri School of Mines and Metallurgy, Rolla, Missouri, U.S.A.

a method of averaging the slip-rotation tendencies of grains with all possible orientations for the determination of the main rotation tendency leading toward the formation of the deformation texture.

The Calnan and Clews method is based on the following assumptions:

1. Only the slip or twinning system which has the maximum resolved shear-stress ratio will be active. The resolved shear-stress ratio is defined as the ratio of the resolved shear stress to the critical shear stress. When the value of this ratio is greater than unity, slip or twinning should occur. For double slip to occur, two slip systems must have equal resolved shear-stress ratios. Multiple slip occurs whenever three or more slip systems have equal resolved shear-stress ratios.

2. Slip and twinning are equally probable when the resolved shear-stress ratio for slip equals the resolved shear-stress ratio for twinning. If the resolved shear-stress ratio for twinning exceeds the resolved shear-stress ratio for slip, twinning will occur.

3. The value of the resolved shear stress is calculated from the position of the effective stress, T_e, rather than from that of the applied stress, T_a. It is possible for T_e to be some distance from T_a. By the use of the concept of effective stress, it is possible to explain why a single grain can deform by multiple slip when the applied stress position is such that only single slip should occur. Thus it is possible for single, double, and multiple slip to occur in the same grain owing to differences in the positions of the effective stress in various parts of the grain. The movements of T_e from T_a can be visualized as the result of grain-boundary influences.

To determine the general rotation tendencies, the resolved shear-stress contour diagram for the slip system having the highest resolved shear-stress ratio is plotted in the unit triangle. If two or more slip systems are active within the unit triangle, the resolved shear-stress diagram for each system is plotted in the portion of the unit triangle in which it is active.[8]

The rotation tendencies for single slip and double slip are determined for each position of T_a within the unit triangle. In single slip, the slip plane normal rotates toward the stress axis in compression and the slip direction rotates toward the stress axis in tension. In double slip, the great circle joining the two active slip plane normals rotates toward the stress axis in compression and the great circle joining the two active slip directions rotates toward the stress axis in tension. In multiple slip no rotation occurs if the stress axis is located symmetrically. If the stress axis is unsymmetrically located, rotation occurs towards a symmetrical position. These rotations are shown by appropriate movements of the stress axis in the unit stereographic triangle, since the slip direction and slip plane normal are fixed.

For simplicity, the movement of T_e is restricted to a contour gradient, that is, T_e is allowed to move only along the most direct route from one resolved shear-stress contour line to the next lower line. Whenever the resolved shear stress exceeds the critical stress necessary for slip to take place, slip may occur or T_e may move to a position of lower resolved shear stress such that the resolved shear stress is no longer greater than the critical shear stress. The movement of T_e and its effect on texture formation is discussed fully by Calnan and Clews.[7–9]

The Calnan and Clews method has been successful in explaining the deformation textures of the hexagonal metals magnesium and zinc[9] and also metals in the face-centred cubic,[7] body-centred cubic,[8] and orthorhombic[10] systems.

IV.—THE CALCULATION OF RESOLVED SHEAR-STRESS VALUES

The resolved shear stress for any slip system is equal to $T_a \cos x \cos \lambda$, where x is the angle between the stress axis and the slip plane normal, λ is the angle between the stress axis and the slip direction, and T_a is the applied stress.

The resolved shear stress for any twinning system is equal to $T_a \cos \gamma \cos \delta$, where γ is the angle between the stress axis and the twin plane normal, δ is the angle between the stress axis and the twinning shear direction, and T_a is the applied stress.

The resolved shear-stress values for all the slip planes in the slip system being considered were calculated, and the resolved shear-stress contour diagram plotted for the slip plane having the maximum value. A similar calculation was made for each twin plane in the twinning systems considered.

Values of x, λ, γ, and δ were determined by direct measurement over a 7-in. Wulff net graduated in 2° intervals. Measurements were made by estimating to the nearest 0·2° and the results of the cosine function plotted. Shear-stress contour diagrams were obtained by making sufficient measurements to locate the approximate position of each contour line. These diagrams are probably accurate to about 2°. Boundary lines between two slip systems or between slip and twinning systems were located by plotting the positions of T_a and measuring the values of the appropriate angles until the following equations were solved:

$$\text{for slip: } \cos x_1 \cos \lambda_1 / C_{s_1} = \cos x_2 \cos \lambda_2 / C_{s_2} \quad (1)$$

$$\text{for twinning: } \cos x \cos \lambda / C_s = \cos \gamma \cos \delta / C_t \quad (2)$$

where C_s is the critical shear stress for slip and C_t is the critical shear stress for twinning.

A mathematical analysis[8] has shown that this boundary may have two possible forms. At least three points were located on each boundary to determine its position and its form.

Values of the ratios between the critical shear stresses had to be assumed. In some cases there was justification for the assumptions made, but in most cases there was a considerable range of possible values.

V.—DEFORMATION BY SLIP

The hexagonal metals subjected to critical study have been found to slip in the $\{0001\}\langle 11\bar{2}0\rangle$ system.[1] This system will tend to give a tension texture of the type $[11\bar{2}0]$. Examination of the wire texture of titanium [11] showed titanium to have a strong $[10\bar{1}0]$ texture. A preliminary report on the plastic flow of titanium [12] showed slip in titanium to occur on both the $\{10\bar{1}0\}$ and $\{10\bar{1}1\}$ planes. These results have not yet led to a determination of the slip direction. Since the slip direction is usually retained in other metals which exhibit slip on several planes, a $\langle 11\bar{2}0\rangle$ slip direction was assumed. The results showed no evidence of $\{0001\}$ slip, but at the low reduction necessary for location of slip elements by the trace method, this mode of slip may be relatively inactive. As will be shown later, $\{0001\}$ slip was essential in the explanation of the compression and rolling textures. The resolved shear-stress contour diagram for each of these three slip systems was developed, and the resulting tension and compression textures were examined. Finally, the three slip systems were combined to give a tension and compression texture that agreed as much as possible with the observed textures.

1. $\{0001\}\langle 11\bar{2}0\rangle$ Slip

Slip on the base plane is simplified by the existence of only one active slip plane. The resolved shear-stress contour diagram is shown in Fig. 1. At both the $[0001]$ point and the $[10\bar{1}0]$-$[11\bar{2}0]$ edge the resolved shear stress is zero and no slip can occur. Within the unit triangle slip occurs on the $(0001)[11\bar{2}0]$ system. Double slip occurs along the $[0001]$-$[10\bar{1}0]$ edge on the $(0001)[11\bar{2}0]$ and $(0001)[2\bar{1}\bar{1}0]$ systems.

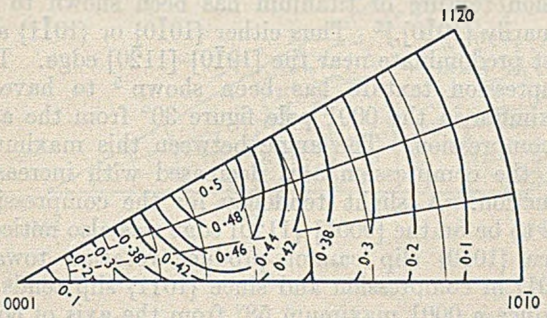

Fig. 1.—Resolved Shear Stress Contours for $\{0001\}\langle 11\bar{2}0\rangle$ Slip.

Single-slip rotations in tension are toward $[11\bar{2}0]$. Double-slip rotations in tension are toward $[10\bar{1}0]$. The tension texture will therefore consist of a moderate $[11\bar{2}0]$ component with a spread of orientations along the $[10\bar{1}0]$-$[11\bar{2}0]$ edge.

In compression both single and double slip rotations lead to a $[0001]$ position, resulting in a strong $[0001]$ compression texture.

Slip on the $\{0001\}\langle 11\bar{2}0\rangle$ system has been examined by Calnan and Clews, and a complete discussion of the rotation tendencies may be found in their treatment.[9]

2. $\{10\bar{1}1\}\langle 11\bar{2}0\rangle$ Slip

The $\{10\bar{1}1\}\langle 11\bar{2}0\rangle$ system contains six slip planes, each of which has two possible slip directions. The resolved shear-stress diagram for this system is shown in Fig. 2. This diagram is more complicated than that for $\{0001\}$ slip, since two different slip systems are active within the unit stereographic triangle. In addition, points *B*, $[11\bar{2}0]$, and $[10\bar{1}0]$ each support multiple slip on four slip systems. In the region *A*–*B*-$[11\bar{2}0]$-$[10\bar{1}0]$ slip occurs on the $(01\bar{1}1)[2\bar{1}\bar{1}0]$ slip system. In the region $[0001]$-*A*–*B* slip occurs on the $(\bar{1}101)[11\bar{2}0]$ slip system. Double slip occurs along the boundaries $[0001]$-$[10\bar{1}0]$, $[10\bar{1}0]$-$[11\bar{2}0]$, $[11\bar{2}0]$-*B*, *B*-$[0001]$, and *A*–*B*.

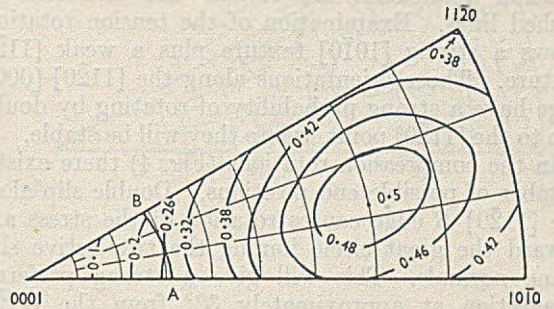

Fig. 2.—Resolved Shear Stress Contours for $\{10\bar{1}1\}\langle 11\bar{2}0\rangle$ Slip.

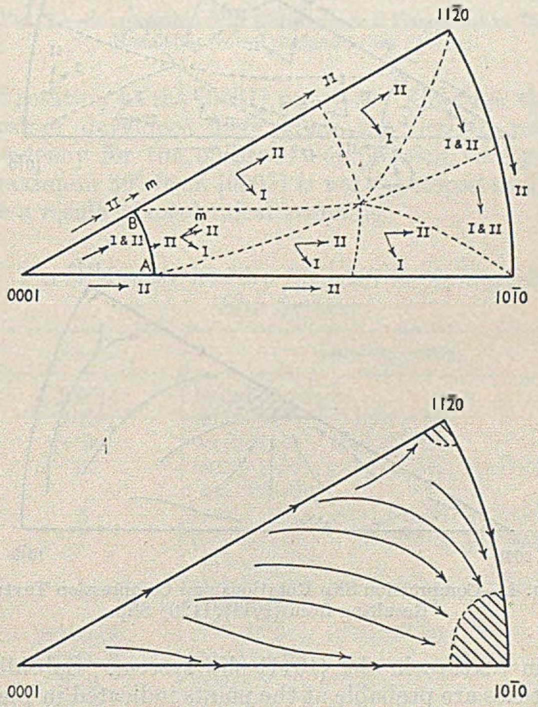

Fig. 3.—Tension Slip Rotations and Tension Texture Resulting from $\{10\bar{1}1\}\langle 11\bar{2}0\rangle$ Slip.

The tension rotations and the resulting tension texture for $\{10\bar{1}1\}$ slip are given in Fig. 3. Owing to the unsymmetrical position of the slip planes at point *B*, multiple slip occurs. Single slip rotations are shown by an arrow marked I, double slip rotations by an arrow marked II, and multiple slip rotations by an arrow marked *m*. Areas within which the rotation tendencies are similar are enclosed by dashed lines. Examination of the tension rotations shows a strong $[10\bar{1}0]$ texture plus a weak $[11\bar{2}0]$ texture. Those orientations along the $[11\bar{2}0]$-$[0001]$ edge have a strong probability of rotating by double slip to the $[11\bar{2}0]$ point, where they will be stable.

In the compression rotations (Fig. 4) there exist a number of possible end positions. Double slip along the $[11\bar{2}0]$-*B* edge causes rotation of the stress axis toward the great circle joining the two active slip-plane normals. This will give a strong preferred orientation at approximately 32° from the $[11\bar{2}0]$ point. Since single slip rotates most of the orientations within the *A*-*B*-$[11\bar{2}0]$-$[10\bar{1}0]$ region to the $[11\bar{2}0]$-*B* edge, the concentration at 32° should be the main texture in the $\{10\bar{1}1\}$ slip system. Subsidiary textures are probable at the points indicated in Fig. 4.

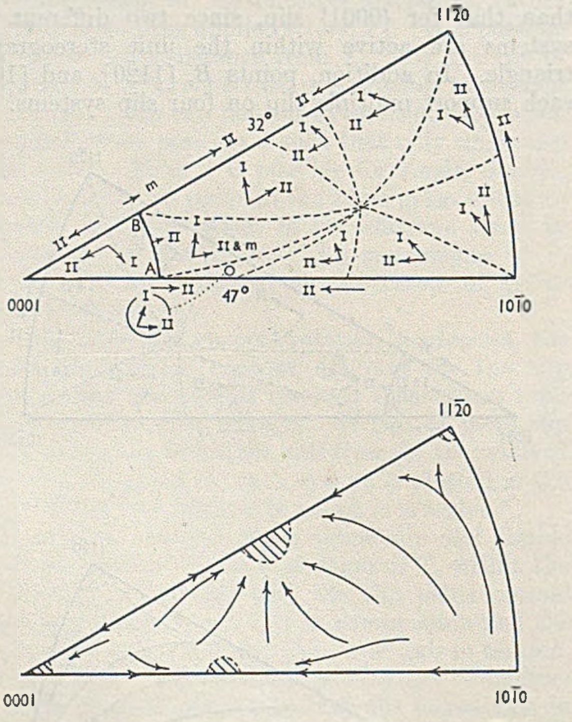

Fig. 4.—Compression Slip Rotations and Compression Texture Resulting from $\{10\bar{1}1\}\langle 11\bar{2}0\rangle$ Slip.

3. $\{10\bar{1}0\}\langle 11\bar{2}0\rangle$ SLIP

This slip system is symmetrical about the midpoint between the $[10\bar{1}0]$ and $[11\bar{2}0]$ points, as is shown in Fig. 5. Within the unit triangle slip occurs on the $(01\bar{1}0)[2\bar{1}\bar{1}0]$ system. Double slip occurs along the $[0001]$-$[10\bar{1}0]$ and $[0001]$-$[11\bar{2}0]$ edges.

The single-slip tension rotations are toward $[2\bar{1}\bar{1}0]$, while double-slip rotations are toward $[11\bar{2}0]$ along the $[0001]$-$[11\bar{2}0]$ edge and toward $[10\bar{1}0]$ along the $[0001]$-$[10\bar{1}0]$ edge. This will result in the formation of a strong $[10\bar{1}0]$ component plus a weak $[11\bar{2}0]$ component in the tension texture.

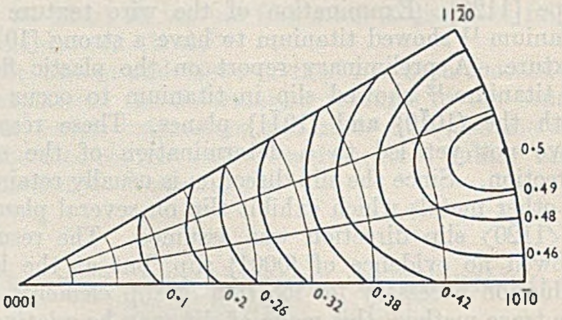

Fig. 5.—Resolved Shear Stress Contours for $\{10\bar{1}0\}\langle 11\bar{2}0\rangle$ Slip.

The single-slip compression rotations are toward $[01\bar{1}0]$, while the double-slip rotations remain the same as in tension. A strong $[11\bar{2}0]$ component plus a weak $[10\bar{1}0]$ component will occur in the compression texture.

4. COMBINED SLIP SYSTEM

Before the three slip systems are combined it is necessary to consider the experimental data. The tension texture of titanium has been shown to be primarily $[10\bar{1}0]$.[11] Thus either $\{10\bar{1}0\}$ or $\{10\bar{1}1\}$ slip must predominate near the $[10\bar{1}0]$-$[11\bar{2}0]$ edge. The compression texture has been shown[5] to have a maximum in the 0001 pole figure 30° from the axis of compression. The angle between this maximum and the compression axis decreased with increased reduction. A slight tendency for the compression axis to be on the $[0001]$-$[11\bar{2}0]$ edge was also noticed. Since $\{10\bar{1}0\}$ slip cannot produce rotation toward $[0001]$ in compression and since $\{10\bar{1}1\}$ slip tends to produce a 0001 maximum 58° from the axis of compression (see Fig. 4), $\{0001\}$ slip must be active at least to a point within 32° of the $[11\bar{2}0]$ point along the $[0001]$-$[11\bar{2}0]$ edge.

The determination of slip elements of titanium[12] indicated that $\{0001\}$ slip was absent and $\{10\bar{1}0\}$ slip was the primary mechanism of slip. Because of these results the $\{0001\}$-$\{10\bar{1}1\}$ slip boundary was adjusted so that the critical shear stress for $\{0001\}$ slip was as large with respect to the critical shear stress for $\{10\bar{1}1\}$ slip as possible without allowing $\{10\bar{1}1\}$ slip to form the maximum along the $[0001]$-$[11\bar{2}0]$ edge 32° from $[11\bar{2}0]$. This was accomplished by placing the boundary between the two systems 30° from $[11\bar{2}0]$. Equation (1) was used for this calculation, and the following ratio of the critical shear stresses was obtained,

$$C_{s0001} = 1{\cdot}1\, C_{s10\bar{1}1} \quad . \quad (3)$$

Although the results of the above-mentioned determination of slip elements in titanium indicated that $\{10\bar{1}0\}$ slip predominates at low reductions, the lack of appreciable $[11\bar{2}0]$ compression texture at higher reductions[5] indicates that it is relatively unimportant or possibly completely absent at high reductions. For the purpose of this development the $\{10\bar{1}0\}$–$\{10\bar{1}1\}$ slip boundary was calculated on the assumption that it crossed the $[0001]$–$[11\bar{2}0]$ edge 5° from $[11\bar{2}0]$. This resulted in a ratio of critical shear stresses of:

$$C_{s10\bar{1}0} = 1{\cdot}078\, C_{s10\bar{1}1} \quad . \quad . \quad . \quad (4)$$

The assumption that $\{10\bar{1}0\}$ slip is occurring is unnecessary at high reductions, but it is included so that its effect at lower reductions may be considered.

Combining equations (3) and (4) gives the following relationship between the critical shear stresses for slip on the three slip systems:

$$C_{s0001} = 1{\cdot}1\, C_{s10\bar{1}1} = 1{\cdot}02\, C_{s10\bar{1}0} \quad . \quad (5)$$

The tension and compression textures resulting from the assumption that the above ratios of critical shear stress were correct are shown in Figs. 6 and 7. The slip systems active in the combined slip system are given in Table I.

Examination of the tension rotations and the resulting tension texture given in Fig. 6 shows that the texture will be predominantly $[10\bar{1}0]$. A weak $[11\bar{2}0]$ texture is also evident.

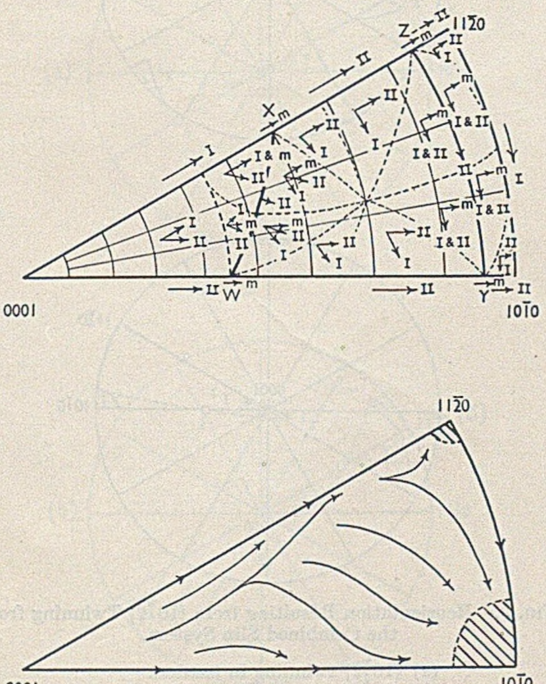

Fig. 6.—Tension Slip Rotations and Tension Texture Resulting from Combined Slip System.

The compression rotations and the compression texture as given in Fig. 7 show a predominant $[0001]$ texture plus a weak secondary $[11\bar{2}0]$ texture. Also of interest is the noticeable increase in density along the $[0001]$–$[11\bar{2}0]$ edge which is the preferred route of rotation to the $[0001]$ position. Although the slip system developed here gives the desired rotation tendency for the observed compression texture, the maximum 30° from $[0001]$ is not developed and must be a result of mechanical twinning.

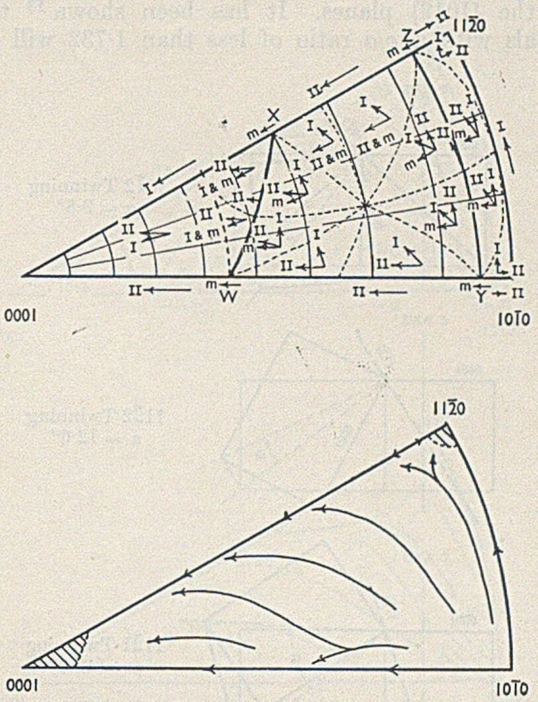

Fig. 7.—Compression Slip Rotations and Compression Texture Resulting from Combined Slip System.

Table I.—*Active Slip Elements in the Combined Slip Systems.*

Position	Active Slip System
$[0001]$	None—Fracture
$[10\bar{1}0]$	$(01\bar{1}0)[2\bar{1}\bar{1}0]$; $(1\bar{1}00)[11\bar{2}0]$
$[11\bar{2}0]$	$(01\bar{1}0)[2\bar{1}\bar{1}0]$; $(10\bar{1}0)[\bar{1}2\bar{1}0]$
W	$(0001)[11\bar{2}0]$; $(0001)[2\bar{1}\bar{1}0]$; $(01\bar{1}1)[2\bar{1}\bar{1}0]$; $(1\bar{1}01)[11\bar{2}0]$
X	$(0001)[11\bar{2}0]$; $(01\bar{1}1)[2\bar{1}\bar{1}0]$; $(10\bar{1}1)[\bar{1}2\bar{1}0]$
Y	$(01\bar{1}1)[2\bar{1}\bar{1}0]$; $(1\bar{1}01)[11\bar{2}0]$; $(01\bar{1}0)[2\bar{1}\bar{1}0)$; $(1\bar{1}00)[11\bar{2}0]$
Z	$(01\bar{1}1)[2\bar{1}\bar{1}0]$; $(10\bar{1}1)[\bar{1}2\bar{1}0]$; $(01\bar{1}0)[2\bar{1}\bar{1}0]$; $(10\bar{1}0)[\bar{1}2\bar{1}0]$
$[0001]$–*W*	$(0001)[11\bar{2}0]$; $(0001)[2\bar{1}\bar{1}0]$
$[0001]$–*X*	$(0001)[11\bar{2}0]$
W–*X*	$(0001)[11\bar{2}0]$; $(01\bar{1}1)[2\bar{1}\bar{1}0]$
W–*Y*	$(01\bar{1}1)[2\bar{1}\bar{1}0]$; $(1\bar{1}01)[11\bar{2}0]$
X–*Z*	$(01\bar{1}1)[2\bar{1}\bar{1}0]$; $(10\bar{1}1)[\bar{1}2\bar{1}0]$
Y–*Z*	$(01\bar{1}1)[2\bar{1}\bar{1}0]$; $(01\bar{1}0)[2\bar{1}\bar{1}0]$
$[10\bar{1}0]$–*Y*	$(01\bar{1}0)[2\bar{1}\bar{1}0]$; $(1\bar{1}00)[11\bar{2}0]$
$[11\bar{2}0]$–*Z*	$(01\bar{1}0)[2\bar{1}\bar{1}0]$; $(10\bar{1}0)[\bar{1}2\bar{1}0]$
$[10\bar{1}0]$–$[11\bar{2}0]$	$(01\bar{1}0)[2\bar{1}\bar{1}0]$
$[0001]$–*W*–*X*	$(0001)[11\bar{2}0]$
W–*X*–*Z*–*Y*	$(01\bar{1}1)[2\bar{1}\bar{1}0]$
Y–*Z*–$[11\bar{2}0]$–$[10\bar{1}0]$	$(01\bar{1}0)[2\bar{1}\bar{1}0]$

VI.—DEFORMATION BY TWINNING

Hexagonal close-packed metals twin most easily on the $\{10\bar{1}2\}$ planes. It has been shown[13] that metals with a c/a ratio of less than 1·732 will not twin by $\{10\bar{1}2\}$ twinning when the axis of compression is along the c-axis of the unit cell. Thus the minimum near [0001] apparent from the 0001 pole figure for compressed and for cold-rolled titanium cannot be the result of twinning on the $\{10\bar{1}2\}$ planes.

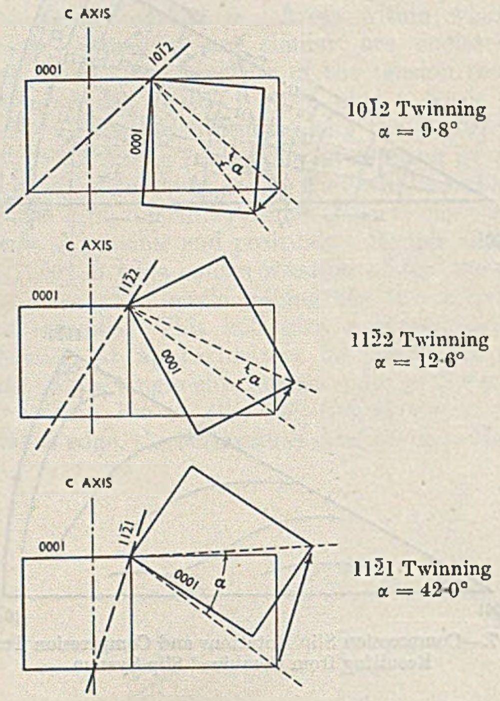

Fig. 8.—Twinning Shear Direction of Twinning on $\{10\bar{1}2\}$, $\{11\bar{2}2\}$, and $\{11\bar{2}1\}$ Planes of Titanium.

To explain the minimum evident in the compression texture, a new type of twinning must be assumed which can occur in compression from the [0001] position. Several types of twinning can be visualized which will take place from this position. The $\{10\bar{1}1\}$ twinning reported in magnesium[14] would be an example. Similarly, both the $\{11\bar{2}1\}$ and $\{11\bar{2}2\}$ twinning reported in titanium[12] have the ability to occur from a [0001] position in compression.

A comparison of the twinning shear angles, the angle between the diagonals of the twinned and untwinned unit cell, of $\{10\bar{1}2\}$, $\{11\bar{2}1\}$, and $\{11\bar{2}2\}$ twinning is given in Fig. 8. It seems likely from inspection of this figure that $\{11\bar{2}2\}$ twinning should occur much more readily than $\{11\bar{2}1\}$ twinning. Attempts to develop a satisfactory picture of the atom movements in $\{11\bar{2}1\}$ and $\{11\bar{2}2\}$ twinning such as has been done for $\{10\bar{1}2\}$ twinning[13] were unsuccessful.

For the purpose of this development of the twinning effects, the following assumptions were made:

(1) $\{10\bar{1}2\}$ and $\{11\bar{2}2\}$ twinning are of about equal frequency and $\{11\bar{2}1\}$ twinning is relatively rare.

(2) The twinning shear stress for $\{11\bar{2}2\}$ twinning is in the direction shown in Fig. 8, and the c-axis, twin plane normal, and twinning shear direction are in the same plane.

(3) The critical shear stresses for $\{10\bar{1}2\}$ twinning and $\{11\bar{2}2\}$ twinning are equal to the critical shear stress for {0001} slip.

The method of twinning analysis shown to give satisfactory results for magnesium and zinc[9] was used.

1. $\{10\bar{1}2\}$ Twinning

For the purpose of calculation the assumption was made that the critical shear stress for twinning on the $\{10\bar{1}2\}$ planes was equal to the critical shear stress for slip on the {0001} planes. Thus, from equation (5):

$$C_{t10\bar{1}2} = C_{s0001} = 1{\cdot}1\ C_{s10\bar{1}1} = 1{\cdot}02\ C_{s10\bar{1}0} \quad (6)$$

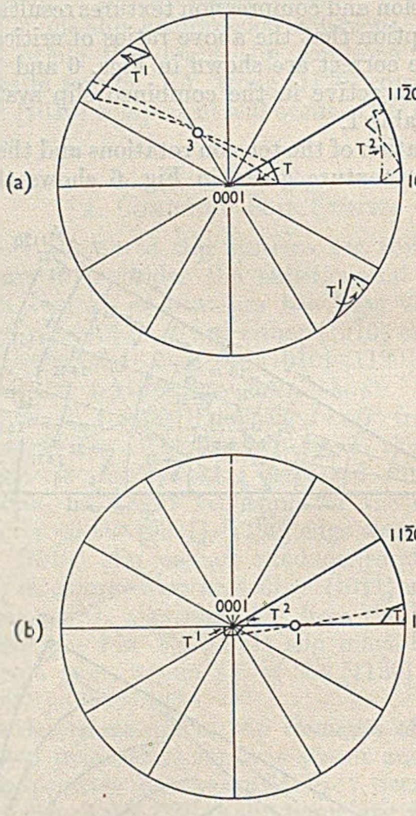

Fig. 9.—Reorientation Resulting from $\{10\bar{1}2\}$ Twinning from the Combined Slip System.

(a) $\{10\bar{1}2\}$ twinning in tension.
(b) $\{10\bar{1}2\}$ twinning in compression.

The boundary between the slip and twinning areas was determined by use of the formulæ:

$$\cos\gamma \cos\delta = n \cos x \cos\lambda \quad \text{in tension} \quad . \quad (7)$$

$$\cos\gamma \cos\delta = -\,n \cos x \cos\lambda \quad \text{in compression} \quad (8)$$

where $n = C_t/C_s$.

The boundaries for twinning in both tension and compression based on the combined slip system shown in Figs. 6 and 7 were calculated for all six of the possible {10$\bar{1}$2} twinning systems. The most favourable system was assumed to be that which included the greatest area of the unit stereographic triangle.

Each point in the twinning area will move to the same angle beyond the twin plane normal as its initial angle from the twin plane normal. The twinning area, T, the active twin plane normal, marked by number, the new twinned orientation, T^1, and the new twinned orientation placed in the unit stereographic triangle, T^2, are shown in Fig. 9.

It is seen that {10$\bar{1}$2} twinning assists slip rotations by twinning toward the [0001] in compression and toward the [10$\bar{1}$0]–[11$\bar{2}$0] edge in tension.

2. {11$\bar{2}$2} TWINNING

The boundary conditions for {11$\bar{2}$2} twinning were determined in the same manner as those for {10$\bar{1}$2} twinning. In this case, however, the signs of the two equations, (7) and (8), were reversed because of the change in the twinning shear direction (see Fig. 8). The shear stress ratios were assumed to be

$$C_{t11\bar{2}2} = C_{s0001} = 1{\cdot}1\, C_{s10\bar{1}1} = 1{\cdot}02\, C_{s10\bar{1}0} \quad (9)$$

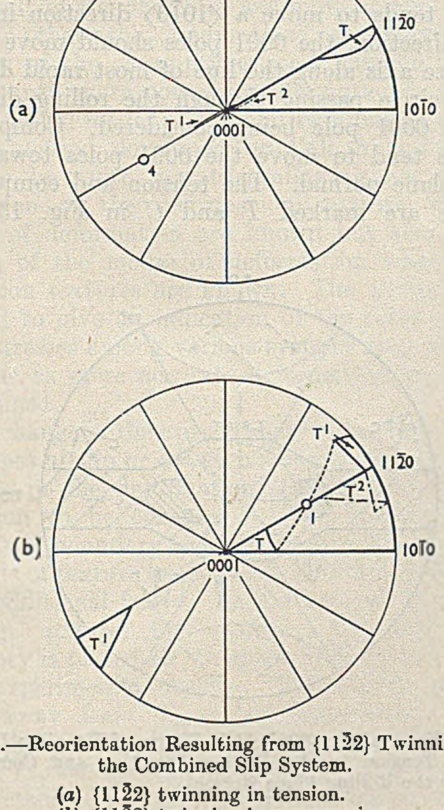

FIG. 10.—Reorientation Resulting from {11$\bar{2}$2} Twinning from the Combined Slip System.
(*a*) {11$\bar{2}$2} twinning in tension.
(*b*) {11$\bar{2}$2} twinning in compression.

The most favourable twinning system was determined in the same manner as in the case of {10$\bar{1}$2} twinning. The results of the twinning re-orientations are given in Fig. 10. {11$\bar{2}$2} twinning opposes slip rotation in compression, but in tension its only effect is to remove those poles in the subsidiary [11$\bar{2}$0] texture.

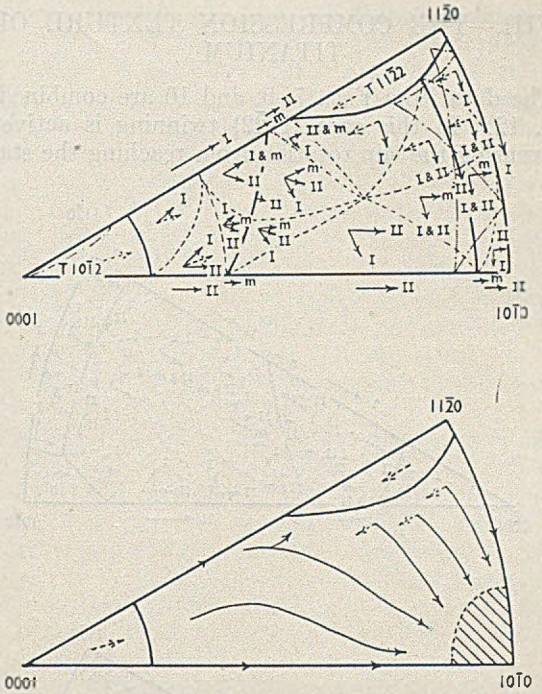

FIG. 11.—Tension Texture Resulting from Combined Slip on the {0001}⟨11$\bar{2}$0⟩, {10$\bar{1}$1}⟨11$\bar{2}$0⟩, and {10$\bar{1}$0}⟨11$\bar{2}$0⟩ Slip Planes and Twinning from the {10$\bar{1}$2} and {11$\bar{2}$2} Planes.

Since, from the geometry of twinning shown in Fig. 8, {11$\bar{2}$1} twinning appeared much less likely to occur than {11$\bar{2}$2} twinning, no calculations were made for this twinning system. The general effects of {11$\bar{2}$1} twinning would be the same as for {11$\bar{2}$2} twinning.

VII.—THE TENSION TEXTURE OF TITANIUM

The results plotted in Figs. 6, 9, and 10 for tension are combined in Fig. 11. In this figure it is seen that {10$\bar{1}$2} twinning aids in developing the [10$\bar{1}$0] texture, while {11$\bar{2}$2} twinning prevents the formation of the subsidiary [11$\bar{2}$0] texture. The net result of slip on three systems and twinning on two is a strong [10$\bar{1}$0] tension texture. This texture should be developed early. As the critical shear stress on the {10$\bar{1}$0} slip planes increases, the boundary between {10$\bar{1}$1} and {10$\bar{1}$0} slip moves toward the [10$\bar{1}$0]–[11$\bar{2}$0] edge. When the critical shear stress has increased until the two systems are equally favoured at [10$\bar{1}$0], when $C_{s10\bar{1}1} = 0{\cdot}878\ C_{s10\bar{1}0}$, there are six active and stable slip systems at [10$\bar{1}$0]. The [10$\bar{1}$0] tension texture would therefore be expected to remain unchanged until the material failed.

VIII.—THE COMPRESSION TEXTURE OF TITANIUM

The data from Figs. 7, 9, and 10 are combined in Fig. 12. In this case $\{11\bar{2}2\}$ twinning is active in preventing the slip rotation from reaching the stable end position. $\{10\bar{1}2\}$ twinning is of little importance in compression. As the slip rotations lead to the twinning region, the grains are twinned to a position near the $[11\bar{2}0]$ point. Thus, as deformation increases, the slip rotations tend to be concentrated more completely along the $[11\bar{2}0]$–$[0001]$ edge of the unit triangle. This accounts for the preferred orientation noticed in the $10\bar{1}0$ and $10\bar{1}1$ pole figures of compressed titanium.[5]

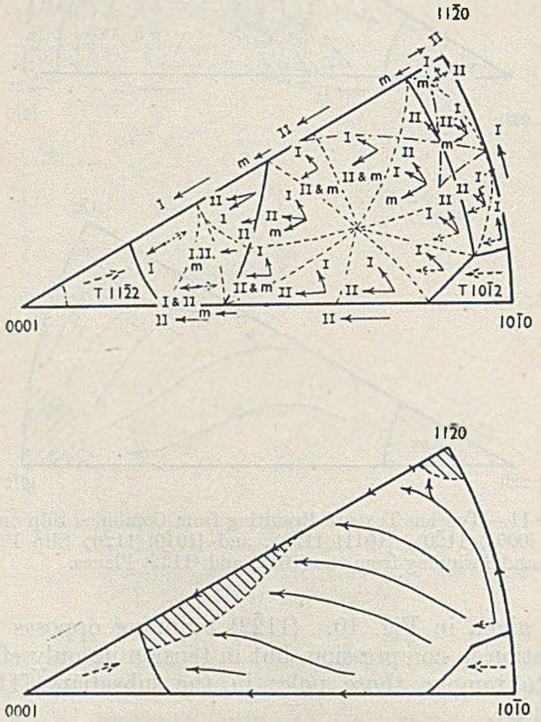

Fig. 12.—Compression Texture Resulting from Combined Slip on the $\{0001\}\langle 11\bar{2}0\rangle$, $\{10\bar{1}1\}\langle 11\bar{2}0\rangle$, and $\{10\bar{1}0\}\langle 11\bar{2}0\rangle$ Slip Planes and Twinning from the $\{10\bar{1}2\}$ and $\{11\bar{2}2\}$ Planes.

As the slip rotations lead toward the $[0001]$ position and the twinning re-orientation leads away from this position, a spread of orientations from the slip-twinning boundary to the $[11\bar{2}0]$ position will occur. An equilibrium texture will arise near the slip-twinning boundary. The decrease of the angle between the compression axis and the $[0001]$ position with increased reduction may be attributed to a relative change in the ratio of the critical shear stress for $\{0001\}$ slip and $\{11\bar{2}2\}$ twinning such that the boundary between slip and twinning moves toward $[0001]$.

The absence of any appreciable $[11\bar{2}0]$ compression texture indicates that $\{10\bar{1}0\}$ slip is probably completely absent at high reductions. The ability of the $\{10\bar{1}1\}$ slip system to trap the stress axis in the minimum occurring in the resolved shear-stress diagram at $[11\bar{2}0]$ (see Fig. 4) would be sufficient to account for the slight $[11\bar{2}0]$ texture apparent at high reductions.

IX.—THE COLD-ROLLED TEXTURE OF TITANIUM

Cold rolling can be considered as tension in the rolling direction and compression on the rolling plane.[15] The observed cold-rolling texture of titanium, $(0001)[10\bar{1}0]$ rotated 30° in the transverse direction, can therefore be visualized as a combination of the $[10\bar{1}0]$ tension texture and the rotated $[0001]$ compression texture. Since the $[0001]$ rotation occurs preferentially about a $\langle 10\bar{1}0\rangle$ axis, both the tension and the compression textures may be satisfied simultaneously in cold rolling.

In Fig. 13 the compression and tension rotations and the twinning re-orientation are shown in a 0001 pole figure. If random initial orientation is assumed, the following tendencies are apparent. Since tension rotation tends to move a $\langle 10\bar{1}0\rangle$ direction into the rolling direction, the 0001 poles should move to the transverse axis along the line of most rapid descent, a great circle passing through the rolling direction and the 0001 pole being considered. Compression rotations tend to move the 0001 poles toward the rolling plane normal. The tension and compression rotations are marked *T* and *C* in Fig. 13. The resultant 0001 pole rotation is shown by an arrow marked *R*. Tension twinning on the $\{10\bar{1}2\}$ planes (Fig. 9) will tend to remove all 0001 poles within approximately 29° of the rolling direction to a

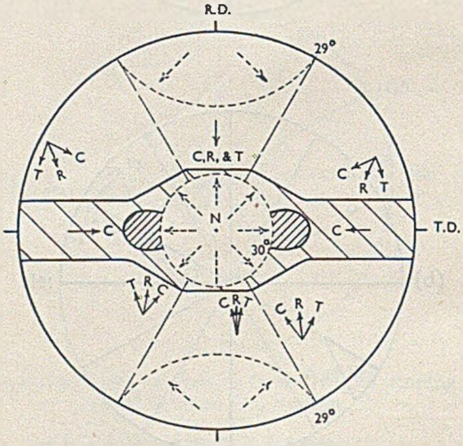

Fig. 13.—Form of the (0001) Pole Figure of Titanium Resulting from Tension in the Rolling Direction and Compression Along the Rolling Plane Normal.

position near the transverse direction. Compression twinning on the $\{11\bar{2}2\}$ planes will twin the 0001 poles from a region within 30° of the rolling plane normal to a region near the circumference of the pole figure (Fig. 10). Twinning re-orientations are indicated by dashed arrows in Fig. 13. Those poles falling within the $\{10\bar{1}2\}$ tension twinning area near the rolling direction will be twinned to the transverse direction, depleting the area enclosed by the long dashes. As the resultant slip rotations tend to move the 0001 poles toward the transverse axis, and from there toward the rolling plane normal, an equilibrium state will gradually be established in which the 0001 poles rotate by compression toward the rolling plane normal and by twinning are removed to the transverse direction to rotate again toward the rolling plane normal. The resulting 0001 pole figure will have a shape similar to that indicated by shading in Fig. 13.

X.—DISCUSSION

By application of the Calnan and Clews method it has been possible to develop a theoretical deformation process based on the experimentally determined deformation textures of titanium. It should be emphasized that the agreement of the theoretically developed textures with those actually observed is the result of the choice of assumptions and does not indicate that the assumptions are correct. The validity of the assumptions made cannot be determined until more complete information is available on the actual modes of slip and twinning in titanium.

The method developed by Calnan and Clews is seen to be quite versatile, allowing not only the prediction of the deformation textures when the modes of deformation are known but also the prediction of the modes of deformation when the deformation textures are known. The ability of their method to give an indication of the ratio of critical shear stresses among various systems may also prove of value as more accurate deformation textures are determined.

The change in the critical shear-stress ratio between two types of slip or between slip and twinning allows changes in the deformation texture with increased reduction to be considered. The assumption that the actual boundary may be located exactly by the methods of texture analysis requires the consideration of an additional factor. In the analysis of the compression texture, for example, the slip-twinning boundary is placed 30° from the [0001] point to agree with experimental results. The ability of T_e to move away from T_a is not considered. If it is assumed that the actual boundary is 10° from [0001] in Fig. 12, the decrease in intensity from 30° to 10° in the measured compression texture can be attributed to the variation in movement of T_e from T_a. That is, if T_e is assumed to have a probability of further movement rather than slip decreasing with increased distance from T_a and equal to zero when T_e has moved 20° from T_a, both the maximum at 30° and the variation between 30° and 10° would be explained. It should be remembered that movement of T_e does not imply movement of T_a. A crystallite oriented so that T_a was at 30° could conceivably twin from this position even though the slip-twinning boundary was at 10° if T_e was allowed sufficient freedom of movement. This will introduce the effect of freedom of movement of T_e to the already discussed change of ratio of the critical shear stresses which should be considered in placing boundaries. Since there is at present no provision for considering the maximum movement of T_e or the effect of increased deformation on the maximum movement in the method of analysis developed by Calnan and Clews, this factor has been neglected. As more critical studies of the deformation textures of metals are conducted, the movement of T_e may be found to give an explanation of the differences in the deformation textures among metals of the same crystal structure.[7]

The existence of an equilibrium type of cold-rolled texture may account for the large amount of deformation by cold rolling which titanium can absorb without failure. The slip planes which support the major portion of the slip are continually changing during the deformation process, so that there is no rapid work-hardening on any one set of slip planes. The absence of any point of zero resolved shear stress is also of interest.

This analysis of the deformation textures of titanium would also be expected to explain satisfactorily the deformation textures of zirconium and beryllium with slight modifications of the critical shear-stress ratios.

XI.—CONCLUSIONS

By suitable choice of slip and twinning elements and their relative critical shear stresses, it was possible to develop a satisfactory explanation of the tension, compression, and cold-rolling textures of titanium, using the theoretical method of texture analysis developed by Calnan and Clews. Slip was assumed to occur on the $\{0001\}\langle 11\bar{2}0\rangle$, $\{10\bar{1}0\}\langle 11\bar{2}0\rangle$, and $\{10\bar{1}1\}\langle 11\bar{2}0\rangle$ slip systems, with $\{10\bar{1}1\}\langle 11\bar{2}0\rangle$ slip being most prominent. $\{11\bar{2}2\}$ twinning was shown to be a possible cause of the minimum near the centre of the 0001 pole figure in the cold-rolled texture of titanium. An equilibrium-type texture existing between the stable end-points for slip and twinning was found to be probable in compression. A stable $[10\bar{1}0]$ texture was developed in tension. The rolling texture consisted of a combination of the tension and compression textures such that tension in the rolling direction kept one set of opposing $\langle 10\bar{1}0\rangle$ poles in position in the rolling direction while the remaining poles were free to rotate in the transverse direction about this axis, according to the compression tendency for the 0001 pole to move continually between positions 30° and 90° from the rolling plane normal. The experimentally determined compression and cold-rolling textures made it possible for the ratio of the critical shear stresses for slip (C_s) and for twinning (C_t) to be calculated. The critical shear stresses were found to be related according to the following approximate equation,

$$C_{s0001} = 1{\cdot}1\, C_{s10\bar{1}1} = 1{\cdot}02\, C_{s10\bar{1}0} = C_{t10\bar{1}2} = C_{t11\bar{2}2}$$

ACKNOWLEDGEMENT

The authors wish to take this opportunity to thank the Titanium Alloy Manufacturing Division of the National Lead Company for support of the fellowship under which this work was conducted.

REFERENCES

1. C. S. Barrett, " Structure of Metals ", p. 289. New York: **1943** (McGraw-Hill).
2. H. T. Clark, Jr., *Trans. Amer. Inst. Min. Met. Eng.*, 1950, **188**, 1154.
3. R. K. McGeary and B. Lustman, *ibid.*, 1951, **191**, 994.
4. A. Smigelskas and C. S. Barrett, *ibid.*, 1949, **185**, 145.
5. D. N. Williams and D. S. Eppelsheimer, *ibid.*, 1952, **194**, 615.
6. D. N. Williams and D. S. Eppelsheimer, to be published.
7. E. A. Calnan and C. J. B. Clews, *Phil. Mag.*, 1950, [vii], **41**, 1085.
8. E. A. Calnan and C. J. B. Clews, *ibid.*, 1951, [vii], 42, 616.
9. E. A. Calnan and C. J. B. Clews, *ibid.*, 919.
10. E. A. Calnan and C. J. B. Clews, *ibid.*, 1952, [vii], **43**, 93.
11. M. K. Yen, *Interim Rep. to Watertown Arsenal*, 1950, **(WHL 401/14-4)**.
12. F. D. Rosi, C. A. Dube, and B. H. Alexander, *J. Metals*, 1952, **4**, 145.
13. C. S. Barrett, *The Cold Working of Metals* (*Amer. Soc. Metals*), **1949**, 84.
14. E. Schiebold and G. Siebel, *Z. Physik*, 1931, **69**, 458.
15. F. Wever, *Trans. Amer. Inst. Min. Met. Eng.*, *Inst. Metals Div.*, **1931**, 51.

THE INFLUENCE OF COMPOSITION ON THE INCIDENCE OF STRAIN MARKINGS IN ALUMINIUM ALLOYS *

By W. H. L. HOOPER,† B.Sc., A.I.M., MEMBER

SYNOPSIS

Using the surface-measuring technique previously described (*J. Inst. Metals*, 1951–52, 80, 17), the form and intensity of stretcher-strain markings in relation to composition and thermal treatment have been investigated. It has been established that, in aluminium–magnesium alloys of commercial and high purity, magnesium itself, rather than impurities or grain-refining additions, is responsible for stretcher-strain effects, which are absent with less than about 1% magnesium, and severe only with more than about 2% of this element. Low-intensity markings are developed in aluminium–copper–magnesium alloys after quenching to retain the alloying constituents in solid solution. It is concluded that, as in mild steel, strain markings are associated with atomic re-arrangement in an unstable, supersaturated solid solution.

I.—INTRODUCTION

OF the aluminium alloys used commercially in sheet-metal work, those containing magnesium as the principal alloying addition appear to be particularly prone to stretcher-strain effects. Strain markings in these materials have been studied and described in some detail,[1, 2] since they are of significantly greater magnitude than similar effects observed in some other aluminium alloys.[3, 4]

A method of approach to the investigation of yield-point phenomena to which considerable attention has been paid is the study of stress/strain curves, the occurrence of discontinuities on which is frequently associated with the incidence of stretcher-strain markings on the specimen under test. For example, MacReynolds [5] has shown that the presence either of small quantities of impurities or of deliberate additions of copper in 99·996% aluminium causes steps to appear in the originally smooth stress/strain curve, indicating a change in the manner of deformation from a process of uniform extension to one involving a series of sudden yields in rapid succession.

The most detailed studies of strain markings in relation to composition have been made on mild steel,[6-8] and it has been established that the sharp yield point which accompanies the formation of strain bands is not an inherent property of pure iron, but depends on the presence of small traces of carbon and is intensified by the presence of nitrogen. Thus Snoek [6] found that pure iron with less than 0·0001% carbon showed no such sharp yield point, but that the addition of 0·003% carbon was sufficient to produce a clear discontinuity in the stress/strain curve. Mild steel, in which these discontinuous straining effects are evident, also exhibits strain-ageing effects, i.e. light straining at room temperature is followed by age-hardening, but no such effect is apparent in pure iron. Edwards, Phillips, and Jones [9] have found that elements such as titanium, which have a strong affinity for carbon, and form carbides in steel, reduce this strain-ageing effect. There is thus strong evidence for the presumption that strain-band formation in steel is associated with the presence of a supersaturated phase.

Existing data referring to aluminium alloys point to the analogy between the behaviour in strain of mild steel and that of industrial aluminium–magnesium alloys in which the magnesium content exceeds the equilibrium α solid-solution limit at room temperature—the magnesium-rich β phase in these alloys can, in fact, be precipitated at temperatures as low as 50° C. However, the possible influence of other elements generally present, such as iron, silicon, and manganese, must be recognized.

II.—SCOPE OF INVESTIGATION

Straining experiments were carried out on alloys in the form of sheet in the soft recrystallized condition resulting from appropriate annealing or heat-treatment. Since it had been established in the earlier published investigation,[2] and amply confirmed in subsequent experiments, that stretcher-strain effects were developed only in sheet with a mean grain-size of less than 0·05 mm., each material was subjected to appropriate processing to obtain the required fine grain. It was necessary to make grain-refining additions to high-purity alloys, which could not otherwise be prepared with a suitably fine-grain structure, and since it was found that small proportions of chromium, manganese, and titanium had

---

* Manuscript received 11 February 1953.

† Research Technical Officer, Imperial Chemical Industries, Ltd., Metals Division, Birmingham.

no significant effect on the stretching characteristics of pure aluminium, these elements were used for the purpose.

Because of the apparent significance of magnesium in relation to strain markings, both high-purity and commercial-grade alloys were prepared over a range of magnesium contents from 0 to 6%, the object being to separate the effect of impurities normally present in industrial alloys, and to determine the relationship between intensity of marking and magnesium content. Additional information was obtained from other representative alloys in the standard industrial range covered by British Standard No. 1470.

III.—PREPARATION OF MATERIAL

In the case of the aluminium–magnesium alloys with less than 1% magnesium made from either pure or commercial aluminium, it was not possible by any combination of rolling and annealing to obtain a suitably fine grain-size. The necessary grain-refining was effected by additions of manganese and titanium, or of chromium, since experiments with high-purity binary alloys had indicated that these elements were not in any way responsible for strain markings. The compositions of the alloys are recorded in Table I.

Table I.—*Composition of Non-Heat-Treatable Alloys.*

Alloy Number	Cu, %	Mn, %	Mg, %	Si, %	Fe, %	Ti, %	Cr, %	Zn, %
				Experimental Alloys				
1	<0·01	0·24	0·12	0·02	0·04	0·11	...	<0·005
2	0·014	0·23	0·27	0·01	0·04	0·12	...	<0·005
3	<0·01	0·23	0·56	0·02	0·04	0·11	...	<0·005
4	0·01	0·30	0·58	0·16	0·20	0·10	...	<0·005
5	<0·01	0·29	0·87	0·03	0·03	0·14	...	<0·005
6	0·01	0·30	0·9	0·10	0·18	0·10	...	<0·005
7	<0·01	0·22	1·11	0·01	0·04	0·002	...	<0·005
8	<0·01	0·27	2·33	0·01	0·035	0·002	...	<0·005
9	<0·01	0·02	3·11	0·017	0·04	0·12	...	<0·005
10	0·02	...	2·59	0·11	0·27	0·01	0·44	<0·005
				Industrial Alloys (B.S. 1470)				
NS3	0·02	1·21	0·01	0·16	0·32	0·07	...	<0·005
NS5	0·08	0·22	3·87	0·18	0·27	0·02	...	<0·005
NS6	0·12	0·21	5·13	0·09	0·21	0·02	...	0·01
NS7	0·01	0·14	6·03	0·12	0·28	0·02	...	<0·005
S1B	0·02	<0·01	<0·01	0·03	0·05	<0·01	<0·01	<0·005
S1C	0·02	<0·01	0·01	0·15	0·3	0·06	...	<0·005

Alloys 1–10, containing up to about 3% magnesium, were prepared under laboratory conditions, from the purest available virgin-metal constituents, in cast slabs of 20 lb. weight. All the remaining alloys, including the higher members of the aluminium–magnesium series, were taken from hot-rolled commercial stock. Heavy cold-rolling reductions, of the order of at least 70–75%, were applied before the final anneal, in order to obtain the necessary fine grain.

The annealing of aluminium–magnesium alloys with up to 1·1% magnesium was carried out at 300° C., grain growth being rapid at higher annealing temperatures. Alloys of greater magnesium content were subjected to a standard annealing treatment of 2 hr. at 400°–430° C. The aluminium–manganese alloy (NS3) was flash-annealed in a salt bath at 500° C.

The three heat-treatable alloys (see Table IV) were obtained in a fully softened condition by annealing at the appropriate temperature and slowly cooling in the furnace. Other specimens of these alloys were prepared in different conditions involving solution-treatment and ageing, as detailed in the table.

The method of preparation of the 8 × 2-in. specimens for stretching has been described previously.[2] In brief, surface treatments involving electropolishing or a chemical bright dip were supplemented where necessary by hand-polishing. Grain-sizes were estimated on etched portions of each specimen by comparison with standard photomicrographs, and values are recorded in Tables II, III, and IV.

IV.—STRETCHING EXPERIMENTS

Strains in the critical range 0–1% with which random-type stretcher-strain markings are associated, were measured with a Lamb roller extensometer of

Table II.—*Stretching Characteristics of Experimental Non-Heat-Treatable Alloys.*

Alloy Number	Principal Alloying Additions			Annealing Treatment	Grain-Size, mm.	Appearance of Specimens during Stretching			
	Mg, %	Ti, %	Mn, %			Extension 0–2%	Maximum Talysurf Deviation, 10^{-3} in.	At 5% Extension	Maximum Talysurf Deviation, 10^{-3} in.
1	0·12	0·11	0·24	4 hr. at 300° C.	0·040	No markings	<0·1	No markings	<0·1
2	0·27	0·12	0·23		0·040	,,	<0·1	,,	<0·1
3	0·56	0·11	0·23		0·040	,,	<0·1	,,	<0·1
4	0·58	0·10	0·30		0·035	,,	<0·1	,,	<0·1
5	0·87	0·14	0·29		0·035–0·040	Slight random markings	0·5	Slight parallel bands	0·15
6	0·90	0·10	0·30		0·030	Very slight random markings	0·2	,, ,,	0·12
7	1·11	...	0·22		0·026	Severe random markings	1·5	Parallel bands	0·20
8	2·33	...	0·27	2 hr. at 400° C.	0·01–0·03	,, ,, ,,	1·8	,, ,,	0·14
9	3·11	0·12	...		0·015	,, ,, ,,	2·0	,, ,,	0·18
			Cr, %						
10	2·59	...	0·44		0·01	,, ,, ,,	1·8	,, ,,	0·18

Table III.—*Stretching Characteristics of Industrial Non-Heat-Treatable Alloys.*

Code Number (B.S. 1470)	Principal Alloying Additions			Annealing Treatment	Grain-Size, mm.	Appearance of Specimens during Stretching			
	Mg, %	Ti, %	Mn, %			Extension 0–2%	Maximum Talysurf Deviation, 10^{-3} in.	At 5% Extension	Maximum Talysurf Deviation, 10^{-3} in.
NS3	...	0·07	1·21	½ hr. at 500° C. in salt bath	0·030	No markings	<0·1	No markings	0·1
NS5	3·87	0·02	0·22	2 hr. at 400° C.	0·015	Severe random markings	2·2	Parallel bands	0·18
NS6	5·13	0·02	0·21	2 hr. at 430° C.	0·025	,, ,, ,,	1·7	,, ,,	0·20
NS7	6·03	0·02	0·14	,, ,,	0·02	,, ,, ,,	1·9	,, ,,	0·17
S1B	99·5% Al			4 hr. at 300° C.	0·035–0·040	No markings	<0·1	No markings	0·1
S1C	99·0% Al				0·035	,,	<0·1	,,	0·1

Table IV.—*Stretching Characteristics of Heat-Treatable Alloys.*

Code Number (B.S. 1470)	Heat-Treatment	Grain-Size, mm.	Appearance of Specimens during Stretching			
			Extension 0–2%	Maximum Talysurf Deviation, 10^{-3} in.	At 5% Extension	Maximum Talysurf Deviation, 10^{-3} in.
HS10 (Cu 0·03, Mn 0·66, Mg 0·75, Si 0·96, Fe 0·28, Ti 0·01%)	2 hr. at 375° C.; furnace-cooled	0·035	No markings	0·1	No markings	0·1
	½ hr. at 540° C.; quenched	0·02	Slight parallel bands at 2% extension	0·1	Slight parallel bands	0·13
	½ hr. at 450° C.; quenched	0·02	,, ,, ,,	0·1	,, ,, ,,	0·11
	½ hr. at 540° C.; quenched; aged 18 hr. at 160° C.	0·02	No markings	<0·1	Fractured at less than 5% extension	...
HS14 (Cu 4·07, Mn 0·56, Mg 0·76, Si 0·46, Fe 0·44, Ti 0·02%)	2 hr. at 375° C.; furnace-cooled	0·01	No markings	<0·1	Parallel bands	0·2
	½ hr. at 495° C.; quenched at 20° C.	0·02	Random markings	0·5	,, ,,	0·22
	½ hr. at 495° C.; quenched at 100° C.	0·02	,, ,,	0·5	,, ,,	0·21
	½ hr. at 450° C.; quenched at 20° C.	0·02	,, ,,	0·5	,, ,,	0·22
	½ hr. at 450° C.; quenched at 100° C.	0·02	,, ,,	0·6	,, ,,	0·20
	½ hr. at 450° C.; quenched in oil at 20° C.	0·02	,, ,,	0·7	,, ,,	0·21
	½ hr. at 400° C.; quenched at 100° C.	0·015	,, ,,	0·5	,, ,,	0·18
	½ hr. at 400° C.; quenched in oil at 20° C.	0·015	,, ,,	0·6	,, ,,	0·18
	½ hr. at 495° C.; quenched; aged 8 hr. at 165° C.	0·02	No markings	<0·1	Fractured at less than 5% extension	...
	½ hr. at 495° C.; quenched; aged 7 days at room temperature	0·02	Slight random markings	0·4	No markings	0·1
D.T.D. 363A (Cu 1·31, Mn 0·49, Mg 2·86, Si 0·14, Fe 0·34, Ti 0·11, Cr 0·34, Zn 5·90%)	2 hr. at 375° C.; furnace-cooled	0·025	No markings	<0·1	No markings	0·1
	½ hr. at 460° C.; quenched at 20° C.	0·02	,,	<0·1	Slight parallel bands	0·12
	½ hr. at 460° C.; quenched; aged 18 hr. at 125° C.	0·02	,,	<0·1	Fractured at less than 5% extension	...

the mirror-and-scale type, the stretching operation being interrupted at appropriate extensions for Talysurf traces to be made of the rolled surface. The larger extensions associated with parallel bands were measured with dividers. Relevant data on the stretching characteristics of high-purity and commercial aluminium–magnesium alloys, and the standard B.S. alloys are summarized in Tables II–IV.

1. NON-HEAT-TREATABLE ALLOYS (TABLES II AND III)

(a) *Aluminium–Magnesium*

No markings were detected on alloys 1 to 4, containing 0·1–0·58% magnesium. A specimen of alloy 4 after stretching to 1% elongation is illustrated in Fig. 1 (Plate LXXXIII).

Among alloys based on high-purity aluminium, the lowest magnesium content, 0·87%, at which random markings occurred was in alloy 5, and very faint markings, less than one-third of the depth of similar markings observed previously in the 3% magnesium alloy,[2] were detected at ½% elongation (Fig. 2, Plate LXXXIII). Alloy 6, made from commercially pure metal with 0·90% magnesium, was subject to very slight markings at ½% extension, the deepest being 0·0002 in. It is probable that in commercially pure material, part of the magnesium is combined with silicon, and the amount in solid solution is thus reduced.

Severe markings, of a depth and distribution comparable to that observed in the commercial 3% magnesium alloy described in the earlier paper,[2] occurred at ½% extension in alloy 7 (1·11% magnesium), and a similar intensity was obtained with alloys 8 and 9 (2·33 and 3·11% magnesium, respectively), the former containing manganese and the latter titanium as grain-refining agent. The markings obtained with ½% extension in the latter alloy are shown in Fig. 3 (Plate LXXXIII). Alloys with 3·8, 5·0, and 6·0% magnesium (NS5–7) were also subject to severe random markings, the intensity and distribution of which were not significantly different from those observed in the higher-purity series.

All alloys which were sensitive to random markings with strains of up to 2% were also subject to parallel bands at higher extensions, and the mechanism by which the bands deepened and subsequently caused failure of the sheet was similar to that observed in the previous investigations on the 3% magnesium alloy. Alloys free from random markings showed no parallel bands. Summarized data on the stretching characteristics of the materials described above are included in Tables II and III.

(b) *Aluminium and Aluminium–1¼% Manganese*

High-purity aluminium (S1B), commercial-grade aluminium (S1C), and aluminium–1¼% manganese alloy (NS3) were free from markings at all stages of stretching up to the point of fracture.

2. HEAT-TREATABLE ALLOYS (TABLE IV)

(a) *Aluminium–Magnesium–Silicon* (*HS*10)

(i) *Fully Annealed.*

No markings of any type were detected, either in the first stage of stretching to 2% elongation, or in the second stage from 2% up to fracture.

(ii) *Solution-Treated.*

Solution-treatment was carried out at temperatures of 540° and 450° C., followed in each instance by quenching. No random markings were detected in the critical range of strain, 0–2%, but slight parallel bands occurred at an angle of about 69° to the tension axis at higher strains.

(iii) *Fully Heat-Treated.*

Specimens aged for 18 hr. at 160° C. after solution-treatment fractured at right angles to the tension axis at about 2% extension, the low ductility being probably attributable to the difficulty in getting accurate alignment of the wide specimen. No markings were detected either during stretching or on the fractured halves on subsequent examination.

(b) *Aluminium–Copper–Magnesium* (*HS*14)

(i) *Fully Annealed.*

In fully annealed aluminium–copper–magnesium alloy no random markings were observed on stretching to extensions of 0–2%, but at about 4% elongation parallel bands appeared comparable in depth to those observed in the aluminium–magnesium alloys at 5% extension. With further stretching, failure eventually occurred by necking through a pair of bands.

(ii) *Solution-Treated.*

Slight random markings occurred in sheet specimens of the aluminium–copper–magnesium alloy, solution-treated for ½ hr. at 495° C. and quenched in cold water. The markings occurred in a strain range of 0·05–0·5%, which is narrower than the range of extensions (0·015–2·0%) with which markings are associated in aluminium–3% magnesium alloy sheet.

Previous experience has shown that when aluminium–3% magnesium sheet is quenched from a suitably high temperature, quenching stresses are set up which prevent the formation of random markings. Relief of quenching stresses by some method, such as, for example, low-temperature annealing, causes a return to the condition in which intense random markings occur on stretching. Attempts were therefore made to produce markings of greater intensity in the heat-treatable aluminium–copper–magnesium alloy by reducing quenching stresses. The procedure adopted involved solution-treatment at different temperatures and quenching in cold water, boiling water, or oil. Some results of stretching tests on specimens quenched at 495°, 450°, and 400° C. are given in Table IV.

The markings were most intense in specimens freshly quenched from 450° C., and were most clearly defined after oil-quenching. The intensity was slightly reduced when stretching was carried out after ageing at room temperature for 7 days. A typical example of random markings in solution-treated aluminium–copper–magnesium alloy is illustrated in Fig. 4 (Plate LXXXIV). As stretching continued, random markings in freshly quenched specimens were replaced by parallel bands, which were deeper than bands observed in 3% magnesium alloy sheet stretched the same amount; room-temperature-aged strips, on the other hand, after the disappearance of random markings, stretched smoothly to failure without any further markings occurring. A typical example of parallel bands in aluminium–copper–magnesium alloy sheet is illustrated in Fig. 5 (Plate LXXXIV), which shows a solution-treated specimen stretched 9%, the maximum depth of marking being 0·0003 in.

(iii) *Fully Heat-Treated.*

Solution-treated specimens of aluminium–copper–magnesium alloy, aged for 8 hr. at 165° C., fractured at right angles to the stretching direction at extensions of less than 5%, and no strain markings of any type were detected either during stretching or on the pieces of strip after failure.

(c) *Clad Aluminium–Copper–Magnesium*

Experiments similar to those described above were carried out on specimens of aluminium–copper–magnesium alloy sheet clad on both surfaces with a skin of pure aluminium 5% of the total thickness of the material. Fully annealed specimens developed only parallel bands at extensions of about 5% and over; on the other hand, solution-treated and oil-quenched sheet exhibited random markings at strains between 0·1 and 0·5%, but, as might be expected, the intensity was less than that observed in the corresponding unclad sheet owing to the masking effect of the aluminium skin. A typical area of random markings in clad sheet is illustrated in Fig. 6 (Plate LXXXIV).

(d) *Aluminium–Zinc–Copper–Magnesium* (*D.T.D.* 363*A*)

(i) *Fully Annealed.*

Specimens annealed at 375° C. and furnace-cooled extended, without developing any strain markings, until fracture was imminent, when several distinct parallel bands appeared at an angle of about 64° to the tension axis, necking through one pair of bands eventually leading to failure.

(ii) *Solution-Treated.*

Sheet, solution-treated for ½ hr. at 460° C. and quenched, developed slight parallel bands at about 5% extension. Further bands appeared as stretching was continued to failure, but did not reach measurable depth at any stage of straining.

(iii) *Fully Heat-Treated.*

Specimens aged for 18 hr. at 125° C. after solution-treatment fractured at about 2% extension, no markings being detected. Fracture occurred at right angles to the axis of tension.

V.—DISCUSSION

The experiments described have established that random markings occur in aluminium–magnesium alloys over a wide range of magnesium contents, the lower limit being between 0·6 and 0·9%, and the upper limit greater than 6%. Maximum intensity of markings, measured on Talysurf tracings, has been plotted against magnesium content in Fig. 7, in which the curve reaches a maximum at a little over 1% and continues without significant variation to the maximum of 6% investigated.

Unalloyed aluminium, aluminium–manganese alloy, and aluminium–magnesium alloys containing 0·6% magnesium and less, were free from any type of marking at all extensions. The relatively coarse grain-size (0·04 mm.) of these low-magnesium alloys cannot account for their freedom from random markings, since material which, in the fine-grained condition, is subject to random markings always exhibits parallel bands in both fine- and coarse-grained states. However, no parallel bands were observed in these alloys when stretching was continued to the point of fracture. On the other hand, the heat-treatable aluminium–magnesium–silicon and aluminium–zinc–copper–magnesium alloys, although without detectable random markings in all conditions of heat-treatment, developed parallel bands when stretched in the solution-treated condition.

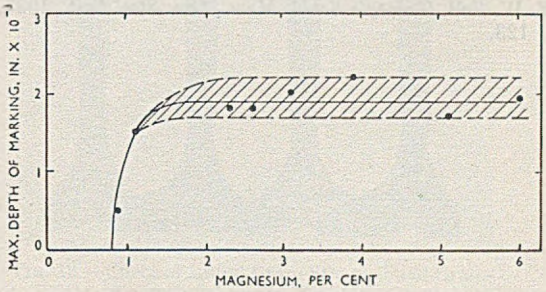

Fig. 7.—Maximum Depth of Random Markings in Aluminium–Magnesium Alloys.

Random markings in aluminium–copper–magnesium-type alloy sheet have not previously been reported, yet solution-treated material of this type is often subjected to stretching operations, for example, in flattening after quenching and in the stretch-forming of aircraft panels. The alloys are, of course, generally coated with pure aluminium, which, as already indicated, renders the markings less conspicuous. Moreover, the markings are less severe than those on aluminium–magnesium alloys, and since they occur with very small extensions and disappear at an elongation of 0·5%, they are probably pulled out in most flattening or forming operations. The occurrence of random markings in solution-treated and quenched aluminium–copper–magnesium alloy sheet appears, upon first consideration, to be anomalous, since in aluminium–magnesium alloys random markings can be avoided by quenching from comparable temperatures. The conclusion that this effect is associated with internal stresses receives some support from the observation that the markings were more intense with less drastic quenching. Ageing at 165° C. completely removed any tendency to strain marking, a result which might be related to the removal of magnesium from solid solution by the precipitation of a magnesium-rich phase.

Both aluminium–magnesium and aluminium–copper–magnesium alloys, in the physical condition in which strain marking is developed on stretching, are supersaturated in respect of solute elements or compounds. In both types of alloy, moreover, some decomposition of the solid solution is known to be induced by straining. The analogy with mild steel, therefore, appears to be close, and current theories, associating strain markings with atomic movements in the lattice analogous to those experienced in precipitation-hardening processes, receive further support.

ACKNOWLEDGEMENT

The encouragement and advice accorded to the author by Mr. R. Chadwick in discussions during the course of the investigation and in preparing the paper for publication is gratefully acknowledged.

REFERENCES

1. G. A. Knight and G. Murray, *Sheet Metal Ind.*, 1946, **23**, 1741.
2. R. Chadwick and W. H. L. Hooper, *J. Inst. Metals*, 1951–52, **80**, 17.
3. J. C. Arrowsmith, K. J. B. Wolfe, and G. Murray, *ibid.*, 1942, **68**, 109.
4. E. W. Fell, *Carnegie Schol. Mem., Iron Steel Inst.*, 1937, **26**, 123.
5. A. W. MacReynolds, *Trans. Amer. Inst. Min. Met. Eng.*, 1949, **185**, 32.
6. J. L. Snoek, *Physica*, 1941, **8**, 711.
7. J. R. Low, Jr., and M. Gensamer, *Trans. Amer. Inst. Min. Met. Eng.*, 1944, **158**, 207.
8. L. B. Pfeil, *J. Iron Steel Inst.*, 1928, **118**, 167.
9. C. A. Edwards, D. L. Phillips, and H. N. Jones, *ibid.*, 1940, **142**, 199P.

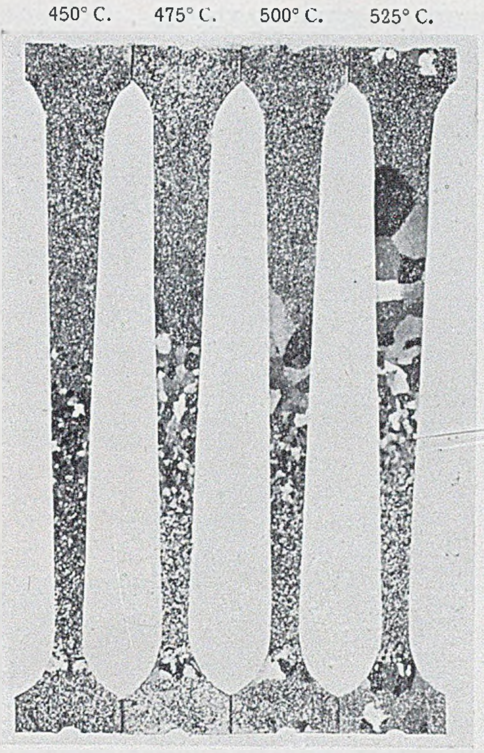

FIG. 11.—Effect of Temperature on Final Grain-Size. Super-purity aluminium pulled 2–20% and recrystallized for 30 min. at various temperatures. Initial grain-size 0·3 mm. × ⅓.

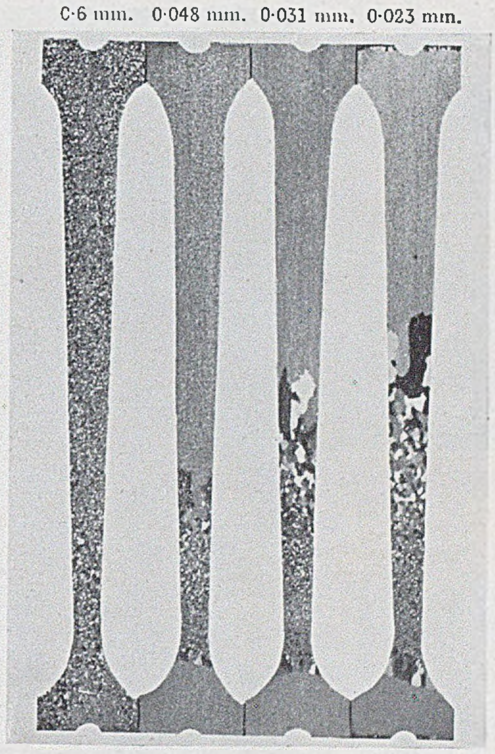

FIG. 12.—Effect of Initial Grain-Size on Final Grain-Size. Commercial-purity aluminium pulled 1–18% and recrystallized for 30 min. at 600° C. from various initial grain-sizes. × ⅓.

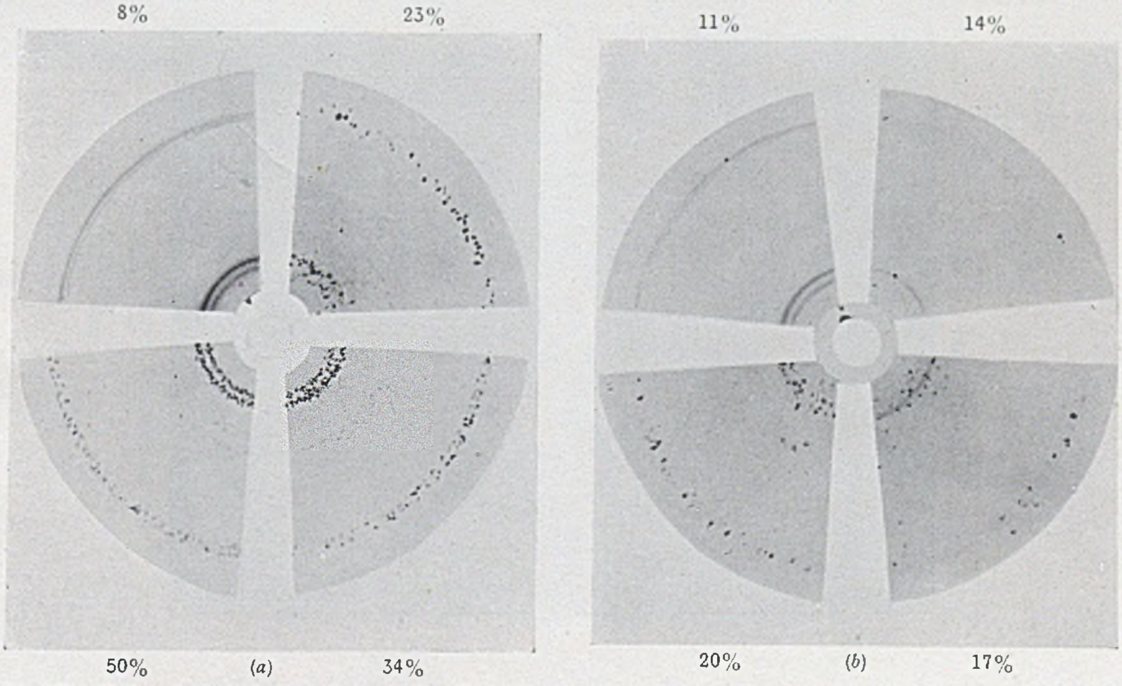

FIG. 13.—X-Ray Back-Reflection Photographs Taken at Various Points along a Wedge-Rolled Specimen. Critical reduction = 21%.

GRAIN REFINEMENT OF COPPER-ALUMINIUM ALLOYS.

FIGS. 1–4.—Transverse Sections of Laboratory Ingots. × $\frac{2}{3}$.

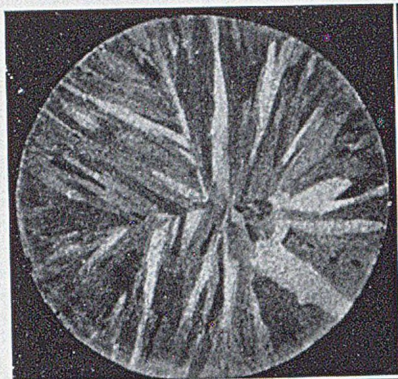

FIG. 1.—10% Al.

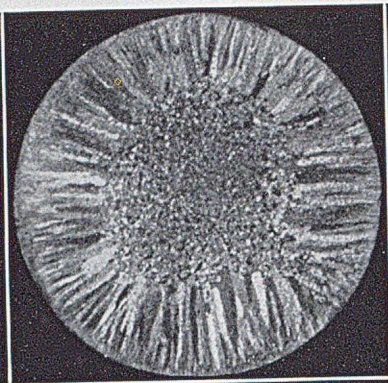

FIG. 2.—10% Al with 0·01% B.

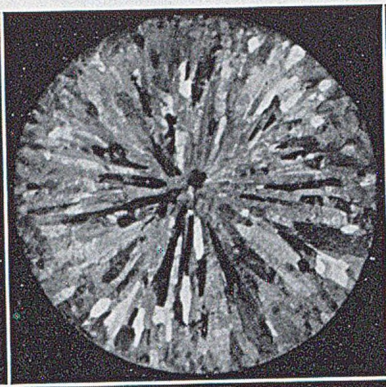

FIG. 3.—12·5% Al.

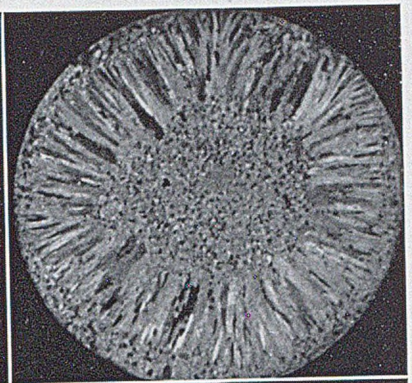

FIG. 4.—12·5% Al with 0·01% B.

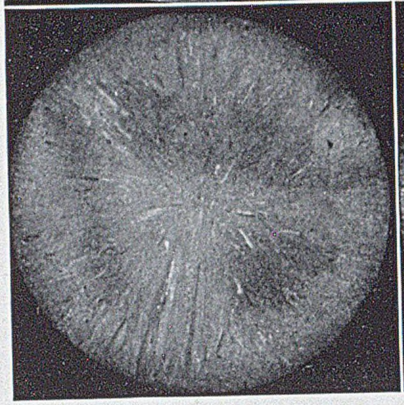

FIG. 5.—Standard Ingot.

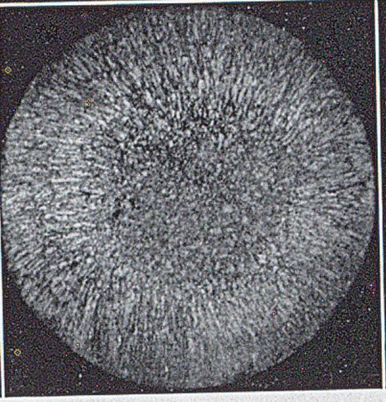

FIG. 6.—0·04% Ca Addition.

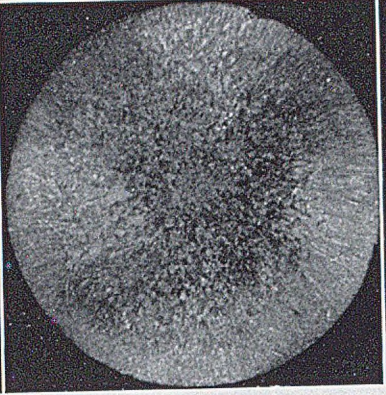

FIG. 7.—0·0025% B Addition.

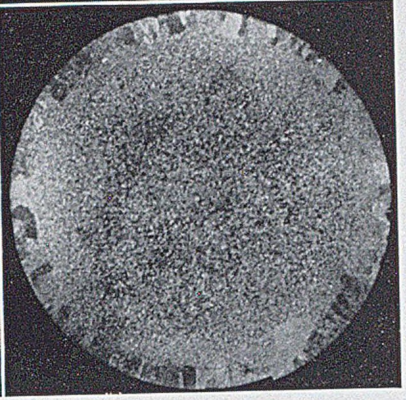

FIG. 8.—0·01% B Addition.

FIGS. 5–8.—Transverse Sections of Commercial Ingots of Copper–10% Aluminium Alloy. × Approx. $\frac{1}{3}$.

MICROSTRUCTURES OF TITANIUM-TIN ALLOYS.

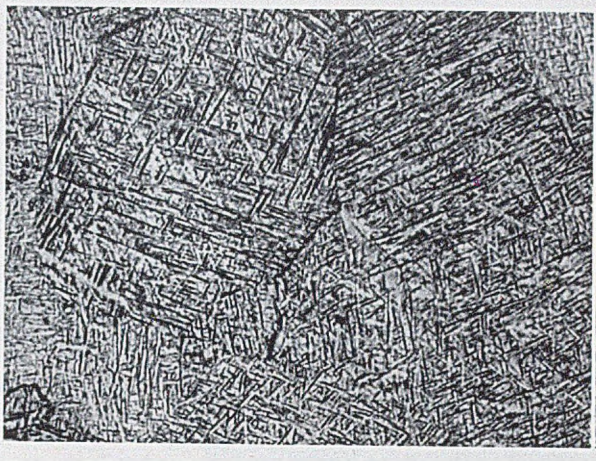

FIG. 7.—7·7 at.-% Tin Alloy (Commercial Titanium), Quenched from 1020° C. α in acicular form due to rapid $\beta \longrightarrow \alpha$ change. × 200.

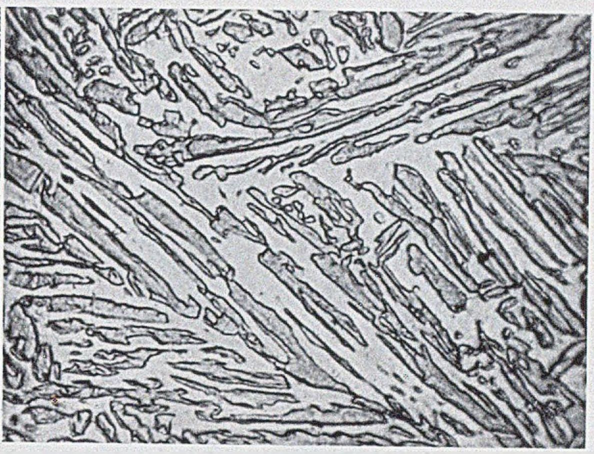

FIG. 8.—15·3 at.-% Tin Alloy (Commercial Titanium), Quenched from 850° C. $\alpha + \gamma$. ×1500.

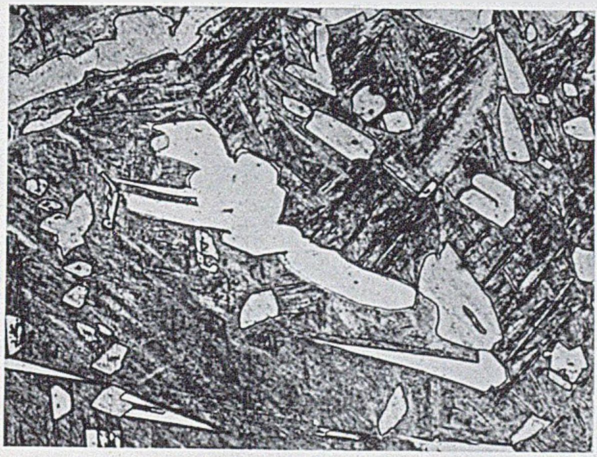

FIG. 9.—7·7 at.-% Tin Alloy (Commercial Titanium), Quenched from 950° C. Equilibrium α in matrix of acicular α. × 200.

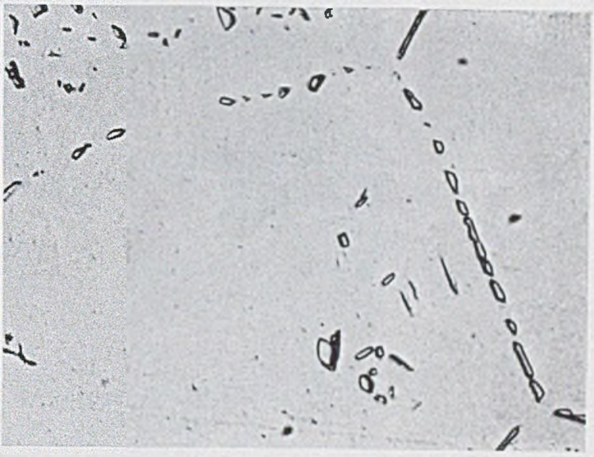

FIG. 10.—11·0 at.-% Tin Alloy (Refined Titanium), Quenched from 880° C. α with a little γ. × 1000.

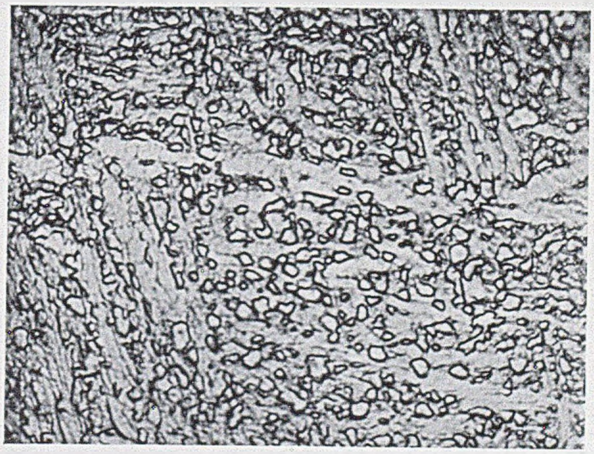

FIG. 11.—11·0 at.-% Tin Alloy (Refined Titanium), Quenched from 890° C. γ in matrix of acicular α. × 1500.

All specimens were etched in 2 wt.-% $HNO_3 + 1$ wt.-% HF in water.

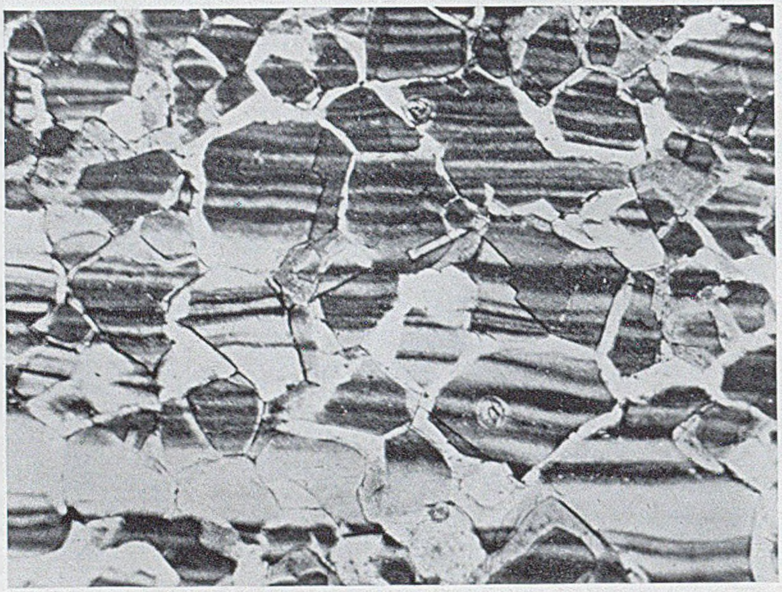

FIG. 7.—Structure of Fine-Grained Alloy E after 144 hr. at 860 lb./in.^{2} Stress (12% extension). × 270.

Stretcher-Strain Markings in Aluminium Alloys and Corresponding Talysurf Traces.

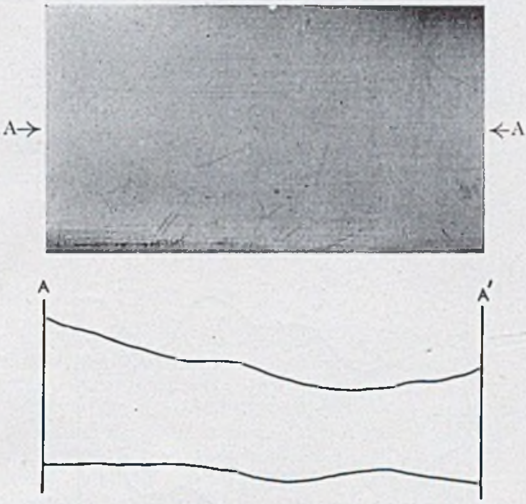

Fig. 1.—Aluminium–0·58% Magnesium Alloy. Annealed 4 hr. at 300° C. Permanent extension 1%.

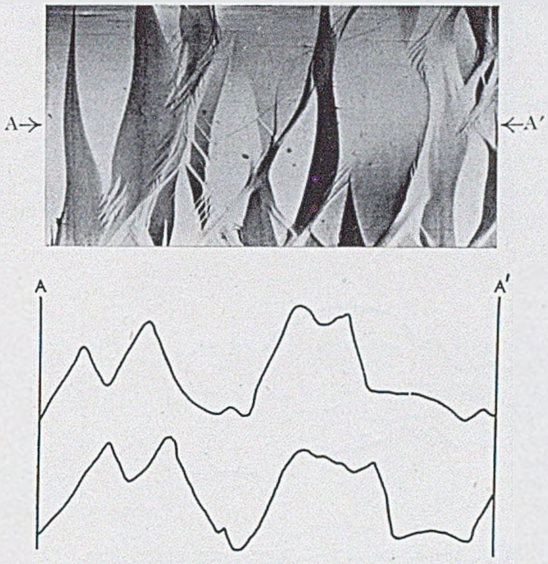

Fig. 3.—Aluminium–3·11% Magnesium Alloy. Annealed 2 hr. at 400° C. Permanent extension ½%.

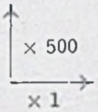

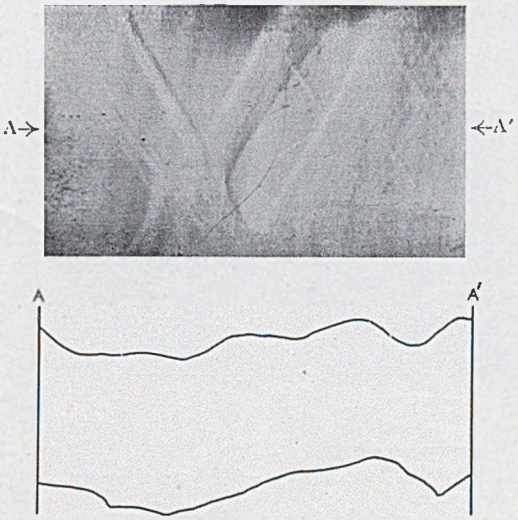

Fig. 2.—Aluminium–0·87% Magnesium Alloy. Annealed 4 hr. at 300° C. Permanent extension ½%.

STRETCHER-STRAIN MARKINGS IN ALUMINIUM ALLOYS AND CORRESPONDING TALYSURF TRACES.

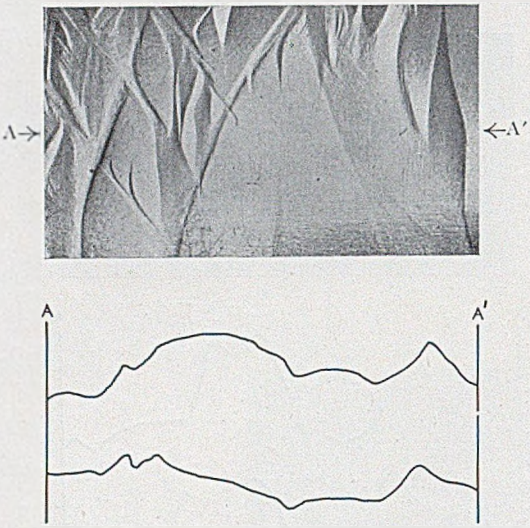

FIG. 4.—Aluminium–Copper–Magnesium Alloy. Solution-treated ½ hr. at 450° C. and quenched in oil. Permanent extension 0·3%.

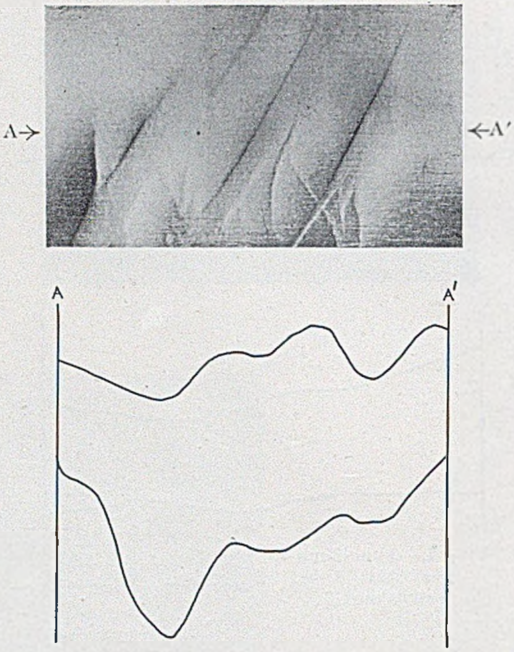

FIG. 6.—Aluminium–Copper–Magnesium Alloy, Clad with Pure Aluminium. Solution-treated ½ hr. at 450° C. and quenched in oil. Permanent extension 0·3%.

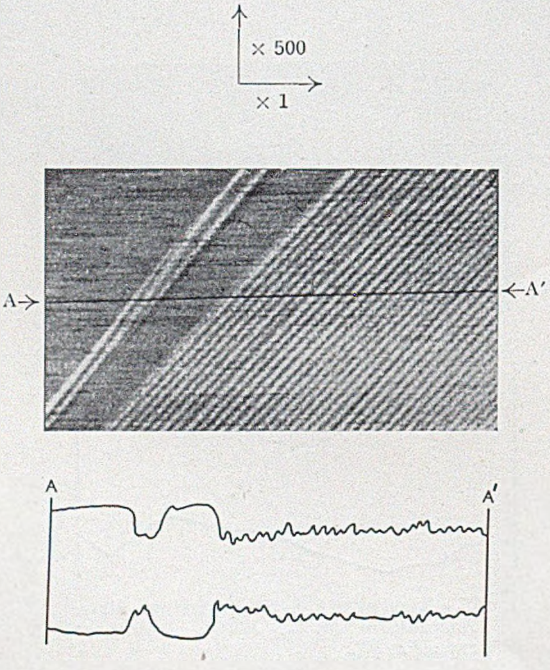

FIG. 5.—As Fig. 4. Permanent extension 9%.

METALLURGICAL ABSTRACTS

GENERAL AND NON-FERROUS

VOLUME 20 JULY 1953 PART 11

1 — PROPERTIES OF METALS

***The Discontinuous Elongation of Aluminium Crystals.—IV.** Tomoyosi Kawada (*J. Phys. Soc. Japan*, 1952, **7**, (3), 240–244).—[In English]. In continuation of previous work (*ibid.*, 1950, **5**, 68 ; *M.A.*, **19**, 337) the discontinuous elongations (of the order a few μ) of commercial coarse-grained Al polycrystals, and Al crystals of purity 99·99%, under tension, were studied at 20°–350° C. Discontinuous elongation occurred only when the slip lines terminated at a grain boundary and did not occur when the slip lines crossed a grain boundary. No discontinuity was observed in the elongation of an Al single crystal. A mechanism of the discontinuities is discussed.—J. S. G. T.

***Effects of Machining Specimens on the Results of Tension Tests of Annealed [Aluminium and] Aluminium Alloys.** (Stickley and Bogardus). See col. 751.

***Absorption of Carbon Monoxide by a Barium Getter. I.—Experiments at Low Temperatures. II.—Theory of Physical Adsorption. III.—Lattice Imperfections. IV.—The Gettering Process in Barium: Sorption Properties of Oxygen on Barium.** Tetsuya Arizumi and Seiichi Kotani (*J. Phys. Soc. Japan*, 1952, **7**, (2), 152–158 ; 158–163 ; 163–166 ; (3), 300–307).—[In English]. [I.—] The adsorption properties of a flashed Ba getter, for CO, at −180° to 0° C., were studied by the const.-flow and const.-vol. techniques, and the results are compared with those obtained with the Cu–CO system. The adsorption by Ba at −180° C. is not very different from that at room temp. By raising the temp. of the Ba getter from −180° C. in steps, the absorbed gas was at first desorbed and then re-absorbed. [II.—] A simple theory of CO adsorption by a Ba getter was found to hold only when the getter had already adsorbed considerable quantities of CO. The large adsorptive power of a fresh Ba getter is attributed to the existence of many lattice imperfections. The activation energies of phys. absorption, desorption, and activated adsorption for the Ba–CO system are, resp., 1·0, 1·4, and 6·5 kg. cal./g.-mol. A theory of adsorption, presuming the existence of lattice imperfections, is developed. [III.—] The theory developed in [II], extended to take into account numerous lattice imperfections, is found to agree qual. with the experimental results. [IV.—] The adsorption of O by Ba was studied at −180° to −30° C. Below −150° C. O is adsorbed mainly at active centres. The activation energy for phys. adsorption is 0·3 to ~0·9 kg.cal./g.-mol. At −150° to −30° C. O is adsorbed in the activated state, and its activated energy is 5·8 kg.cal./g.-mol. Above −30° C. O combines chem. with Ba.—J. S. G. T.

***Size Effects in the Supraconductivity of Cadmium.** M. C. Steele and R. A. Hein (*Phys. Rev.*, 1952, [ii], **87**, (5), 908).—A letter. The critical magnetic field for the destruction of supraconductivity increases more rapidly with decreasing temp. for high-purity Cd spheres 2–3 × 10^{-3} cm. radius than for spheres 6–12 × 10^{-2} cm. radius. The zero-field critical temp. was the same for both samples, but apparently higher than that of massive Cd.—P. C. L. P.

Melting Point of Chromium. F. W. David (*Engineer*, 1953, **195**, (5062), 176).—A letter. Referring to a note previously published in *Engineer* on the paper by Bloom, Putnam, and Grant (*J. Metals*, 1952, **4**, 626 ; *M.A.*, **20**, 66), D. draws attention to the recent detn. of the m.p. of Cr by Carlile, Christian, and Hume-Rothery (*J. Inst. Metals*, 1949–50, **76**, 169 ; *M.A.*, **17**, 915) and by Greenaway, Johnstone, and McQuillan (*J. Inst. Metals*, 1951–52, **80**, 109 ; *M.A.*, **19**, 317), who obtained values of 1860° and 1845° C., resp., for high-purity material (0·1% impurity in the case of the material used by Greenaway *et al.*).—D. K. W.

***Creep Fracture of Copper as a Nucleation Process.** Takeo Yokobori (*J. Phys. Soc. Japan*, 1952, **7**, (1), 48–51).—[In English]. The creep fracture of Cu wire was studied experimentally, and the results are interpreted by the aid of the theory developed elsewhere (*ibid.*, p. 44 ; *M.A.*, **20**, 745). In accordance with the theory, a linear relation was found between the log of the breaking stress, S, and the log of the time, t, required for fracture. In accordance with the theory, the reciprocal of the temp., T, and the log of the time, t, required for fracture under const. load, were found to be linearly related, in accordance with the equation $\log t = \Delta f/KT + C$, where Δf is the free energy of activation for the motion of a dislocation, and C is a const. The dependence of t upon the length of the wire, and the fluctuation characteristics of creep fracture are studied and interpreted in terms of nucleation theory.—J. S. G. T.

Measurement of the Specific Heat at Room Temperature of Copper in the Form of Wire by Electrical Heating. A. R. Ingles (*Amer. J. Physics*, 1952, **20**, (5), 289–292).—I. describes an experiment suitable for advanced students, based on the original work carried out by Lapp and Grew to determine the sp. heat of Ni at various temp.—W. A. M. P.

***Self-Diffusion on the Surface of Copper.** Erich Menzel (*Z. Physik*, 1952, **132**, (4), 508–528).—Spherical single crystals of Cu were chem. attacked to produce etch pits, and then heated at high temp. while the surface was observed opt. The time taken for a definite change in the surface reflection (corresponding to rounding of the etch-pit edges) was taken to be proportional to the reciprocal of the velocity of migration over the surface. When the crystal was held in air at a pressure of 10^{-3} mm. Hg, the surface change was found to obey the Boltzmann law in the region 700°–1080° C., the activation energy for surface diffusion being 13 ± 2 kg.cal./mole. Different results were obtained in a H atmosphere and indicated a chem. reaction between H and adsorbed O. Immediately below the m.p. the equilibrium form of the crystal was a smooth sphere.—J. W. C.

Germanium, the Unknown Element. —— (*Canad. Metals*, 1952, **15**, (12), 28).—A brief note on the properties, extraction, purification, and appn. of Ge.—W. A. M. P.

---

* Denotes a paper describing the results of original research. † Denotes a first-class critical review.

***Copper as an Acceptor Element in Germanium.** C. S. Fuller and J. D. Struthers (*Phys. Rev.*, 1952, [ii], 87, (3), 526–527).—A letter. The diffusion of radioactive Cu^{64} into a single crystal of Ge at 825° C. has been correlated with the formation of thermal acceptors. Annealing at 500° C. causes the Cu to precipitate and the specimen to return to its original *n*-type condition. At 1100° C., Cu diffuses into Si at a rate comparable with that of Cu into Ge.—P. C. L. P.

***Impurity Effects in the Thermal Conversion of Germanium.** W. P. Slichter and E. D. Kolb (*Phys. Rev.*, 1952, [ii], 87, (3), 527–528).—A letter. No detectable difference exists between the resistivity of high-purity Ge crystals kept in contact with the melt for a prolonged period during growth and the resistivity of rapidly grown crystals. Conversion of the crystal to *p*-type by heat-treatment was not found unless the crystal had been in contact with a soln. contg. Cu. In the crystal examined, about one hole was developed per Cu atom.—P. C. L. P.

***The [Electrical] Conductivity of Non-Polar [Germanium] Crystals in Strong Electrostatic Fields.** J. Yamashita and M. Watanabe (*J. Phys. Soc. Japan*, 1952, **7**, (3), 334–335).—[In English]. Ryder and Shockley (*Phys. Rev.*, 1951, [ii], 81, 139; *M.A.*, 19, 627) discovered that the elect. conductivity of a pure Ge crystal showed marked deviation from Ohm's law in strong electrostatic fields. By solving Bloch's integral equation for transport in non-polar semi-conductors, to a second order of approximation, Y. and W. obtain an expression for the dependence of the elect. current upon field strength. The critical field strength, at which deviation from Ohm's law begins, is deduced and is in qual. agreement with observations in so far as this critical field decreases with decreasing temp. The calculated critical field value for Ge is $\sim\frac{1}{3}$ of that observed. The critical field is sensitive to the presence of impurities.—J. S. G. T.

***Interpretation of the Low-Temperature Hall Curve of a Degenerate Germanium Sample.** D. M. Finlayson, V. A. Johnson, and F. M. Shipley (*Phys. Rev.*, 1952, [ii], 87, (6), 1141–1142).—A letter. The Hall coeff. of a Ge sample contg. a small amount of Sb has been found to have a max. near 120° K. The decrease in the Hall coeff. at low temp. is reconciled to a decrease in the carrier *d* by allowing for the dominating effect of impurity scattering at low temp.—P. C. L. P.

***Mobility of Electrons in Germanium.** P. P. Debye and E. M. Conwell (*Phys. Rev.*, 1952, [ii], 87, (6), 1131–1132).—A letter. New measurements of the Hall coeff. and resistivity of high-purity *n*-type Ge have given values of the electron mobility greater than any previously reported and in agreement with the drift mobility. The variation of the mobility with As content agrees with that predicted by impurity scattering. —P. C. L. P.

***Electron-Hole Recombination in Germanium.** R. N. Hall (*Phys. Rev.*, 1952, [ii], 87, (2), 387).—A letter. A simple theory of the recombination rate of holes and electrons at centres lying in the forbidden energy-band region, is used to deduce the variations of average lifetime with impurity content and temp., choosing parameters which give agreement between theory and experiment at room temp. Between +20° and −20° C., the variation of lifetime suggests that the recombination centres are 0·22 eV. above the valence band or below the conduction band.—P. C. L. P.

***Determination of the Absolute Grain-Boundary Energy of Gold at 1300° K.** F. H. Buttner, H. Udin, and J. Wulff (*J. Metals*, 1953, **5**, (2), 313–317).—During the course of surface-tension experiments on Au (*Trans. Amer. Inst. Min. Met. Eng.*, 1951, **191**, 1209; see *M.A.*, 19, 500) conditions of thermal and phase equilibrium were maintained about fine wire held at high temp. for long periods of time, and grain-boundary grooves appeared on the surface of the wire. The angular dimensions (θ) of these grooves have been used to determine—by a method which is described in detail—the energy of the grain boundaries. An overall average of $\theta = 164{\cdot}5°$ was obtained; this, in conjunction with the previously determined value for the surface tension, leads to an average grain-boundary energy of 365 ± 50 dynes/cm.^{2} at 1300° K. 37 ref.—E. N.

***Gyromagnetic Ratios of Iron, Cobalt, and Many Binary Alloys of Iron, Cobalt, and Nickel.** S. J. Barnett and G. S. Kenny (*Phys. Rev.*, 1952, [ii], 87, (5), 723–734).—After a review of previous work on gyromagnetic effects, a detailed description is given of the methods used to eliminate errors in the present work, in which the gyromagnetic ratios of Fe and Co were redetermined. The gyromagnetic ratios of Co–Fe, Co–Ni, and Fe–Ni alloys varied approx. linearly with compn. The Co–Fe alloys contained 0·4–0·6% Mn, while Al and Si were present as impurities in the Co–Ni and Fe–Ni samples. —P. C. L. P.

***Heat Conductivity of Supraconductive Lead Below 1° K.** J. L. Olsen and C. A. Renton (*Phil. Mag.*, 1952, [vii], 43, (344), 946–948).—The thermal conductivity of supraconductive Pb, σ, between 0·4° and 0·9° K. may be expressed by the formula $\sigma = AT^3$, though σ increases more rapidly above 0·9° K. The experimental value of A is considerably less than that calculated theoretically, assuming negligible electronic scattering of the lattice vibrations. The heat resistance increases when the specimen is brought isothermally into the intermediate state by appn. of a magnetic field. —P. C. L. P.

***The Heat Capacity of Mercury from 15° to 330° K.: Thermodynamic Properties of Solid, Liquid, and Gas: Heat of Fusion and Vaporization.** R. H. Busey and W. F. Giauque (*J. Amer. Chem. Soc.*, 1953, **75**, (4), 806–809).—Observations from measurements of the heat capacity of Hg from 15° to 330° K. were combined with available calorimetric and vapour-pressure data and the Sackur–Tetrode equation, to determine thermodynamic properties. The following values (cal./mole) were obtained: heat of fusion of Hg at the m.p. 548·6; heat of vaporization at the b.p. 14,127; entropy of liq. Hg at 298·16° K., 18·19.—J. R.

***The Diffusion Coefficients of Certain Metals in Mercury.** W. Charles Cooper and N. Howell Furman (*J. Amer. Chem. Soc.*, 1952, **74**, (24), 6183–6186).—Previous work on the detn. of the diffusion coeff. of various metals in Hg by e.m.f., conductance, and polarographic methods is reviewed, the reported results being compared with each other and with those obtained by F. and C. for Sn and Bi (1·68 and $0{\cdot}99 \times 10^{-5}$ cm.^{2}/sec., resp.), using a polarographic technique earlier described (*ibid.*, 1950, **72**, 5667; *M.A.*, 18, 624). Consideration of the relationship between diffusion coeff. and atomic radii indicates the probability of molecules of Cu–Hg and Bi–Hg compounds occurring in dil. mercurial soln.—J. R.

***Properties of Molybdenum Made by Arc Casting and Powder Metallurgy.** James H. Bechtold and Howard Scott (*Metal Progress*, 1952, **61**, (4), 82–88).—The inherent differences in mech. properties between arc-cast and powder-met. Mo after hot-rolling $\frac{5}{8}$-in. rods at 1900°–1700° F. (1040°–925° C.) are illustrated. U.T.S. and % elongation curves at temp. from −100° to 200° C. for both materials show that their properties are very similar. Creep-rupture curves at 1600° F. (870° C.) in H for arc-cast and powder-met. Mo also show close similarity. 100-hr. rupture strengths of Mo, pure Fe, Co, Refractaloy 70, and Stellite No. 31 are given for purposes of comparison. The influence of stress distribution on the transition temp. was studied, using a theoretical stress-concentration factor of 3·1. This condition raised the transition temp. to 257° F. (125° C.). The cold brittleness of Mo was found to be associated with a well-defined transition from ductile to brittle fracture on a tensile test only slightly below room temp.—R. P. H. F.

***Carriers of Electricity in Metals [Molybdenum and Zinc] Exhibiting Positive Hall Effects.** Sheldon Brown and S. J. Barnett (*Phys. Rev.*, 1952, [ii], 87, (4), 601–607).—The sign of the current carriers in Mo and Zn, which have positive Hall coeff., is negative, while the value of e/m is within 3% of that for slowly moving free electrons. The same result was also obtained with the Mo at liq.-air temp.—P. C. L. P.

***Nature of the Creep Curve [Especially for High-Purity Nickel].** Thomas H. Hazlett and Earl R. Parker (*J. Metals*, 1953, **5**, (2), 318–323).—A study has been made of the effects of stress, temp., alloying, and structure on the creep characteristics of some metals, particularly specially prepared high-purity Ni contg. Fe 0·030, Si 0·003, Ca 0·001, Mg 0·020, and S 0·002%, balance (99·944%) Ni, and its solid-soln. alloys with 0·25, 1, and 2% Ti. The tests were carried out in independent single creep-test units, at const. stress (3700–8000 lb./in.^{2}) rather than const. load, to total strains of 0·15, at temp. up to 750° C. The results show that structurally stable metals like Ni, tested under conditions of const. stress, exhibit a continuous decrease in creep rate up to the point of initiation of failure; there is no region of const. creep rate. The creep curve may be accurately represented by the empirical equation, (1) $\varepsilon - \varepsilon_0 = At^b$, at const. temp., or (2) $\varepsilon - \varepsilon_0 = Bt^b e^{-Q/RT}$, over a considerable temp. range; ε = total true strain, ε_0 = instantaneous strain at loading, t = time, A = a const. which varies in a regular manner with stress and alloy content, and exponentially with $1/T$, B and b = const., T = abs. temp., R = the gas const., and Q = the "experimental activation energy". An analysis of the results of other workers on the creep of mild steel, Pt, and Cu, and of Pb and high-purity Al, confirms equations (1) and (2), resp.; equation (2) is also substantiated by the data obtained for the Ni–Ti alloys, and for single crystals of Zn tested in shear—thus indicating that the continuously decreasing creep rate is not solely a grain-boundary phenomenon, although it does vary with grain-size. 8 ref.—E. N.

***On the Problem of the Magnetic Transformation [of Nickel].** Friedrich Fraunberger (*Z. Physik*, 1952, 132, (2), 212–220).—Experimental results for the H.F. resistance of Ni wires, the magnetocaloric effect, susceptibility, sp. heat, &c., are shown to imply that the magnetic transformation takes place in several steps. It is suggested that there is a relation between the magnetic state and the Debye characteristic temp.
—J. W. C.

***Electrical Conductivity of Thin Films of Platinum Covered with a Dielectric Coating by Vacuum Evaporation.** Charles Feldman and Boris Vodar (*Compt. rend.*, 1952, 235, (6), 414–417).—Using the method previously described (F., *ibid.*, 1952, 234, 1858; *M.A.*, 20, 388), F. and V. give the results of experiments on the elect. conduction of thin films of Pt on glass when a much thicker (of the order of 1000 Å.) coating of a dielectric (such as SiO_2) is deposited on them by vacuum evaporation. At ordinary temp. there is no great variation in the resistance, and no difference in ageing between the covered and the uncovered films was observed. The usual relation between the resistance and the temp. was confirmed for both types, but covering the film with SiO_2 caused an increase in the temp. coeff. and a diminution of the stress coeff. This is the same effect as that observed as a result of gas adsorption and the reverse of that of annealing (not hitherto recorded).—J. H. W.

***Coefficients of Accommodation of Complex Molecules upon Metals: The Case of Acetaldehyde at 273° K. on Platinum at 1000°–1300° K.** Xavier Duval and Michel Niclause (*J. Chim. Phys.*, 1952, 49, (2), 51–59).—A general relation, established for the elect. power dissipated from a heated metal filament stretched axially within a cylindrical vessel, exhausted to a very low pressure, in terms of the thermal conductivity of the gas and other phys. data relating to the system, is applied to determine the coeff. of accommodation (α) of gases upon the filament. Results relating to the accommodation coeff. of acetaldehyde molecules at 273° K. upon a Pt filament at 1000°–1300° K. are tabulated and discussed. Values of α range from 0·1 to 0·4, and decrease when the temp. of the filament increases, so that the molecules of acetaldehyde which leave the filament have a mean internal energy corresponding to a temp. much below that of the filament, e.g. $<700°$ K. when the filament is at 1300° K. 26 ref.—J. S. G. T.

***(I) Non-Uniform Nature of Selenium Rectifiers. (II) Electron Multiplication in Hard Flows of Selenium Rectifiers.** Masao Tomura and Yukiaki Abiko (*J. Phys. Soc. Japan*, 1952, 7, (2), 167–170; 220–221).—[In English]. [I.—] Small Se rectifiers, all cut from one normal-sized rectifier, were found to differ in respect of spreading resistance, contact potential, max. back voltage, which depended more especially upon the dimensions of the rectifiers. Local thin patches, separated by a mean distance of several mm., occur. Rectifiers having no local thin patches are characterized by back voltages as high as 100 V. [II.—] In continuation of previous work (*ibid.*, 1950, 5, 349; *M.A.*, 19, 695), the occurrence of electron multiplication and the occurrence of noises due to electron avalanches, and their dependence on temp. and voltage, are briefly discussed.—J. S. G. T.

***Electrical Dispersion of the Selenium Rectifier at High Frequency.** Jiro Yamaguchi, Takeshi Miyauchi, and Hideo Mori (*J. Phys. Soc. Japan*, 1952, 7, (2), 171–173).—[In English]. Frequency characteristics of Se rectifiers were studied; elect. dispersion, observed at ~1 Mc./s. at room temp., is attributed to the relaxation effect of an electron transferred from an impurity centre to the conduction band.—J. S. G. T.

***An Application of the Cellular Method to Silicon.** D. K. Holmes (*Phys. Rev.*, 1952, [ii], 87, (5), 782–784).—The energy limits of the filled and conduction bands of Si have been calculated as a function of internuclear sepn., assuming that the top of the filled band and the bottom of the conduction band occur at the centre of the Brillouin zone. The calculated energy gap is considerably greater than that observed, which might be due to incorrectness of the assumption made. The effective mass of electrons occupying a level at the bottom of the conduction band has been computed.—P. C. L. P.

***Mechanical Properties of Thin Films of Silver.** J. W. Beams, W. E. Walker, and H. S. Morton, Jr. (*Phys. Rev.*, 1952, [ii], 87, (3), 524–525).—A letter. The strength of a thin Ag film electrodeposited on to a small cylindrical steel rotor has been determined from the conditions necessary to remove the films by centrifugal force. The U.T.S. is ~40,000 lb./in.^{2} for films 0·001–0·00003 in. thick, but thinner films rapidly increase in relative strength.—P. C. L. P.

***The Solubility of Oxygen in, and the Oxides of, Tantalum.** R. J. Wasilewski (*J. Amer. Chem. Soc.*, 1953, 75, (4), 1001–1002).—A note. Lattice-parameter values for Ta contg. 0–1·96% O show linearity between parameter increase and increasing O; the O solubility limit was found to be 0·9 wt.-% at 1050° C., but there are indications of much higher solubilities at higher temp. No confirmation of the existence of Ta_2O_4 was obtained, and any structure intermediate between Ta_2O and Ta_2O_5 is considered doubtful. Reaction of Ta_2O_5 with Ta metal is very rapid in the range 1700°–2200° C., indicating rapid diffusion of O and accounting for the difficulty in obtaining O-free Ta on slow cooling through this range after sintering.—J. R.

***Optical Polarization in Single Crystals of Tellurium.** J. J. Loferski (*Phys. Rev.*, 1952, [ii], 87, (5), 905–906).—A letter. The transmission of polarized infra-red radiation through a single crystal of Te has been measured as a function of λ in the region 3–9 μ, and of the relative orientation of the *c*-axis of the crystal to the plane of polarization. The absorption coeff. was determined by using crystals of different thicknesses, and its variation with λ is discussed in relation to the energy gap between the filled and conduction electron energy levels.—P. C. L. P.

***The Electrical Resistance of Thin Layers of Tin with Lattice Defects.** Johannes Niebuhr (*Z. Physik*, 1952, 132, (4), 468–481).—Thin layers of Sn were deposited on quartz plates at condensation temp. below 200° K., and their elect. resistance measured between 10° and 420° K. The layers had thicknesses from 200 to 2000 Å.; the results were reproducible and independent of condensation rate. Temp./elect. resistance curves are given for various condensation temp. and layer thicknesses, and the variation of the sp. resistance with layer thickness for various condensation temp. is obtained. The results are compared with theories due to Fuchs and to Sondheimer.—J. W. C.

***Measurements on the Temperature, Current, and Magnetic-Field Phase Diagram of Supraconductivity [of Tin].** K. Mendelssohn, C. Squire, and Tom S. Teasdale (*Phys. Rev.*, 1952, [ii], 87, (4), 589–591).—No paramagnetic effect at the transition of a Sn sample has been found in experiments where the magnetic field, current, and temp. were varied separately, in steps, so as to cause supraconductivity. Currents of 6–10 amp. with magnetic fields of 16–30 Oe., were employed so that the transition temp. occurred at 3·5°–3·6° K. The results do not disprove the existence of a paramagnetic effect of a transient nature.—P. C. L. P.

***Microstructure and Mechanical Properties of Iodide Titanium.** F. C. Holden, H. R. Ogden, and R. I. Jaffee (*J. Metals*, 1953, 5, (2), 238–242).—The effects of heat-treatment on the structure and mech. properties of commercially produced iodide Ti have been studied. The as-deposited rods, contg. N 0·004–0·008, Mn 0·005–0·013, Fe 0·0035–0·025, Al 0·013–0·015, Mo 0·0015, Pb 0·0045–0·0065, Cu 0·0015–0·002, Sn 0·001–0·01, Mg 0·0015–0·002, Ni 0·003, and H 0·0091 wt.-%, were arc-melted with a W electrode in a water-cooled Cu crucible under high-purity A, to produce a 2-in.-dia. ingot having the same hardness (85 D.P.N.) as the initial stock. As the grain-size of equiaxed α annealed metal increases from 0·01 to 0·25 mm., the U.T.S., impact energy, and hardness decrease slightly, and there is a corresponding increase in ductility; coarse-grained material hardens considerably more than fine-grained material starting from a lower initial flow stress. Large-grained (0·2–0·3 mm. dia.) serrated α structure material produced by furnace-cooling from the β field has mech. properties very similar to those of equivalent large equiaxed α grains. Quenching from the α or β fields changes the distribution of TiH, the second phase present in the metal, and increases the hardness and strength, particularly the yield and flow stresses, and the level of the impact energy. Overall average values for the mech. properties are : P.S. (0·2%) 20,000 and U.T.S. 35,000 lb./in.^{2}, elongation 65%, reduction in area 85%, and D.P.N. (5-kg. load) 90. Photomicrographs show the typical structures encountered. 6 ref.—E. N.

***Creep Properties of Commercially Pure Titanium.** W. R. Kiessel and M. J. Sinnott (*J. Metals*, 1953, 5, (2), 331–338).—A study has been made of the creep characteristics of commercially pure Ti sheet—contg. C 0·037, Si 0·023, W 0·50, Ni 0·083, Fe 0·08, and O + N probably 0·2%—in the annealed (for 1 hr. at 1600° F. (870° C.) in A), cold-worked, and cold-worked and recovered states at 75°–750° F. (25°–400° C.). The results show that : (1) cold working up to 40% by rolling improves the creep-resistance because of the residual strains left in the lattice; (2) recovery in sheet rolled >60, 40, and 7%, occurs at room temp., between room temp. and 210° F. (100° C.), and between 210° and 400° F. (205° C.), resp.; (3) sheet of the given compn. exhibits strain-ageing which markedly improves its creep-resistance—an effect which is most noticeable when creep testing is carried out at 400° F.; (4) cold working and/or strain-ageing causes a considerable reduction in the amount of first-stage creep; and (5) relationships appear to exist between (i) the amount of internal strain induced by cold rolling and the creep-resistance at temp. below which recovery occurs, and (ii) the short-time U.T.S. and the creep-resistance of metal which has been cold-worked and recovered. 20 ref.—E. N.

Titanium Metal and Its Future. (Burston *et al.*). See col. 813.

***An Abnormal After-Effect in Metals [Zinc and Steel].** Charles S. Barrett (*Acta Met.*, 1953, 1, (1), 2–7).—[In English]. The untwisting of metal wires, previously given plastic strains of 0·2–0·3% in torsion, was observed opt., the wires being immersed in a stream of water. After some time, the water was suddenly replaced by a dilute acid soln., used as an etchant to remove oxide layers. During relaxation, the strain decreased linearly with log time; this is the normal after-effect. When the etchant was applied, there was usually a transient increase of strain, and the subsequent untwisting was always less rapid than originally. The effects were observed for single and polycryst. specimens of pure and impure Zn and mild steel. The existence of a Bauschinger effect in single crystals was also confirmed. The results are explained by assuming that dislocations pile up behind an adherent oxide layer; when this layer is removed, some dislocations escape to the surface, thus increasing the twisting. The subsequent slower untwisting is due to the balance between dislocations which relax back to their original positions and those which relax out to the surface. 18 ref.—J. W. C.

***Effects of Small Additions of Oxygen on Lattice Constants and Hardness of Zirconium.** R. M. Treco (*J. Metals*, 1953, 5, (2), 344–348).—The effects of small addn. (up to 2·5 at.-%) of O on the lattice parameters, hardness, and *d* of high-purity Zr has been studied. The iodide crystal bar, of given compn., low in Hf (0·0142 at.-%), and contg. 0·0147 at.-% O, had lattice const. of $a = 3{\cdot}2256_2 \pm 0{\cdot}00014$ and $c = 5{\cdot}1370_9 \pm 0{\cdot}00036$ kX; these increased linearly with increasing O content, but the *c/a* ratio, 1·5926, remained const.; extrapolated values for O-free metal gave $a_0 = 3{\cdot}2258_0 \pm 0{\cdot}00064$ and $c_0 = 5{\cdot}1373_2 \pm 0{\cdot}00105$ kX. Equations which were derived for relating lattice parameters to O content were not sufficiently accurate to justify their use for analytical purposes. Small amounts of O produced large increases in hardness, as little as 2·0 at.-% embrittling the metal to such an extent as to preclude cold working and machining. This, together with the fact that there is little tendency to form mech. twins, suggests that the O atoms occupy preferred positions in the lattice, thus interfering with the normal slip process, and it is probable that slip and twinning occur, not on the usual hexagonal basal plane, but in a manner similar to that in α-Ti, where slip occurs in the $(10\bar{1}0)$ and $(10\bar{1}1)$ planes, and in a $[1\bar{1}20]$ direction, while twinning takes place in the planes $(10\bar{1}2)$ and $(11\bar{2}2)$. The X-ray *d* of O-free metal was calculated as 6·507 g./cm.^{3} at 25° C.; the *d* increased with increasing O contents, despite the observed linear increase in unit cell vol., while the effects of minor impurities were found to vary with the sp. element. It is considered that good agreement in the calculated and measured *d* values is consistent with the initial assumption of interstitial and substitutional soln. of O and Hf atoms resp. 9 ref.—E. N.

***High-Temperature Experiments with Zirconium and Zirconium Compounds.** W. J. Kroll, W. R. Carmody, and A. W. Schlechten (*U.S. Bur. Mines, Rep. Invest.*, 1952, (4915), 31 pp.).—A report of the chem. reactions of Zr and Zr compounds investigated during the development of processes for the prodn. of ductile Zr; it is stated that the results are also applicable to Ti and Ti compounds. The prodn. of $ZrCl_4$ by the following methods was considered and the conditions and yields investigated : (1) Direct chlorination of ZrO_2–C mixtures; (2) chlorination of the carbide with HCl; (3) reaction between chlorides (e.g. Mg and Ca) and ZrO_2; (4) reaction between K_2ZrF_6 and $CaCl_2$; and (5) reaction between ZrSi and $FeCl_2$. The sepn. of Zr by the formation of the sulphide or of K_2ZrF_6 was also investigated. Direct prodn. of alloys was carried out by the reduction of ZrO_2 by C in the presence of other metals, reduction of Zr double chlorides or fluorides by (e.g.) Mg–Cu alloys, by fusion electrolysis to form an alloy with the cathode metal, and by reduction of compounds with Al. The power of various metals to reduce $ZrCl_4$ was investigated, and Al was found to be most effective. Electrolytic methods were developed for plating other metals with Zr. A number of experiments on the fusibility of $ZrCl_4$–NaCl mixtures are also reported. The prodn. of Zr powder by Mg reduction of the oxide, reduction of the chloride, and by fusion electrolysis is described. An appendix on the detn. of O in Zr by chlorination methods is included. 32 ref.—D. M. P.

***Final Report on Metallurgical Investigation of Materials Subjected to Liquid Lead–Bismuth Alloy Environment.** R. C. Grassi, D. W. Bainbridge, and J. W. Harman (*U.S. Atomic Energy Commission Publ.*, 1952, (**AECU–2201**), 72 pp.).—Stress-rupture data were obtained for Mo at 1600° and 1800° F. (870° and 980° C.) and for Nb at 1800° F. in He, Pb, and Bi. An anomalous increase in effective strength was found for Mo at both 1600° and 1800° F. in Pb and Bi; at 1800° F. the load for fracture in 100 hr. was 13% greater in Bi than in He and 7% greater in Pb. No significant surface attack by the liq. metals was noted. The strength of Nb was slightly less in Pb than in He for tests of <100 hr. Pb caused no major soln. attack, but micrographic studies showed the presence of a new surface phase with a slight penetration. Bi caused the development of surface fissures in Nb, and the attack was accompanied by a marked loss in strength and ductility. When Nb was welded to Mo, large grains were developed, together with the formation of an unknown precipitate in the grain boundaries which resulted in marked weakening of the material in liq. Bi at 1800° F. In static soln. tests in Pb and Pb–Bi, Fe, Cr, Ni, and Mn were found to dissolve in appreciable amounts from a low-alloy steel, an austenitic stainless steel, and various ferritic stainless steels in the temp. range 1400°–2000° F. (760°–1095° C.). The liq. became rapidly saturated with Fe, which was displaced from soln. with further soln. of Cr; this effect was more pronounced in Pb than in Pb–Bi alloy. Ni also appeared to have a precipitating influence with respect to Fe and Cr. For all the materials studied, the eutectic Pb–Bi alloy was more reactive than Pb and dissolved ~5 times the amount of all steels tested. Metallographic evidence suggested that surface decarburization occurred for some steels and the degree of general attack increased with the concentration of Cr and Ni in the steel. No evidence of attack was obtained for Mo in Pb at 1400°–2000° F., and it appeared that Nb was unattacked by Pb. A review is given of the complete results to date, and suggestions are made for further work.—B. W. M.

***Theory of Time-Dependent Rupture and Interpretation of Some Stress-Rupture Data.** D. N. Frey (*Amer. Soc. Test. Mat. Preprint*, 1952, (80), 7 pp.).—The mechanism of rupture processes is considered, and it is suggested that two types of processes occur. At short times and high stresses, dislocations condense to form a microcrack of critical size; at long times and low stresses, where creep is negligible, rupture is of a truly brittle nature. Microcracks initially present grow by random thermal oscillations to critical size. The increased time to rupture brought about by pptn. in austenitic alloys can be explained on this basis. Circumferential notches increase the rupture time for short times, but decrease it for long times, and this is also explicable on the theories put forward. 11 ref. —P. T. G.

***Failure and Fracture of Metals as a Nucleation Process.** Takeo Yokobori (*J. Phys. Soc. Japan*, 1952, 7, (1), 44–47).—[In English]. Discontinuous plastic phenomena in metals, e.g. yielding and brittle fracture, are regarded as Markoff processes, and are discussed math. from the standpoint of nucleation theory. Among matters discussed are: (1) the relation between strength and deformation or stress velocity; (2) the temp. dependence of strength; (3) the size-effect; (4) the transition temp. from ductile to brittle fracture; (5) fluctuation characteristics of strength, and (6) theoretical criteria of failure and fracture of polycryst. metals. 20 ref. —J. S. G. T.

***Failure and Fracture of Metals as a Rate Process.** Takeo Yokobori (*J. Phys. Soc. Japan*, 1952, 7, (1), 122–123).—[In English]. Math. deductions from a theory of the failure and fracture of metals which regards yielding as a process of nucleation and the growth and movement of dislocations, are shown to be in good agreement with many experimental data relating to the fracture of the harder metals. Creep fracture after necking is better explained as a growth process of a crack nucleus than as a nucleation process.—J. S. G. T.

Effect of Radiation on Elastic Constants. F. R. N. Nabarro. G. J. Dienes (*Phys. Rev.*, 1952, [ii], 87, (4), 665–666).—Two letters. N. claims that the approximation used by Dienes (*ibid.*, 1952, [ii], **86**, 228; *M.A.*, **20**, 450), in which a lattice distorted by interstitial atoms and vacancies is treated as deforming homogeneously, overestimates the difference between the effects of interstitial atoms and vacant lattice sites in equal numbers. Different estimates are obtained by applying elasticity theory. D. replies that N.'s elasticity-theory calculations underestimate the effect of interstitial atoms, and that if a more probable radius of effect of an interstitial atom were used, elasticity theory would have given a result in approx. agreement with the original calculations. —P. C. L. P.

†Mechanical Effects of Interfaces. Bruce Chalmers (*Metal Interfaces* (*Amer. Soc. Metals*), **1952**, 299–311).—Variations in the mech. properties of metals, viz. elastic and plastic properties and fracture, associated with (1) the external surface and (2) interfaces between crystals of either (*a*) the same or (*b*) different phases of a metal, are very briefly discussed. Effects occur in polycryst. metals that cannot be detected or predicted in single crystals. 33 ref.—J. S. G. T.

†Stress Relaxation Across Interfaces. A. S. Nowick (*Metal Interfaces* (*Amer. Soc. Metals*), **1952**, 248–268).—Mech. properties due to stress relaxation across interfaces, the effect of impurities on grain-boundary relaxation, and the activation energy for interface relaxation, are briefly reviewed. Experimental methods for studying relaxation effects include stress relaxation at const. strain, creep at const. stress, creep recovery, internal friction, and dynamic modulus. 28 ref. —J. S. G. T.

***Prediction of Creep Curves from Stress/Strain Data.** Yoh-Han Pao and Joseph Marin (*Amer. Soc. Test. Mat. Preprint*, 1952, (141), 7 pp.).—A method is developed for predicting tension creep/time relations for const. stresses from tensile stress/strain relations at various strain rates. The essential difference between the proposed procedure and formerly proposed " equations of state " procedures is that the mech. equation of state is applied to the creep strains and creep rates only, rather than to the total strains and total strain rates. Graphical and numerical procedures have been used, and no actual equation has been formulated. The method was applied to test data obtained using Plexiglas II, and the agreement between actual and predicted creep/time curves was good. 7 ref.—P. T. G.

***A Statistical Interpretation of the Effect of Understressing on Fatigue Strength.** E. Epremian and R. F. Mehl (*Amer. Soc. Test. Mat. Preprint*, 1952, (90), 7 pp.).—Specimens subjected to fatigue at or below the endurance limit will undergo a larger number of cycles to failure, as compared with virgin material, when tested at a higher stress. To investigate this effect of understressing, specimens of Armco Fe and of a steel were tested in groups of 20 at several stresses in the endurance range and were then retested at a higher stress. It is concluded that the effect of understressing can, in part if not wholly, be interpreted as a statistical phenomenon based on selectivity and the statistical nature of the endurance limit, and that contrary to general belief, cold work does not play a dominant role. The importance of the statistical approach to fatigue problems is emphasized.—P. T. G.

***An Investigation of the Coaxing Effect in Fatigue of Metals.** G. M. Sinclair (*Amer. Soc. Test. Mat. Preprint*, 1952, (92), 9 pp.).—The fatigue-resistance of some metals may be improved by understressing followed by a process of gradually increasing the amplitude of the alternating stress in small increments (" coaxing "). The effects of various coaxing procedures on the fatigue resistance of ingot Fe, two steels, 75S-T6 Al alloy (Zn 5·6, Mg 2·5, Cu 1·6, Cr 0·3%), and annealed 70 : 30 brass, were studied. The fatigue-resistance of unstrained ingot Fe and the steels was considerably increased by coaxing, but that of strained and aged ingot Fe, the Al alloy, and the brass was not improved. It is concluded that the coaxing effect is due to a time-dependent localized strengthening of the metal by strain-ageing and not to the ability of the metal to be strengthened by cold work. 12 ref. —P. T. G.

***On the Theory of Dipole Interactions with Metals.** S. J. Czyzak (*Amer. J. Physics*, 1952, 20, (7), 440–446).—Practical appn. in which interactions of organic mol. and metallic surfaces play an important part include adhesion, lubrication, friction, wetting, and phys. absorption. The classical and quantum-mech. interactions of molecular dipoles and metallic surfaces are derived and numerical calculations given for several mol.–metal pairs. The effect of the polarity of the mol. on the interaction energy with metallic surfaces, and the problem of adhesion are also discussed. 21 ref. —W. A. M. P.

***Theoretical Problems Relating to the Determination of Coefficients of Auto-Diffusion in Solids by the Method of Isotopic Heterogeneous Exchanges.** Gaston Berthier (*J. Chim. Phys.*, 1952, 49, (10), 527–536).—Based upon Fick's diffusion law, the method and notation of vectorial analysis are applied to develop a theory and formulæ applicable to the detn. of coeff. of auto-diffusion in solids by the method of isotopic exchanges. Tables facilitating calculations relating to plane, cylindrical, and spherical diffusion are provided, and the possibilities of the method are illustrated by appn. to the work of Haïssinsky and Peschanski on S (*ibid.*, 1950, **47**, 191).—J. S. G. T.

***Theory of Grain-Boundary Diffusion.** R. Smoluchowski (*Phys. Rev.*, 1952, [ii], **87**, (3), 482–487).—The variation of the structure of grain boundaries with the relative angle of disorientation (*J. Appl. Physics*, 1951, **22**, 1260; *M.A.*, **19**, 599) is used to deduce the apparent activation energy for grain-boundary diffusion, taking loss of material from the boundary into surrounding grains into account. In certain circumstances it is possible to get a small or a negative apparent activation energy. The theory is in agreement with the experimental work on the diffusion of Zn in Cu (Flanagan and S., *ibid.*, 1952, **23**, 785; *M.A.*, **20**, 226). —P. C. L. P.

†Metal Surface Phenomena. Herbert H. Uhlig (*Metal Interfaces* (*Amer. Soc. Metals*), 1952, 312–333).—U. considers that there are no special forces at the surface of a metal; surface forces are the same as those operating within the crystal lattice, and differ only in magnitude from the latter. After clarification of this matter the subjects of phys. and chem. adsorption are discussed. It is considered that adsorbed layers account largely for: (1) friction and lubrication phenomena; (2) catalytic activity; (3) passivity and corrosion-resistance, particularly of the transition metals, which are themselves passive or constitute the major components of passive alloys. 38 ref.—J. S. G. T.

†The Atomistic Theory of Metallic Surfaces. Conyers Herring (*Metal Interfaces* (*Amer. Soc. Metals*), 1952, 1–19; discussion, 19).—The work-function and surface energy of metal surfaces, free from contamination, are discussed theoretically, starting from elementary considerations relating to the formation of a superficial double layer by a process of electron spreading, and leading up to a brief discussion of the free-electron theory of surface energy. Other matters briefly discussed include: (1) the double layer of an idealized metal with a homogeneously-distributed positive charge and a stepped or flat surface; (2) semi-empirical deductions relating to surface energy, e.g. that metals tend to have smaller values of the ratio shear modulus/bulk modulus than non-metals; (3) theory of the elastic const. of metals; and (4) the relation of the work-function to electron-emission phenomena. H. considers that all theoretical papers relating to the properties of metal surfaces are open to serious objections, and suggests that the surface lattice spacing may be a few % less than that in the interior. 12 ref.—J. S. G. T.

†Measurement of Solid/Gas and Solid/Liquid Interfacial Energies. Harry Udin (*Metal Interfaces* (*Amer. Soc. Metals*), 1952, 114–133).—Experimental methods, developed within the last 4 years, for measuring solid/gas and solid/liquid interfacial energies are briefly reviewed, and results relating to Cu, Ag, and Au at temp. of 1040°–1360° K. are given and briefly discussed. For many metals the ratio solid : liquid energy/g.-atom of surface atoms is ~½ the heat of fusion, indicating that interfacial atoms may be considered as half-melted, each atom having, on the average, an equal number of liquid and solid near neighbours. The interfacial tension solid Cu/Pb vapour is 800 dynes/cm.; that of solid Cu/liq. Pb is ~360 dynes/cm. The surface tension of Cu is 1800 dynes/cm. O appears to be strongly adsorbed at grain boundaries as well as at the surface of Ag. Imperfect wetting, e.g. as in the case of Pb on Cu, appears to be exceptional among metal pairs. Although a number of transition metals wet refractory carbide surfaces, only Co-bonded carbide performs well in a tool-bit. 26 ref.—J. S. G. T.

***The Specific Heats of Several Metals Between 1·8° and 4·2° K.** I. Estermann, S. A. Friedberg, and J. E. Goldman (*Phys. Rev.*, 1952, [ii], **87**, (4), 582–588).—The sp. heats of Cu, Mg, Ti, Zr, and Cr of purities 99·6, 99·96, >99, 99·5, and 99·9%, resp., have been measured in the liq.-He temp. range with the aid of a resistance thermometer made of a Ge alloy contg. a small amount of In. The results for all the metals could be fitted to equations of the type $C_v = \gamma T + \beta T^3$, while the values of γ and β for Cu agreed closely with those obtained by Keesom and Kok (*Physica*, 1936, **3**, 1035). The experimental value of γ for Mg of $3{\cdot}25 \times 10^{-4}$ cal./°K.^{2}/mole is compared with that expected assuming two free electrons, and with the value of γ for Zn. The values of γ for Ti, Zr, and Cr of 8·00, 6·92, and $3{\cdot}80 \times 10^{-4}$ cal./°K.^{2}/mole, resp., are discussed in relation to the various theories of the electronic structure of the transition metals.—P. C. L. P.

The Influence of Lattice Vibration Spectrum on Electronic Thermal Conductivity. F. H. J. Cornish and D. K. C. MacDonald (*Phil. Mag.*, 1952, [vii], **43**, (344), 991).—A letter. The assumption of a const. lattice wave velocity is shown not to be responsible for the incorrect prediction of a min. in the thermal conductivity of a pure monovalent metal.—P. C. L. P.

***The Fundamentals of the Welding of Electric Contacts under Heavy Current Conditions.** Else Holm and Ragnar Holm (*Amer. Soc. Test. Mat. Bull.*, 1952, (188), 39–44).—Welding or sticking of elect. contacts is liable to occur in many types of equipment. Under heavy current conditions the welding is due to melting or softening of the metal, and the joint may be stronger than the opening forces available. A method for calculating the strength of a weld as function of the max. current and the hardness of the annealed metal, is put forward, which applies under certain simplified conditions, one of which is that the metal does not oxidize. Results obtained with Ag confirmed the predictions of the theory. Measurements with steel, Ni, Mo, and W showed what proportions of the calculated values were obtained for metals that do oxidize. —P. T. G.

***Theoretical and Experimental Heat Capacities of Supraconducting Metals.** R. D. Worley, M. W. Zemansky, and H. A. Boorse (*Phys. Rev.*, 1952, [ii], **87**, (6), 1142–1143).—A letter. The variation of the heat capacity of supraconducting metals with temp. is shown to agree with the theory suggested by Koppe (*Ann. Physik*, 1947, [vi], **1**, 405). The discrepancy between measurements and theory for Nb and V at low temp. is somewhat greater than the limits of experimental error.—P. C. L. P.

***Effect of Surface Energy on the Supraconducting Phase Transition.** M. P. Garfunkel (*Phys. Rev.*, 1952, [ii], **87**, (1), 108–110).—Simple thermodynamics is used to deduce the relationship between the amount of superheating or supercooling and the surface energy between the supraconducting and normal-conducting phases. The expected amount of hysteresis is related to the geometry of the specimen with respect to the magnetic field.—P. C. L. P.

Supraconductivity Below 1° K. M. C. Steele (*Phys. Rev.*, 1952, [ii], **87**, (6), 1137–1138).—A letter. A discussion, in terms of the temp. variation of the magnetization curves of supraconductors, is given of the paramagnetic effect found by Daunt and Heer (*ibid.*, 1949, [ii], **76**, 1324; *M.A.*, **17**, 625), when supraconducting specimens of Al and Zn were allowed to warm up from very low temp. under the influence of an applied magnetic field.—P. C. L. P.

Electron-Lattice Interaction and Supraconductivity. K. S. Singwi (*Phys. Rev.*, 1952, [ii], **87**, (6), 1044–1047).—A theory of supraconductivity is proposed which, like that of Bohm and Staver (*ibid.*, 1951, [ii], **84**, 836; *M.A.*, **20**, 77), attributes the existence of the supraconducting state to the fact that fast-moving electrons can move more readily in the wake of one another. Short wave-length phonons are considered to be important in electron-lattice interaction because of the small dependence of the transition temp. on film thickness. The present theory can treat these, whereas the model of B. and S. breaks down.—P. C. L. P.

***Determinantal Eigenfunctions for the Theory of Supraconductivity.** William Band ([*U.S.*] *Nat. Bur. Stand. Circ.*, 1952, (519), 23–25).—Use of the Pauli exclusion principle applied to an electron assembly, combined with phys. ideas about phase coherence among zero-point Debye modes (*Phys. Rev.*, 1950, [ii], **79**, 739, 1005; *M.A.*, **18**, 455, 502), enables a qual. explanation to be given of the Meissner effect, which includes more than the diamagnetic effects observed in large supraconductors, and is necessarily associated with the observed ability of the supercurrent to jump over lattice imperfections even in non-inductive linear supraconductors too thin to show any diamagnetic effects. If it can be proved that a magnetic field would increase the negative resonance energy, the destruction of supraconductivity by a magnetic field and the fact that this occurs as a first-order phase change, can be well understood. B. suggests that the combination referred to appears to be highly promising in the matter of developing a theory of supraconductivity. In particular, his theory does not require unreasonably great lattice interactions to stabilize the supercurrent.—J. S. G. T.

Statistical Thermodynamics of the Supraconducting State. Hiroshi Ichimura (*J. Phys. Soc. Japan*, 1952, **7**, (3), 233–240). —[In English]. A statistical-mech. theory of the supraconducting state, in which the second-order effect of the lattice vibration on the electrons, introduced by Fröhlich (*Phys. Rev.*, 1950, [ii], **79**, 845; *M.A.*, **18**, 502), is regarded as the source of the attraction in the momentum space, is developed. The existence of a special equilibrium state, stable below a certain temp., is established; this state being regarded as the supraconducting state, satisfactory agreement is found between theoretical and observed values of ΔC, the jump in the values of the sp. heat at the transition temp. and the threshold magnetic field for the metals Al, V, Zn, Sn, Ta, Hg, and Pb. —J. S. G. T.

***The Thermodynamics of a Fermi Gas with Interchanges.** Wolfhart Zimmermann (*Z. Physik*, 1952, **132**, (1), 1–22).—Math. A method for developing the thermodynamic theory is explained and applied to Fröhlich's theory of supraconductivity (*Phys. Rev.*, 1950, [ii], **79**, 845; *M.A.*, **18**, 502). The results found by F. for $T = 0$ are confirmed, but it is shown that the theory in its present form cannot explain the anomalies found in the sp. heats of supraconductors.—J. W. C.

Similarity Properties of the Two-Fluid Model of Supraconductivity. E. Maxwell (*Phys. Rev.*, 1952, [ii], **87**, (6), 1126–1127).—A letter. M. shows that the exact geometrical similarity of the threshold curves for the supraconductivity of different isotopes of the same substance, supports the Gorter and Casimir two-fluid theory, which separates the electrons into normal and supraconducting types (*Physikal. Z.*, 1934, **35**, 963; *M.A.*, **2**, 144).—P. C. L. P.

***Gyromagnetic Effect in a Supraconductor.** R. H. Pry, A. L. Lathrop, and W. V. Houston (*Phys. Rev.*, 1952, [ii], **86**, (6), 905–907).—The experiments of Kikoin and Gubar with a supraconducting Sn sphere (*J. Physics* (*U.S.S.R.*), 1940, **3**, 333; *M.A.*, **8**, 261) have been repeated to remove ambiguity about the direction of the gyromagnetic effect. The measurements agreed with those of K. and G. and gave an effect rather less than that expected for completely free electrons. —P. C. L. P.

***A Note on Wooldridge's Theory of Secondary Emission.** E. M. Baroody (*Phys. Rev.*, 1952, [ii], **86**, (6), 915–916).—B. shows that the broad max. in the secondary emission coeff. against primary energy, obtained by Wooldridge (*ibid.*, 1939, [ii], **56**, 562), results from neglect of the consequences of the momentum received from the primary electron. This momentum is sufficient to eliminate or substantially modify the theoretical shape of the curve.—P. C. L. P.

***Theory of the Production of Secondary Electrons in Solids.** A. J. Dekker and A. van der Ziel (*Phys. Rev.*, 1952, [ii], **86**, (5), 755–760).—A theoretical treatment is given of the prodn. of secondary electrons, assuming that the interaction energy, V, between a primary electron with a radius vector, $\mathbf{R}$, and a lattice electron with a radius vector, $\mathbf{r}$, is $V = e^2/|\mathbf{R} - \mathbf{r}|$. It is applied to weakly bound electrons, to completely free electrons, and to tightly bound electrons whose wave-functions are similar to the atomic wave-functions. The energy loss along the path of the primary electron has the same kind of dependence on the primary energy in the free electron and tightly-bound cases, but it is different from the dependence found where the electrons are weakly bound. After making simplifying assumptions, the mechanism of the escape of secondary electrons from the surface is brought into the treatment, which is discussed in relation to previous theories.—P. C. L. P.

***The de Haas–van Alphen Effect.** D. Shoenberg ([*U.S.*] *Nat. Bur. Stand. Circ.*, 1952, (519), 261–264).—The de Haas–van Alphen effect relates to the periodic field-dependence of the magnetic susceptibility of metal single crystals. The effect, already known to occur in Bi, Zn, Ga, Sn, and graphite, has now been found to occur also in Cd, In, Sb, Al, Mg, and Be. The effect should occur in every metal at sufficiently high fields and sufficiently low temp., and should be most easily observed in metals in which the Fermi surface crosses Brillouin zone boundaries. Al is the first metal of cubic symmetry in which the effect has been observed. Characteristics of the effect, as exhibited by different metals, are briefly discussed, and a modification of Landau's formula for the periodic field-dependence of the effect (see S., *Proc. Roy. Soc.*, 1939, [A], **170**, 341, Appendix; *M.A.*, **6**, 201), which provides a possible explanation of experimental facts that hitherto did not fit the theory, is proposed and discussed.—J. S. G. T.

***Interpretation of the de Haas–van Alphen Effect.** L. Onsager (*Phil. Mag.*, 1952, [vii], **43**, (344), 1006–1008).—A letter. The explanation of the oscillatory variation of the magnetic susceptibility of many metals at low temp. (the de Haas–van Alphen effect), in terms of the helical motion of free electrons is generalized to take account of the periodic field within the crystal. A relation is obtained between the oscillatory diamagnetism and the geometry of the Fermi surface.—P. C. L. P.

***Some Magnetic Properties of Metals. I.—General Introduction, and Properties of Large Systems of Electrons. II.—The Influence of Collisions on the Magnetic Behaviour of Large Systems.** R. B. Dingle (*Proc. Roy. Soc.*, 1952, [A], **211**, (1107), 500–516; 517–525).—[I.—] Math. After a general introduction surveying some of the problems of magnetic susceptibility which are examined in this and subsequent papers, a detailed analysis is made of the magnetic behaviour of a large system of N electrons, viz. (1) the Schrödinger equation is solved, assuming that the system is unbounded; modifications caused by the finite size of the system are then determined for the limiting case in which the system is much larger than the electronic orbits, (2) an expression is then obtained for the *d* of states, (3) the free energy of the system is evaluated assuming $kT < E_0$, where E_0 is the degeneracy parameter, (4) the magnetic susceptibility, thermodynamic potential, and sp. heat are discussed for the two cases N const. and E_0 const., and (5) the non-periodic magnetic susceptibility at high temp. is evaluated. 34 ref. [II.—] Math. The effect of collisions on the magnetic properties of a large system of free electrons is analysed. The result shows that although the non-periodic term in the susceptibility is hardly affected the periodic terms are reduced by a factor. 8 ref.—E. N.

***Comparison of Magnetoelastic Energy Losses and Magnetic Hysteresis in Ferromagnetic Materials.** G. Bonfiglioli, A. Ferro, and G. Montalenti (*Phys. Rev.*, 1952, [ii], **86**, (6), 959–961).—Experiments on Ni, Fe, and several steels indicate that the magnetic hysteresis energy losses in a loop going to magnetic saturation are greater than, though of the same order as, the magnetoelastic energy losses in a stress cycle between stresses near the Y.P. The attempt made to analyse the implications of the result is only partially successful.—P. C. L. P.

***The Gyromagnetic Ratios of the Ferromagnetic Elements.** G. G. Scott (*Phys. Rev.*, 1952, [ii], **87**, (5), 697–699).—A sensitive torsional pendulum has been used to determine the gyromagnetic ratio of high-purity Ni and Fe, and of two samples of Co contg. ~1% of Ni. The slight difference in the results for the two Co samples is not thought to be directly attributable to a difference in impurity contents.—P. C. L. P.

***The Spherical Model of a Ferromagnet.** T. H. Berlin and M. Kac (*Phys. Rev.*, 1952, [ii], **86**, (6), 821–835).—Two modifications to the Ising model of a ferromagnet are described and analysed. The Gaussian model is shown to become invalid below a critical temp., though the spherical model, whose behaviour is examined in detail, is valid at all temp. The three-dimensional lattice shows ferromagnetic behaviour and provides a framework within which to discuss the nature of the ferromagnetic transition.—P. C. L. P.

***Molecular-Field Treatment of Ferromagnetism and Antiferromagnetism.** J. Samuel Smart (*Phys. Rev.*, 1952, [ii], **86**, (6), 968–974).—The Weiss-type treatment is extended to take account of both first- and second-nearest neighbour interaction. All four possible combinations of the signs of the Weiss coeff. are considered, and the extents of ordering of spins in b.c.c. and f.c.c. lattices below the Curie temp. are deduced. The conclusions are in qual. agreement with experimental data on antiferromagnetic compounds, though some puzzling features remain.—P. C. L. P.

***An Approximate Quantum Theory of the Antiferromagnetic Ground State.** P. W. Anderson (*Phys. Rev.*, 1952, [ii], **86**, (5), 694–701).—Spin-wave theory is used to calculate the ground-state energy and wave-functions of certain simple lattices, where the atomic spins are coupled antiferromagnetically. The results justify the basis upon which other theoretical treatments have been built. A brief discussion is given of the implications of the conclusions about the extent of long-range order, to the theory of metallic binding. 17 ref.—P. C. L. P.

***Energy of a Bloch Wall on the Band Picture. II.—Perturbation Approach.** Conyers Herring (*Phys. Rev.*, 1952, [ii], **87**, (1), 60–70).—Cf. *ibid.*, 1952, [ii], **85**, 1003; *M.A.*, **20**, 460. H. recently (*loc. cit.*) calculated the energy associated with the boundary between two ferromagnetic domains, by considering the precession of electron spins necessary to keep alignment with the magnetization vector within the transition region. An alternative calculation more closely related to the band theory of metals is given in the present paper, using a running spin-wave model and self-consistent field methods. An explicit soln. is obtained for a real metal, assuming that the torque exerted on the spin of an electron is proportional to the departure of the spin orientation of the electron states in that region from the local mean orientation. Comparison is made with the somewhat similar assumptions used in the collective electron model of ferromagnetism. Appn. of the treatment to Ni, using theoretically derived parameters, gave a value of the Bloch wall coeff. of the correct order of magnitude but appreciably smaller than that observed experimentally. The idealized case of a free-electron gas is treated without approximations. A discussion of the behaviour of spin waves in a metal shows their ability to carry a current. For spin waves of long wavelength, the present treatment is shown to include Slater's theory of spin waves in a ferromagnetic insulator as a special case.—P. C. L. P.

***A Soluble Problem in Energy Bands.** J. C. Slater (*Phys. Rev.*, 1952, [ii], **87**, (5), 807–835).—The behaviour of electrons in a simple cubic lattice is considered with particular ref. to wave-functions of a type intermediate between the ranges of validity of the free-electron and tight-binding approximations. The simple cubic lattice was chosen because the soln. is separable into soluble one-dimensional equations. The behaviour of the wave-functions of valence electrons is determined by being squeezed between the quite different patterns associated with bound and free electrons. The effect of various perturbations, including a doubling of the periodicity, is considered, and this is taken to the limit in suggesting an approach to the behaviour of electrons in b.c.c. and f.c.c. lattices. A detailed discussion is given of the complications introduced when different types of band overlap.—P. C. L. P.

***Electronic Energy Bands in Crystals.** R. H. Parmenter (*Phys. Rev.*, 1952, [ii], **86**, (4), 552–560).—The behaviour of electrons in an unbounded cryst. solid is considered. The tight-binding approximation which is often used to determine the Bloch sums of the overlap and exchange integrals is rejected as unsatisfactory for valence electrons and excited states. By partial expansion and math. manipulation, the slowly convergent Bloch sums in ordinary space are converted into rapidly convergent series in momentum space. Transformation of the result to make it of use in calculations, gives an answer identical with that obtained by the method of orthogonalized plane waves (Herring, *ibid.*, 1940, [ii], **57**, 1169; *M.A.*, **7**, 437). Appn. of the approach to the valence electrons of Li, shows that the effective mass of the electrons at the bottom of the valence band, averaged over the different crystallographic directions is 0·8075 electron masses, which is greater than that calculated by Silverman and Kohn (*ibid.*, 1950, [ii], **80**, 912; *M.A.*, **19**, 101, 260). The calculated width of the filled part of the valence band is 4·06 eV., which is in better agreement with the observed value of $4{\cdot}1 \pm 0{\cdot}3$ than the 3·51 eV. calculated by S. and K. The theoretically expected soft X-ray K emission band of Li does not agree well with the observations of Skinner (*Reports on Progress in Physics*, 1938, **5**), which show a pronounced drop at the top of the filled part of the band.—P. C. L. P.

***Statistics of the Recombination of Holes and Electrons.** W. Shockley and W. T. Read, Jr. (*Phys. Rev.*, 1952, [ii], **87**, (5), 835–842).—A treatment of the rates of recombination of holes and electrons is given on the basis that the recombination occurs by trapping in energy levels within the energy gap between filled and conduction bands. The rate-limiting process is assumed to be the availability of electrons to enter the traps. Predictions are made about the dependence of the lifetime of injected current carriers upon the extent to which the bands were occupied initially, and upon the d of injected carriers.—P. C. L. P.

***The Binding Energy of the Thomas–Fermi Atom.** J. M. C. Scott (*Phil. Mag.*, 1952, [vii], **43**, (343), 859–867).—The theoretical variation of the total binding energy of atoms with at. number Z is calculated to be as $Z^{7/5}$ on the Thomas–Fermi statistical model taking boundary and exchange effects into account. This result agrees with deductions from observations on atoms of medium at. wt. It is shown how the variation with $Z^{7/3}$, as found by experiment, could arise for the light elements. A rough estimate is made of the necessary relativity correction for the heavy atoms.—P. C. L. P.

***Variational Methods for Periodic Lattices.** W. Kohn (*Phys. Rev.*, 1952, [ii], **87**, (3), 472–481).—The variational method is developed for the soln. of the Schrödinger equation in a periodic potential produced by a lattice. The results obtained by the use of: (i) Wigner–Seitz polyhedra; (ii) the semi-empirical approximation of Kuhn and Van Vleck; and (iii) Slater's method of taking the actual shape of the polyhedra into account, which assumes spherical symmetry of the potential field, are all derived by the variational method using suitable approximations. Improvements to existing calculation procedures are suggested, and a comparison is made between Slater's and the variational treatment of the energy of the electrons in a b.c.c. lattice.—P. C. L. P.

2 — PROPERTIES OF ALLOYS

***Effects of Machining Specimens on the Results of Tension Tests of Annealed [Aluminium and] Aluminium Alloys.** G. W. Stickley and K. O. Bogardus (*Amer. Soc. Test. Mat. Preprint*, 1952, (66), 6 pp.).—Tension tests were made on specimens from annealed Al and Al-alloy rod of 13 different compn., using full-sized (unmachined) specimens, and specimens annealed after machining and machined after annealing. Specimens annealed after machining and machined after annealing from Al and Al-alloy sheet of 10 different compn. were also tested. The Y.P. of annealed 99·6% Al (2500 lb./in.^{2}) was more than doubled by machining from rod. The effect of machining was less for materials with higher Y.P., but did not become insignificant until a Y.P. of 10,000 lb./in.^{2} was reached. The effects on the Y.P. of sheet specimens were smaller and insignificant for materials having a Y.P. of 8000 lb./in.^{2} or more. Machining annealed round specimens reduced the elongation values for materials with Y.P. $< \sim 5000$ lb./in.^{2}, but there was no effect on the elongation for sheet specimens. In neither case was there any significant effect on the U.T.S. As re-annealing after machining is not always satisfactory, the best way of eliminating machining effects in very soft metals is to use full-size specimens. If this is impractical, specimens machined from a cold-worked temper (at least half-hard) and then annealed should be used.—P. T. G.

***An Investigation of the Plastic Behaviour of Metal [Aluminium-Alloy] Rods Subjected to Longitudinal Impact.** (Campbell). See col. 791.

***Influence of Testing Frequency on the Fatigue Strength of Steels and Light Alloys.** (Wyss). See col. 791.

***Some Observations on Correlations Between the Creep Behaviour and the Resulting Structures in [Aluminium] Alpha Solid Solutions.** Oleg D. Sherby and John E. Dorn (*J. Metals*, 1953, **5**, (2), 324–330).—An extension of previous work (cf. *Trans. Amer. Inst. Min. Met. Eng.*, 1952, **194**, 959; see *M.A.*, **20**, 560). Metallographic and X-ray-diffraction examination of specimens in various stages of creep show that the creep behaviour is directly related to the grain substructures which are developed; for a given creep stress the substructures are functions of the creep strain independent of the test temp. (above 400° K.). For each new creep stress a unique set of grain substructures is developed as a function of creep strain; this is one of the factors responsible for the failure of the mech. equation of state for creep. 11 ref.
—E. N.

***On the Change of Dilatation of Aluminium Alloys Containing 10% $MgZn_2$, and 10% $MgZn_2$ and 1·5% Cu.** Hideo Nishimura, Yōtaro Murakami, and Hisao Ōtsuji (*Suiyokwai-Shi*, 1952, **12**, (3), 105–108).—[In Japanese]. The dilatometric change accompanying the pptn. from solid soln. of Al alloys contg. 10% $MgZn_2$, and Al alloys contg. 10% $MgZn_2$ and 1·5% Cu has been investigated by a differential dilatometric method after various heat-treatments.—AUTHORS.

***Solid Solutions and Grain Boundaries: Progress Report [Aluminium–Zinc Alloys].** B. L. Averbach *et al.* (*U.S. Atomic Energy Commission Publ.*, 1952, (**NYO-3809**), 2 pp.).—The thermodynamic properties of Al–Zn alloys were determined from e.m.f. measurements in a molten-salt electrolyte contg. $AlCl_3$ and NaCl. The data showed that the thermodynamic activity of Al shows positive deviations from Raoult's law and a positive heat of mixing, and the soln. appears to be regular in that the entropy of mixing is close to the ideal configurational entropy.—B. W. M.

***Thermal and Dilatometric Investigation of the Alloys of Cobalt with Chromium and Molybdenum.** A. G. Metcalfe (*J. Metals*, 1953, **5**, (2), 357–364).—Thermal analysis and dilatometry at temp. have been used to study the binary and ternary alloys of Co with up to 50% Cr and Mo, from the liquidus down to ~1050° C., and particular attention has been paid to the $\alpha \rightarrow \gamma$ and $\sigma \rightarrow \delta$ transformations which can be easily overlooked in quenched specimens. The alloys were prepared from Co, Cr, and Mo of 99·92, 99·88, and > 99·8% purity, resp., irrespective of their O content, all metals being assumed to contain this gas. The alloys were vacuum-melted and cast, deoxidation being carried out with C; the ingots were homogenized by heating for 36–48 hr. at 1300°–1325° C. *in vacuo*. The experimental techniques employed and the methods of calibrating the W/Mo thermocouples which were used, are described in detail. The results are discussed in relation to those of other workers, and binary phase diagrams are presented which incorporate modifications arising from the new observations. *Co–Cr*: (1) the transformation of f.c.c. Co (α) to the high-temp. h.c.p. form (γ) occurs at temp. which increase with Cr content; (2) the eutectic is at 1401° C. and 42·5 % Cr; (3) the liquid partaking in the peritectic reaction contains 53% Cr; (4) the peritectoid reaction at 1323° C. is, γ (38% Cr) + δ (46% Cr) = α (39% Cr); δ is the high-temp. form of the intermetallic compound Co_2Cr_3; and (5) the peritectoid formation of σ from δ is placed at 1285° C. *Co–Mo*: (1) the eutectic is placed at 1345° C. and 35% Mo; and (2) the peritectoid formation of θ takes place at 1205° C. The ternary system Co–Cr–Mo is discussed, and diagrams are presented showing the liquidus and the $\alpha \rightarrow \delta$ transformation temp. Four-phase equilibria within the system are considered; there is a non-variant point of equilibrium between the phases α, γ, δ, and σ at 1288° C., and a compn. of Cr 42, Mo 1·5%, balance Co. All compn. are in wt.-%. 20 ref.—E. N.

***Development of Mechanical and Magnetic Hardness in a 10% V–Co–Fe Alloy.** Richard W. Fountain and Joseph F. Libsch (*J. Metals*, 1953, **5**, (2), 349–356).—The Co–Fe–V alloys used in this study consisted of: (1) commercial Vicalloy I, contg. 10% V, and (2) alloys prepared by powder-metallurgy methods, and contg. Co 52, V 0–14%, balance Fe. The following techniques were employed in the investigation: metallography, thermal and X-ray analysis, hardness and elect.-resistivity measurements, and detn. of the magnetic properties—coercive force, saturation, and residual induction. Increasing V addn. to Co–Fe alloys: (*a*) lower the $\gamma \rightarrow \alpha$ transformation temp., thus promoting the formation of non-magnetic γ; (*b*) decrease the intensity of the ordering reaction of the α phase; and (*c*) lower the saturation and residual inductance, and increase the coercive force—max. values for the latter occur in alloys contg. Co 52, Fe 36–38, and V 12–10%, and are ascribed to the formation and pptn. of γ in the magnetic α phase. Although mech. hardening is primarily a result of γ pptn., ordering in the α phase may make a contribution at temp. above 600° C. 11 ref.—E. N.

***Supraconductivity in the Cobalt–Silicon System.** B. T. Matthias (*Phys. Rev.*, 1952, [ii], **87**, (2), 380).—A letter. It has been found that the compound $CoSi_2$ is supraconducting, with a critical temp. of 1·27° K. A rapidly cooled, two-phase ($CoSi_2$ + Si) alloy had a transition temp. of 1·33° K., though this could be lowered by annealing. $CoSi_2$ is believed to be a novel kind of supraconducting compound formed between two non-supraconducting elements.—P. C. L. P.

***The Solubility of Indium in Copper.** E. A. Owen and E. A. O'Donnell Roberts (*J. Inst. Metals*, 1952–53, **81**, (10), 479–480).—The X-ray measurements that have been made to determine the solubility of In in Cu, and thus the α-phase boundary of the Cu–In system over the range of temp. from 710° to 470° C., are recorded. The max. solubility of In in Cu is found to be $10{\cdot}9_0$ at.-% at 575° C.; the solubility at the peritectic temp. (710° C.) is $10{\cdot}0_5$ and at 500° C., $8{\cdot}1_0$ at.-%.
—AUTHORS.

***Study on Halman Electrical-Resistance Alloy [Cu–Mn–Al]. VIII.—Experiments on Stability of the Resistance of Halman Electrical Resistance Wire. IX.—On the Stability of Resistance.** Kiichiro Shinji (*Suiyokwai-Shi*, 1952, **12**, (3), 95–97; 97–99).—[In Japanese]. Cf. *ibid.*, (2), 1; *M.A.*, **20**, 687. [VIII.—] The following results are reported from experiments: (i) The stability is slightly increased by pickling in acid after soft annealing; (ii) slower cooling after soft annealing increases the stability; (iii) the stability decreases when wire is stressed, e.g. by winding; and (iv) annealing at low temp. of both bare and coated wire is necessary to stabilize the resistance. [IX.—] The rate of decrease of the resistance by annealing at low temp. after winding is not const. It is supposed that the internal stress remaining in the wire after winding consists of that contained in the wire before winding and that added by the winding operation, and it is these stresses which affect the rate of decrease. The change of resistance can be kept within a certain range by winding and annealing at low temp. under const. conditions. An example of the change of resistance by heating and passing an elect. current and the stabilization by a low-temp. anneal after winding is described. The results of heating and cooling on the resistance are described as one example of the remarkable effect of low-temp. annealing on the stability of resistance.—AUTHOR.

***On the Electrical Properties of Alloys of Copper, Manganese, and Zinc.** Hideo Nishimura, Masao Adachi, and Hiroshi Nakagawa (*Bull. Eng. Research Inst. Kyoto Univ.*, 1952, **2**, (Sept.), 48–50).—[In Japanese, with graphs and tables in English]. Results are reported of an investigation of the elect. properties of Cu–Mn–Zn alloys (1·1–17·1% Mn, 2·2–19·3% Zn). In the compn. range tested, the temp. coeff. of resistance is positive. The linear relation between conductivity and temp. coeff., which has been shown by Hansen, Johnson, and Parks (*Trans. Amer. Inst. Min. Met. Eng.*, 1951, **191**, 1184; see *M.A.*, **19**, 530), has been applied to the results.
—AUTHORS.

***The System InAs–InSb.** C. Shih and E. A. Peretti (*J. Amer. Chem. Soc.*, 1953, 75, (3), 608–609).—Thermal-analysis, X-ray, and metallographic studies of the system InAs–InSb are reported. In the phase diagram obtained, the liquidus consists of an uninterrupted line running from the f.p. of InAs (942° C.) to a eutectic point experimentally indistinguishable from the f.p. of InSb (525° C.). The X-ray studies of the solid state showed a small single-phase region at the InAs end of the diagram.—J. R.

***The Magnetic Properties of Supraconducting Alloys of Indium and Thallium.** W. F. Love, E. Callen, and F. C. Nix (*Phys. Rev.*, 1952, [ii], 87, (5), 844–847).—Spheres of solid-soln. In–Tl alloys contg. 5–37 at.-% Tl have been made from 99·98% purity ingredients. The 5 and 10% alloys showed a well-defined critical magnetic field for the destruction of supraconductivity, and considerable reversibility of the magnetization on decreasing the field. The electronic sp. heat deduced from thermodynamic relationships is the same for both alloys, indicating that the effective valency of the components is the same. The breadth of the transition became greater in alloys contg. more Tl, while the magnetic behaviour became strongly sensitive to mech. shock. The critical temp. for the destruction of supraconductivity decreases only slowly on alloying.—P. C. L. P.

***Effect of a Notch and of Hardness on the Rupture Strength of "Discaloy." [Iron–Nickel–Chromium–Molybdenum–Titanium Alloy].** F. C. Hull, E. K. Hann, and H. Scott (*Amer. Soc. Test. Mat. Preprint*, 1952, (75), 10 pp.).—The austenitic alloy tested was of nominal compn. Ni 25, Cr 13, Mo 3, Mn 0·8, Si 0·8, Al $\not>$ 0·4%, with Ti varied between 1·4 and 2·4% (balance Fe). Const.-load creep-rupture tests were carried out at 1000° and 1200° F. (540° and 650° C.) on plain- and notched-bar specimens. All material was first soln.-treated for 1 hr. at 1950° F. (1065° C.) and oil-quenched, which completely dissolved the Ti hardener and produced a fully recrystallized structure of const. grain-size. The specimens were then aged at 1350° F. (730° C.) for 20 hr. (which time produces approx. the max. hardness) and then air-cooled or furnace-cooled in 6 hr. to the test temp. and stabilized at that temp. for 20 hr. The hardness of the aged material increased regularly with Ti content. The creep-rupture strengths at 1000° and 1200° F. increased to a max. then decreased with increasing Ti content, the ductility diminishing with increase of strength to 3% elongation and 4% reduction of area at max. strength. The max. strength occurred at lower Ti contents for notched than for plain specimens. The strength fell more rapidly from the max. with increasing Ti for notched than for plain specimens. The notched-bar strength was greater than the plain-bar strength below a hardness corresponding to ~ 1·9% Ti, and the max. notched-bar strength could only be obtained with a minor sacrifice in plain-bar strength. Close control of Ti content is necessary to obtain the optimum combination of plain- and notched-bar rupture strength. —P. T. G.

***Application of Nucleation Theory to Isothermal Martensite.** J. C. Fisher (*Acta Met.*, 1953, 1, (1), 32–35).—[In English]. Some results of Cech and Hollomon (to be published) for the isothermal formation of martensite in a 73 : 23 : 4 Fe–Ni–Mn alloy are compared quant. with a simplified classical nucleation theory. The rate-limiting step is assumed to be ordinary thermal nucleation (allowing for strain energy) and the growth rate to be very rapid. Each martensite plate is assumed to divide up the vol. available for its growth and to transform a const. fraction (*f*) of this vol. Using tabulated free-energy values, the max. nucleation rate is calculated to occur at −126° C. in excellent agreement with the experimental value of −128° C. The nucleation rate and fraction *f* are both determined as a function of temp. from the experimental results, and the former shows reasonably good agreement with the theoretical curve. 5 ref.—J. W. C.

***Thermal Stabilization of Austenite in Iron–Carbon–Nickel Alloys.** E. R. Morgan and T. Ko (*Acta Met.*, 1953, 1, (1), 36–48).—[In English]. Experiments were made on the thermal stabilization of austenite in alloys of Fe with 0–10% Ni and 0·9–1·3% C. Stabilization occurred during continuous cooling and by holding above and below M_s; stabilization above M_s depressed this temp. Detailed martensitic transformation curves are given for a number of alloys under specified cooling conditions. The mechanism of stabilization is discussed, and it is suggested that it is due to an increase in the resistance of the parent phase to the shearing movements required to produce martensite. This resistance may be due to the formation of Cottrell atmospheres round dislocations. 40 ref.—J. W. C.

***Effect of Sigma on Strength and Ductility of 25 Cr, 20 Ni Steel.** G. V. Smith and E. J. Dulis (*Amer. Soc. Test. Mat. Preprint*, 1952, (82), 11 pp.).—Cf. *M.A.*, 19, 179. Samples of 25 : 20 Cr–Ni austenitic stainless steel initially cold worked 35% were heated at 1700°, 2000°, or 2300° F. (925°, 1095°, or 1260° C.) for 1 hr. and water-quenched and then exposed for 7500 hr. at 1300° F. (705° C.) to promote the pptn. of σ phase. In tension tests at room temp. σ caused increased Y.P. and U.T.S. and reduced elongation and reduction of area. Loss of ductility was most pronounced after annealing at 2300° F., elongation being reduced from 65 to ~1%. The presence or absence of σ was more important than grain-size. Pptn. of σ resulted in severe loss of notch impact strength in the temp. range −315° to +500° F. (−195° to 260° C.). The presence of σ caused moderate loss of creep-rupture strength at 1300° F.—P. T. G.

***Gyromagnetic Ratios of Iron, Cobalt, and Many Binary Alloys of Iron, Cobalt, and Nickel.** (Barnett and Kenny). See col. 740.

***The Optical Constants of Lead Sulphide, Lead Selenide, and Lead Telluride in the 0·5–3 μ Region of the Spectrum.** D. G. Avery (*Proc. Phys. Soc.*, 1953, [B], 66, (2), 134–140).—Using a reflection method, the refractive indices and absorption coeff. of PbS, PbSe, and PbTe have been measured against wave-length. At shorter wave-lengths ($<\sim 2\ \mu$) the values depend on the method of prepn. of the surface, but beyond 2·5 μ, prepn. method has no effect on the results. Mean values of refractive index at 3 μ are PbS 4·10, PbSe 4·59, PbTe 5·35. For PbS, the absorption is independent of impurity concentration. The results are related to the photoconductive properties of these compounds.—E. O. H.

***Inter-Relation Between Optical Constants for Lead Telluride and Silicon.** T. S. Moss (*Proc. Phys. Soc.*, 1953, [B], 66, (2), 141–144).—Measurements of the absorption spectrum of PbTe (cf. Avery, *ibid.*, p. 134 ; preceding abstract) and Si are used to calculate theoretically the refractive indices of these substances at long wave-lengths. Agreement with experimental values is good. It is suggested that the refractive index of PbTe should increase on cooling, with a reverse effect for Si. In an appendix, the results are also applied to Ge.—E. O. H.

Magnesium [Alloys]. Rudolf Freitag (*Metall*, 1952, 5, (5/6), 154–155).—A brief note on the prodn., properties, and appn. of a few of the more important Mg alloys. —E. N.

***Stress and Plastic Strain Relations of a Magnesium[–2% Aluminium] Alloy.** A. E. Johnson and N. E. Frost (*Engineer*, 1952, 194, (5053), 713–719).—Describes work which is part of a general research on the short-time combined-stress properties of some metallic alloys. An Mg–Al alloy has been subjected to test under pure tension (*t*), pure torsion (*s*), and combined stresses of *t*/*s* ratio ranging from 0·2 to 3·25 at temp. of 20°, 50°, 100°, and 150° C. The results are presented graphically and discussed in the light of modern deformation theory.—D. K. W.

***Room- and Elevated-Temperature Properties of Powder-Extruded Magnesium Alloys Containing Aluminium, Beryllium, and Zirconium.** —— (*U.S. Atomic Energy Commission Publ.*, 1950, (COO-20), 21 pp.).—Mixtures of a basic Mg alloy contg. 0·5% Zr with various binary Al–Mg alloy powders were extruded and heat-treated for 16 hr. at 750° F (400° C.). The mech. properties of the alloys at room temp. were as follows :

Alloy Compn.	Tensile Y.P.	Compression Y.P.	U.T.S.	Elongation, %
	Lb./in.^{2} × 1000			
Basic . . .	22	19	35	13
Basic + 4% Al . .	51	45	53	4
Basic + 12% $A_{30\cdot7}$.	45	39	50	9
Basic + 20% $A_{19\cdot7}$.	45	40	51	13
Basic + 40% A_{10} .	40	36	49	13

where A_x is a binary Mg–Al alloy contg. x% Al. Tensile tests at temp. up to 750° F. (400° C.) showed a rapid decrease in strength with increase in temp., but all the Al-contg. alloys were superior to the basic alloy at all temp. A homogenizing heat-treatment of 16 hr. at 1050° F. (565° C.) applied to the basic alloy powder before extrusion resulted in a marked lowering of the strength properties of the extruded mixture. In the as-extruded condition, the creep-resistance of the mixtures at 200° and 300° F. (95° and 150° C.) was greater than that of the basic alloy. Heat-treatment at 750° F. for 16 hr. increased the creep-resistance of the basic alloy and decreased that of the mixtures.—B. W. M.

An Examination of Joule's Work on the Metallurgy of Amalgams. H. J. Axon (*Metallurgia*, 1953, **47**, (279), 27–28).—Joule's work on the constitution of binary alloys of Hg is reviewed in the light of modern knowledge. The systems of Hg with Fe, Cu, Ag, Zn, Pb, and Sn are each considered.—F. M. L.

***Effect of Notch Geometry on Rupture Strength [of Nickel–Cobalt–Chromium–Iron Alloys] at Elevated Temperatures.** E. A. Davis and M. J. Manjoine (*Amer. Soc. Test. Mat. Preprint*, 1952, (78), 21 pp.).—Creep-rupture tests were carried out at 1000° or 1200° F. (540° or 650° C.) on plain bars and notched bars with varying geometry of the notch on the following alloys: (1) a stainless steel contg. Cr 19, Ni 9, Mo 1·4, W 1·2, Nb 0·4, and Ti 0·3%, (2) a steel contg. Cr 12, W 3%, and pptn.-hardening alloys contg., (3) Ni 39, Co 20, Cr 18·5, Fe 15, Mo 3, Ti 2·5, Al 0·2%, and (4) Ni 42, Co 22, Cr 18, Fe 14, Ti 2·2, Al 0·2%. Alloys (3) and (4) were tested in various conditions of heat-treatment. The effect on notch sensitivity of the following factors were investigated besides notch shape: stress level, grain-size, hardness, ductility, and heat-treatment. Increasing the sharpness of the notch with const.-depth notches could raise or lower the notch sensitivity, depending on the ductility and microstructure of the alloy. Metals with high ductility exhibited a strengthening effect due to sharp notches, the strengthening effect decreasing and the notch sensitivity increasing as the ductility decreased. For metals with <10% unnotched elongation, the notch effect was strengthened or weakened, depending on notch sharpness. For the same unnotched ductility or hardness, the notch sensitivity increased with increasing grain-size. Stress level had no appreciable effect on notch sensitivity. The time taken to initiate a crack which propagated was much longer than the time taken for this crack to travel across the min. section of a notched specimen. It is suggested that failure probably starts near the surface at the root of the notch. It generally propagates along grain boundaries. 9 ref.—P. T. G.

***Solid Solutions and Grain Boundaries: Progress Report. [Nickel–Gold Alloys].** B. L. Averbach *et al.* (*U.S. Atomic Energy Commission Publ.*, 1952, (**NYO-582**), 4 pp.).—The X-ray diffuse scattering from Ni–Au alloys was measured at 80° K. Abs. intensities in electron units were obtained from thin plates quenched from 900° C. by comparison with the scattering from paraffin or lucite. It is considered that the diffuse scattering arises from two factors, (*a*) the average local atomic arrangement in the alloy and (*b*) the size difference between the Ni and Au atoms. A math. treatment of the Fourier transform has led to an improved method for calculating the short-range order and the size-effect parameters and has shown that the short-range order is of the Cu–Au type. Evaluation of the atomic dia. of the Au and Ni atoms in solid soln. with 60, 70, and 80 at.-% Ni indicates that each atom has a size approx. midway between the average size calculated from the lattice parameters of the alloy and pure metal, resp. Measurements of the variation of the Hall coeff. with compn. and temp. of Ni–Au alloys show that the calculated effective number of conduction electrons as a function of compn. agrees approx. with values calculated from magnetic data. Measurements of the diffuse X-ray scattering from Al–Zn solid soln. at 400° C. indicate a preference for like nearest neighbours for the short-range order.—B. W. M.

***Solid Solutions and Grain Boundaries: Progress Report on Thermodynamic Properties of Solid Nickel–Gold Alloys.** L. L. Seigle, Morris Cohen, and B. L. Averbach (*U.S. Atomic Energy Commission Publ.*, 1952, (**NYO-3807**), 22 pp.).—The free energies, enthalpies, and entropies of mixing of solid Ni–Au alloys contg. 5–95 at.-% Ni were determined by means of elect.-potential measurements in the range 700°–900° C. The thermodynamic activities indicated a large positive deviation from Raoult's law, and this is in conformity with the solid miscibility gap in the equilibrium diagram. The positive enthalpies of mixing are attributed to the lattice distortion resulting from the difference in size between the Ni and Au atoms, and this factor, rather than the relative bond energies between like and unlike pairs of atoms, leads to the formation of the two solid soln. at lower temp. The entropies of mixing for the Ni–Au solid soln. are almost twice those of ideal soln., and are probably due to an increase in heat capacity. Good agreement was found between the experimental activities and those computed from the phase diagram, but this may not be significant, since the calculations were based on ideal entropies of mixing which results in a compensating error in the calculated enthalpies. It is suggested that the effect of Au on the magnetic susceptibility of Ni indicates that the 6*s* electron in Au attains a lower energy state in the alloys by entering the unfilled 3*d* band of Ni.—25 ref.—B. W. M.

***Magnetostrictive Vibration of Prolate Spheroids: Nickel–Iron and Nickel–Copper Alloys.** J. S. Kouvelites and L. W. McKeehan (*Phys. Rev.*, 1952, [ii], **86**, (6), 898–904).—The magnetic characteristics of commercial-purity Ni–Fe and Ni–Cu alloys have been investigated, using the experimental and analytical methods described by Bock, K., and McK. (*ibid.*, 1951, [ii], **84**, 957; *M.A.*, **20**, 91). The effect was studied of annealing and slow cooling in a magnetic field on the properties of Ni–Fe alloys. The relative change of Young's modulus varied with the relative magnetization in the same manner for all the Ni–Fe alloys tested. In the cold-drawn condition, the relative change in the Young's modulus of the 68% Ni alloy (Permalloy) was different, though heat-treatment at 700° C. made it behave similarly to the other specimens.—P. C. L. P.

***The Magnetic Behaviour of Rhenium–Palladium Alloys.** Jules Wucher and Nicolas Perakis (*Compt. rend.*, 1952, **235**, (6), 419–421).—Re–Pd alloys were melted in a H.F. furnace under low-pressure A in pure Al_2O_3 crucibles. The thermomagnetic properties studied were the coeff. of magnetization of the alloys at 15° C., their molecular coeff. of magnetization at 15° C., the paramagnetic Curie point, and the Curie atomic const. compared with that of Pd between −180° and +460° C. Micro-examination showed that the alloys contg. 17·1, 25, and 40 at.-% Re are two-phase, while those contg. up to 9·5 at.-% are one-phase. The coeff. of magnetization diminishes very rapidly as the Re increases from 0 to 17 at.-%, and thereafter is virtually const., so that this compn. can be considered the limit of solid solubility. Re appears to dissolve in Pd by giving up its peripheral electrons and the 0·65 holes/atom of Pd being closed up, a new phase of practically const. paramagnetism is formed with the solid soln. saturated with Re.—J. H. W.

A Sterling Silver Containing Aluminium. G. E. Gardam (*Metallurgia*, 1953, **47**, (279), 29–33).—"Firestain", which occurs in the normal Cu-contg. standard Ag, is eliminated by including in the alloy a small amount (1–1·3%) of Al. This addn. also inhibits grain growth and confers on the alloy enhanced pptn.-hardening properties.—F. M. L.

***The Solubility of Oxygen in, and the Oxides of, Tantalum.** (Wasilewski). See col. 742.

***Mechanical Properties of High-Purity Titanium–Aluminium Alloys.** H. R. Ogden, D. J. Maykuth, W. L. Finlay, and R. I. Jaffee (*J. Metals*, 1953, **5**, (2), 267–272).—Small melts of the binary alloys were prepared from iodide Ti and 99·99% Al by arc melting in a water-cooled Cu hearth under an A atmosphere, the resulting buttons being fabricated without further treatment. Their working and mech. properties were then investigated; the results show that increasing addn. of Al: (1) increase the recrystn. and softening temp. of Ti, and restrict the amount of hot and cold working that can be employed, until at $>$7·5% Al the alloys are no longer amenable to fabrication; γ-phase alloys contg. 37–43% Al, however, are soft but of only limited workability; (2) up to 3% slowly improve the mech. properties of the alloys; thereafter, and particularly in the range 4–5% Al, the values increase rapidly; material contg. $<$7·5% Al is very ductile, but is not susceptible to heat-treatment by β quenching or subsequent ageing; (3) increase the elastic modulus of Ti by ~200,000 lb./in.^{2} for every addn. of 1% Al, up to a max. of 5%; the values decrease linearly with increasing temp. by $\sim 1 \times 10^6$ lb./in.^{2}/100° C.; the γ-phase alloys have a modulus of $\sim 21 \times 10^6$ lb./in.^{2}; (4) lower the *d* of the alloys by ~0·02 g./c.c. for each 1% Al added, the values being 4·5, 4·35, and 3·80 g./c.c. for material contg. 0, 7·5, and 37% Al; (5) cause the D.P.N. values to increase rapidly up to the limit (26%) of solubility of Al in α-Ti, after which the values decrease in the $(\alpha + \gamma)$ phase field, become const. in the γ region, and thereafter rise sharply again as increasing amounts of $TiAl_3$ are present, and (6) above 4% improve the oxidation-resistance of alloys within the α solid-soln. region; an alloy contg. 8% Al suffers ~40% less oxidation than does pure Ti after a 24-hr. exposure at 850° C. to still air; γ-phase alloys likewise are markedly superior to unalloyed Ti. Single-phase α alloys (*a*) are strain-hardening to a considerable extent, but at a lower rate than unalloyed Ti, and (*b*) can be welded in a He atmosphere, using a D.C. W electrode arc, without any loss of bend ductility in the heat-affected zone. All compn. are in wt.-%. 4 ref.—E. N.

***Titanium–Carbon Phase Diagram.** Irving Cadoff and John P. Nielsen (*J. Metals*, 1953, **5**, (2), 248–252).—A metallographic, X-ray-diffraction, and thermal study has been made of the system from 0 to 24% C, using alloys prepared from iodide Ti ($\nless$99·95%) and spectroscopic-grade C by arc melting with a W electrode in a water-cooled Cu crucible under an atmosphere of A. From the results, which are described in detail, partial phase diagrams have been produced. Increasing addn. of C raise the $\alpha \rightarrow \beta$ transformation temp. of Ti from 882° to a max. of 920° ± 3° C. at 0·48 ± 0·02% C, this point corresponding to that of the peritectoid reaction $\beta + \delta \rightarrow \alpha$. The solubility of C in β-Ti increases from 0·15% at 920° to a max. of 0·8% at 1750° ± 20° C., this point corresponding to that of the peritectic reaction, liquid $+ \delta \rightarrow \beta$. The solubility of C in liq. Ti is just under 0·2% at the peritectic temp., above which the liquidus and solidus lines rise continuously with increasing C content to the TiC m.p., ~3140° C. C expands the lattice—particularly the α parameter—of Ti to a greater extent than does O or N. There is no evidence of any intermediate phase other than TiC in any of the temp. ranges above 600° C. Photomicrographs show the typical structures encountered. All compn. are in wt.-%. 13 ref.—E. N.

***Titanium–Manganese System.** D. J. Maykuth, H. R. Ogden, and R. I. Jaffee (*J. Metals*, 1953, **5**, (2), 225–230).—The system has been investigated from 0 to 69·5% Mn, using alloys prepared from high-purity metals—iodide Ti crystal bar and degassed (from H) electrolytic Mn. The experimental methods used for melting, fabrication, heat-treatment, metallography, and the elect. resistance, X-ray diffraction, and thermal detn. are described in detail. From the results a partial phase diagram has been constructed, which shows: (1) an intermetallic compound, δ, located at ~66·9% Mn, which melts incongruently at 1330° C.; it has an X-ray-diffraction pattern identical with that previously reported for $TiMn_2$ (i.e., hexagonal *C*14 ($MgZn_2$)-type structure with $a =$ 4·18 and $c =$ 7·88 Å., resp.); (2) that at 67% Mn small quantities of a new higher-Mn phase appear—in the form of Chinese script eutectic particles, the amount increasing as the compn. rises to 69·5% Mn; (3) an intermetallic compound, γ, with a compn. near 53% Mn, which originates in a peritectic reaction at 1200° C., between δ and the melt contg. 45% Mn; although the indicated compn. corresponds roughly to TiMn, the diffraction pattern does not fit the b.c.c. CaCl-type lattice of the TiX compounds of the neighbouring transition elements, and the crystal structure has not been identified; (4) a eutectic reaction at 42·5% Mn, 1175° C., between β-Ti contg. 33% Mn and γ; (5) that the solubility of Mn in β-Ti decreases almost linearly from a max. of 33% at 1175° C. to ~20% at 550° C.; (6) a sluggish eutectoid reaction, $\beta \rightarrow \alpha + \gamma$, at 550° C. and ~20% Mn; (7) a lowering of the β transus temp. with increasing addn. to 550° C. at the eutectoid compn.; and (8) that the solubility of Mn in α-Ti reaches a max. of ~0·5% at the eutectoid temp. Photomicrographs show the typical structures encountered; all compn. are in wt.-%. 10 ref. —E. N.

***Titanium–Nickel Phase Diagram.** Harold Margolin, Elmars Ence, and John P. Nielsen (*J. Metals*, 1953, **5**, (2), 243–247).—The Ti–Ni phase diagram has been studied up to 68% Ni, using iodide Ti-base alloys, by metallographic, X-ray, and m.p. methods, and from 68 to 90% Ni by examination of the as-cast structure of sponge Ti (99·75%)-base alloys. The experimental procedures employed are fully described. From the results, which are compared with those of other workers, complete and partial phase diagrams (above 500° C.) have been prepared, the main features of which are: (1) a eutectoid reaction at 770° ± 5° C., when β contg. 6–7% Ni decomposes into α contg. $<$0·2% Ni and Ti_2Ni (~38% Ni), (2) a eutectic at 28–29% Ni and 955° ± 5° C., with the liquid solidifying into β (13% Ni) and Ti_2Ni; (3) a peritectic reaction at ~1015° C.: liquid (~37·5% Ni) + TiNi (~53% Ni) $\rightarrow$ Ti_2Ni; (4) a second eutectic at ~65% Ni and ~1110° C., with the liquid solidifying into TiNi (~59% Ni) and $TiNi_3$ (~78·6% Ni); (5) a third eutectic at 1287° C. and 84% Ni, when the liquid forms $TiNi_3 + \gamma$. The transformation of β-Ti is discussed; it may occur by a nucleation-and-growth process or by a martensitic reaction; it is stimulated by the presence of α and Ti_2Ni, and is suppressed by water-quenching when the phase contains $\nless$8% Ni. Photomicrographs show the typical structures encountered; all compn. are in wt.-%. 14 ref.—E. N.

***Titanium–Tungsten and Titanium–Tantalum Systems.** D. J. Maykuth, H. R. Ogden, and R. I. Jaffee (*J. Metals*, 1953, **5**, (2), 231–237).—The entire alloy range in both systems has been studied, with special ref. to high-purity alloys at the Ti ends, in the prepn. of which iodide Ti crystal bar was used together with W and Ta of 99·9+% purity. From the results, which are discussed in detail, partial and complete phase diagrams (above 400° C.) have been prepared which show the following features. *Ti–W*: (1) A high-temp. peritectic at ~1880° C. and a compn. slightly above 50% W, between liquid contg. ~25% W and terminal W solid soln. contg. ~8% Ti, which produces a wide two-phase region of β + W in the intermediate portion of the diagram; (2) a max. solubility of ~8% Ti in W at 1880° C., decreasing to $<$5% at ~700° C.; (3) a max. solubility of ~50% W in β-Ti at the peritectic temp. decreasing to ~28% at ~715° C., where the β-phase field terminates in a eutectic reaction, $\beta \rightarrow \alpha + W$; (4) addn. of W to Ti depressing the β transus from 882° to 715° C. at the eutectoid compn.; and (5) ~0·8% W soluble in α-Ti at 715° C.—an amount which has practically no effect on lattice parameters, thus making X-ray observations useless in determining α solubilities. *Ti–Ta*: (1) The formation of a continuous series of solid soln., the solidus curve rising smoothly from the m.p. of Ti to that of Ta, and a relatively narrow solid-liquid range; (2) an α field which, although closed, has an appreciable range, the solubility of Ta in α-Ti increasing with decreasing temp. to a max. of ~12·5% at 550° C.—the increasing Ta contents expanding the *c* axis and having no significant effect on the *a* parameter of the Ti lattice; and (3) increasing addn. of Ta to Ti progressively lowering the β transus to ~600° C. at 70% Ta. Photomicrographs show the typical structures encountered. The experimental methods used for alloy propn., fabrication, and heat-treatment, and for the metallographic, elect.-resistance, X-ray, and thermal detn. are described in an Appendix. All compn. are in wt.-%. 7 ref.—E. N.

Thermal Conductivity, Electrical Resistivity, and Thermoelectric Power of Titanium Alloy RC-130-B. W. W. Tyler and A. C. Wilson (*U.S. Atomic Energy Commission Publ.*, 1952, (**KAPL-803**), 41 pp.).—Various phys. measurements were made on Type-316 stainless steel and a Ti alloy RC-130-B contg. C 0·14, Al 3·99, and Mn 4·7%, in the temp. range 20°–300° K. The thermal conductivity of the Ti alloy was approx. half that of the steel, and varied from 0·004 cal./cm./sec./°K. at 20° K. to 0·02 at 300° K.; the elect. resistivity is ~150 μΩ and relatively independent of temp. The Wiedemann–Franz ratio is ~5 times the theoretical value at 20° K. and decreases to about twice the theoretical value at 300° K. The abs. thermoelect. power is negative throughout the temp. range studied and is ~5 μV./°K. at 300° K.—B. W. M.

***Vanadium–Oxygen Solid Solutions.** A. U. Seybolt and H. T. Sumsion (*J. Metals*, 1953, **5**, (2), 292–299).—A study has been made of V-rich V–O solid soln., employing the methods of X-ray and neutron diffraction, elect. resistance, thermo-elect. effect, thermal analysis, and microscopy. The Ca-reduced V used contained Fe 0·007, Si 0·02, Ca 0·06, C 0·224, O 0·004, N 0·0017, H 0·003, and V ~99·6 wt.-%; the various alloys were prepared by vertically suspending V strips in an absorption apparatus at 900°–1000° C., and adding the O gas a few c.c. at a time. The hardness of the alloys was found to increase with increasing O content, rising to ~1000 D.P.N. at 17% O; slowly cooled material was only a few points lower in hardness than quenched material; alloys contg. >0·15% O were relatively unworkable and partially brittle at room temp. From the results, and those of other workers above 20% O, a V–O phase diagram has been prepared which shows that: (1) a polymorphic transformation exists in V at 1550° ± 10° C.; (2) α solid soln. exists up to 3·2% O; it has a b.c.c. structure, in which linear lattice expansion takes place up to a max. of 0·66% O, (3) β solid soln. exists between 14·7 and 22% O, being separated from α by a two-phase (α + β) region; it has an ordered b.c. tetragonal structure whose *c*/*a* ratio increases with increasing O content; it forms by a peritectoid reaction, $\alpha + VO \rightarrow \beta$, at 1270° C.; (4) the homogeneity range of VO is 47·4–56·5% O; a two-phase (β + VO) region separates it from β; (5) VO apparently melts incongruently at ~1900° C., and probably takes part in a peritectic reaction, an assumption which fits in with the deduced existence of the high temp. γ solid-soln. phase; and (6) a suggested eutectoid horizontal extends from ~6% O to VO, at an arbitrary temp. of 1450° C.; the eutectoid point is in the region of 40% O. Photomicrographs show the typical structures encountered; except where stated otherwise, all compn. are in at.-%. 14 ref.—E. N.

***High-Temperature Experiments with Zirconium and Zirconium Compounds.** (Kroll, Carmody, and Schlechten). See col. 744.

***System Zirconium–Chromium.** R. F. Domagala, D. J. McPherson, and M. Hansen (*J. Metals*, 1953, **5**, (2), 279–283).—Thermal-analysis, metallographic, and incipient-melting techniques have been employed to resolve, accurately, phase relationships in the 0–50 at.-% Cr region, while the remainder of the diagram is outlined on a basis of cast structures and thermal analyses. An arc furnace with non-consumable electrode was used to prepare the alloys from "low-Hf" iodide Zr (99·8%) crystal bar, and Johnson–Matthey or National Research Cr of 99·9 and 99·5% purity, resp.; the experimental procedures employed are described in detail. Partial and complete equilibrium diagrams, at temp. above 500° C. are presented, which show: (1) that the solubility of Cr in β-Zr decreases from a max. of 4·5% at the eutectic temp. to ~1% at the temp. of the eutectoid reaction; (2) <0·28% Cr soluble in α-Zr at all temp.; (3) a eutectic between β-Zr and $ZrCr_2$ at 18% Cr and 1280° ± 10° C.; (4) a single intermediate phase, $ZrCr_2$, at 53% Cr, which melts at an open max. at 1700° ± 25° C.; it has a h.c.p. structure with, in an alloy contg. 53·1% Cr, an observed *c*/*a* ratio of 1·65, and calculated parameters of *a* = 5·079 and *c* = 8·262 Å., and *c*/*a* = 1·627; (5) a eutectoid reaction $\beta \rightarrow \alpha + ZrCr_2$ at 835° ± 10° C., and 1 ± 0·25% Cr; (6) a second eutectic between $ZrCr_2$ and Cr-rich solid soln. at 70% Cr and 1635° ± 15° C.; and (7) <3% Zr soluble in Cr. The results are compared with those of other workers. Photomicrographs show the typical structures encountered. Except where stated otherwise, all compn. are in wt.-% 8 ref.—E. N.

***System Zirconium–Copper.** C. E. Lundin, D. J. McPherson, and M. Hansen (*J. Metals*, 1953, **5**, (2), 273–278).—A study has been made of the entire range of this system, using alloys prepared from "Grade 3" iodide Zr crystal bar (99·8%) and spectrographic-grade (99·99%) Cu, by melting under He in a water-cooled Cu block in a W-electrode arc-furnace. From the results of the thermal analyses and metallographic examinations, partial and complete phase diagrams at temp. above 400° C. have been prepared; they show that: (1) the $\alpha \rightarrow \beta$ transformation temp. of Zr is decreased from 862° C. to ~822° C. by increasing amounts of Cu; (2) up to 3·8% Cu is soluble in β-Zr at the eutectic temp. of 995° C., and <0·18% Cu is soluble in α-Zr at all temp.; (3) a eutectoid reaction occurs at 1·6% Cu and 822° ± 10° C., (4) five intermetallic phases form, viz., (*a*) Zr_2Cu (25·83%Cu) at~27% Cu and 1000° ± 10° C; it has a f.c. tetragonal structure with, in an alloy contg. 26·9% Cu, *a* = 4·536 and *c* = 3·716 Å., and *c*/*a* = 0·819, (*b*) ZrCu (41·06% Cu) at 935° ± 10° C., (*c*) Zr_2Cu_3 (51·09% Cu) at 50% Cu and 895° ± 10° C., (*d*) Zr_2Cu_5 (63·52% Cu), by a peritectic reaction between the melt contg. 61% Cu and $ZrCu_3$ at 1070° ± 10° C., and (*e*) $ZrCu_3$ (67·63% Cu), which exists at ~71·5% Cu and melts with an open max. at 1100° ± 10° C.; (5) five eutectics occur, viz., between (*a*) Zr and Zr_2Cu at 21% Cu and 995° ± 10° C., (*b*) Zr_2Cu and ZrCu at 37% Cu and 928° ± 10° C., (*c*) ZrCu and Zr_2Cu_3 at 47% Cu and 890° ± 10° C., (*d*) Zr_2Cu_3 and Zr_2Cu_5 at 53% Cu and 885° ± 10° C., and (*e*) $ZrCu_3$ and Cu at 91% Cu and 965° ± 10° C.; and (6) the solid solubility of Zr in Cu is <1%. Photomicrographs show the typical structures encountered. All compn are in wt.-%. 8 ref.—E. N.

***Effects of Small Additions of Oxygen on Lattice Constants and Hardness of Zirconium.** (Treco). See col. 743.

***The Electrical Resistances of Alloys of a Noble Metal and a Transition Metal.** A. N. Gerritsen and J. O. Linde (*Physica*, 1952, **18**, (11), 877–890).—[In English]. The elect. resistances of a series of wires of Au and Cu, contg. small amounts of Mn and Cr, have been measured at low temp. (2°–100° K.). In the region 2°–20° K., the curves show anomalies, the resistance passing through a min. then a max. as the temp. is lowered. The results are analysed in terms of the change in resistance/at.-% solute, and possible causes of the resistance min. are discussed. 23 ref.—E. O. H.

Problems of Metallic Fatigue at High Temperature. Thomas J. Dolan (*Metal Progress*, 1952, **61**, (4) 97–104).—D. states that although up to 1939 alloys in the high-temp. field were principally of the Ni–Cr family a wide variety of complex alloys have recently been studied, based on Co, Cr, Fe, Ni, Mo, W, V, Nb, Al, Si, and Ta to increase their high-temp. strength. It is stated that the use of cast alloys in preference to forged alloys is due to their superior properties in both creep and stress-to-rupture tests of long duration. However, the position is reversed in short-time high-temp. tests. The analyses and fatigue results for a large number of alloys including Hastelloy B, Inconel X, Refractalloy 26, and Stellite 23 are tabulated, the fatigue results quoted for these alloys are 66,000, 65,000, 52,000, and 44,000 lb/in.^{2}, resp.
—R. P. H. F.

***On the Wear and the Frictional Properties of Duplex Bearing Alloys.** Kiyoshi Matsubara (*J. Mech. Lab., Tokyo,* 1952, **6**, (6), 221–228).—[In Japanese, with figures and graphs in English]. The wear of duplex bearing alloys (Sn-base, Pb-base white-metal, and gun-metal) which slide on a standard steel under dry conditions under very light loads, has been studied. Wear tests of white metal have already been studied by Zimmerman (*Metals and Alloys,* 1931, **2**, 95) and Herschman and Basil (*Proc. Amer. Soc. Test. Mat.*, 1932, **32**, (II), 536; see *Met. Abs.* (*J. Inst. Metals*), 1932, **50**, 429), but these authors did not explain the mechanism, presumably because they used a heavy-load method, i.e. Amsler-type wear-testing machine. M. used a new wear-testing machine which allows 2 cylindrical test-pieces axially opposite to each other to slide successively over the same track under a load of 50–2000 g./cm.². The results are compared with the rule of metallic junctions by Bowden and Tabor (" The Friction and Lubrication of Solids," **1950**: Oxford), and the following conclusions are obtained: (1) the coeff. of wear is ~1·0 on Sn-base, ~2·6 on Pb-base, and ~3·2 on gun-metal; (2) the mechanism of wear and friction can be explained experimentally by the effect of velocity and load; and (3) the experimental results confirm the rule of metallic junctions in the main, but some differences do occur between the rule and M.'s results. 13 ref.—Author.

***Final Report on Metallurgical Investigation of Materials Subjected to Liquid Lead–Bismuth Alloy Environment.** (Grassi, Bainbridge, and Harman). See col. 744.

***A Search for New Supraconducting Compounds.** B. T. Matthias and J. K. Hulm (*Phys. Rev.*, 1952, [ii], **87**, (5). 799–806).—The possibility of supraconductivity in ~90 compounds at temp. down to 1·28° K. has been tested for magnetically, and several new supraconducting compounds found, including $SrBi_3$ and $BaBi_3$. No compound exhibiting semi-conductor characteristics became supraconducting nor did any compound contg. >50 at.-% B. The results support the possibility that metallic bonding of a special character is essential for supraconductivity. The behaviour of the Bi-contg. and of the interstitial compounds with the transition metals, suggests that a cubic or tetragonal lattice is more favourable to supraconductivity than a hexagonal structure. —P. C. L. P.

3 — STRUCTURE

(Metallography; Macrography; Crystal Structure.)

[For all abstracts on the constitution of alloy systems, including X-ray studies, see 2—Properties of Alloys.]

***Slip and Grain-Boundary Sliding [in Aluminium and Magnesium] as Affected by Grain-Size.** Nicholas J. Grant, Italo S. Servi, and Arup Chaudhuri (*J. Metals*, 1953, **5**, (2), 217–218).—2S Al was recrystallized to yield a mixed grain-size, and specimens were tested in creep at 900° F. (485° C.) at 880 lb./in.² to total elongations of 3·5 and 9%. Similarly, a high-purity Mg specimen was tested at 500° F. (260° C.) and 670 lb./in.². Photomicrographs were taken which show slip in coarse grains and grain-boundary sliding in fine-grained zones; medium grains exhibit both phenomena. The results support the previously reported evidence (cf. S. and G., *Trans. Amer. Inst. Min. Met. Eng.*, 1951, **191**, 917; see *M.A.*, **19**, 531) that grain boundaries have a blocking effect on slip at high temp., and at a given grain-size for a given stress, will undergo sliding as a primary mechanism of deformation.—E. N.

***Grain-Boundary Sliding and Migration, and Intercrystalline Failure [of Aluminium] under Creep Conditions.** Hsing C. Chang and Nicholas J. Grant (*J. Metals*, 1953, **5**, (2), 305–312). —Cf. *Trans. Amer. Inst. Min. Met. Eng.*, 1952, **194**, 619; see *M.A.*, **19**, 65. Specimens of high-purity Al were deformed by creep at temp. of 400°, 700°, 900°, and 1100° F. (205°, 370°, 485°, and 595° C.) at initial stresses of 50–1200 lb./in.², and the processes of boundary sliding and migration were studied microscopically. The direction of boundary sliding is governed, primarily, by the direction of the shearing stress acting on the boundary surface. The driving force which controls the direction of boundary migration is a combination of strain energy and surface energy, the latter being the more important at high temp. The zigzag nature of the movement of the grain-boundary triple-point appears to be a necessary consequence of the highly co-operative processes of grain-boundary sliding and migration, because the direction of migration depends mainly on the direction in which the grain boundary slides as the initial step. Grain-boundary sliding and migration are observed also in 2S Al at 900° and 1100° F., but, as a result of the alloy and excess phase content, the amount of migration is much smaller and has a more irregular course than in the high-purity metal. 3S alloy (Al–1¼% Mn) at 1100° F. exhibits normal boundary sliding (leading to intercryst. fracture) without any clear evidence of migration. The results are discussed at length, and a theory is presented regarding the role the grain boundary plays under creep conditions, which not only affords an explanation for the intercryst. failure of commercial alloys but also leads to the conclusion that an optimum grain-size should exist for good high-temp. properties of high-purity materials. 7 ref.—E. N.

***On an Etching Reagent to Reveal the Heterogeneities of Composition in Aluminium Alloys.** (Mme) Charlotte Bückle, (Mlle) Christiane Changarnier, and Jean Calvet (*Compt. rend.*, 1952, **235**, (18), 1040–1041).—An aq. soln. of 4% $KMnO_4$ + 2% Na_2CO_3 gives better results in revealing the compn. gradients of heterogeneous solid soln. of Al alloys than the commonly used Na_2CO_3 soln., acid mixtures, and anodic oxidation. This reagent, already used in rapid attack on steels, scarcely attacks Al alloys, and in general does not corrode the surfaces or grain boundaries. Its action is due to the formation of a thin film of an oxidation product, whose thickness, and hence interference colour, varies to a sensible degree with the compn. of the solid soln. Electropolishing gives the best results, but simple rubbing on emery paper is often sufficient. Certain constituents (e.g. Al_3Fe, Al_3Ni, Si) are coloured by the reagent; others (e.g. Al_3Mg_2, Al_2Cu. $SiMg_2$, Al_6Mn, Al_2Ca, Al_3Ti) are unaltered. Prolonged attack by the reagent reveals the crystal structure by grain coloration in certain alloys, particularly the Al–Cu alloys. —J. H. W.

***Electrolytic Polishing of Al–Si–Fe Alloys for Microscopical Examination.** G. Meynet and R. Assibat (*Rev. Aluminium*. 1952, (188), 180–182).—By using a polishing cycle of a few sec. on a Disa-Electropol machine, a good polish can be obtained on the 10% and 20% Si alloys without causing the Si particles to appear in relief. The specimen is rubbed down to 000 emery and polished with Al_2O_3, washed for 1 min. in conc. chromic acid, and dried. It is then placed in an electrolyte consisting of 20% perchloric acid, 70% ethyl alcohol, and 10% butyl cellosolve; the current used is 3–3·5 amp./cm.² at 100 V., and bath temp. is 18°–20° C. The ratio of specimen area : cathode area should be $\nless$ 1/100. —A. W. B.

***X-Ray Line Broadening from Filed Aluminium and Tungsten.** G. K. Williamson and W. H. Hall (*Acta Met.*, 1953, **1**, (1), 22–31).—[In English]. Methods of separating particle-size and strain effects in line broadening are discussed with ref. to previous work (*Proc. Phys. Soc.*, 1951, [B], **64**, 937, 946; *M.A.*, **19**, 654). New results are reported for line breadths in annealed and cold-worked Al and W, the measurements being made on powder specimens using a Geiger-counter spectrometer. For the annealed metals there was an increase in line breadth at high angles, and this is attributed to phys. rather than instrumental broadening. The phys. broadening was analysed by the Hall method (*ibid.*, 1949, [A], **62**, 741; *M.A.*, **17**, 822), and both size effects and strain effects were observed, the latter predominating. The broadening from filed commercial Al was larger than that from high-purity Al, and the difference is probably due to changes in the rate of recovery, taking place spontaneously at the high local temp. caused by the filing. This interpretation was confirmed by examining high-purity material filed at liq.-air temp., when the broadening increased. Similar results were obtained for W. Cold-worked W showed large particle size and strain broadening, which mostly disappeared after recovery at 1100° C., but was still a little higher than for recrystallized W. The results are regarded as confirmation for the dislocation theory, and indicate the presence both of randomly distributed dislocations, and of dislocation walls after recovery. Fourier analysis of the line shapes of W confirmed the results obtained from the line breadths, and also gave more definitive evidence of the formation of polygon walls, the strain after recovery being confined to regions of the order of 30 atoms wide. 42 ref.—J. W. C.

***An Electron-Microscope Study of the Development of Fatigue Failures [in Aluminium, Brass, and Iron].** W. J. Craig (*Amer. Soc. Test. Mat. Preprint*, 1952, (167), 13 pp.).—A pictorial comparison is made of deformation marks on the surface of α-brass, ingot Fe, and Al (99·97%) under both static and repeated loading. Under static loading the deformation is shown to be a general process taking place in all crystals, whereas under conditions of repeated loading the deformation is extremely localized and takes place in a few crystals or portions of crystals only. The appearance of the individual deformation marks produced by static as compared to repeated loading differed with the metal: (*a*) in α-brass no differences were observed; (*b*) in Fe there were slight differences; (*c*) in Al there were marked differences. 9 ref.—P. T. G.

***The Growth of Crystals of the Hexagonal Metals [Cadmium, Magnesium, and Zinc] from Their Vapours.** A. J. Forty (*Phil. Mag.*, 1952, [vii], **43**, (344), 949–957).—Opt.-microscopic examination of the (0001) surfaces has revealed spiral growth hills on Cd and Mg crystals grown from the vapour phase, indicating the screw-dislocation mechanism of growth. The growth steps, which are probably monomolecular in many examples, appear more obvious on exposure to air and Plasticene. The Zn crystals showed no spiral growth patterns, though closed loops were found surrounding impurity nuclei which are probably of ZnO. The possibility of obtaining further evidence by plastic-deformation experiments is discussed.—P. C. L. P.

***Frequency of Annealing Twins in Copper Crystals Grown by Recrystallization.** W. G. Burgers, J. C. Meijs, and T. J. Tiedema (*Acta Met.*, 1953, **1**, (1), 75–78).—[In English]. Strips of cold-rolled Cu sheet were annealed at 850° C. to obtain a sharp cubic texture, and then converted into single crystals by recrystn. at 930° C. The crystals were usually twinned on the {111} plane most nearly ‖ a {111} plane of the cubic texture. Crystals with an orientation derivable from the original texture by a rotation of 30° about a ⟨111⟩ axis showed many twins, but crystals derivable from the texture by a rotation of 15° or less showed very few twins. When a crystal was grown in a bent strip, there was usually a marked difference in twinning frequency before and after the bend. The results are explained on the assumption that twin crystals are formed when the growing crystal encounters regions of the matrix nearer to one of its possible twin orientations than to its own orientation. This would be expected if twins are formed either by "stimulation" or by growth faults. 16 ref.—J. W. C.

***The Study of Diffusionless Phase Changes in Solid Metals and Alloys [Gold–Cadmium Alloy].** T. A. Read, M. W. Burkart, J. Intrater, M. Wechsler, and D. S. Lieberman (*U.S. Atomic Energy Commission Publ.*, 1953, (**NYO-936**), 5 pp.).—A single crystal of 50 : 50 Au–Cd alloy was quenched from 450° C. and the variation of rocking curve width of the 100 and 200 reflections was determined with a double-crystal spectrometer as a function of time after quench. The widths for the two reflections increased similarly, but the % spread in sin θ did not, suggesting that the line broadening is due to a spread in the orientation of mosaic blocks rather than in the value of the lattice const.—B. W. M.

***[Structure of] Martensite.** F. C. Frank (*Acta Met.*, 1953, **1**, (1), 15–21).—[In English]. The structure of martensite is expressed in terms of a f.c. tetragonal cell (*F*), instead of the more usual b.c.c. cell (*I*). For all observed lattice orientations, the close-packed planes of the two lattices are ‖, and this suggests they meet edge to edge in the surface of contact. There must actually be a small bend of ~1° at this surface because of the different interplanar spacings. For the Kurdjumow–Sachs orientation, it is further assumed that close-packed rows in the contact surface are common to both lattices. The known lattice parameters then enable the habit plane to be calculated: using the standard variant $(111)_{\gamma} \parallel (111)_{\alpha F} \equiv (101)_{\alpha I}$, $[01\bar{1}]_{\gamma} \parallel [01\bar{1}]_{\alpha F} \equiv [11\bar{1}]_{\alpha I}$, the habit plane is $(522)_{\gamma}$ in agreement with experiment. The positions of the atoms along the $[01\bar{1}]$ rows are obtained by a heterogeneous shear in units of 6 planes in opposite $[01\bar{1}]$ and $[0\bar{1}1]$ directions. The surface of contact contains a grid of screw dislocations ‖ $[01\bar{1}]$ rows, the motion of which generates the heterogeneous shear. The results are compared with Bowles' analysis, the minor differences being connected with the bend in the (111) planes. The heterogenous shear can occur simultaneously with the "first" deformation. 8 ref.
—J. W. C.

***A Study of Segregation in Metals [Lead].** W. R. Thomas and W. C. Winegard (*Canad. Metals*, 1952, **15**, (11), 26).—Segregation has been detected in a single crystal of Pb, and some experimental work with bi- and polycryst. specimens is briefly described.—W. A. M. P.

***Cold-Rolling and Annealing Textures of Molybdenum Single Crystals.** N. K. Chen and R. Maddin (*J. Metals*, 1953, **5**, (2), 300–304).—Single crystals of Mo (0·1 in. dia., and 1 in. long) were grown by a method previously described (cf. C., M., and Pond, *Trans. Amer. Inst. Min. Met. Eng.*, 1951, **191**, 461; see *M.A.*, **19**, 217). They were then cold rolled (with respect to sp. crystallographic planes and directions), without intermediate anneals, by ~0·001 in./10 passes, to a final reduction in thickness of 87–98% (requiring ~800 passes), after which the orientations were determined by the conventional Laue transmission method. The specimens were then annealed in A for 14 min. at 1350° C. and their orientations again determined. *Rolling Textures.*—These are $(001)[110] + (111)[11\bar{2}]$, and $(001)[110]$, according to whether the initial orientations of the crystals are remote from or close to a cube position, resp. Compression rolling produces a fibre texture which is mainly [001] ⊥ the axis of compression. *Recrystn. Textures.*—Specimens having a $(001)[110] + (111)[11\bar{2}]$ deformation texture retain this texture after recrystn.; $(001)[110]$ deformation textures, however, undergo a rotation of ~20° about the pole of the rolling plane. The results are discussed; they are shown to be quite different from what has been previously reported as the rolling textures of b.c.c. metals; a possible explanation for this must be sought from the initial orientations chosen as the rolling plane and the rolling direction. 10 ref.
—E. N.

***Effects of Dislocations on Mobilities in Semi-Conductors [Silicon and Germanium].** D. L. Dexter and F. Seitz (*Phys. Rev.*, 1952, [ii], **86**, (6), 964–965).—A theoretical treatment is given of the scattering of electrons by randomly-arranged edge-type dislocations in the Si or Ge lattice. This contribution is compared with those from the lattice and impurity atoms, and consideration is given to the experimental conditions necessary for elect. measurements to give useful information about dislocations in semi-conductors.
—P. C. L. P.

***The Effect of Added Metallic Impurity and of Closed Moulds on the Growth from the Melt of Single Crystals of Tin.** A. J. Goss (*Proc. Phys. Soc.*, 1953, [B], **66**, (2), 65–73).—The results of growing Sn single crystals in open moulds are described, where addn. of Cd, Zn, Pb, Ag, In, and Sb were made to the melt. The amount of impurity was in every case less than the solubility limit. In general, the chances of successfully growing good single crystals are lowered when these impurities are present. The surface of the specimen is also affected. The use of closed vertical moulds did not seem to influence these results.—E. O. H

***Microstructure and Mechanical Properties of Iodide Titanium.** (Holden, Ogden, and Jaffee). See col. 743.

Titanium Metallography: Simple, Safe. —— (*Iron Age*, 1952, **170**, (9), 112).—The method of polishing and etching of Ti specimens is described.—S. R. W.

***Mechanism of Plastic Flow in Titanium: Determination of Slip and Twinning Elements.** F. D. Rosi, C. A. Dube, and B. H. Alexander (*J. Metals*, 1953, **5**, (2), 257–265).—Coarse-grained (2–8 mm. dia.) specimens of 99·77% Ti which have been deformed several % either by extension, bending, or compression in a vice, show well-marked slip bands and twins, the former being rather fine and straight and having a somewhat regular spacing of $\sim 1{\cdot}5 \times 10^{-2}$ mm. Back-reflection Laue X-ray patterns show that: (1) there are at least two types of slip—a prismatic type, $\{10\bar{1}0\}$, which predominates, and a secondary, pyramidal type, $\{10\bar{1}1\}$, which occurs rarely, and is difficult to detect; in both cases a digonal axis of indices $<11\bar{2}0>$ is the effective slip direction; basal slip appears to be absent; and (2) the twinning habit, like the slip process, is very different from that generally associated with the hexagonal metals, and takes place on pyramidal planes of low indices; three twin types are found, viz. (i), $\{10\bar{1}2\}$—which are thick and lenticular, being similar in habit to those of the same form observed in Cd, Mg, Zn, and Be, (ii) $\{11\bar{2}1\}$—appearing as thin lamellæ similar to the Neumann bands characteristic of twinning in Fe, and (iii) $\{11\bar{2}2\}$—which are infrequent, have a shape intermediate between the other two types, and show a distinct preference for appearing in pairs. An attempt is made to correlate the characteristic shapes of the three twin types with the amount of twinning shear. The effect of slip and twinning on the ductility of Ti and other h.c.p. metals is discussed in relation to the differences in their c/a ratios. 24 ref.—E. N.

***Plastic Deformation of Alpha-Uranium: Twinning and Slip.** R. W. Cahn (*Acta Met.*, 1953, **1**, (1), 49–70).—[In English]. The crystallographic elements of twinning, slip, and kinking in orthorhombic α-U were determined. Coarse-grained U was examined microscopically under polarized light, and back-reflection Laue photographs were taken in a precision camera of new design. Twins and slip lines were formed by heating and cooling (because of anisotropic expansion), by deformation, and by abrasion. Methods used for determining the complex twinning modes are described in detail. The principal slip plane is (010), and the slip direction [100]; {110} is a minor slip plane. Kink bands were observed $\perp$ [100]. Twins of both the first and second kinds are formed and are tabulated below. K_1 is the composition plane, η_1 the direction of shear, K_2 the second undistorted plane, and η_2 its intersection with the plane of shear. The amount of shear is s. Types 2 and 3 are reciprocal twins; type 3 occurs rarely and type 4 very rarely. The type-2 twins are the only known examples of twins of the second kind in metals. Twinning is the principal mode of deformation at lower temp., but is superseded entirely by slip above ~350° C. The conditions under which kinking should be preferred are discussed. The probable atom movements for the main types of twin are derived graphically. The plane of shear is always very close to a rational plane, though the significance of this is unknown. The crystallography of twin intersections is considered in two Appendices. 35 ref.—J. W. C.

Type	K_1	K_2	η_1	η_2	s	Kind
1	(130)	$(1\bar{1}0)$	$[3\bar{1}0]$	[110]	0·299	Compound
2	Irrational approx. $(\bar{1}72)$	(112)	[312]	Irrational	0·228	Second
3	(112)	Irrational approx. $(\bar{1}72)$	Irrational	[312]	0·228	First
4	(121)	Irrational	Irrational	[311]	0·329	First

***A Note on Twinning in Alpha-Uranium.** F. C. Frank (*Acta Met.*, 1953, **1**, (1), 71–74).—[In English]. A discussion of Cahn's results (*ibid.*, p. 49; preceding abstract) is given in terms of a comparison with the twinning modes of Zn. The lower symmetry of U should introduce extra modes, first because some of the reciprocal twins of Zn become different modes (twins of the second kind), and second because each symmetry plane present in Zn but absent in U becomes a possible twinning plane. Of the 5 types expected, 3 are found together with 1 other. The extra plane (121) is regarded by C. as not definitely established. For reciprocal pairs of twins, those of the second kind seem to be preferred, and the possible reasons for this are discussed, in terms of the relative immobility of low index (rational) habit planes. 2 ref. —J. W. C.

***A Method for the Quantitative Determination of Preferred Orientation [in Uranium].** J. H. Bach and J. B. Burnham (*U.S. Atomic Energy Commission Publ.*, 1952, **(AECD-3450)**, 10 pp.).—A rapid method is described for determining textures in worked U rods. X-ray reflections from the surface crystals were picked up in an X-ray spectrometer, and it was found that the intensity of the (111) reflection remained almost const. This reflection was used as an internal standard for estimating the intensities of other reflections, thereby avoiding errors due to differences in the state of surface oxidation from sample to sample and variations in the slit adjustment and beam intensity. The ratio of the measured intensity from a given plane to the calculated intensity on the basis of a random orientation, was taken as an indication of preferred orientation. The method is less precise than a pole-figure procedure, but gave satisfactory results for U in agreement with those of Harris (*Phil. Mag.*, 1952, **43**, 113; *M.A.*, **20**, 103). For U rolled at 600° C. with 90% reduction in area, the orientation was duplex with both the (010) and (110) poles $\parallel$ the rolling direction: for cast U, no preferred orientation was found.—B. W. M.

***The Location of Oxygen Atoms in Vanadium–Oxygen Alloys by Means of Neutron Diffraction.** C. W. Tucker, A. U. Seybolt, H. T. Sumsion, E. O. Wollan, and W. C. Koehler (*U.S. Atomic Energy Commission Publ.*, 1952, **(KAPL-829)**, 25 pp.). A comparison was made of X-ray and neutron-diffraction techniques for locating O atoms in V–O alloys. For alloys of high O content, such as VO, either method is satisfactory, but in the region of low O content, neutron diffraction has a marked advantage owing to the large scattering factor for O with neutrons compared with that for V. In an alloy contg. 21 at.-% O, the O atoms were found to occupy octahedral positions of a b.c. tetragonal lattice as inferred by Klemm and Grimm (*Z. anorg. Chem.*, 1942–43, **257**, 42), using X-ray diffraction. 9 ref.—B. W. M.

***Metallographic Identification of Non-Metallic Inclusions in Zirconium.** H. A. Saller and R. F. Dickerson (*U.S. Atomic Energy Commission Publ.*, 1951, **(BMI-74)**, 27 pp.).—The identification of various inclusions on mech. polished microsections of Zr is described. The two etching soln. used were: (*a*) 10–15 ml. HNO_3, 40 ml. HCl, and 3 drops HF, and (*b*) 10 wt.-% aq. $NH_4F.HF$. Carbides occur as globules in stringers, appear isotropic under polarized light, and etch to light-grey. Oxide is present both in the grains and grain boundaries, and is difficult to identify in β-quenched material. No inclusion has been identified as nitride, but bands which etch up in the matrix with $NH_4F.HF$ are believed to be N-rich areas. A spiny inclusion found in continuous stringers and polishing in slight relief is considered to be a hydride. The structures are illustrated by typical photomicrographs. —B. W. M.

***Kinetics of Thermal Re-Orientations in Cold-Rolled Zirconium.** R. K. McGeary and B. Lustman (*J. Metals*, 1953, **5**, (2), 284–291).—The metal used was an arc-melted ingot—showing only a single-phase structure—of high-purity Zr crystal bar contg. as impurities: C 0·04; Fe 0·05; Hf 0·014; W 0·01; Ti, Ni, and Al 0·003; Si and N 0·002;

Cr and Cu 0·001 wt.-%. This, after hot working and annealing to produce an equiaxed grain structure (~0·1 mm. dia.), and removal of the surface layers, was cold rolled to a 97% reduction, from 0·135 to 0·004 in. thickness. Specimens were then isothermally annealed *in vacuo*, at temp. of 98°–600° C., and both cold-rolled and annealed materials were studied by X-ray diffraction, by metallography, and by hardness measurements and from the results, and consideration of those of other workers, an analysis has been made of the mechanism of annealing. Cold rolling produces a high degree of preferred orientation in which prism poles, {1010}, are ⊥ the rolling direction. The processes which occur during annealing are : (1) polygonization—this may occur during the first stages of heating, or even during cold rolling ; it is not accompanied by re-orientation, and cannot be detected metallographically ; (2) recrystn. *in situ* (metallographic evidence of polygonization) —which occurs after annealing at relatively low temp., and corresponds to a re-orientation in which the ideal cold-rolling texture is sharpened ; this process may occur by selective growth of favourably oriented domains, ~2 μ dia. ; and (3) complete re-orientation—which occurs after further heating, and corresponds to 20° or 40° rotations about {0001} poles ; it takes place in two steps, the first at const. domain size, the second accompanied by domain growth. Data are presented which show that re-orientation is not governed by (*a*) the simple conventional mechanism of nucleation and growth, or (*b*) the discontinuous growth of favourably oriented domains. Activation energies for domain growth and for annealing orientations have been calculated. 27 ref.—E. N.

***Allotropy in the Phase $ZrCr_2$.** W. Rostoker (*J. Metals*, 1953, 5, (2), 304).—Differences in the reports of various workers on the structure of the phase $ZrCr_2$ are critically examined, and it is shown that the conflicting results can be resolved by assuming a high- and a low-temp. modification for $ZrCr_2$. X-ray-diffraction analysis of specimens annealed at temp. between 700° and 1200° C. and subsequently quenched show that such a transition—from the low-temp. $MgZn_2$-type structure (*C*14, hexagonal lattice, 12 atoms/unit cell) to the high-temp. $MgCu_2$-type structure (*C*15, cubic lattice, 24 atoms/unit cell)—takes place at some temp. between 900° and 944° C. Lattice parameters of the two modifications have been calculated. $ZrCr_2$, therefore, behaves in a reverse fashion to $TiCr_2$, for in the latter the $MgCu_2$ structure is the low-temp. modification and the $MgZn_2$ structure is the high-temp. modification. 3 ref.—E. N.

***The Use of Diamond Abrasives for a Universal System of Metallographic Polishing.** L. E. Samuels (*J. Inst. Metals*, 1952–53, **81**, (10), 471–478).—An investigation has been carried out to determine the most efficient and economical methods of using diamond abrasives for metallographic polishing. It has been found that the abrasive is most efficiently used when dispersed in a carrier paste, the polishing rate then being 4–5 times that of dry appn., and that it can be used economically only in the finer grades (0–10 μ particle-size range). The polishing rates are then extremely high ; even with hand polishing, the rates are frequently higher than that of electrolytic polishing. The results of the work are applied to the development of a system of metallographic polishing, the costs of abrasive for which are sufficiently low to permit its use for general, and even routine, polishing. To bridge the gap over which diamond abrasives cannot be used economically, a cast wax-abrasive lap has been developed, the characteristics of which are such as utilize the full potential of the subsequent diamond stages. Consideration has also been given to final polishing treatments necessary to give truly scratch-free surfaces. The system finally developed is very rapid and produces a polish of very high quality, with a surface free from objectionable deformation.—Author.

***An Experimental Study of Electrolytic Polishing.** I. Epelboin (*J. Chim. Phys.*, 1952, 49, (2), C214–C218 ; discussion, C218).—During the process of electrolytic polishing, the apparent resistance, *R*, of the polishing bath, and the modulus of the impedance, *R′*, of the bath, both expressed in terms of the bath voltage, attain max. values for the same value of the polishing voltage, *U*, despite the fact that *R* and *R′* are very different. This fact is utilized in order to determine optimum conditions for polishing. Likewise it can be used to determine the optimum compn. of the polishing electrolytic bath to be used for polishing any specified specimen, since best polishing is obtained by the use of that electrolyte which gives the highest value of the max. resistance. It is found that the desirable compn. of the polishing bath is determined by the degree of hydration of the dissolved ions, in accordance with the mechanism of the polishing process proposed by Darmois, viz. direct passage of metallic ions into soln. by reason of the contact p.d. created by anions adsorbed at the anode.—J. S. G. T.

***The Water Content of Solutions Used in Electrolytic Polishing.** I. Epelboin (*J. Chim. Phys.*, 1952, 49, (7/8), C137–C140 ; discussion, C140–C141).—E. has shown that, using an electrolyte contg. ClO_4^- and PO_4^{3-} ions, optimum polishing conditions are obtained when the elect. resistance of the electrolytic cell passes through a max. (*Compt. rend.*, 1948, 226, 324 ; *M.A.*, 15, 574). Optimum conditions for the electrolytic polishing of Co, Pb, Fe, Ni, Sn, Cu, and other metals, using ClO_4 or PO_4 anions are given and discussed, together with the electrolytic polishing of Pt by CN or Cl ions. The creation of an anhydrous anionic layer would appear to be necessary to effect electrolytic polishing, but this, alone, is not sufficient. A theory of electrolytic polishing should explain, in particular, the role played by the anion, and the restricted relation between the water content and that of any other solvent used in the electrolytic bath. 17 ref.—J. S. G. T.

***A Combination of Electron Microscopy and Optical Phase-Contrast Microscopy.** Shigeto Yamaguchi (*J. Appl. Physics*, 1952, 23, (12), 1404–1405).—A letter. Electron-microscopic negatives taken of an oxide replica of a Permalloy crystal surface were opt. enlarged with ordinary and dark-ground phase-contrast microscopes. The latter removed the images of unwanted oxide grains, and improved the contrast of etch-pit markings. The phase-contrast acts as a filter, eliminating the contrast between shades of grey and consequently bringing out the contrast between these and bright regions.—R. W. C.

***Effective Atomic Diameter and Various Kinds of Atomic Distances in the Crystal Lattices of the Elements.** Robert Forrer (*J. Chim. Phys.*, 1952, 49, (9), 504–512).—In previous work, F. has defined an effective atomic dia. in terms of an interaction distance (*ibid.*, 1949, 46, 561 ; *M.A.*, 18, 176). These interactions are characteristic of metals, but occur also in numerous metalloids, salts, and combinations. In the case of I, four kinds of atomic distances are clearly distinguished, viz. covalent distance, interaction distance, a distance approx. that of the effective atomic dia., and a slightly greater distance attributable to feeble van der Waals forces. It is now shown that continuity characterizes, to a very great extent, the appn. of the notions of these four distances to the periodic classification of the elements ; Si and Ge exhibit discontinuities in this respect. It is considered that, in general, an atom opposes a number of quite distinct barriers to the approach of its neighbours.
—J. S. G. T.

***Theory of Catalysis of Nucleation by Surface Patches.** David Turnbull (*Acta Met.*, 1953, 1, (1), 8–14).—[In English]. The theory of heterogeneous nucleation on catalytic surfaces, which are of the order of size of the critical nuclei for homogeneous nucleation, is discussed. This hypothesis is able to explain the apparent multiplicity of nucleation frequencies observed in the solidification of Hg droplets catalysed by " HgX ", and of Sn droplets catalysed by oxide. Quant. agreement with previous experimental results is obtained by plausible assumptions about the size distribution of patches. For the Sn droplets, it is also necessary to assume a steady nucleation rate, which may be that of homogeneous nucleation. The theory explains the athermal formation of crystal nuclei in solidification processes. Although developed for surface patches, it is readily adapted to nucleation on small catalysts distributed through the vol. of a phase. 12 ref.—J. W. C.

***Centres of Disturbance in [Catalytic] Surfaces.** Georg-Maria Schwab (*Z. Elektrochem.*, 1952, **56**, (4), 297–301; discussion, 301–302).—[In German]. Paper presented at a Symposium held by the Deutsche Bunsengesellschaft at Berlin, Jan. 1952. Simple electrostatic ideas are used to calculate the energy resident at disturbance centres in cation-disturbed crystal lattices. From this it is possible to deduce what kinds of disturbance centres are to be anticipated in different regions of crystal surfaces of various kinds, and possible consequences concerning the catalytic action of the disturbed lattice are briefly discussed.—J. S. G. T.

***The Structure of Surfaces and Their Adsorption, Considered as a Co-Operative Problem.** N. Cabrera (*Z. Elektrochem.*, 1952, **56**, (4), 294–296).—[In French]. Paper presented at a Symposium held by the Deutsche Bunsengesellschaft at Berlin, Jan. 1952. It is suggested that the adsorption of a monolayer on a crystal surface could produce a kind of surface fusion at a transition temp., T_c, well below the m.p. of the crystal, and it is shown that this surface fusion would produce a pronounced min. value of the heat of adsorption at T_c, and possibly also a marked change in surface tension.

—J. S. G. T.

***†Grain Shapes and Other Metallurgical Applications of Topology.** Cyril Stanley Smith (*Metal Interfaces* (*Amer. Soc. Metals*), **1952**, 65–108; discussion, 108–113).—The role of topology, and more especially space-filling requirements, in determining the internal structure of metals and alloys is very interestingly developed. Starting with a relation resembling, very closely, the well-known Eulerian relation between the number of polygons, edges, and corners required to fill space of either 2 or 3 dimensions, S. draws attention to math. relations between the number of grains with n sides, the number of grain boundaries, and the number of grain corners necessary to fill a space of two or three dimensions. The high frequency of pentagons as grain faces is a direct result of topological considerations, but grains with only pentagonal faces cannot fill space *in extenso*. The conflict between space-filling requirements and those of local surface-tension equilibrium is shown to be responsible for grain growth, because of the inevitable introduction of curvatures. Recrystn. can be regarded as the migration of a high-energy interface into a network of numerous low-energy interfaces, following simple surface-tension rules geometrically similar to those determining abnormal grain growth. Simple relations between the intercepts of random lines and random planes with an array of lines and spaces in three-dimensional space allow one to deduce accurately the ratio of grain-boundary area : vol., and the ratio of grain edge : grain face-area directly from the examination of two-dimensional sections alone, without making any assumptions regarding grain shape and size. Simple appn. of topology are suggested for the study, *inter alia*, of relations between phase fields in ternary diagrams, and of cryst. interfaces. It is shown that perfectly coherent interfaces are possible between lattices differing in co-ordination number, even though they may differ in orientation and spacing; the martensite/austenite interface is possibly of this kind. 26 ref.—J. S. G. T.

†Phase Transformations at Interfaces. Alfred H. Geisler (*Metal Interfaces* (*Amer. Soc. Metals*), **1952**, 269–295; discussion, 295–298).—Internal surfaces in metals, e.g. grain boundaries, can act as preferred sites for the accelerated nucleation of transformations such as pptn. and eutectoid decompn.; the preferred site is generally one of discontinuity or imperfection in the crystal lattice; the mechanism of the acceleration is speculative. Localized formation of particles of the new phase may produce a susceptibility to intergranular corrosion and brittle fracture. Pptn. at interfaces is responsible for the initial hardening of some alloys. The activation energy for the initial hardening is $\sim\frac{1}{3}$–$\frac{1}{2}$ of that for vol. diffusion, indicating that interface diffusion plays a prominent role. A nodular process, nucleated almost exclusively at grain boundaries, is found with the three main types of transformation in solid soln. This nodular process is perhaps the slowest reaction, with the exception of spheroidization. and grain-boundary diffusion is not the controlling factor, although diffusion along interfaces may play a part in the process. 41 ref.—J. S. G. T.

***Statistical Theory of Rotational Phase Transition.—I.** Takehiko Oguchi and Yutaka Takaci (*J. Phys. Soc. Japan*, 1952, **7**, (2), 145–152).—[In English]. Anomalous sp. heats of molecular crystals at relatively low temp. are attributed to transition from an ordered state of orientation of the axes of mol. to a disordered state due to thermal agitation; this phenomenon is attributed to what is known as rotational phase transitions. A math. theory of the phenomenon is developed, for the case of the two-dimensional sq. lattice, along the lines of Kikuchi's theory of the order–disorder transformation in binary alloys. The discontinuity in the sp. heat at the transition point is derived. 9 ref.

—J. S. G. T.

***A Study [of the Deformation] of Two-Phase Alloys by Cold Rolling.** Genjirô Mima and Shigenori Hori (*Nippon Kinzoku Gakkai-Si* (*J. Japan Inst. Metals*), 1952, **16**, (7), 361–365).—[In Japanese, with tables and graphs in English]. Generally indust. alloys consist of several phases, e.g. solid soln., intermetallic compounds, and non-metallic inclusions. The deformation by rolling of these alloys differs from that of alloys with homogeneous structures. M. and H. have studied by statistical methods, using a microscope, the internal stresses set up by rolling in 2-phase alloys of Cu–Zn, Cu–Sn, Cu–Al, and Sn–Sb. The results show that in an alloy contg. a second phase which is softer or harder than the matrix the softer second phase is deformed more, whereas the harder second phase is deformed less than the matrix. Continued rolling with progressive reduction leads to similar flow-strength in both phases. The following corrected Unckel's formula (*J. Inst. Metals*, 1937, **61**, 171; *M.A.*, **4**, 672) satisfied the results of the experiments: $\frac{\Delta h}{h} \Big/ \frac{\Delta H}{H} = a^{1 - V_t/V_m}$, where $\Delta h/h$ = degree of deformation of the second phase, $\Delta H/H$ = average % of reduction, V_t/V_m = relative hardness of the two phases, and a was obtained by experiment and found to be 3·0.

—AUTHORS.

***Plastic-Deformation Features on the Cleavage Surfaces of Metal Crystals.** J. Holden (*Phil. Mag.*, 1952, [vii], **43**, (344), 976–983).—Interferometric study of the cleavage surfaces of single crystals of Zn, Mg, Bi, and Sb, after subjection to a variety of plastic-deformation experiments, has given information on the twin bands, band planes, and kink bands that are formed. The polygonized structure found after inhomogeneous deformation and subsequent annealing, is related to the growth mosaic structure of metal crystals. Evidence has been obtained on the glide deformation in Zn and Mg single crystals at different temp.—P. C. L. P.

***Similar Glide Processes in Ionic and Metallic Crystals.** P. L. Pratt (*Acta Met.*, 1953, **1**, (1), 103–104).—[In English]. A letter. The strain-hardening curve of NaCl is parabolic when single glide occurs, and linear when double glide occurs. The results are compared with those for metallic crystals. Hexagonal metals show single glide and give linear curves, whilst for f.c.c. crystals the shape of the hardening curve should depend on the initial orientation, which determines whether or not double glide is present from the beginning of deformation. Experimental evidence in favour of this prediction is summarized. 10 ref.—J. W. C.

***Theory of Slip-Band Formation.** John C. Fisher, Edward W. Hart, and Robert H. Pry (*Phys. Rev.*, 1952, [ii], **87**, (6), 958–961).—The approx. const. glide produced per avalanche in the plastic deformation of metals is attributed to the termination of the dynamic generation of dislocation loops from a Frank–Read source (*ibid.*, 1950, [ii], 79, 722; *M.A.*, **18**, 465) by their own back-stress field. In agreement with observation, it is shown that approx. 300 loops can be produced before loop generation stops unless the applied stress be raised.—P. C. L. P.

***The Continuity of Slip Lines Across a Grain Boundary.** G. J. Ogilvie (*J. Inst. Metals*, 1952–53, **81**, (10), 491–495).—Slip lines on the surfaces of polished and subsequently strained specimens of Al and 70 : 30 brass are sometimes continuous across a grain boundary. Investigation of the interior of the brass specimens shows that this is not merely a surface effect, but that the intersection of the slip planes does in fact lie in the grain boundary. It is shown that this intersection lies at an angle of $<2^\circ$ from one of the $\langle 110\rangle$, $\langle 112\rangle$, or $\langle 123\rangle$ directions in both the slip planes concerned. When the duration of annealing, before the final deformation, is increased, there is, within a given surface area, an increase in the number of grain-boundary sections where slip lines cross. It is therefore suggested that the boundary configuration favourable to slip-line crossing has a low interfacial free energy. It is shown that approx. half the adjacent crystal pairs in a random aggregate are favourably oriented for slip-line crossing to occur.—AUTHOR.

†**The Quantitative Explanation of [Actual] Crystal Structures in Terms of Dislocations.** Albert Kochendörfer (*Z. Elektrochem.*, 1952, **56**, (4), 283–294). [In German]. Paper presented at a Symposium held by the Deutsche Bunsengesellschaft at Berlin, Jan. 1952. Stepwise and screw dislocations in slip planes and latent dislocations are explained and used to account quant. for crystal defects, i.e. respects in which the structures of actual crystals differ from those of ideal crystals. Thus, more especially, mosaic structure and grain boundaries are discussed in terms of regular dislocations or in terms of definite collections of defects, whilst latent and mobile dislocations are considered as sources of crystal defects of high concentration, together with other phenomena requiring such high concentration of defects. 31 ref.
—J. S. G. T.

***The Formation of Immobile Dislocations During Slip.** A. H. Cottrell (*Phil. Mag.*, 1952, [vii], **43**, (341), 645–647).—A new mechanism whereby dislocations on intersecting slip planes in a f.c.c. lattice can react to form immobile dislocations is proposed, which is more effective than that suggested by Lomer (*ibid.*, 1951, [vii], **42**, 1327; *M.A.*, **19**, 721). The role of such dislocations in work-hardening is discussed.
—P. C. L. P.

***Scattering of Electrons in Metals by Dislocations.** D. L. Dexter (*Phys. Rev.*, 1952, [ii], **86**, (5), 770–774).—A comparison is made between four recent theoretical treatments of the increase in the elect. resistivity of metals on cold working, arising from scattering of electrons by edge-type dislocations. A new treatment on similar lines indicates that the *d* of edge dislocations would have to be an order of magnitude greater than that estimated from energy-storage measurements. The discrepancy is possibly attributable to the neglect of effects such as those of clustered vacancies and screw dislocations.—P. C. L. P.

***Microscopic Studies in Beryl Crystals. III.—The Movement of Dislocations.** L. J. Griffin (*Phil. Mag.*, 1952, [vii], **43**, (343), 827–846).—Study of the surface of beryl crystals has given evidence of the prior movement of certain dislocations over short distances. The frequent observation of certain characteristic groupings of dislocations is interpreted to give evidence of the generation of dislocations by Frank–Read sources (*Phys. Rev.*, 1950, [ii], 79, 722; *M.A.*, **18**, 465).—P. C. L. P.

***Critical Shear Stresses in Body-Centred Cubic Lattices.** R. Smoluchowski (*Phys. Rev.*, 1952, [ii], **86**, (5), 787–789).—An explanation of the observed relative values of the critical shear stress on different planes of certain b.c.c. materials (Opinski and S., *J. Appl. Physics*, 1951, **22**, 1380, 1488; *M.A.*, **19**, 778, 837) is put forward, based on the atomic configuration of dislocations. The calculated temp. variation of the critical shear stresses agrees with observations on Fe–Si alloys. The elimination of slip on the {112} and {123} planes by the addn. of $>7{\cdot}5$ at.-% Si is attributed to local displacements around the smaller Si atoms. Other work is discussed on the temp. variation of the observed slip planes in b.c.c. materials.—P. C. L. P.

†**The Mathematical Theory of Stationary Dislocations.** F. R. N. Nabarro (*Advances in Physics*, 1952, **1**, (3), 271–394).—The various possible types of dislocations are defined and theorems proved about their properties, including their interaction and behaviour in motion. The importance of the mechanism for the generation of large numbers of dislocation loops proposed by Frank and Read (*Phys. Rev.*, 1950, [ii], **79**, 722; *M.A.*, 18, 465) in the theory of slip-band formation is pointed out. The various dislocation models of a grain boundary are included in the discussion of the properties of arrays of dislocations. The dependence of the thermal activation energy necessary for creep to occur, upon the applied stress, is considered for various types of dislocation models of the creep process. The theory of the properties of elastic dislocations is compared with that of dislocations in crystal lattices, and important differences are pointed out. N. also discusses the compression-wave theory of slip proposed by Frenkel and Kontorowa (*Physikal. Z. Sowjetunion*, 1938, **13**, 1; *M.A.*, 5, 222) and its extensions. Finally, those aspects of dislocation behaviour which depend upon the particular crystal lattice are reviewed, including those phenomena which have been explained on the basis of dislocation reactions. About 170 ref.—P. C. L. P.

†**Energies and Structure of Grain Boundaries.** K. T. Aust and B. Chalmers (*Metal Interfaces* (*Amer. Soc. Metals*), **1952**, 153–178).—The two theories, viz. the amorphous-cement and the transition-lattice theories, advanced to explain grain-boundary structures, are critically discussed in the light of experimental evidence. Properties of grain boundaries—melting, mech. and viscous behaviour, and chem. effects—indicate the latter theory as the more acceptable, but conclusive evidence for this preference was lacking, until recent measurements of the free surface energies showed that the boundary energy of Sn, Pb, Si ferrite, and Ag depends upon the difference of orientation of grains on either side of the boundary; it is concluded that different boundaries differ in structure and therefore cannot be amorphous. A sp. form of the transitional lattice is the dislocation model. For large differences of grain orientation across the boundary, alternative descriptions of the transition structure, e.g. those of Mott and of Kê, may be preferable. 85 ref.—J. S. G. T.

†**Theory of Internal Boundaries.** Harvey Brooks (*Metal Interfaces* (*Amer. Soc. Metals*), **1952**, 20–64; discussion, 64).—The present status of the theory of internal boundaries is comprehensively reviewed, particular attention being devoted to the dislocation model of internal boundaries and its success and limitations in predicting observed energy relations of grain and interphase boundaries. The main conclusions reached are: (1) any grain boundary may be described as an array of one or more types of dislocations; (2) any two lattices which can be generated from each other by a homogeneous linear transformation of co-ordinates may meet in a boundary represented by arrays of dislocations; (3) a phase or grain boundary is a transitional region between perfect crystals; (4) the elastic part of boundary energy can be computed from elasticity theory and agrees with the value found by experiment; (5) for coherent twin or interphase boundaries, there exists a dislocation description for which the *d* of dislocations vanishes; (6) for solid interfaces, surface free energy, and surface stress must be distinguished from one another; and (7) the energy of coherent boundaries depends only on the distortion of interatomic bonds near the boundary, and there is no longer-range elastic energy. 40 ref.
—J. S. G. T.

***Study of the Surface Tension of a Grain Boundary in a Metal as a Function of the Orientation of the Two Grains Which the Boundary Separates.** J. Friedel, D. B. Cullity, and C. Crussard (*Acta Met.*, 1953, **1**, (1), 79–92).—[In French]. Relative grain-boundary energies were obtained by measurement of dihedral angles in polycryst. Al discs. The grain orientations were not random, but had two textures: a cubic texture and a "*Z*" texture obtainable from this by a rotation of $\sim 40^\circ$ about a $\langle 111\rangle$ axis. Grain orientations were obtained by Laue photographs and by etch-pit methods. The effect of the grain-boundary orientation was also studied. Grain boundaries between two crystals of random orientation were found to have nearly const. energy, which decreases when there is a common plane of symmetry. The energy becomes lower still when the grain boundary lies in this plane of symmetry, and practically disappears for crystals which are $\parallel$ or in spinel twin orientation. A rather approx. method of calculating surface and grain-boundary energies, based on a central force model, is described, and results are given for Al, Cu, α-Fe, and γ-Fe. The method is suitable for large-angle grain boundaries, where the dislocation model is inappropriate. The calculations for Al agree well with experimental results. 37 ref.—J. W. C.

***†Boundary Migration During Grain Growth.** R. L. Fullman (*Metal Interfaces* (*Amer. Soc. Metals*), 1952, 179–207).—An extension of the quant. analysis of the kinetics of grain growth, using more detailed models than those hitherto employed, is developed. In metals, grain dia. frequently ∝ the annealing time raised to a power n which generally differs from $\frac{1}{2}$. Assumptions made in the theory are removed, singly, in order to determine their possible effect upon this grain-growth index. The presence of inclusions can account for the cessation of grain growth, but cannot account for the small values of n commonly observed. Reasonable changes in average grain-boundary interfacial free energy probably have no significant influence on n. Variation in grain-boundary free energy with grain orientation may cause a short-range preferred orientation during grain growth, which might influence n significantly. Adsorption of soluble impurities on grain boundaries could change n from $\frac{1}{2}$ to $\frac{1}{3}$ at most. Polygonization has probably no significant influence upon grain growth, but residual strains remaining after recrystn., might affect n. Tentative evidence supporting the possibility that recrystn. does not remove all strain is presented and briefly discussed. Subjects requiring investigation in the study of grain growth are suggested. 55 ref.—J. S. G. T.

†Interface Migration in Recrystallization. Paul A. Beck (*Metal Interfaces* (*Amer. Soc. Metals*), **1952**, 208–247).—Important variables affecting the rate of grain-interface migration in recrystn., and some features of recently-discovered types of interface migration, closely connected with recrystn., are reviewed. Matters discussed include: the effects of strain, temp., orientation and impurities, strain-induced boundary and sub-boundary migration, sub-grain growth, and the driving energy of interface migration in recrystn. 67 ref.—J. S. G. T.

***Grain-Boundary Diffusion: Annual Report.** R. Smoluchowski *et al.* (*U.S. Atomic Energy Commission Publ.*, 1952, (**NYO-3185**), 6 pp.).—A study of grain-boundary diffusion of Zn in columnar Cu showed that, as in the case of diffusion of Ag in Cu, no preferential grain-boundary diffusion occurs until a certain critical angle is reached, after which penetration increases to a max. at an angle of 45°. The critical angle increases rapidly with temp. Calculations from data at 550°, 600°, and 650° C. lead to the anomaly that very low or negative activation energies are obtained at angles slightly greater than the critical value. This is explained on the basis of a change from a pure dislocation type of boundary to one in which dislocations merge and form rods of highly distorted material at the critical angle. Further increase of angle results in the rods merging to form a more or less uniform boundary. The activation energies are 34,000 and 24,500 cal./mole for vol. diffusion and diffusion in the distorted material. In Fe–Co alloys, the normal recrystn. texture is the sum of three ideal textures, one of which is identical with the as-rolled texture. Both increasing the recrystn. temp. and the appn. of a magnetic field result in a decrease in the importance of the as-rolled texture and corresponding increases in the other two.
—B. W. M.

***Investigation of Diffusion Phenomena: Progress Report.** R. Smoluchowski *et al.* (*U.S. Atomic Energy Commission Publ.*, 1952, (**NYO-3483**), 3 pp.).—To show the presence of Al in the grain boundaries of the Cu component of a Cu–Al diffusion couple, an etch was developed contg. 15 ml. 10% $(NH_4)_2S_2O_8$, 2·5 ml. NH_4OH, and 15 ml. H_2O. A bicrystal of Si–Fe with an orientation difference of 47° between the grains ([011] common) was plated with radioactive Fe on one side and diffused in H for 145 hr. at 704° C. Vol.-diffusion penetration was found to be ~0·0008 in., compared with a grain-boundary diffusion between 0·0010 and 0·0015 in.—B. W. M.

Theory of Grain-Boundary Diffusion. (Smoluchowski). See col. 747.

***Determination of the Lattice Disorientation in Single Crystals by X-Ray Diffraction.** Honoré Lambot and Lawrence Vassamiller (*Compt. rend.*, 1952, **235**, (19), 1136–1138).—Details of the X-ray technique for the examination of single crystals are given.—J. H. W.

Summarized Proceedings of a Conference on X-Ray Analysis, Edinburgh, April 1952. C. A. Beevers and A. E. De Barr (*Brit. J. Appl. Physics*, 1952, **3**, (10), 305–306).—*H. S. Peiser* and *J. R. Rait* lectured on " The Metals Industry and X-Ray Methods ", special attention being given to the close relation between structure and properties of steels and the consequent importance of determining the structure. *P. Gay*, *P. B. Hirsch*, and *A. Kelly* estimated dislocation d and internal strains in cold-worked metals by microbeam methods, while *G. K. Williamson* studied these points by Geiger-counter precision methods. *J. Adam* reported that ordered Cu_3Au, while under neutron bombardment, disordered and re-ordered simultaneously. *J. Thewlis* showed that Li^6F and Li^7F had different lattice const. (4·0271 and 4·0262 kX, resp., at 25° C.). Theory agrees with these values. *C. J. Milner* described a new preferred-orientation camera. *A. R. Lang* described some novel arrangements for Geiger-counter diffraction measurements in which the diffracted beam is monochromated. Background is supressed and high θ angles can be observed.—R. W. C.

***X-Ray Study of Radiation Damage: Progress Report.** B. E. Warren (*U.S. Atomic Energy Commission Publ.*, 1952, (**NYO-3731**), 4 pp.).—A method has been developed for separating the line-broadening effects due to small particle size, lattice distortion, and stacking faults in f.c.c. materials. Stacking faults due to slip cannot produce line-broadening for planes of the type $(\pm h \pm k \pm 2l) = 6n$, so that if peak shapes are measured for several orders of (111) or (200), and the peak shapes expressed by Fourier coeff. $A_L(l_0)$, where $l_0{}^2 = h^2 + k^2 + l^2$, a plot of $\ln A_L(l_0)$ against $l_0{}^2$ for various values of L will separate the three effects. The intercept on the axis gives the Fourier coeff. for particle-size broadening alone, the slope gives the distortion in the material, and the departure of the (333) or (600) points from the curve through the other reflections gives a measure of the broadening due to stacking faults. A method is given for correcting for instrumental broadening. Measurements on a 98 : 2 Cu–Si alloy showed that the damage produced by 30 days' irradiation was insufficient to be detected by X-rays. Marked line-broadening was obtained on LiF single crystals after irradiation for 2 days, and in cold-worked filings of α-brass due to both particle size and distortion.—B. W. M.

***The Effect of Accelerating Voltage and Specimen Morphology on Electron-Diffraction Patterns.** S. G. Ellis (*J. Appl. Physics*, 1952, **23**, (9), 1024–1028).—Experiments with uniform films of Al showed that the contrast between diffraction rings and background improves considerably as the voltage is raised as long as the specimen is thin (of the order of the reciprocal of the absorption coeff.). There is not much scope for increasing the limiting thickness that can be dealt with by raising the voltage. Using the results, calculations are made for specimens which have local thick regions (e.g. pyramids). Here voltage has less effect on the contrast. (If the thick regions are sufficiently thick, they will not produce enough background to obscure the rings.) Some artifices of technique for improving contrast are reviewed.
—R. W. C.

***A Collective Description of Electron Interactions.** R. Kronig (*Phys. Rev.*, 1952, [ii], **86**, (5), 795).—A letter. In connection with recent papers by Bohm and Pines (*ibid.*, 1951, [ii], 82, 625; 1952, [ii], 85, 338; *M.A.*, **19**, 355; **20**, 413), K. points out that he and Korringa used a similar approach and derived similar conclusions previously (*Physica*, 1943, **10**, 406, 800; *M.A.*, 12, 208).—P. C. L. P.

***Scattering of Electrons from Point Singularities in Metals.** D. L. Dexter (*Phys. Rev.*, 1952, [ii], **87**, (5), 768–777).—Estimates are made of the contributions to the elect. resistance of metals from vacancies, interstitial atoms, and substitutional impurity atoms. Generally, the lattice distortion around the imperfection does not increase the scattering significantly and may be neglected. The resistance change in a monovalent metal given by one interstitial atom and one vacancy should be either equal to or slightly greater than that due to two solute atoms of the element of one larger atomic number. A discussion is given of the effects of alloying by elements of different valency and by other monovalent metals on the resistivity of Cu, Ag, and Au alloys. Arguments are given to support the view that the charge on the Cu, Ag, and Au ion is $+1e$ or nearly so, though the large effects given by Zn and Cd in Au are not understood. D.'s calculations indicate that vacancies will scatter electrons to a lesser extent than is assumed by Seitz (*Advances in Physics*, 1952, **1**, 43; *M.A.*, **20**, 170), so if most of the observed increase in resistivity on cold working at liq.-air temp. is attributed to vacancies, there would have to be many more of them; in fact a reasonable energy of vacancy formation would imply that most of the energy of cold work is stored at liq.-air temp.—P. C. L. P.

5—POWDER METALLURGY

***Room- and Elevated-Temperature Properties of Powder-Extruded Magnesium Alloys Containing Aluminium, Beryllium, and Zirconium.** (——). See col. 756.

***Properties of Molybdenum Made by Arc Casting and Powder Metallurgy.** (Bechtold and Scott). See col. 740.

***Field of Cemented Carbides Expanded by Titanium Compositions.** John C. Redmond and John W. Graham (*Metal Progress*, 1952, **61**, (4), 67–70).—The general properties of a new group of cemented carbides based on Ti and sold under the trade name of Kentanium are reviewed, and a comparison is made of the properties of these alloys with WC and the Superalloys. The Ti carbide alloys are bonded with 10–30% Ni. An U.T.S. of 80,000–100,000 lb./in.^{2} at 70° F. (21° C.) is quoted for the Kentanium alloys, as compared with 110,000–180,000 lb./in.^{2} for the Superalloys. At 2000° F. (1095° C.) the position is reversed, in that the U.T.S. quoted for Ti carbide alloys is 30,000 lb./in.^{2} as compared with 13,000 lb./in.^{2} for the Superalloys. Stress-rupture curves show that Kentanium alloys K 151A and K 152B have 125% and 170%, resp., of the stress-rupture strength of Inconel X. The oxidation attack on Kentanium alloys K 151A and K 152B in air at 1800° F. (980° C.) for 118 hr. is given as 0·00085 in. and 0·00115 in., resp. The ductility of Kentanium alloys is said to be low. The stress-rupture elongation at 1600° F. (870° C.) has seldom been $>2\%$; it is slightly greater at higher temp. It is claimed that improved powder-met. and sintering techniques have been developed so that the necessity for the machining of sintered components has been eliminated. A Ti carbide impellor and a high-temp. pressure vessel are illustrated, and other appn. are indicated.—R. P. H. F.

Powder Metallurgy 1925–1950–19??. A. J. Langhammer (*Metal Progress*, 1952, **61**, (1), 72–75).—A brief historical review of powder metallurgy is followed by a discussion of the recent developments in the manufacture of self-lubricating bearings and an account of their greatly improved performance. The saving resulting from the prodn. of a variety of parts by powder-met. methods is illustrated. Recent improvements in briquetting presses and other equipment are mentioned, and the need for metal powders of high purity and improved phys. properties, is stressed. The opinion is expressed that in the future a large increase in the use of Fe powder products is likely.—R. P. H. F.

Considering Powder Metallurgy. H. W. Greenwood (*Engineer*, 1953, **195**, (5065), 269–270).—A review of recent developments in the powder-metallurgy field, and an appraisement of the potentialities of the technique in prodn. and research.—D. K. W.

Report of [A.S.T.M.] Committee B-9 on Metal Powders and Metal-Powder Products. —— (*Amer. Soc. Test. Mat. Preprint*, 1952, (15), 7 pp.).—Tentative Specification (B222-50T) for Sintered Metal-Powder Structural Parts is recommended for adoption as standard. A proposed tentative recommended practice for Evaluating the Microstructure of Apparent Porosity in Cemented Carbides is given.—P. T. G.

Treatise on Powder Metallurgy. Vol. III.—Classified and Annotated Bibliography. (Goetzel). See col. 814.

6—CORROSION AND RELATED PHENOMENA

***The Resistance of Light Alloys to Marine Corrosion.** André Guilhaudis (*Rev. Aluminium*, 1952, (186), 85–96; (187), 127–133; (188), 175–179).—The marine testing stations of the Société Péchiney at Salin-de-Giraud and St. Jean-de-Luz are described, and arrangements for atmospheric, half-tide, and full-immersion tests are illustrated. Results are then given for the effect of 2 years' exposure under these conditions for a range of materials including 99·0%, 99·7%, and 99·99% Al, Al–1¼% Mn, and stronger alloys. Most specimens were of 1 mm. thickness. With the Al–5% Mg alloy (A-G5) it was found that cold work had no effect on corrosion-resistance, but an increase of the Cu content from 0·035 to 0·16% markedly lowered the corrosion-resistance and the elongation values. Reheating of the material to $\sim$175° C. for several hr. did not lead to intercryst. corrosion. Cold work also did not affect the corrosion-resistance of the Al–Mg–Si alloy (A-SG). Tests on Al–Cu–Mg (A-U4G) specimens showed that their mech. properties were much affected by 2 years' exposure, but the extent depended on the thickness of the material. Partial recrystn. has little effect on the Al–5% Mg alloy, but increases the severity of the corrosion at the boundary of the recrystallized zone in the Al–Cu–Mg alloy. The effect of rain and the different behaviour of the two faces of test specimens are discussed, and a comparison made between the results of half-tide and atmospheric exposure tests on the Al–Cu–Mg alloy. The Al–Zn–Mg–Cu alloy (A-Z8GU) has been tested after immersion and exposure tests up to 1 year, and whereas, in the atmosphere, there was some loss of elongation, under immersion conditions complete loss of strength occurred. Cladding of A-U4GT with pure Al and A-Z8GU with Al–3% Zn offers good protection to both alloys over the 2-year period, even when immersed. Finally, comparative test figures are given for Cu, Ni, Sn, Zn, mild steel, 18 : 8 stainless steel, and 65 : 35 brass after 2 years' exposure in these conditions.—A. W. B.

***The Effect of Climate and Atmospheric Pollution on Corrosion [of Zinc and Ferrous Materials].** J. C. Hudson and J. F. Stanners (*J. Appl. Chem.*, 1953, **3**, (2), 86–96).—Read before a joint meeting of Sections of the Society of Chemical Industry. Results of corrosion tests in which unprotected Zn and ferrous specimens are continuously exposed to different atmospheres throughout the world are presented and discussed. The degree of correlation between corrosion, both of the Zn and the ferrous samples, and S pollution of the atmosphere at British sites clearly demonstrates that the SO_2 concentration in the air is the determining factor in the rate of corrosion of these metals in this country. The corrosion rate for Zn is proportional to the S pollution, but the rate for Cu-bearing steel increases more slowly with increasing pollution, indicating that in certain enclosed situations where S pollution is very high it may be more economical to increase the thickness of unpainted steel rather than protect it with Zn.—J. R.

Report of [A.S.T.M.] Committee A-5 on Corrosion of [Galvanized] Iron and Steel. —— (*Amer. Soc. Test. Mat. Preprint*, 1952, (4), 17 pp.).—A proposed tentative specification for " 1·25-oz. Ordered Coating (Pot Yield) Zinc-Coated (Galvanized) Iron or Steel Roofing Sheets " is given, dealing with flat and corrugated sheets with a $1\cdot25$ oz./ft.^{2} Zn coating. Details are given of proposed revisions of tentative specification A93-50T for "Zn-coated (Galvanized) Iron or Steel Sheets, Coils and Cut Lengths". Small revisions are recommended to specifications A326-49T and A111-51, dealing with galvanized wire, and a number of specifications involving galvanized or terne-coated goods are reaffirmed. The activities of sub-committees are reviewed, and the report of Sub-Committee XIV on its inspection of black and galvanized sheets is given. This includes the detailed results for the exposure to the atmosphere of corrugated galvanized sheets with various weights of coating at five sites for periods up to 25 years.—P. T. G.

Trends in Corrosion Control. Herbert H. Uhlig (*Metal Progress*, 1952, 61, (3), 82–88).—Methods of corrosion prevention such as the use of paints, metallic coatings, and non-metallic coatings are discussed. Current trends in corrosion prevention such as the broader appn. of cathodic protection, corrosion-resistant metals and alloys, and the general use of inhibitors, paints, ceramics, and plastics designed for optimum protection at ordinary and elevated temp. are given.—R. P. H. F.

Theory of Overvoltage and the Mechanism of Corrosion. R. Audubert (*J. Chim. Phys.*, 1952, 49, (7/8), C97–C103; discussion, C103–C104).—General principles of the modern theory are briefly reviewed and applied to discuss the theoretical fundamentals of the process of corrosion. Theoretical results have been compared with experimental results relating to Mg, Zn, Cd, Al, Fe, and Hg in acid soln. of various concentrations, and confirm one another. More especially, A. considers that the linear relation deduced between the electrode potential and the activity of the active ions has been verified experimentally.—J. S. G. T.

Liquid Sodium: A Non-Corrosive Coolant. R. F. Koenig and S. R. Vandenberg (*Metal Progress*, 1952, 61, (3), 71–75).—See *M.A.*, 20, 265.—R. P. H. F.

***Final Report on Metallurgical Investigation of Materials Subjected to Liquid Lead–Bismuth Alloy Environment.** (Grassi, Bainbridge, and Harman). See col. 744.

7—PROTECTION

(Other than by Electrodeposition)

***Priming Paints for Light Alloys.** J. G. Rigg and E. W. Skerrey (*J. Inst. Metals*, 1952–53, 81, (10), 481–489).—The results obtained from the exposure of light alloy specimens for 6 months in rural, indust., and marine atmospheres, with various primers under Al top coats, have been published previously, and the present paper gives the further information obtained on continuation of the tests for 3½ years. The results confirmed earlier indications. Zn chromate and Zn tetroxychromate primers were superior in protective value to Fe oxide primer, although the latter provided satisfactory protection, especially to Al in the less severe environments. Red Pb primer was definitely harmful on light alloys, and especially on Mg in corrosive environments. In these tests both types of chromate primer were found to be slightly preferable to red Pb on mild steel. Zn chromate and Zn tetroxychromate pigments are preferred for primers for composite structures of steel and light alloys in severe exposure conditions, while Fe oxide is adequate for milder conditions.—Authors.

Aluminium Coatings Applied to Steel by Many Methods. E. M. Smith (*Materials and Methods*, 1952, 36, (6), 105–108).—The well-known methods of spraying, calorizing, hot-dipping, cladding, electroplating, and vapour-plating for coating steel with Al are reviewed. It is claimed that although these methods are not new the continued improvement of the bond and the appearance of the coating have resulted from improved methods of prodn. Spraying is said to be the easiest method of appn. Calorizing is specially adaptable to large bulky steel articles. The main difficulties of producing hot-dipped Al coatings are given, and it is pointed out that this is the only available method for the Al coating of steel wire and strip. The cladding of steel with Al is said to be specially adaptable to the high-speed prodn. of sheet by rolling. The electroplating and vapour-plating of steel with Al is discussed and appn. of each of the methods is indicated.—R. P. H. F.

Steel Protection by Sprayed Aluminium. —— (*Engineering*, 1953, 175, (4540), 158).—A brief report on the corrosion resistance exhibited by an Al sprayed steel building erected in 1937, in a highly corrosive steel works atmosphere. Signs of rusting are now apparent, and 15 years is thought to be the max. life that can be reasonably expected from the coating under these particular conditions.—D. K. W.

Aluminized Coatings [on Steel]. M. G. Whitfield and V. Sheshunoff (*Machine Design*, 1952, 24, (5), 139–140).—The possibilities of the aluminizing processes for the protection of Fe and steel parts against corrosion and also to give them heat-resistance are considered. The various processing methods are outlined, and it is shown that considerable advantages can result from the use of Al alloys, particularly the Al–Si type, in place of pure Al. Details of costs are given, and information is presented on the properties and finish of treated parts. The appn. of aluminized parts are discussed. The Al coating in its polished condition resembles Cr-plated objects.—D. M. L.

High-Temperature Oxidation Prevented by Sprayed Aluminium. —— (*Electroplating*, 1953, 6, (2), 74).—A note on the aluminizing process for the protection of steel, and sometimes other metals, against high-temp. oxidation. After Al spraying (0·006–0·008 in.) the Al is alloyed with the steel by any of 3 methods, 2 of which involve a furnace treatment.—H. A. H.

Tungsten Carbide Thin Coatings Have Many Applications. —— (*Canad. Metals*, 1952, 15, (11), 80–82, 84).—The appn. of flame-plated WC coatings are reviewed. These coatings are claimed to be harder than Cr plate, and to last 15–20 times longer during abrasion tests. See also *M.A.*, 20, 497. —W. A. M. P.

***An Investigation of the Method of Inhibiting the Formation of Blisters on Galvanized Sheet.** Hiroshi Sawamura and Taiji Ogino (*Suiyokwai-Shi*, 1952, 12, (3), 123–126).—[In Japanese]. Various experiments are reported on the behaviour of H retained by thin sheets during acid washing and hot galvanizing. Since the number of sheet samples was small, general conclusions could not be drawn from the results. —Author.

A Coating Alloy for High-Temperature Use. —— (*Engineer*, 1953, 195, (5065), 274).—A brief note giving the principal properties of a Ni-base alloy, known as C26, contg. Cr, Al, and Mo developed primarily for the facing of I.C. engine valve seats. The alloy resists oxidation at temp. up to 1250° C, and Pb oxybromide attack at temp. up to 800° C. —D. K. W.

Ceramic Coatings [for High-Temperature Parts]. John V. Long (*Machine Design*, 1952, 24, (5), 122–126).—The necessity to develop substitutes for the expensive heat-resistant alloys has resulted in the use of ceramic parts as well as ceramic coatings for normal metal parts. L. outlines the development of the coatings, particularly the Solaramic process. The advantages of ceramic coatings are listed, attention being directed to the influence of these on the heat-flow characteristics, fatigue strength, service life, and corrosion- and oxidation-resistance. Design requirements for coated parts are discussed, and accounts are given of the phys. characteristics of the coatings, processing methods, and possible future developments of low-alloy coatings.—D. M. L.

8 — ELECTRODEPOSITION

Chromium-Plated Aluminium Cylinder Barrels. (Meyer-Rässler). See col. 804.

Speedy [Copper] Plating of Small-Diameter Steel Tubing. —— (*Iron Age*, 1952, **170**, (19), 174–175).—A process is described by which tubes $\frac{5}{8}$–$\frac{3}{16}$ in. in dia. are coated with 0·0004 in. of Cu at 40–150 ft./min. in a single pass through a special bath contg. 7 oz. Cu cyanide and 35–40 oz. $NaCO_3$/U.S. gal. at 200°–205° F. (93°–97° C.). Current of 2500–4000 amp. at 10–15 V. is applied at a c.d. of 10–20 amp./in.^{2}. The tubes are fed continuously, the tail end of one being butt-welded to the lead end of the next, by grooved Cu guide-rolls through which the current is passed. Brief details of Zn/Cu/Cr coatings on tubes are also given.—S. R. W.

White Brass Plating: One Solution to the Nickel Freeze. Webster B. Knight (*Metal Progress*, 1952, **61**, (3), 61–64).—Five alternatives to the conventional Cu/Ni/Cr plate are described: (1) the Cr plating of Type-430 stainless steel; (2) a heavy Cu plate, followed by a flash of Ni and Cr + lacquer; (3) a heavy Cu plate, followed by a flash of Cr + lacquer; (4) a bright Zn plate, chromate dip + lacquer; and (5) white brass plating, followed by a Cr flash. The advantages and disadvantages of each process are enumerated. The factors controlling the successful appn. of white brass plating are claimed to be: super-purity Zn (99·99%) and electrolytic Cu for the prodn. of plating electrodes; and anodes of 80 : 20 Zn–Cu, used in a soln. of Zn cyanide, Na cyanide, and NaOH (8 oz./U.S. gal. each) and 2 oz./U.S. gal. of Cu cyanide, at room temp. at a c.d. of 28 amp./ft.^{2}, with the addn. of brighteners such as Na molybdate. The Cu–Zn equilibrium diagram is illustrated, and the limits of the ε phase illustrated with special ref. to the 80 : 20 Zn–Cu alloy which consists entirely of ε phase at room temp. The metallurgy of anodes is described, and the results of salt-spray tests on 0·0003-in.-thick deposits of white brass plated on steel radiator grills after 24-, 36-, and 48-hr. periods, are reviewed. It is claimed that the prodn. of crack-free Co deposits in barrel-plating has been accomplished, and that the possibility of producing crack-free Co deposits in still tanks is being investigated.
—R. P. H. F.

***The Determination of Total Sulphate in Nickel-Plating Solutions, Using Disodium Ethylenediaminetetra-acetate.** K. E. Langford (*Electroplating*, 1953, 6, (2), 41–42, 58).—A volumetric method is described for the detn. of total sulphate in Ni-plating soln. Although not as accurate as grav. procedures, it is useful for routine checks, &c. 1 ml. of the Ni soln. is diluted to 100 ml., raised to the boil and 20 ml. of $N/5$-$BaCl_2$–$N/10$-$MgCl_2$ added. After mixing and cooling, 2 g. NH_4Cl, 2 g. KCN, 10 ml. NH_4OH, and 6 spots of indicator (0·5 g. Erichrome Black T and 4·5 g. hydroxylamine hydrochloride in 100 ml. alcohol or indust. spirit) are added. Titration is then performed with $N/5$-di-Na ethylenediamine tetra-acetate to the blue end-point, allowing the precipitated $BaSO_4$ to settle for final confirmation (X). If Y ml. is the "blank" on 20 ml. of the $N/5$-$BaCl_2$–$N/10$-$MgCl_2$ soln., then $Y - X =$ ml. of $N/5$-$BaCl_2$ equivalent to the SO_4. (1 ml. $N/5$-$BaCl_2 = 0{\cdot}02809$ g. $NiSO_4.7H_2O$ or 0·02629 g. $NiSO_4.6H_2O$.
—H. A. H.

***Alternating-Current Electrolysis. II.—Silver Nitrate Solutions.** A. N. Kappanna and K. M. Joshi (*J. Indian Chem. Soc.*, 1952, **29**, (4), 211–216).—An account of some experimental work on the electrolysis of $AgNO_3$ soln. with symmetrical A.C., using Pt electrodes in the frequency range 3–50 c./s. Ag is deposited on both electrodes, but the current efficiency is very low, varying between 0 and 5%, and is different at the two different electrodes. The current efficiency decreases with increase in frequency at the same c.d.; it increases at the same frequency with increase in c.d. As the electrolysis proceeds, the current efficiency decreases. It is higher in dil. soln. than in conc. soln. Some explanations are offered for these phenomena.—W. A. M. P.

***Electrochemistry of Fluoride Solutions. III.—Electrodeposition of Zinc from Fluoride Solutions.** Erach R. Talaty (*J. Indian Chem. Soc.*, 1952, 29, (3), 147–156).—Cf. *ibid.*, 1951, 28, 523; *M.A.*, **20**, 356. A detailed study of the electrolysis of acid ZnF_2 soln. has been made, and experimental data are given on (*a*) decompn. potentials, (*b*) cathode and anode discharge potentials on polished Pt electrodes, and (*c*) the electrodeposition of Zn under various conditions. The Zn deposits on Fe cathodes are adherent, but are dark and porous. Good deposits can only be obtained with the aid of addn. agents, such as thiourea, gelatine, and glucose with $(NH_4)_2CO_3$. It is concluded that although the max. permissible c.d. for fluoride baths is not high, the deposits obtained from baths contg. thiourea compare favourably with the best obtained from acid sulphate baths.—W. A. M. P.

***Triangular Logarithmic Net for the Calculation of Plating Thicknesses.** D. R. Curry (*Electroplating*, 1952, **5**, (12), 397–399).—A simple system is described whereby the weights of various metals electrodeposited on different surface areas, as obtained, for example, from the stripping of plated articles, can be rapidly and simply converted to thickness (thousandths of an in.).—H. A. H.

[Plating] Process Control. —— (*Product Finishing* (*Lond.*), 1953, **6**, (1), 40–44).—Recommendations are made regarding the min. sci. apparatus required for equipping an electroplating laboratory.—H. A. H.

9 — ELECTROMETALLURGY AND ELECTROCHEMISTRY

(Other than Electrodeposition.)

Remarks Regarding the Theory of the Production of Aluminium by Electrolysis. R. Piontelli (*J. Chim. Phys.*, 1952, **49**, (6), C29–C33; errata, (7/8), C147).—An electrochem. and a thermodynamic discussion of the customary electrolytic process for producing Al leads to the conclusion that the cathodic sepn. of Al is a direct process, i.e. the electrochem. process involved consists of the direct reduction of the constituent of the electrolyte contg. Al. The electrolytic deposition of Na, on the other hand, is considered to be a "parasitic" process, attributable more especially to anomalies of compn. of the cathode layer, or operation of the vat. 8 ref.—J. S. G. T.

***Cathodic Deposits, Consisting of Monatomic Layers of Bismuth, upon Platinum and Gold.** A. Coche, J. Danon, and M. El. Guébély (*J. Chim. Phys.*, 1952, **49**, (6), 363–366).—The partition of micro-quantities of Bi between an electrolytic soln. contg. Bi ions and a Au cathode, for electrolytes of concentration $10^{-12}N$ to $3 \times 10^{-7}N$ is found, experimentally, to be in accordance with two Freundlich isotherms with resp. exponents 0·80 and 1·3. The critical potential for the deposit of Bi upon Pt varies with the concentration of the electrolyte in accordance with Nernst's electrochem. equation. Herzfeld's equation is obeyed only qual. The partition of micro-quantities of Bi between soln. and electrode in the case of a Pt electrode is in accord with a single Freundlich isotherm with exponent 0·95. 10 ref.—J. S. G. T.

***Electronic- and Solvent-Transfer in Aqueous Solutions of Bi- and Tri-Valent Chromium.** M. Haïssinsky (*J. Chim. Phys.*, 1952, **49**, (7/8), C133–C135; discussion, C135–C136).—Electronic exchange between Cr^{2+} and Cr^{3+} ions in HCl soln. is complete in the few min. necessary for the chromatographic separation of the bi- and tri-valent ions; the time of semi-exchange in H_2SO_4 soln. is of the order of 3–5 min. These velocities of exchange are considerably higher than those measured by other experimenters for the velocity of exchange between co-ordination H_2O of Cr^{3+} and the solvent.

The results are interpreted in terms of a mechanism of electronic transfer by the formation of complex, ephemeral ionic associations between cations and anions.—J. S. G. T.

***The Electrolytic Precipitation of Metal Powders: Significance of Diffusion Processes at the Cathode.** N. Ibl and G. Trümpler (*Helv. Chim. Acta.*, 1952, **35**, (1), 363–374).—[In German]. A study has been made of the phenomena which accompany the electrodepn. of Cu powders from aq. soln. contg. $CuSO_4$ 0·3–0·1 mole/l. The results are discussed, and correlated with those of other workers on the depn. of Zn and Ag powders. Powder formation takes place after certain current limits are attained. The time, τ, (in sec.) which elapses before powder begins to form corresponds to the "transition time" calculated from the diffusion laws postulated by Sand, and, if i = c.d. (in m. amp./cm.^{2}), then $i\sqrt{\tau}$ = a const. which decreases with increasing dilution of the electrolyte. The min. c.d. necessary for powder prodn. is discussed, as well as the conditions which exist at vertical electrodes.

—E. N.

***Kinetics of the Reaction Metallic Copper/Copper Ion.** E. Quagliozzi and A. Rescigno (*Helv. Chim. Acta*, 1952, **35**, (4), 1227–1330).—[In German]. A Cu foil, irradiated so as to contain the radioactive isotope ^{64}Cu was immersed in an aq. soln. of pure $CuSO_4$. The exchange of Cu between the foil and soln. was studied, and found to take place according to the reaction $Cu \rightleftharpoons Cu^+ \rightleftharpoons Cu^{2+}$, the equilibrium const. of which have been determined.—E. N.

***Electron-Transfer Reactions at Lead Electrodes [of Storage Batteries].** H. R. Thirsk and W. F. K. Wynne-Jones (*J. Chim. Phys.*, 1952, **49**, (1), C131–C133; discussion, C133–C134).—[In English]. Theories relating to reactions occurring at the Pb plates of storage batteries are briefly reviewed, and it is considered that it is difficult to reconcile accepted theory with certain chem. and electro-chem. observations, and an alternative mechanism, conforming to the overall reaction of the "double sulphation" theory is proposed. During the formation process, it is suggested that conversion of $PbSO_4$ begins near the $Pb/PbSO_4$ interface and continues through the deposit, without any further attack on the Pb, in the absence of forming agents. When forming agents are present, attack continues on the Pb surface, maintaining a layer of high $PbSO_4$ concentration near the Pb surface. When the PbO_2 layer reaches the Pb surface, further OH' or SO_4'' discharge on the PbO_2 grains occurs, and electronic conduction takes place through the combined $Pb–PbO_2$ conducting path. The final stage is the discharge of anions with the prodn. of O at high overvoltage at the PbO_2 surface. In the reduction process, it is suggested that the solid PbO_2 layer with its high free-electron content reacts at the PbO_2/soln. interface by direct electron transfer in the solid state. Subsequently, the Pb^{2+} ion in the solid reacts with the SO_4 of the soln. 11 ref.

—J. S. G. T.

***Passivation of Lead in Sulphuric Acid, and Processes Occurring in the Positive Plate of the Lead Accumulator.** W. Feitknecht and A. Gaumann (*J. Chim. Phys.*, 1952, **49**, (1), C135–C144; discussion, C144).—The anodic passivation of Pb in H_2SO_4 was studied by measuring, at const. current, the change of voltage of a storage cell, the resistance of the cell, and the anode potential. Formation of the sulphate layer and its transformation into PbO_2 were studied by the electron microscope. Passivation is attributed to an increase of activation polarization, represented by the equation $Pb \rightarrow Pb^{\cdot\cdot} + 2e$, after formation of a layer of $PbSO_4$ fixed at points of the Pb surface, so that the reaction $Pb + 2H_2O \rightarrow PbO_2 + 4e + 4H^{\cdot}$ can occur, with the prodn. of a thin layer of PbO_2, permeable only to electrons. The transformation of $PbSO_4$ into PbO_2 takes place in a thin layer of electrolyte in accordance with the equations:

$$\left.\begin{array}{l}\text{Surface } PbO_2: 2OH' \rightarrow 2e + 2OH \\ \qquad\qquad PbSO_4 \rightarrow SO_4'' + Pb^{\cdot\cdot}\end{array}\right\} Pb(OH)_4^{\cdot\cdot} \rightarrow PbO_2 + 2H^{\cdot}.$$

Pb anodes lose their passivity when, in accordance with the reaction $PbO_2 + 4H^{\cdot} + 2e \rightarrow Pb^{\cdot\cdot} + 2H_2O$, the primary layer of PbO_2 is destroyed.—J. S. G. T.

Electrolytic Manganese Acceptance Grows. C. L. Mantell (*Iron Age*, 1952, **170**, (12), 168–172).—Electrolytic Mn having high purity (99·97%) is replacing Ni and is opening up a new field of Mn-base alloys. The chem. compn., the properties, and the allotropy of Mn are given in tabular form, and a flow-sheet describes briefly the method of manufacture. Negligible S, P, and C contents, together with freedom from Si, are of special value in steel prodn. 11 ref.—S. R. W.

***The Production of Silicon–Titanium Alloys by Igneous Electrolysis.** Maurico Dodero (*J. Chim. Phys.*, 1952, **49**, (6), C11–C14; discussion, C14).—The type of electrolysis discussed is illustrated by the electrolysis of a fused mixture of Na silicate and NaF; Na, the primary product of the electrolysis is seen burning at the cathode with liberation of Si. The course of the electrolysis of (1) fused alkali and alkaline-earth silicates mixed with TiO_2, and (2) K fluosilicate mixed with TiO_2, and the resulting products are briefly discussed. Hitherto, the electrolysis of fused baths contg. silicates or fluosilicates mixed with TiO_2 has led to the prodn. of free Si and silicide. The possibility of producing the Si–Ti eutectic contg. 8·5% Si by igneous electrolysis, by electrolysis of mixtures of fluosilicate and fluotitanate of K, is suggested.

—J. S. G. T.

***Electrolytic Deposits from Very Dilute Solutions, and Heterogeneity of the Surface of the Electrodes.** J. Danon and M. Haïssinsky (*J. Chim. Phys.*, 1952, **49**, (1), C123–C130; discussion, C130).—The critical potential for the cathodic deposition of Bi upon a polarized Au cathode in very dil. HNO_3, is found to vary with the concentration in accordance with Nernst's electrochem. equation for concentrations down to $3 \times 10^{-16}\,N$. Without previous polarization, the deposition, at this concentration, is characterized by the existence of a sub-voltage. Herzfeld's equation is not obeyed, and the qual. validity of the equation is attributed to an exponential distribution of active centres upon the electrode surface. The distribution of Bi between a nitric soln. of Bi^{3+} ions of concentration 10^{-12}–$8 \times 10^{-7}\,N$ and a Ag electrode, at potentials equidistant from the critical potentials, follows two Freundlich isotherms, corresponding, in the case of very dilute concentrations, to two values of the exponent resp. $>$ and < 1. It follows that, with only slight coating of the electrode surface, it is the heterogeneity of the coating, together with an exponential distribution of the energies of absorption, which determine details of the deposition; with thicker deposits, attraction between the deposited Bi atoms comes into play.—J. S. G. T.

***Oscillographic Polarographic Waves for the Reversible Deposition of Metals on Solid Electrodes.** Talivaldis Berzins and Paul Delahay (*J. Amer. Chem. Soc.*, 1953, **75**, (3), 555–559).—An equation is derived for oscillographic polarographic waves corresponding to the reversible deposition of an insoluble substance. Theoretical results are compared with experimental data, and discrepancies are accounted for by variations of the activity of the deposit. Experimental and calculated waves for the deposition of Cd on Pt are compared.

—J. R.

Phenomena at Electrodes in Electrolysis. E. Darmois (*J. Chim. Phys.*, 1952, **49**, (2), C151–C153; discussion, C153).—The initial process in electrolysis is the formation of a layer of adsorbed ions at the electrodes, the so-called Stern layer, and this is mainly responsible for the prodn. of electrode potentials. Sutra has arranged electrolytic ions in 3 categories dependent upon their resp. crystal radii (*ibid.*, 1946, **43**, 189). Characteristics of the different classes of ions are discussed, with a brief ref. to the potential necessary to effect electrolytic polishing of metals; in this process dissoln. of the metal begins at certain "active" points, and the adsorption energy of the process decreases in proportion as the surface becomes plane. 5 ref.—J. S. G. T.

***Variation of Reaction Velocities, at an Electrode, with the Solvent.** J. O'M. Bockris (*J. Chim. Phys.*, 1952, **49**, (7/8), C41–C45; discussion, C45–C46).—The kinetics of electrodeposition and the effect of the nature of the electrolyte upon the rate of deposition become important in the case of the electrodeposition of metals which are deposited badly from aq. soln. Electrodeposition upon cathodes of Hg, Ni, Cu, Sn, Bi, W, Au, and Ta was studied for aq. soln. of HCl and H_2SO_4, and in a few cases NH_4Cl, with and without addn. of CH_3OH, glycol, H.COOH, $(C_2H_5)_2O$, and C_2H_5OH. Deposition upon Hg and Cu is very little different whether from H_2O or ether. Considerably more work is necessary before knowledge of the effect of the solvent upon electrodeposition can be regarded as precise. 42 ref.—J. S. G. T.

†Aspects of the Theory of Electrode Processes with Electron Transition. R. Piontelli (*J. Chim. Phys.*, 1952, **49**, (1), C53–C65; discussion, C65).—The thermodynamics of electrode voltages in redox electrolytic systems is discussed in considerable detail. 10 ref.—J. S. G. T.

***Kinetics of the Primary Reactions in Electrolysis, Determined by Cathodic Oscillography Utilizing the Technique of Polarography.** (Mme) M. Fournier (*J. Chim. Phys.*, 1952, **49**, (2), C183–C192; discussion, C192–C193).—The effect of an A.C. upon polarographic records was studied by means of voltage/time records derived from cathodic oscillographic observation and by determining the effect of an A.C., superposed on a const. D.C., upon the current intensity/voltage diagrams derived from polarographic studies. The various ions studied include Tl, Cu, Cd, Pb, Zn, Mn, Fe, Co, and Ni.—J. S. G. T.

Some Examples of Perturbations Brought into Electrolysis by Supplementary Factors. Pierre Jolibois (*J. Chim. Phys.*, 1952, **49**, (7/8), C106–C107).—Attention is directed to perturbations that can occur in electrolysis owing to variation of *d* and compn., illustrated by the progress of the electrolysis of a soln. contg. H_2SO_4, NaOH, and Na_2SO_4, and by the presence of H_2SO_4 in the cathode vessel of an electrolyte system comprising an anode vessel and a cathode vessel, both contg. $CuSO_4$, connected by a capillary tube.—J. S. G. T.

***Overvoltage and the Mechanism of Electrolysis of Oxidation–Reduction Systems.** René Audubert (*J. Chim. Phys.*, 1952, **49**, (1), C106–C109; discussion, C109).—A comparison of experimental results with deductions from the modern theory of overvoltage, applied to electro-reduction and electro-oxidation processes, e.g. the $Fe^{3+} \rightarrow Fe^{2+}$ reduction process, is used to give precision to the processes involved in the mechanism of electrolysis. The deductions are applicable only to very strongly acid or very strongly alkaline soln.; in other cases it is probable that the different effects discussed are superposed.—J. S. G. T.

***†(I) Theoretical Study of Overvoltage in Oxidation–Reduction Systems. (II) Experimental Study of Overvoltage in Some Oxidation–Reduction Systems. (III) Interpretation of Measurements of Overvoltage in Oxidation–Reduction Systems.** Eugène Lewartowicz (*J. Chim. Phys.*, 1952, **49**, (10), 557–563; 564–572; 573–581).—[I.—] Audubert's theory of overvoltage (*ibid.*, 1924, **21**, 351), in which the theory of probability is applied to calculate values of electrode potentials, is applied to oxidation–reduction electrochem. processes, and equations relating c.d. to electrode potentials are developed. Overvoltage, taking diffusion into account, and the significance of activation energies and transfer coeff. are discussed. 57 ref. [II.—] Apparatus used and experimental conditions necessary to overcome the numerous difficulties met with in the study of oxidation–reduction systems are discussed. Experimental results relating, *inter alia*, to overvoltage in the oxidation–reduction systems Fe^{2+}–Fe^{3+} and Ce^{3+}–Ce^{4+} are given. The roles played by compn. of the soln., treatment of electrodes, mech. agitation, and temp. are discussed. 7 ref. [III.—] Results obtained in [II.] are used: (1) to verify the formulæ in Audubert's theory; (2) to determine values of transfer coeff., activation energies, and exchange currents; (3) to show the importance of diffusion; and (4) to show that except in the case of the oxidation of $Ce^{3+} \rightarrow Ce^{4+}$, oxidation and reduction are effected by direct electronic exchanges. 11 ref.—J. S. G. T.

Hydrogen Overvoltage. Geneviève Sutra (*J. Chim. Phys.*, 1952, **49**, (1), C66–C68; discussion, C68–C69).—A theory of H overvoltage in which it is assumed that ions are absorbed at the surface of the cathode together with a number of H_2O mol., and that H is formed within the metal is developed. H overvoltages at electrodes of Pt, Au, Ag, Ni, W, Mo, Sn, graphite, Ta, and Hg are tabulated.—J. S. G. T.

***Thermodynamics and Electrochemical Kinetics of Hydrogen Overvoltage.** Pierre van Rysselberghe (*J. Chim. Phys.*, 1952, **49**, (1), C47–C51; discussion, C51–C52).—The relation between H overvoltage and c.d. is discussed in detail. A thermodynamic activity coeff., relating to the activated complex, is explicitly introduced into the theory, and the activated layer and electrode are assimilated to an atomic H reversible electrode.—J. S. G. T.

***The Significance of Dual Mechanisms in Hydrogen Overvoltage.** Roger Parsons (*J. Chim. Phys.*, 1952, **49**, (1), C82–C87; discussion, C87).—[In English]. It is suggested that the term "dual mechanism" should be restricted to the occurrence of two consecutive or alternative reactions, having activated complexes of equal or nearly equal standard free energy with respect to the free energy of the initial state. Possible types of behaviour of electrodes evolving H are discussed, and predictions of the effect of a catalytic poison, e.g. As_2O_3, upon overvoltage at a Pt electrode agree with observations. 9 ref.—J. S. G. T.

***Adsorption and Hydrogen Overvoltage.** P. J. Hillson (*J. Chim. Phys.*, 1952, **49**, (1), C88–C94; discussion, C94–C96).—The intensity of adsorption of capillary-active substances, e.g. caproic alcohol, hexylamine, and toluene sulphonic acid, on electrodes of Ni, W, Ag, Ta, and Au, at which H was evolved, was studied by determining their effects upon the overvoltage and capacity of the electrodes in HCl soln. The metals were found to differ markedly in respect of their behaviour towards the capillary-active substances, and these differences are correlated with the energies of adsorption of H and of O by the resp. metals and with the H overvoltage in pure soln.—J. S. G. T.

---

11 — ANALYSIS

***The Determination of Aluminium and Zinc After Their Chromatographic Separation from Tin–Lead Alloys.** J. R. Bishop and H. Liebmann (*Analyst*, 1953, **78**, (923), 117–122).—2 g. solder in the form of fine filings or drillings is dissolved in HBr + Br_2. $HClO_4$ is added to the soln., which is then evaporated to fumes of $HClO_4$ to volatilize Sn. Pb is removed by adding HCl and filtering off $PbCl_2$, the filtrate being evaporated to fumes of $HClO_4$ and again taken up in a smaller quantity of HCl to precipitate more $PbCl_2$. The soln. is then transferred to a cellulose pulp chromatographic column and Zn eluted with a mixture of const.-boiling HCl 4 and *n*-butanol 96 parts. The column is then eluted with a mixture of const.-boiling HCl 4 and methyl ethyl ketone 96 parts to remove all metals except Al and Ni, which are recovered by elution with dil. HCl. Zn and Al are determined in the respective soln. by normal polarographic methods.—F. M. L.

***Spectrophotometric Determination of Aluminium in Thorium: Extraction of Aluminium with 8-Quinolinol in Chloroform.** D. W. Margerum, Wilbur Sprain, and Charles V. Banks (*Analyt. Chem.*, 1953, **25**, (2), 249–252).—Al is determined spectrophotometrically in Th by direct extraction into a soln. of 8-hydroxyquinoline in chloroform. Extraction of Th is prevented by using either 4-sulphobenzenearsonic acid or conc. acetate buffer. In the latter case allowance must be made for the acetic acid dissolved in the chloroform phase when making the spectrophotometric measurements. —F. M. L.

***The Determination of Aluminium by the Fluorophotometric Method.** J. B. Zimmerman (*U.S. Atomic Energy Commission Publ.*, 1952, (**NP-4182**), 11 pp.).—A method is described for the detn. of Al by measurement of the fluorescence of the 8-hydroxyquinolate. The complex is precipitated from a soln. buffered at *p*H 1·6. The precipitate is extracted with $CHCl_3$ and the fluorescence of this soln. is measured under exposure to ultra-violet light of wave-length 560 mμ. Interfering elements such as Fe, Mn, or Cr are first removed from the soln. either by sepn. with the Hg cathode or pptn. with NaOH. The intensity of fluorescence is linear with respect to Al content for the range 1–50 γ Al/30 ml. soln. Comparison of experimental values obtained by normal and fluorometric methods is given.—C. E. A.

***Separation of Antimony by Solvent Extraction.** Charles E. White and Harry J. Rose (*Analyt. Chem.*, 1953, **25**, (2), 351–353).—Sb is oxidized to the pentavalent condition with ceric sulphate, complexed with a mixture of oxalic and citric acids, and then extracted into ethyl acetate.—F. M. L.

***Photometric Determination of Bismuth in Lead and Its Alloys by Means of Thiourea.** Heinz Pohl (*Angew. Chem.*, 1952, **64**, (22), 608–610).—P. describes a method for the photometric detn. of Bi in Pb and its alloys with Sb. The major part of the Sb is first separated and removed with the Pb, the remainder being bound as a complex by means of tartaric acid and NaF. Bi contents of 0·5–0·001% can be determined with an accuracy of ±3%, and it is claimed that the time taken per detn. is approx. 60 min.—W. F. H.

***Extension of Sensitivity of Polarographic Analysis with Rotating Amalgam Electrodes [for Determination of Cadmium and Cobalt Ions].** W. Donald Cooke (*Analyt. Chem.*, 1953, **25**, (2), 215–218).—An amalgamated Ag wire rotated at high speed has been used to increase the sensitivity for the detn. of Cd and Co^{III} ions.—F. M. L.

***5 : 6-Benzoquinaldinic Acid as an Analytical Reagent. I.—Estimation of Copper.** Anil Kumar Majumdar and Ajit Kumar Mallick (*J. Indian Chem. Soc.*, 1952, **29**, (4), 255–262).—5 : 6-benzoquinaldinic acid completely precipitates Cu between *p*H 0·82 and 9·40, and has been used for the estn. of Cu and its sepn. from Mg, Ca, Sr, Ba, phosphate, arsenate, arsenite, citrate, and tartrate. The Cu salt may be dried either at 110° C. as $Cu(C_{14}H_8NO_2)_2.15H_2O$ or at 180° C. as $Cu(C_{14}H_8NO_2)_2$.—W. A. M. P.

***Determination of Milligram and Sub-Milligram Quantities of Copper by the Iodate Titration of Cuprous Thiocyanate.** Krisna Tantranon and B. B. Cunningham (*Analyt. Chem.*, 1953, **25**, (1), 194–195).—Small amounts of Cu are precipitated as CuCNS, which is then suspended in conc. HCl and titrated with KIO_3, using chloroform to detect when all free I has been removed and the end-point, therefore, reached.
—F. M. L.

Analytical Methods for Germanium. Horatio H. Krause and Otto H. Johnson (*Analyt. Chem.*, 1953, **25**, (1), 134–138).—A review, with 111 ref.—F. M. L.

***Determining Low Concentrations of Hafnium in Zirconium: A Spectrographic Method.** D. M. Mortimore and L. A. Noble (*Analyt. Chem.*, 1953, **25**, (2), 296–298).—0·003–0·4% Hf in Zr is determined by converting the sample to oxide, mixing it with a buffer comprising a 1 : 1 mixture of graphite and BaF_2 to steady the arc and enhance the Hf spectrum, and then arcing at 30 amp. and 230 V. The spectra are recorded in the 3rd-order ultra-violet, using a filter to suppress the 2nd-order (CN) band.—F. M. L.

***Determination of Hydrogen in Magnesium, Lithium, and Magnesium–Lithium Alloys.** M. W. Mallett, A. F. Gerds, and C. B. Griffith (*Analyt. Chem.*, 1953, **25**, (1), 116–119).—H has been satisfactorily determined in Mg and Mg–Li alloys by the Sn-fusion method. If a sample could be adequately protected from reaction with atmospheric moisture during prepn. for analysis, this method could also be applied to Li. The apparent H content of Mg–Li alloys, and especially of Li, increases when the metal is exposed to air. Satisfactory results for Mg–16% Li alloys were obtained by sealing the metal in a welded steel capsule and extracting H at 800° C. The method, however, is more complicated and time-consuming than the Sn-fusion method.—F. M. L.

***Spectrophotometric Titrations with Ethylenediaminetetraacetic Acid : Determination of Iron, Copper, and Nickel.** Philip B. Sweetser and Clark E. Bricker (*Analyt. Chem.*, 1953, **25**, (2), 253–255).—The spectrophotometer is used to determine the end-point in the titration of Fe^{III}, Cu, and Ni with a standard soln. of disodium dihydrogen ethylenediaminetetra-acetate.—F. M. L.

***Determination of Osmium: Application of Polarographic Kinetic Hydrogen Peroxide Current.** I. M. Kolthoff and E. P. Parry (*Analyt. Chem.*, 1953, **25**, (1), 188–189).—The catalytic reduction current of H_2O_2 during the reduction of OsO_4 is used to determine small amounts of Os.—F. M. L.

***Rapid [Photometric] Determination of Silicon in Copper and Copper Alloys.** Masao Adachi, Hirozō Kimura, and Nobuyoshi Aoki (*Bull. Eng. Research Inst. Kyoto Univ.*, 1952, **2**, (Sept.), 51–54).—[In Japanese, with tables and graphs in English]. The reaction to form a yellow heteropoly acid between soluble silicic acid and molybdate ion, has been applied to the photometric analysis of Si in Cu and Cu alloys. Less than 5% Si can be determined rapidly by this procedure; 0·05% P and 1% Fe and As do not interfere. 8 ref.—AUTHORS.

***Photometric Determination of Silicon in Ferrous, Ferromagnetic, Nickel, and Copper Alloys: A Molybdenum Blue Method.** C. L. Luke (*Analyt. Chem.*, 1953, **25**, (1), 148–151).—The sample is dissolved in a mixture of HCl and HNO_3, HNO_3 is destroyed by boiling with formic acid, and all interfering metals are removed by extraction into a soln. of Na diethyldithiocarbamate in chloroform. Si is then determined in the aq. phase by the usual photometric Mo blue method.—F. M. L.

***Spectrographic Determination of Small Quantities of Silver [in Lead].** W. D. Treadwell, E. Amrein, and A. E. R. Bodmer. (*Helv. Chim. Acta*, 1952, **35**, (3), 765–770).—[In German]. The spectrographic detn. of Ag in Pb–Ag alloys contg. 0·001–1·6 wt.-% Ag is described, using a Feussner excitation circuit, and the Ag lines 3280·7 and 3382·9 Å. in comparison with the Pb lines 3572·7 and 3639·6 Å. In the alloy range 0·1–1·6% Ag, the Ag line intensities are found to be approx. twice as great in freshly prepared alloys as in alloys aged for 6 weeks at room temp. Ageing causes pptn. of the Ag at the Pb grain boundaries; the Ag crystallites formed are much greater in dia. and have a lower vapour pressure than those occurring in freshly prepared alloys. The sensitivity of the spectrographic detn. is so great that the transition from homogeneous solid soln. to the heterogeneous condition can be followed by the decrease in intensity of the Ag lines. The alterations in the hardness of the alloys, which accompany the ageing, are discussed.—E. N.

Detection and Determination of Thallium. J. R. A. Anderson (*Analyt. Chem.*, 1953, **25**, (1), 108–112).—A review, with 61 ref.—F. M. L.

***Analytical Procedure for the Determination of Thorium.** R. Kronstadt and A. R. Eberle (*U.S. Atomic Energy Commission Publ.*, 1952, (**RMO-838**), 9 pp.).—A detailed procedure is given for the detn. of Th in the presence of rare-earth elements by the spectrophotometric measurement of the colour developed with Thoron [1-(*o*-arsenophenylazo)-2-naphthol-3 : 6-disulphonic acid]. Th and rare-earths are first separated by pptn. as oxalates, using La as a carrier. Removal of the rare-earths is then effected by iodate pptn., using Hg as carrier. The colour developed with Thoron, after liberation and removal of I, is measured at a wave-length of 545 mμ. The method covers a range of 20–200 γ ThO_2 with a precision of ±1%. The accuracy is claimed to be ±2%.—C. E. A.

***Spectrophotometric Determination of Uranium by Thiocyanate Method in Acetone Medium.** C. E. Crouthamel and C. E. Johnson (*U.S. Atomic Energy Commission Publ.*, 1952, (**AECD-3328**), 16 pp.).—U to $5 \times 10^{-5} M$ can be determined colorimetrically by measurement of the absorption at 375 mμ of a $(C_2H_5)_2O/H_2O$ extract of the thiocyanate complex. The method shows freedom from interference by fairly large amounts of Cu, Zr, Sn, Hg, Mn, SO_4'', F', Cl', NO_3', CH_3COO', and by small amounts of SiF_6'', PO_4'''. At low levels Ni, Cr, Fe, Pb, Co, Mo, and citrate interfere. $(C_2H_5)_2O$ extraction of the original soln. helped to reduce the interference by some of these ions. 11 ref.—C. E. A.

***Determination of Small Amounts of Zinc in Aluminium Alloys: Rapid Electrogravimetric Method Utilizing Isotope Dilution Technique.** Kurt Theurer and Thomas R. Sweet (*Analyt. Chem.*, 1953, **25**, (1), 119–121).—Loss of Zn by co-pptn. or mech. means during manipulation or by incomplete deposition on the cathode during electrolysis is nullified by using the isotope-dilution technique and the radioactive tracer ^{65}Zn.—F. M. L.

***Determination of Zinc in Zinc-Cadmium Alloys [by Spectrography, Electrometric Titration, and Polarography].** Walter Scheller and W. D. Treadwell (*Helv. Chim. Acta*, 1952, **35**, (3), 754–762).—[In German]. *Spectrographic Method.* —Up to 10% Cd in Cd–Zn alloys and sublimates can be determined, using a spark discharge, a pure Cd rod as the second electrode, and the Zn line 4810·5 Å. in comparison with the Cd line 4678·2 Å. *Electrometric Titration.*—The method can be employed for soln. having Zn contents down to 5 γ/ml., when titration is carried out with $10^{-3}M$-$K_4Fe(CN)_6$; Cd interferes and must be separated by pptn. as CdS. The influence of the presence of K^+, NH_4^+, and H_2SO_4 on the accuracy of the results is discussed. *Polarographic Method.*—If Cd is previously separated by pptn. with H_2S, the Zn content of soln. contg. down to 0·3 γ/ml. can be determined polarographically, if a base electrolyte 1·0·5*N* in NH_4OH and NH_4Cl is used. The apparatus and techniques employed in the three methods are described in detail; the results obtained are critically compared.—E. N.

***Spectrophotometric Determination of Zirconium.** A. D. Horton (*U.S. Atomic Energy Commission Publ.*, 1952, (**AECD-3482**), 15 pp.).—The procedure is given for the detn. of trace amounts of Zr, using Thoron [1-(*o*-arsenophenylazo)-2-naphthol-3 : 6-disulphonic acid] as a colorimetric reagent. The method covers a range of 10–100 γ Zr, measured at a wave-length of 555 mμ with a precision of 6–3%. F^-, PO_4^{3-}, ClO_4^- must be reduced to low concentration. Fe^{3+}, Ti^{3+}, Ti^{4+}, Cr^{3+}, Cr^{6+}, U^{6+}, MoO_4^{2-} can be present to ~10 : 1 ratio relative to Zr. The reaction takes place in an unbuffered acid soln., and $NH_2OH.HCl$ is suggested for suppressing the effect of Fe^{3+}, Sn^{4+}, and CrO_4^{2-}.—C. E. A.

The Identification of Alloys and Stainless Steels by Electrographic Methods. G. C. Clark and E. E. Hale (*Analyst*, 1953, **78**, (924), 145–147; discussion 147–148).—A method is described for the identification of stainless steels and other alloys used in chem.-plant construction. The constituents shown on the electrogram are identified by a series of spot tests.—F. M. L.

A Brief Survey of the Development of Electrographic Analysis, with Special Reference to Recent British Apparatus. P. R. Monk (*Analyst*, 1953, **78**, (924), 141–144).—A review, with 17 ref.—F. M. L.

Non-Ferrous Metallurgy [Non-Ferrous Metal Analysis]. M. L. Moss (*Analyt. Chem.*, 1953, **25**, (1), 37–41).—A review of progress in non-ferrous metal analysis, with 118 ref. —F. M. L.

Recent Developments in Metallurgical Analysis. II.—Titrimetric Analysis. III.—Gravimetric Analysis. T. S. West (*Metallurgia*, 1953, **47**, (279), 45–51; (280), 97–106).—Cf. *ibid.*, 1952, **46**, (278), 313; *M.A.*, **20**, 592. [II.—] A review, with 81 ref. [III.—] A review, with 77 ref.—F. M. L.

Analysis of High-Temperature Alloys by X-Ray Fluorescence. Ruben M. Brissey (*Analyt. Chem.*, 1953, **25**, (1), 190–192).—A technique using Geiger counters to measure the intensity of the radiations.—F. M. L.

***The Determination of Trace Elements by Neutron Radioactivation Analysis.** G. W. Leddicotte and S. A. Reynolds (*Amer. Soc. Test. Mat. Bull.*, 1953, (188), 29–31).—Most elements when exposed to the neutron source of a chain-reacting pile become activated to form artificially radioactive species which have characteristic types of radiation and rates of decay. Identification of the radiation provides a method of analysis which has great sensitivity of detection for most elements and in which there is normally no serious interference by other elements. Some appn. of the method are listed and some advantages and limitations briefly discussed. 11 ref.—P. T. G.

Analytical Procedures Based on Complex Formation. Z. G. Szabó and M. T. Beck (*Analyt. Chem.*, 1953, **25**, (1), 103–108).—A theoretical consideration.—F. M. L.

12—LABORATORY APPARATUS, INSTRUMENTS, &c.

(See also "Testing" and "Temperature Measurement and Control".)

†Measurement of Solid/Solid Interfacial Energies. James B. Hess (*Metal Interfaces* (*Amer. Soc. Metals*), 1952, 134–150; discussion, 150–152).—Experimental techniques that have been proposed or employed for the measurement of solid/solid interfacial energies are catalogued and briefly discussed. The best scheme is considered to be the one of measuring microscopically the dihedral angles between intersecting interfaces in equilibrium; it has obtained both the greatest experimental use and the most thorough theoretical development. The technique can be extended to yield abs. interfacial energies, and to determine the energy of a sp. interface rather than of a statistical average. 37 ref.—J. S. G. T.

Low-Temperature Test Chamber. —— (*Engineering*, 1953, **175**, (4546), 332–333).—Describes a self-contained low-temp. test chamber which can be fitted to certain types of tensile and fatigue testing machines for determining the properties of materials at temp. down to −196° C. Liq. N, solid CO_2 in a low-freezing liquid, or ice-H_2O coolants may be used. A coolant-circulation system permits temp. control to within ±2° C.—D. K. W.

Gaugemeter for Strip-Mills. R. B. Sims (*Engineering*, 1953, **175**, (4537), 33–35).—Established instruments for continuously measuring the thickness of strip leaving a mill are of two classes: (*a*) the contact micrometer and (*b*) the radiation-type gauge. Both have disadvantages of fragility and appreciable lag in response to changes in thickness of the strip. In addn. the micrometer gauge is not applicable to hot mills, and the radiation type is very expensive. S. describes a gaugemeter which overcomes the disadvantages of these types. The instrument depends upon the measurement of the work-roll setting and loading on the strip mill. The adjustment of the elect. circuit associated with the instrument in relation to the characteristics of the mill is discussed, and data are presented, indicating the accuracy attainable.—D. K. W.

Metals Melted Without Crucibles. E. C. Okress and D. M. Wroughton (*Iron Age*, 1952, **170**, (5), 83–86).—Cf. O., W., Comenetz, Brace, and Kelly, *J. Appl. Physics*, 1952, **23**, 545; *M.A.*, **20**, 287. See also *M.A.*, **20**, 203.—S. R. W.

Erratum: Electromagnetic Levitation of Solid and Molten Metals. E. C. Okress, D. M. Wroughton, G. Comenetz, P. H. Brace, and J. C. R. Kelly (*J. Appl. Physics*, 1952, **23**, (12), 1413).—Two math. expressions derived in the original paper (*ibid.*, (5), 545; *M.A.*, **20**, 287) are modified. A coil has recently been made that supported 80 g. of bright molten Al in a vacuum of 7×10^{-6} mm. Hg.—R. W. C.

Sensitive Recording Alternating-Current Hall-Effect Apparatus. E. M. Pell and R. L. Sproull (*Rev. Sci. Instruments*, 1952, **23**, (10), 548–552).—The theories, advantages, and disadvantages of various methods used for measuring the Hall effect are discussed. A new, sensitive apparatus is described, in which the magnetic field automatically reverses every 6 sec.; full circuit details are given.—E. J.

13 — PHYSICAL AND MECHANICAL TESTING, INSPECTION, AND RADIOLOGY

Report of [A.S.T.M.] Committee E-1 on Methods of Testing. —— (*Amer. Soc. Test. Mat. Preprint*, 1952, (50), 21 pp.).—Revisions to the Tentative Methods of Tension Testing of Metallic Materials (E8-51T) are given. A standard hardness-conversion table for Ni and high-Ni alloys giving the relationship between D.P.N., B.H.N., and Rockwell hardness numbers, is recommended for immediate publication as standard. A proposed tentative method of test for the Diamond Pyramid Hardness of Metallic Materials describing apparatus, prepn. of specimens, procedure, and calibration of apparatus is given. —P. T. G.

***An Investigation of the Plastic Behaviour of Metal [Aluminium-Alloy] Rods Subjected to Longitudinal Impact.** J. D. Campbell (*J. Mechanics Physics Solids*, 1953, **1**, (2), 113–123).—Apparatus is described whereby stress/strain curves may be obtained under impulsive loading. The stress is produced by means of a falling weight, while tht deformation is measured by strain gauges and displayed on an oscilloscope. Calibration methods are described, and the results of tests on an Al–2% Mg–¼% Mn alloy are given. Under dynamic conditions the 0·1% P.S. is raised 15% above the value in a static test.—E. O. H.

***Influence of Testing Frequency on the Fatigue Strength of Steels and Light Alloys.** Th. Wyss (*Amer. Soc. Test. Mat. Bull.*, 1953, (188), 31–34).—The fatigue strength for 10^6 cycles was determined for several different grades of C and alloy steel at 350 and 10,500 c./min. and for four Al alloys at 350 and 8000 c./min. The Al alloys approximated to 17S-T, 24S-T, 75S-T, and 51S-T. The tests were carried out under fluctuating axial tensile stress with min. stress zero. Fatigue strengths at higher frequencies were only slightly greater than at low frequencies, except for one grade of low-C steel and the Al alloy high in Zn, where the difference was 3·1%. It is pointed out that tests at higher frequencies result in considerable economy of time. The equipment used is briefly described.—P. T. G.

How Can We Appraise Metals for High-Temperature Service? Thomas J. Dolan (*Metal Progress*, 1952, **61**, (3), 55–60).—The factors affecting fatigue strength are enumerated, and a comprehensive discussion of the fatigue of metals at elevated temp. is given. The importance of correctly evaluating stress history is indicated. The various laboratory testing techniques are enumerated, and their resp. shortcomings are discussed. A testing machine capable of superimposing an alternating load on a steady load, and another machine capable of superimposing an alternating bending on a steady bending stress are mentioned. The effects of stress-raisers are discussed.—R. P. H. F.

Which Method to Evaluate Surface Roughness? Irwin Goldman (*Materials and Methods*, 1952, **36**, (6), 89–93).—The methods reviewed include photomicrograph, plastic replica, surface analyser, microscopic, and other special methods of the evaluation of surface roughness. The special methods include the electron-microscope method, electron-diffraction method, parallel-plane clearance method, gas and liquid adsorption methods, and the electrolytic method. The microscopic method is preferred, as it is said to give the most revealing information even with the subtlest surface characteristics.—R. P. H. F.

***Microscopic Observation of the Skin Structure of Finished Surfaces. I.—Measurement of Superfinished Surfaces.** Atsushi Inoue and Sueko Mori (*J. Mech. Lab., Tokyo*, 1952, **6**, (5), 175–178).—[In Japanese]. An experimental technique for observing the microstructure of stressed skin surfaces (of worked steels contg. 0·1–0·9% C) by using an oblique section is described. The skin structure of superfinished surfaces, 1–2 μ thick, has been checked by the technique. —AUTHORS.

Pneumatic Gauging Applied to the Measurement of Surface Finish. M. Graneek and H. L. Wunsch (*Engineer*, 1952, **194**, (5043), 387–389).—G. and W. describe an instrument designed to fill the gap between the expensive stylus recording instrument, and the comparison block methods for measuring surface roughness. Variations in flow of air escaping from an orifice held against the surface under test, are detected by a sensitive pneumatic comparator. Two types of comparator are described, and the design of orifice and the significance of various wave-forms on the surface under test, are discussed.—D. K. W.

Null Method of Measuring Periodic Strains. J. H. Littlewood and C. Maskery (*Engineering*, 1953, **175**, (4546), 350–351).—Describes an electronic method for measuring periodic strains such as are encountered in fatigue testing. The circuit compares the dynamic and static components of strain with the static strain in a calibrating beam, by a system of strain gauges. A good accuracy has been maintained whilst eliminating the need for highly stabilized voltage supplies. —D. K. W.

Testing Today and Tomorrow. F. G. Tatnall (*Metal Progress*, 1952, **61**, (1), 64–67).—The appn. of electronics in testing equipment is indicated, and an attempt is made to forecast how such devices may help to attain future needs. The original use of strain gauges in impact testing is discussed, and the use of strain gauges in creep and fatigue testing is indicated. Non-destructive testing is briefly mentioned, and ref. is made to A.S.T.M. Tech. Publication No. 112, which classifies 12 basic test methods. Finally, the factors which modify basic strength data are given.—R. P. H. F.

Ultrasonic Detector Reveals Flaws. W. J. Stirling (*Canad. Metals*, 1952, **15**, (10), 58, 60, 62–63).—W. A. M. P.

Ultrasonic Examinations of Weldments and the Establishment of Safe Acceptable Limits for Defects. Frank C. Parker (*Non-Destructive Testing*, 1953, **11**, (3), 12–20).—Illustrated examples are given to indicate the scope of ultrasonic inspection of castings and welds. In the absence of standards of acceptance for the ultrasonic inspection of welds, P. has used the existing A.S.M.E. and A.S.T.M. weld-acceptance codes as a basis. A curve is given relating height of the ultrasonic (shear wave) trace to the cross-sectional area of the residual metal for ½ in. steel. Defects in castings and forgings are more readily assessed by ultrasonics than are those in welds.—L. M.

Quality Control Applications of Non-Destructive Tests in the Airframe Industries Which Will Effectively Lower Production Costs. B. W. Clawson (*Non-Destructive Testing*, 1953, **11**, (3), 25–27).—In reviewing non-destructive testing as a feature of quality control, C. quotes examples indicating how: (1) prodn. costs were reduced; (2) better products resulted, and (3) spectrography saved time in chem. analysis. C.'s firm has written the appropriate non-destructive testing schedule into prodn. drawings and has provided acceptance standard radiographs to guide their radiologists in casting acceptance.—L. M.

Commercial Interpretation of Magnetic-Particle Tests Correlated with Radiography and Physical Tests. A. F. Cota and J. J. Chyle (*Non-Destructive Testing*, 1953, **11**, (3), 34–40).—An illustrated account is given of a comparison of radiography and magnetic-particle inspection applied to welds. It is concluded that: (1) radiography detected all the defects investigated; (2) radiography takes longer than magnetic-particle inspection; (3) the magnetic method is most suitable for detecting surface defects but can detect defects existing two or three weld layers deep; (4) for good magnetic inspection the surface should be free of surface irregularities, slag, and spatter; (5) neither method is self-sufficient, nor are they sufficient as co-ordinated inspection in all cases; and (6) acceptance standards should be correlated with destructive tests and actual loading.—L. M.

Industrial Fluoroscopy. D. T. O'Connor (*Non-Destructive Testing*, 1952, **11**, (2), 11–22).—The 1952 Mehl lecture to the Society for Non-Destructive Testing. Fluoroscopic inspection is critically and extensively reviewed with particular ref. to: (1) its scope and limitations; (2) sensitivity of defect detection; (3) effect of object movement during inspection; (4) effect of scattered radiation; (5) image definition; (6) merit of Be window in the X-ray tube; (7) screen brightness in relation to defect detection, tube current, and kilovoltage; (8) design of equipment for handling castings during fluoroscopy; and (9) its merits relative to radiography. O'C. confirms that roughly 15% of the casting defects detected by fluoroscopy are missed by radiography, and that fluoroscopy cannot compete with radiography if extreme sensitivity for the smallest defects is required. Ref. is made to an improved fluoroscopic technique in which the screen image and the specimen are visible simultaneously, the latter being illuminated by red light.—L. M.

Semi-Empirical Equations for the Spectral Energy Distribution in X-Ray Beams. C. Robert Emigh and Lawrence R. Megill (*Non-Destructive Testing*, 1953, **11**, (3), 30–33).—Data from filtration curves for 37·7 and 50·7 kV. (peak) X-rays have been matched to a Laplace transformable equation to an accuracy $>1\%$; and thereby spectral energy curves for these radiations have been calculated, with an estimated accuracy of 5% of the max. value. The max. value of $f(\lambda)$ occurs at wave-lengths of 0·55 and 0·45 Å., resp., for 37·7 and 50·7 kV. (peak) X-rays. The methods of calculation and measurement are described.—L. M.

---

15 — FOUNDRY PRACTICE AND APPLIANCES

Light Metal Castings for Aircraft Structures. Keith F. Finlay (*Metal Progress*, 1952, **61**, (1), 81–83).—The lack of progressive design in the light alloy casting field is attributed to the conservative attitude of designers. It is pointed out that although Ti is considered by some to be the paragon of metals, its *d* is twice that of the Al alloys 24S and 75S, and ref. is made to some damaging characteristics associated with the fabrication of Ti which will limit its appn. The high quality of German foundry technology is acknowledged, and the use of Mg castings in the as-cast rather than in the wrought and heat-treated condition, in enemy aircraft, is emphasized. The advantages claimed for the use of castings are their dimensional accuracy, the elimination of machining, the freedom from residual stresses, heat-treating cracks, warpage, &c.—R. P. H. F.

The Impending Revolution in [Aluminium Alloy] Casting Processes. H. H. Harris (*Metal Progress*, 1952, **61**, (3), 65–69).—H. reviews the recent developments in the foundry, and states that although aircraft designers allow approx. 33,000 lb./in.^{2} U.T.S. for Al sand castings as compared with 70,000–75,000 lb./in.^{2} for Al forgings, advanced casting processes in commercial prodn. are producing Al castings with U.T.S. $>60,000$ lb./in^2., Y.P. $>50,000$ lb./in.^{2}, and elongation of $\geqslant 10\%$, thus approx. equalling the values obtainable with forgings, with the inherent advantages of castings. The developments in casting techniques discussed include casting under pressure, casting out of contact with air, steam, hydrocarbons, refractory sands, and the accurate control of metal temp. throughout the casting process. Attention is drawn to the fact that no casting can be dimensionally more accurate than the pattern or the machines employed in mould prodn., and therefore the necessity for greater precision in tooling and accuracy of patternmaking is stressed.—R. P. H. F.

Aluminium Pressure Die-Casting Dies: Their Failure by Surface Cracking. H. J. Sharp (*Metal Ind.*, 1953, **82**, (8), 141–143; (9), 164–166; (10), 181–184).—By far the most common failure of die-casting dies is characterized by the appearance of a network of surface cracks extending over the casting faces. These cracks are usually referred to as "heat-checking", "crazy-cracking", or "die-crazing". S. investigated the mechanism of failure and the variables involved in the casting process, compared the main types of steel used, and described the heat-treatment procedure. He concludes that a die life of 200,000–500,000 Al castings can be obtained by carburizing the dies at their casting faces and heat-treating them to a surface hardness of 50–55 Rockwell C, providing that correct operating methods are used. Final failure of such dies will be by corrosion-fatigue.—J. H. W.

Secondary Aluminium: And No Apology! M. J. Davison (*Canad. Metals*, 1952, **15**, (11), 74, 76).—The use of secondary Al in the foundry industry is discussed. D. regrets the use of the term "secondary".—W. A. M. P.

An Unusual Tin Bronze Casting. Harold J. Roast (*Metal Progress*, 1952, **61**, (3), 76–78).—R. describes a visit to a large American factory and the plant used for the prodn. of a 20,000-lb. pump casing in a Sn bronze of the following compn.: Cu 90%, Sn 8%, Pb 2%. The 30,000-lb. charge is melted in 4 hr. in a reverberatory furnace; no deoxidizing is accomplished in the furnace, but 2 oz. of 15% phosphor-Cu is placed in the ladle before pouring, for deoxidation. The tapping and pouring temp. are 2280° F. (1250° C.) and 2160° F. (1180° C.), resp. The mould is made of silica sand bonded with 12% Portland cement and 6% water. Cast Fe chills 2 in. thick are placed in the drag to control local cooling rates. A test-bar from the casting gave Y.P. 20,000 lb./in.^{2}, U.T.S. 30,560 lb./in.^{2}, and 3% elongation.—R. P. H. F.

***Influence of Aluminium on Properties of Cast Gun-Metal and Removal of Aluminium by Slag.** Ake V. Larsson (*Trans. Amer. Found. Soc.*, 1952, **60**, 75–82; discussion, 82–83).—Disc castings and D.T.D. test-bars were used to study the effect of Al on pressure-tightness and mech. properties of 83 : 6 : 5 : 6 gun-metal. Both properties deteriorate rapidly when Al exceeds 0·01%. By adding 1·5% of flux, consisting of NaF 30, CaF 20, Na_3AlF_6 20, Na_2SO_4 20, and Na_2CO_3 10%, Al can be reduced from 0·3 to $<0{\cdot}01\%$ in the alloy.—V. K.

Melting and Casting Aluminium Bronzes.—I.–II. James G. Dick (*Canad. Metals*, 1952, **15**, (12), 36, 38; (13), 32, 34, 36).—[I.—] Melting practice is briefly discussed. [II.—] Shrinkage, alloy compn., heat-treatment, and the effects of other elements in the alloys are similarly discussed. W. A. M. P.

Light Alloys' Modern Foundry. —— (*Canad. Metals*, 1952, **15**, (11), 52–54).—Canada's largest Mg foundry is described. —W. A. M. P.

Biggest in Canada: Domal's New Magnesium Foundry. ——(*Modern Metals*, 1952, **8**, (10), 52–53). A description is given of a new Mg foundry; a particular feature is the sand-handling facilities.—R. J.

Titanium and Zirconium Casting Now Practicable. W. E. Kuhn (*Materials and Methods*, 1952, **36**, (6), 94–95).—The vacuum-casting and pressure-casting methods of producing heavy rods and precision parts in Ti and Zr are reviewed. The use of inert-arc melting of the required alloy on a water-cooled Cu hearth, followed by casting into graphite or Cu moulds, is described. Precision castings and rods up to 7 in. in length and varying in dia. from $\frac{1}{8}$ to $\frac{1}{4}$ in. are illustrated. The possible fields of appn. of the inert-arc melting process and the commercial prodn. of small complex parts by this method are discussed.—R. P. H. F.

How to Increase Your [Zinc] Die-Casting Output? L. F. Spencer (*Iron Age*, 1953, **171**, (2), 93–98).—S. discusses the proper selection and heat-treatment of die steels for Zn die-casting. This is governed by the type of die-casting metal and its m.p., and if carefully made can keep heat checking and metal wash of dies at a min. Nitriding improves die life and prevents the sticking of the casting to the die cavity.—J. H. W.

***Practical Consequences of Space, Time, and Temperature Relations During Casting of Metals.** J. S. Abcouwer (*Trans. Amer. Found. Soc.*, 1952, **60**, 90–100).—Fourier's equations of heat flow are applied to the problem of heat flow in sand moulds. A method of applying the results obtained to dimensioning of risers is outlined. 24 ref.—V. K.

***A Test for Hot-Tearing Tendency.** E. A. Lange and R. W. Heine (*Trans. Amer. Found. Soc.*, 1952, **60**, 182–195; discussion, 195–196).—A hot-tear testing device was constructed which allows the combined effects of hot strength, ductility, and contraction to be measured. The test-bar is cast into a core-sand mould, one end of the bar being fixed, whilst the other is attached to a spring and dial through a water-cooled stud. Full dimensional details of design of the apparatus which was found suitable for studying hot tearing of cast Fe are given. The test could be readily modified for other alloys.—V. K.

Feeding Heads.—I.–II. M. R. Hinchcliffe (*Metal Ind.*, 1953, **82**, (3), 43–46; (4), 67–70).—H. first examines the grounds underlying the detn. of the proportions of ordinary feeding heads. The methods whereby the amount of feeding head can be reduced without interfering with the efficacy of feeding resolve themselves into the provision of thermal insulation by material other than surplus liq. metal. Such materials fall into three broad classes: (1) purely insulating material, such as gypsum; (2) exothermic chem. mixtures that generate heat on contact with the liq. metal and deposit a quantity of new superheated liq. ferro- or other alloy as a product of the reaction, such as "Risotherm"; and (3) similar materials that do not modify the quantity or quality of the feed metal and provide a high degree of insulation after the reaction has ceased, such as "Feedex". H. describes the appn. of the material in the last category in conjunction with a neck-down technique for feeding heads. —J. H. W.

Special Mixture Overcomes Feeding Problem. —— (*Canad. Metals*, 1952, **15**, (10), 30–32).—Light-alloy casting feeder heads may be kept molten for a prescribed time by the use of "Feedex" mixture. The size of the feeder head is therefore reduced, and several other advantages are claimed. —W. A. M. P.

Risering Castings: A Progress Report for 1948–1951. J. B. Caine (*Trans. Amer. Found. Soc.*, 1952, **60**, 16–22).—Cf. *Amer. Foundryman*, 1952, **21**, (4), 143; *M.A.*, **20**, 205.—V. K.

***A Study of the Principles of Gating as Applied to Sprue-Base Design.** K. Grube, J. G. Kura, and J. H. Jackson (*Trans. Amer. Found. Soc.*, 1952, **60**, 125–136).—Different types of transition from the downrunner to the runner bars were studied in relation to the degree of turbulence created by the flow of water in lucite moulds. The appn. of a well basin at the bottom end of the downrunner was most effective in reducing the turbulence and aspiration. The optimum cross-section of the well is 5 times the downrunner area, and its depth is equal to the depth of the runner bar. This area can be made smaller with larger gating ratios, i.e. with downrunner area to runner-bar area 1 : 2, or larger.—V. K.

Gases and Naturally Occurring (Congenital) Blowholes in Foundry Practice. Albert M. Portevin (*Trans. Amer. Found. Soc.*, 1952, **60**, 109–124).—The laws and data of solubility of gases in metals and alloys are reviewed. The appn. of such basic knowledge to the problems of gas porosity in castings and degassing of metals is discussed at length.—V. K.

An Appraisal of the Shell Moulding [Croning] Process. Harold J. Roast (*Metal Progress*, 1952, **61**, (4), 71–74)—Cf. *M.A.*, **20**, 658.—R. P. H. F.

The Shell Moulding Process. F. L. Church (*Modern Metals*, 1952, **8**, (3), 28–30, 31–33).—R. J.

Low-Cost Shell-Moulding Machine. —— (*Modern Metals*, 1952, **8**, (10), 58–59).—A new simple shell-moulding machine has been developed for use in the small jobbing foundry. Its main features are: (1) flexibility, (2) low cost of construction, and (3) efficiency.—R. J.

Design and Production of Shell-Mould Patterns. —— (*Iron Age*, 1952, **170**, (24), 172–174).—The design of shell mould patterns involves intricate problems because of the severe heating and cooling cycles. Results of experience with various prodn. patterns are reviewed. With special heat-treatment, anodizing, and new parting agents, Al can be used with advantages over cast Fe, particularly where machining is necessary. Plates 16 × 24 in. in size have been made to within 0·0015–0·0020 in. tolerance and the warpage eliminated by increased section and strain relieving. —S. R. W.

Sand Control, with Particular Reference to the Prevention of Scabbing. W. B. Parkes (*Trans. Amer. Found. Soc.*, 1952, **60**, 23–37; discussion, 37).—The incidence of scab defect in sand moulds is explained in terms of the expansion characteristics of the moulding-sand mixture. By either sand grading or special addn. (coal dust, wood flour, asbestos fibre) the effective plasticity of sand surface at high temp. is increased and the formation of scabs reduced or eliminated. 13 ref.—V. K.

Practical Aspects of Olivine as a Moulding Material. John Sissener and Bjorn Langum (*Trans. Amer. Found. Soc.*, 1952, **60**, 38–42; discussion, 43).—Cf. *Amer. Foundryman*, 1952, **21**, (4), 138; *M.A.*, **20**, 206.—V. K.

***Study of the A.F.S. Fineness Test.** H. A. Stephens (*Trans. Amer. Found. Soc.*, 1952, **60**, 53–67; discussion, 67).—Fine sands of different grading were sieved using A.S.T.M. and B.S.S. sieves with different types of sieving machines. The sieving value was found to be mainly affected by the characteristics of the sieve material, size of the sample, and time of sieving. If the sieving test is standardized, it could be used for calibrating unknown sieves under different sieving conditions.—V. K.

***Heat Flow in Moist Sand.** [—II.] Victor Paschkis (*Trans. Amer. Found. Soc.*, 1952, **60**, 163–168; discussion, 168).—Cf. *ibid.*, 1951, **59**, 381; *M.A.*, **20**, 294. The effect of 4 and 6% moisture content in sand on the rate of heat transfer in comparison to dry sand was determined for the mould surface temp. of 2000° and 2600° F. (1095° and 1425° C.). For 2000° F. the ratios of heat extracted during the first min. are: dry : 7% : 6% = 1 : 1·21 : 1·16, while for 2600° F. = 1 : 1·19 : 1·11. This ratio falls off during the subsequent periods so that the solidification time of thin castings only will be affected by the moisture content. —V. K.

Role of the Research Foundry Unit. G. A. Lillieqvist (*Trans. Amer. Found. Soc.*, 1952, **60**, 6–15; also *Proc. Inst. Brit. Found.*, 1952, **45**, A34–A44; discussion, A45–A47; *Found. Trade J.*, 1952, **93**, (1875), 145–151; (1876), 187–191; discussion, (1877), 217–219; *Foundry*, 1952, **80**, (10), 114–119, 258, 260, 262, 264).—An example of organizing a foundry research laboratory is described. For illustration a number of research investigations which have led to improvements in foundry processes are given. Fluidity measurements, hot tears, deoxidation, and special addn. to the melt are quoted. 7 ref.—V. K.

Die-Casting. (Herb). See col. 815.

17 — FURNACES, FUELS, AND REFRACTORIES

Advantages and Disadvantages of Light-Metal Melting Equipment. Hiram Brown (*Amer. Foundryman*, 1952, **22**, (6), 36–41).—Fuel and elect. furnaces are discussed.—V. K.

Rotary Melting Furnaces: Some Results Obtained from an Interesting Type of Equipment. —— (*Canad. Metals*, 1952, **15**, (12), 40).—W. A. M. P.

Design of an Oil-Fired Galvanizing Furnace. William D. Bawden (*Wire and Wire Products*, 1953, **28**, (2), 151–154, 222).—A paper delivered to the Wire Association, in Cleveland, Ohio. The designer's objects were efficiency, longest possible pot life, a low dross prodn., the avoidance of hot spots, and ease of furnace operation. B. describes how the design for a furnace with a working load of 300–2000 lb./hr. is evolved from a basis of 20 lb. Zn/lb. of prodn. Temp. are controlled automatically at 840° F. (450° C.). 6 ref.—C. P. F.

[High-Vacuum Furnace for] Metal Alloying. —— (*Elect. Rev.*, 1952, **150**, (3873), 355–356).—A short description is given of a high-vacuum furnace developed by Gerätebau-Anstalt Balzers, Liechtenstein, for the melting and casting of special alloys.—S. R. W.

Continuous Furnace for Fast Annealing of Tinplate. M. D. Stone and E. A. Randich (*Metal Progress*, 1952, **61**, (2), 62–66).—The tower-type furnace described consists of four 34-ft. vertical passes for heating and eight 38-ft. passes for holding and cooling. A controlled atmosphere is provided in the furnace and also a chem. strip cleaning plant immediately ahead of the annealing furnace for the removal of oil before annealing. With cold reductions of from 80 to 90% annealing temp. of 1250°–1350° F. (675°–730° C.) are satisfactory as compared with 1750° F. (955° C.) for reductions of 55–65%. The capacity of the plant is claimed to be 30 tons/hr. of 0·0075–0·015-in.-thick strip, 18–37 in. wide, travelling at speeds of 1000 ft./min.—R. P. H. F.

Magnethermic Induction Billet Heaters. ——(*Modern Metals*, 1952, **7**, (12), 36–37).—The use of L.F. induction heating methods is increasing rapidly in the U.S.A. The main use is for pre-heating extrusion billets of Al, but other uses are for heating slugs for forging, for Cu and Mg alloys, and in some cases for steel.—R. J.

Saturable Reactor Control of Electric Furnaces.—I. R. M. Sills (*Indust. Heating*, 1952, **19**, (4), 608–610, 612, 614, 616, 618, 620, 622, 628).—The process of development of saturable reactor furnace controls is reviewed and the advantages of the method indicated. The improved control obtainable gives a specially uniform temp. control and prevents cycling. The use of proportional power control in the processes of Al brazing and metal-powder sintering is described. Temp. accuracies of ±5° F. (2·5° C.) are claimed for the method. Continuous radiant heating can be usefully controlled by saturable reactors. A large proportion of the installations are for continuous heating processes where rapid accurate heating is essential, e.g. strip heating.—D. M. L.

***Centrifugal Furnaces [Actuated] by the Accumulation of Solar Energy.** Félix Trombe and Marc Foëx (*Compt. rend.*, 1952, **235**, (11), 571–573).—T. and F. describe the construction and operation of a solar energy furnace in which are combined the advantages of working without a crucible with those of heating in a calorifuge, which even at high temp. is practically isothermal and in respect of absorbed and transmitted radiations behaves like a black body. The furnaces have a capacity of 300–1000 c.c. of metal (Al, Duralumin, Fe, &c.) and rotate at between 200 and 5000 r.p.m. The circular face opposite to the axis of rotation has an 18-mm. hole in the centre through which the radiation is focused by a 2-m. parabolic mirror.—J. H. W.

***On the Construction of a Semi-Industrial Solar Furnace at the Mont Louis Laboratory (Eastern Pyrenees).** Félix Trombe (*Compt. rend.*, 1952, **235**, (14), 704–705).—The construction of a solar furnace with a working temp. of 2900°–3000° C. and capable of melting 60 kg./hr. of Fe, is described.—J. H. W.

***Some Details of the Setting-Up of the Semi-Industrial Solar Furnace at Mont Louis.** Félix Trombe (*Compt. rend.*, 1952, **235**, (20), 1211–1213).—T. gives details of the setting-up of the 90 m.² paraboloid in relation to the solar furnace.—J. H. W.

***Properties of Some Niobium Oxide Basic Ceramics.** E. A. Durbin, H. E. Wagner, and C. G. Harman (*U.S. Atomic Energy Commission Publ.*, 1952, (**BMI–792**), 15 pp.).—Experiments were made on Nb_2O_5 and certain compn. of binary mixtures with Al_2O_3, ZrO_2, MgO, and TiO_2. The materials were wet milled for 20 hr. in a neoprene-lined ball mill, using Burundum cylindrical grinding media. The milled product was dried, screened, and pressed into compacts, which were calcined, crushed, and screened. Test specimens were made from the powder by pressing hydrostatically at 100,000 lb./in.² and sintering in air in the range 1345°–1495° C. The sintered products were sound, having apparent porosities in the range 5–16%, and were characterized by low thermal expansions, low E, and large increases in strength combined with small increases in E with increasing temp. The mean coeff. of linear thermal expansion in the temp. range 25°–500° C. varied from $1{\cdot}05$–$4{\cdot}82 \times 10^{-6}$/°C. for the binary mixtures compared with $-0{\cdot}61 \times 10^{-6}$/°C. for pure Nb_2O_5.—B. W. M.

***The Measurement of Thermal Conductivity of Refractory Materials.** F. H. Norton and W. D. Kingery (*U.S. Atomic Energy Commission Publ.*, 1952, (**NYO-602**), 40 pp.).—The thermal conductivities of TiO_2, mullite, and ZrO_2 were measured in the range 200°–1400° C. by the ellipsoid envelope method and of Al_2O_3, BeO, and MgO to 1800° C. by employing H.F. heating. A new derivation of the heat flow equations for ellipsoidal specimens and calculations of the effect of porosity are given. The conductivity of TiO_2 having a bulk d of 4·11 g./c.c. decreased from 0·011 cal./sec./°C./cm²./cm. at 200° C. to ~0·0075 at 1200° C., that of mullite from 0·012 at 200° C. to ~0·008 at 1400° C., and that of ZrO_2 (bulk d, 3·69 : total porosity, 19·1%) from 0·01 at 200° C. to ~0·008 at 1400° C. The temp. dependence of conductivity for Al_2O_3, BeO, and MgO are given by the equations, $k = 17{\cdot}0/T + 3 \times 10^{-29}T^8$ (Al_2O_3, range 273°–2073° K.), $k = 20{\cdot}3/T + 3 \times 10^{-29}T^8$ (MgO, 273°–2073° K.), and $k = 58{\cdot}2/T + 3 \times 10^{-29}T^8$ (BeO, 1073°–2073° K.). A min. conductivity followed by a sharp rise above 1600° C. for these materials is believed to be due to the radiant transmission by the specimens, which were all found to be translucent. The effect of this translucency is analysed, and it is considered that above 1600° C. radiation shield insulation and opaque insulators will become rapidly more efficient than translucent insulators as the temp. increases.—B. W. M.

---

19 — WORKING

Extruding Aluminium in Giant Presses. T. F. McCormick (*Modern Metals*, 1952, **8**, (11), 54, 56–57).—McC. discusses the use of 13,200-ton extrusion presses for Al alloys. Problems of large-capacity presses are discussed, together with some of the special features, e.g. the prodn. of stepped and tapered sections.—R. J.

What You Should Know About Stretch-Forming [of Aluminium]. E. V. Sharpnack (*Iron Age*, 1952, **170**, (7), 138–140).—The advantages and disadvantages, and the technique of stretch-forming of Al are briefly given.—S. R. W.

The Mass Production of a Motor Car Cowl [in Aluminium-13% Silicon Alloy]. Charles Roinet (*Rev. Aluminium*, 1952, (**188**), 186–195).—An illustrated account of the prodn. of this unit by machine moulding. Its finished weight is 60 kg. in the Al–13% Si alloy (A–S13), and it meets an overall tolerance of ±2 mm.—A. W. B.

How Oak Ridge Machines Beryllium. J. N. Case and E. R. Watkins (*Machinist* (*Eur. Edn.*), 1953, **79**, (6), 221–225).—C. and W. describe the special precautions taken to protect workers for the U.S. Atomic Energy Commission in the finish machining of Be and give the latest information on deep-hole drilling, milling, and other machining operations.—J. H. W.

Why the 250-lb. Copper Wire-Bar? —— (*Metal Ind.*, 1953, **82**, (5), 83–85; (6), 101–102).—It is suggested that the Cu wire industry should work on a larger scale. The effects of this on the wire-drawing operations and the manner in which the industry has grown in Britain, Australia, and the U.S.A. are discussed. The advantages and disadvantages of siting rod mills at refineries are set out. On balance it is considered likely that standard bars much heavier than 250 lb. will one day be made. 30 ref.—J. H. W.

***Drop-Hammer Forming Magnesium Sheet.** F. L. Coenen (*Modern Metals*, 1953, **9**, (1), 33–34; 36–37).—C. describes the results of an experimental programme designed to investigate problems in the drop-hammer forming of Mg sheet. Factors studied were time and temp. limits which produce max. formability with min. loss of structural properties, heating and forming equipment, tooling and lubrication, and tolerances. Practical recommendations are given based on this experimental work.—R. J.

Magnesium Castings Drilled, Reamed, C'Bored at High Speed. W. G. Patton (*Iron Age*, 1952, **170**, (23), 162–164).—A new in-line automatic machine performs 200 drilling, reaming, and countersinking operations on a Mg alloy casting in 8 min. The machine operates on two faces of the casting, which is held on to a double roller chain by toe clamps. The chain carries the casting from station to station by operation of a series of relay switches.—S. R. W.

Forging Titanium. R. Bullock (*Modern Metals*, 1953, **9**, (1), 46–48).—Describes the forging of a 200-lb. compressor wheel made in a Cr–Fe–Ti alloy, and various other forgings such as aircraft pistons, wheel forgings, gears, &c.—R. J.

Cold Forming Titanium. J. W. Gullikson (*Modern Metals*, 1953, **9**, (1), 48, 52).—G. describes his experiences in the deep drawing and shallow forming of Ti. Reductions of 35–40% were obtained. Surface prepn. such as Bonderizing, anodizing, &c., was necessary to prevent die roughening and galling. —R. J.

Titanium Can Be Deep Drawn. J. W. Gullikson (*Iron Age*, 1953, **171**, (7), 136–139).—The chief difficulty in deep drawing commercially pure Ti sheet is scouring due to the pick-up of Ti particles. This has been partly overcome by Bonderizing before appn. of a high-pressure lubricant and also by electrolytic treatment. Reductions as high as 38% have been obtained on 0·078-in. sheet in one draw. —J. H. W.

How to Grind Titanium? Leo P. Tarasov (*Iron Age*, 1953, **171**, (7), 335–346).—T. gives the latest information on grinding Ti which makes the process a little easier than grinding high-speed steel.—J. H. W.

Spun and Drawn Zinc Parts Have Many Applications. Ernest V. Gent (*Materials and Methods*, 1952, **36**, (6), 102–104).—The requirements for the spinning and drawing of a variety of Zn parts are given, and the methods of finishing are briefly mentioned. Reductions/draw, tolerances, and lubricants used in drawing are discussed.—R. P. H. F.

Extrusion with Glass Lubrication. H. W. Perry (*Metal Ind.*, 1953, **82**, (5), 87–88).—The use of glass lubrication for extruding ferrous alloys in France reduces damage to dies. It is suggested that this technique should be applied to the extrusion of non-ferrous metals and alloys.—J. H. W.

12,000-Ton Forging Press. —— (*Engineer*, 1953, **195**, (5067), 347–349; also *Engineering*, 1953, **175**, (4545), 301; *Light Metals*, 1953, **16**, (180), 95–96; *Metal Ind.*, 1953, **82**, (11), 201–205; *Metal Treatment*, 1953, **20**, (90), 110, 112; *Aircraft Prodn.*, 1953, **15**, (174), 124–125; *Shipbuilder*, 1953, **60**, (536), 210).—A description of the 12,000-ton hydraulic forging press installed at the Redditch Works of High Duty Alloys, Ltd.—D. K. W.

Roll-Size Effects in Rolling of Strip. N. H. Polakowski (*Metal Progress*, 1952, **61**, (2), 67–71).—Cf. *M.A.*, 19, 876. The soln. to the following problems namely—does roll dia. limit the max. reduction and the min. thickness of strip during cold rolling, and secondly, does roll dia. affect the power requirements for thin strip, are presented. The soln. to the first problem is stated to be that for equal drafts the contact length decreases when roll dia. is reduced, and therefore the thickness to which the final strip can be rolled is also reduced in approx. the same proportion. The contact area consists of an active and an inactive portion. Thus the soln. to the second problem is stated to be that by increasing roll dia. the inactive portion can be considerably increased, but the active length is not greatly affected by change in roll dia., and thus the active length-to-thickness ratio is virtually independent of roll dia. Hence the power requirements do not depend on roll dia., whereas strip thickness does. —R. P. H. F.

Strip Rolled to 0·0002 in. on New Small Mill. Robert L. Stockus (*Iron Age*, 1952, **170**, (10), 156–159).—A small Sendzimir mill, ZR32-4, which will cold roll elect. alloys to 0·0002 in., is described.—S. R. W.

Advances in Machining and Cutting Operations. Taylor White (*Metal Progress*, 1952, **61**, (1), 84–86).—The developments in tool steels since 1890 are reviewed. The advent of WC cutting tools is claimed to have revolutionized the machining of the hard alloy steels. Advances in powder metallurgy resulted in the use of TaC and BC powders embodied in WC tools. The development of new machines and techniques resulted from advances in four main fields, namely dies, equipment, met. control, and design. The need for mass-prodn. methods is said to have resulted in the improvement of the machinability of materials either by the addn. of alloying elements, or by their mech. and thermal treatment before machining. The appn. of special coatings to deep-drawing stock is mentioned. The improvements both from the mech. and met. points of view are claimed to be unlimited.—R. P. H. F.

Unorthodox Methods of Machining Hard Materials. P. Grodzinski (*Metallurgia*, 1953, **47**, (279), 34–38).—A review, with 29 ref.—F. M. L.

---

20 — CLEANING AND FINISHING

(See also " Protection " and " Electrodeposition ".)

The Finishing of Aluminium and Its Alloys. A. P. Fenn (*Metallurgia*, 1953, **47**, (280), 70–72, 90).—A review.—F. M. L.

Pickling and Bright-Dipping of Copper and Copper-Rich Alloy Components. E. E. Halls (*Electroplating*, 1953, **6**, (2), 43–50).—A review of acid treatments for Cu and Cu-rich alloys for removing superficial oxide or the prodn. of a relatively bright appearance without attacking the base metal. The problem is approached with special ref. to the formulation of recommended procedures for the wide range of Cu-rich materials passing through the plating shops of engineering factories or to trade platers. H_2SO_4; H_2SO_4–$Na_2Cr_2O_7$; H_2SO_4–HNO_3; HCl; and HNO_3–H_2SO_4–H_3PO_4 soln. are considered; special treatments are recommended for nickel silvers, Al bronzes, and Cu–Be alloys. Finally, figures are given showing the rate of attack of many of the acid soln. on some Cu-rich alloys.—H. A. H.

American Practice in Finishing Zinc-Base Die-Castings: Productivity Team Report. —— (*Electroplating*, 1952, **5**, (12), 409–410).—H. A. H.

Metal Cleaning and Finishing Since the War. Vernon A. Lamb (*Metal Progress*, 1952, **61**, (1), 76–80).—The progress that has been made since the end of the war in the fields of fundamental research and development in metal cleaning and finishing is reviewed. The availability of radioactive tracers and their appn. to problems of current and metal distribution, the mechanism of Cr plating, &c., are discussed. Advances in chem. and electrochem. methods for achieving bright finishes, including chem. dip polishing, electropolishing, and the periodic reverse current process are mentioned. The work of a number of people on an improved Cr-plating soln. called the high-speed self-regulating soln. is cited. The plating and protection of Mg is discussed. New instruments for measuring the thickness and adhesion of electrodeposits, hot hardness, and surface tension are briefly mentioned.—R. P. H. F.

Laundering Applied to Metals. —— (*Canad. Metals*, 1952, **15**, (12), 58, 60).—A brief note on the cleaning of metal components by degreasing and shot-blasting. Shot-peening is also mentioned.—W. A. M. P.

Faster Grinding with Abrasive Belts. H. N. Acker (*Canad. Metals*, 1952, **15**, (11), 46, 48).—The use of abrasive belts and contact wheels is discussed.—W. A. M. P.

21 — JOINING

***Fundamentals of Glass-to-Metal Bonding. I.—Wettability of Some Group I and Group VIII Metals by Sodium Silicate Glass.** V. F. Zackay, D. W. Mitchell, S. P. Mitoff, and J. A. Pask (*J. Amer. Ceram. Soc.*, 1953, **36**, (3), 84–89).—In order to evaluate the degree of wetting of Cu, Ag, Au, Pd, Pt, and Ni by Na silicate glasses contg. 30·8, 33·6, and 36·9% Na_2O in vacuum, He, H, O, and air, the contact angle at 900° C. was measured after attainment of a const.-angle reading. There is no relation between the position of the element in the Periodic System and the contact angle. No reaction between metal and glass occurs in an inert atmosphere, whereas the chem. reactions that occur in O and H improve spreading. Grain-size has no marked effect on the contact angle in any atmosphere. The wettability is related to the solubility of the gas atmosphere in the metal. The role of the polarizing power of the metal in determining the contact angle is discussed.—I. S. S.

Metal Stitching [Can Help to Reduce Costs of Fastening]. ——(*Machine Design*, 1952, **24**, (5), 151–153).—The great advantages of metal stitching as a joining method for thin-section metals are indicated. Stitches are formed in $\frac{1}{6}$ sec. from high-C steel wire. The different types of wire employed are discussed, and details are given of the form of stitches used, the strength of stitched joints, and the metals most usually joined by this process. Recommended material thicknesses are tabulated.—D. M. L.

How to Design Good Joints for Brazing. W. J. Van Natten (*Iron Age.*, 1953, **171**, (3), 95–98).—A general survey is made of the factors involved in the design of good joints in the brazing of Al, Mg, Ni, and their alloys and ferrous metals. Lap joints are used whenever possible; butt joints are used only when service requirements are not severe and leak tightness and strength are relatively unimportant.—J. H. W.

Hints for Silver-Brazing of Stainless Steel. J. P. Emmerich (*Weld. J.*, 1952, **31**, (1), 50–53).—Technique for Ag-brazing is described. Groups of stainless steels and their scaling temp. and Ag brazing alloys (Ag, Cu, Zn, Cd) and their flow points are tabulated.—K. B.

For Aluminium Radiators: A New Aluminium Brazing Sheet. —— (*Modern Metals*, 1952, **8**, (6), 52–54).—Describes a composite brazing sheet coated on one side with a low-m.p. brazing alloy and on the other with a corrosion-resistant clad alloy. It is claimed that this material has substantially reduced the problems of joining and corrosion-resistance associated with the use of Al for radiators.—R. J.

The Joining of Aluminium and Its Alloys. W. V. Binstead (*Metallurgia*, 1953, **47**, (280), 81–88).—A review.—F. M. L.

The "Aircomatic" Welding Process for Aluminium. —— (*Engineering*, 1953, **175**, (4548), 397).—Describes an A-arc process for the welding of Al and Al alloys. A continuously fed filler rod is employed.—D. K. W.

***Metal Transfer in Sigma Welding [of Aluminium Plate].** R. T. Breymeier (*Weld. J.*, 1952, **31**, (5), 393–399).—The effect is reported of current direction, amperage, and the gas used on the appearance of beads made in $\frac{1}{2}$-in. and $\frac{1}{4}$-in. Al plate by the shielded inert-gas metal-arc process. The addn. of O to A has little effect on the metal deposition rate with D.C.-reverse polarity and does not materially change the drop rate. Usable bead forms can be produced with D.C.-straight polarity and at higher deposition rate than with reverse polarity.—K. B.

***Fatigue Tests on Aluminium Alloy Spot-Welded Joints.** Marshall Holt and E. C. Hartmann (*Weld. J.*, 1952, **31**, (4), 183s–187s).—Results are compared of fatigue tests of spot-welded joints in sheets, 0·064 in. thick, of various high-strength Alclad Al alloys. 10 ref.—K. B.

Technical Factors in Cold-Welding Aluminium. W. E. McCullough (*Modern Metals*, 1952, **8**, (11), 40, 42, 44).—The theory of the cold-welding process is briefly discussed, and examples are given of the properties obtained and actual and potential appn.—R. J.

***Hot-Rolled Copper Rod Butt-Welding.** Clement Blazoy (*Wire Production*, 1953, **2**, (4), 4–7).—B. stresses that to wire-users the ultimate criterion of the success of butt-welding is whether, and to what extent, welds in rod become regions of weakness in drawn wire. Experiments on $\frac{5}{16}$-in. H.C. Cu rod with butt-welders rated at 25 kVA., are reported, from which it is agreed that the absence of oxide in small lenticular regions around the welds is due to the fact that Cu solidifies before the Cu–CuO eutectic and the liq. oxide is always squeezed out. Elect. resistance tests show no difference between lengths of wire with and without welds, whilst the welded joints had 98% of the tensile strength of the wire.—C. P. F.

Jet Engines Push Welded Molybdenum [and Molybdenum Alloys] Study. Willard M. Boam (*Iron Age*, 1952, **170**, (2), 145–148).—After a brief survey of the high-temp. properties of Mo and its alloys, B. reviews tests on the weldability of Mo alloys. He-shielded W electrodes were used. Incomplete shielding resulting from poor torch design, too rapid welding speed, and improper cleaning results in porosity and brittleness owing to low oxidation-resistance. For good welds complete absence of O is essential. Deoxidation with C results in the formation of a carbide network and cracking. No welds with good ductility were made.—S. R. W.

Welding Characteristics of Materials [Inconel W and Titanium Alloys] for Aircraft Gas Turbines. A. J. Rosenberg (*Weld. J.*, 1952, **31**, (5), 407–413).—Satisfactory resistance and inert-arc welding of Inconel W and of Ti alloys is reported. Arc welding of Inconel W is difficult. Weld properties and microstructures are shown.—K. B.

Welding Titanium. A. J. Rosenberg (*Modern Metals*, 1953, **9**, (1), 52–54, 56).—Ti can be welded by conventional methods. R. describes inert-arc welding, spot welding, seam and flash welding, and considers the fatigue strengths of some of the joints.—R. J.

Welding Heat-Exchangers for the Chemical Industry. John W. Mortimer (*Weld. J.*, 1952, **31**, (5), 387–392).—Types of heat-exchangers are described and illustrated. Arc, automatic arc, and inert-arc welding procedures are discussed for Cu, Ni, Al, and their alloys.—K. B.

Continuous Inert Arc Welding. —— (*Canad. Metals*, 1952, **15**, (12), 45–46).—A brief account of a semi-automatic, inert-gas shielded-arc welding process for joining light-gauge material.—W. A. M. P.

Melting Rate of Coated Electrodes. J. ter Berg and A. Larigaldie (*Weld. J.*, 1952, **31**, (5), 268s–271s).—9 ref.
—K. B.

***Heat Flow in Welding.** A. A. Wells (*Weld. J.*, 1952, **31**, (5), 263s–267s).—It is shown that heat dissipation may be used for predicting size of weld and that the shape of weld ripples indicates the heat input used. Experiments on steel are discussed; some equations are applied to Al and Cu. 9 ref.—K. B.

Hard-Facing for Impact. Howard S. Avery (*Weld. J.*, 1952, **31**, (2), 116–143; discussion, 143–145).—Aspects of impact as a wear factor are analysed, and the appn. of various hard-facing alloys, including Ni- and Co-base alloys, are discussed. 16 ref.—K. B.

***The Fundamentals of the Welding of Electric Contacts under Heavy Current Conditions.** (Holm and Holm). See col. 748.

Ultrasonic Examinations of Weldments and the Establishment of Safe Acceptance Limits for Defects. (Parker). See col. 792.

Progress in the Welding Industry. B. Karnisky (*Metal Progress*, 1952, **61**, (1), 59–63).—The aspects of welding reviewed include residual stresses, weldability, and alternative steels to replace materials contg. large amounts of Ni such as 18 : 8 stainless steel, &c. The use of welded Al members to replace structural steels is discussed. The prevention of brittle fractures and the desirability of higher welding speeds are indicated.—R. P. H. F.

22—INDUSTRIAL USES AND APPLICATIONS

Economical Introduction of Aluminium. K. Specht (*Aluminium*, 1952, **28**, (3), 76–77).—S. shows how to calculate, with the help of nomograms, the cost saving resulting from the use of Al.—M. A. H.

The Outlook for Aluminium in the Electrical Industry. H. W. Biskeborn (*Modern Metals*, 1953, **8**, (3), 56–58, 60, 62).—B. describes some of the accepted and potential appn. of Al in the elect. industry. Covered conductors, cable sheathing, and structural appn. are the chief uses at present. Among potential uses B. considers bus-bars, fuse wire, lightning conductors, &c.—R. J.

Aluminium-Sheathed Cable. B. O. Ashford, J. A. Donelan, and J. R. Penrose (*G.E.C. Journal*, 1952, **19**, (4), 222–228).—Processes by which Al strip is cold formed around elect. cables and welded longitudinally into continuous sheathing are described and illustrated. The advantages and mech. properties of the Al-sheathed cables are discussed.—J. R.

Aluminium as a Cable-Sheathing Material. D. McAllister (*Engineer*, 1952, **194**, (5056), 819–823; (5057), 854–857).—A. enumerates the advantages and disadvantages of Al and Pb for use as cable-sheathing materials and outlines the methods which have received most attention, for sheathing with the former. The relevant phys., mech., and chem. properties of Al and their influence on the characteristics of Al-sheathed cable are discussed. Notes are given on installation and jointing.—D. K. W.

Aluminium Cable Sheathing. —— (*Engineer*, 1952, **194**, (5044), 411–412; also *Engineering*, 1952, **174**, (4522), 404–405; *Metallurgia*, 1952, **46**, (276), 175–178; and *Light Metals*, 1952, **15**, (176), 357–360).—An account of an Al cable-sheathing process at Johnson and Phillips, Ltd., London, in which pre-extruded Al tube is drawn down over the cable core.—D. K. W.

The Manufacture of [Corrugated] Aluminium-Sheathed Electric Cable. —— (*Engineering*, 1952, **174**, (4528), 614–615; also *Engineer*, 1952, **194**, (5048), 548–549; *Metallurgia*, 1952, **46**, (271), 237–240; and *Light Metals*, 1952, **15**, (177), 394–396).—An account of an Al cable sheathing process at Pirelli-General Cable Works, Ltd., Eastleigh, in which Al strip is formed into tube around the cable core. The butting edges of the strip are continuously joined by A-arc welding. —D. K. W.

Discussion of Aluminium Conductor Connectors. H. W. Biskeborn (*Wire and Wire Products*, 1952, **27**, (12), 1297, 1320).—A summary of various views of American practice as expressed in letters and editorials.—C. P. F.

Progress and Future of Structural Aluminium. C. Marsh (*Light Metals*, 1952, **15**, (172), 219–220).—A. W. B.

Modern Structural Engineering in Light Metals. E. W. Pleines (*Aluminium*, 1952, **28**, (3), 69–74).—A review of the tech. and economical advantages of light-metal construction is followed by a description of the construction of hangars at London Airport.—M. A. H.

The Light Alloy Decking of the Havre Bascule Bridge. Jean Reinhold (*Rev. Aluminium*, 1952, (**190**), 285–290).—In the reconstruction of a bascule bridge in the docks at Le Havre, flooring in an Al-5% Mg alloy was chosen instead of wood previously used, with a 10% reduction in the weight of the leaf and at a lower cost than for steel or wood. A special extruded section 324 mm. wide was used to provide the flooring in the form of lapped beams. Precautions taken to prevent bi-metallic corrosion included zinc coating of steel fixing accessories, bitumen-impregnated tape between the steel/Al interface, measures to reduce condensation on internal surfaces, and finally the use of a Zn chromate primer and bitumen paint.—A. W. B.

Aluminium Roof of the Westfalenhalle at Dortmund. H. Kentzler and J. Schroeder (*Aluminium*, 1952, **28**, (4), 121–123).—A brief illustrated description of the lay-out is given. —M. A. H.

[Aluminium Alloys in] Dredgers, Draglines, and Cableways for the Donzère–Mondragon Canal. Jean Reinhold (*Rev. Aluminium*, 1952, (**187**), 137–148).—Al-alloy construction has been used in draglines for this project to increase their span. Three floating dredgers were equipped with light-alloy conveyor beams to enable a greater reach to be obtained. The cableway of 2066 ft. span also includes numerous Al components.—A. W. B.

The Choice of [Aluminium] Alloys for Ship Structures. —— (*Aluminium Courier*, 1952, (**20**), 9).—The two types of wrought Al-alloy used in shipbuilding today are: (1) the alloys of Al with up to 5% Mg (most generally used in Europe) and (2) alloys in the Al–Mg–Si group (most widely used in America). The nomenclature adopted in British Standards classification is expounded.—C. P. F.

Light-Alloy Barge. —— (*Engineering*, 1953, **175**, (4542), 208).—A description is given of an 80-ft., 150-ton-capacity Al alloy barge for service in the Middle East.—D. K. W.

Aluminium Alloys in General Engineering. M. H. P. Levie (*J. Junior Inst. Eng.*, 1952, **63**, (3), 93–101).—L. reviews the properties and suitability of different Al alloys. In wrought alloys the cold-workable commercial Al, Al–Mn, Al–Mg, and the heat-treatable Duralumin-type alloys are mentioned. The casting alloys are considered from the aspect of ease of casting with the development of max. properties. Al–12% Si, Al–Cu–Si, and Al-Cu-Ni-Mg alloys are given as most useful. Peculiarities in designing structures and components from Al alloys are discussed briefly, with an account of methods for joining them.—S. Ma.

Practical Applications of Aluminium Casting Alloys, Particularly in Motor Vehicles. Curt Bücken (*Metall*, 1952, **6**, (5/6), 123–128).—Recommended Al alloy compn. and casting procedures are discussed in regard to their appn. to the prodn. of bicycle frames, and to the various parts of internal-combustion engines—particularly those for autocycles, low-powered motor-cycles, &c.—and to light-weight containers (e.g. beer barrels).—E. N.

A New German Light Omnibus. ——(*Automobiltechn. Z.*, 1952, **54**, (6), 141–143).—An illustrated description, with details of design, of a new light-weight omnibus, all the main parts of which are made of Al alloy.—W. F. H.

Mass Production of Light-Metal Car Bodies. J. Baron (*Aluminium*, 1952, **28**, (3), 62–68; (4), 107–111).—After a historical review, B. describes indust. experience in modern methods concerning choice of alloy and gauge of sheet, and of deep-drawing techniques for various components; the use of cast components; methods of joining; and finishing. —M. A. H.

Chromium-Plated Aluminium Cylinder Barrels. E. Meyer-Rässler (*Rev. Aluminium*, 1952, (**188**), 200–204).—The advantages of hard Cr-plated cylinders are discussed and test data are given. Wear was only 0·05 mm. after 100,000 km. compared with 0·3 mm. for cast Fe. Several plating procedures are mentioned, but no useful details are included. Methods for modifying the Cr surface to increase its oil-retaining properties are also reviewed. A thickness of 0·1 mm. (0·004 in.) is recommended.—A. W. B.

Considerations on Some Railway Applications of Light Bearing Alloys. L. Paglialunga (*Alluminio*, 1952, **21**, (1), 43–47).—The Rome Tramways and Electric Railways Corp. have had some experience of using light alloy axle bearings of I.S.M.L. "Lubrical" alloy (Sn 6·5, Cu 1%, balance Al), and the main characteristics of this alloy are reported as good resistance to elevated temp. and high fatigue strength. —I. S. M.

[Use of Aluminium in] A Railway Refrigeration Unit. Maurice Victor (*Rev. Aluminium*, 1952, (**187**), 166–169).—Al was extensively used in the construction of a mobile refrigeration plant which is used to treat simultaneously four railway wagons of fruit or vegetables. The Al–5% Mg alloy has been used in the refrigerator and ducting and a Duralumin-type alloy for the framework.—A. W. B.

Aluminium in Aircraft. —— (*Aluminium Courier*, 1952, (**19**), 4–9).—Records the use of Al in aircraft from 1887.

Alloys of Al have been used in aero engines since 1903, playing a prominent part in reducing the wt./h.p. of the piston-type engine from 16 lb. in the Wright engine to under 1 lb./h.p. in the engines of today.—C. P. F.

The "Prouvé" [Aluminium] Schools. Maurice Victor (*Rev. Aluminium*, 1953, **(190)**, 267–269).—An illustrated description of prefabricated school buildings utilizing Al alloys in their construction, together with masonry and other traditional non-metallic materials.—A. W. B.

Aluminium in the "Franklin D. Roosevelt" Metro Station. Maurice Victor (*Rev. Aluminium*, 1953, **(190)**, 291–294).—Anodized Al in the form of panels, display cases, and nameplate letters has been widely used in the modernization of a French "Metro" station.—A. W. B.

"Aluman" Roofs in Switzerland. E. Müller (*Aluminium Suisse*, 1952, **2**, (4), 126–131).—[In French and German]. After referring to installations of commercial-purity Al roofing in Italy and Germany before 1925, ref. is made to buildings in Switzerland which since that date have used Al–1¼% Mn alloy (Aluman) for roofing with success. Means of fixing the roofing sheets adopted for different roofing methods are briefly mentioned.—A. W. B.

Corrugated Aluminium for General Building in Israel. —— (*Light Metals*, 1952, **15**, (172), 244–245).—A. W. B.

A Completely Insulated Aluminium Window. —— (*Modern Metals*, 1952, **8**, (6), 25–26).—The known disadvantage of Al window-frames—condensation of moisture on the frames—has been overcome by manufacturing a double frame with an insulating medium in between.—R. J.

Aluminium Honeycomb Sandwich Has Light Weight, High Strength, Good Stability, and Uniform Density. Phillip O'Keefe (*Materials and Methods*, 1952, **36**, (6), 96–98).—Cf. *M.A.*, **19**, 892.—R. P. H. F.

Aluminium in Paper-Making Plant. —— (*Light Metals*, 1952, **15**, (172), 238).—A. W. B.

Aluminium as a Structural Material in the Chemical Industry. E. Franke (*Aluminium*, 1952, **28**, (3), 75–76).—A brief review is given of relevant publications in 1950.—M. A. H.

Use of Aluminium Pipe in Oil-Country Applications. William B. Moore, Jr. (*Petroleum Eng.*, 1952, **24**, (4), D28, D30, D32).—A number of appn. of Al pipe in the oil industry are described. These include its use in heat-transfer equipment, shot-hole casing, temporary portable lines, and pipelines.—G. T. C.

Aluminium in the Petroleum Industry. —— (*Modern Metals*, 1952, **8**, (6), 34–36).—Extensive use is being made of Al piping for carrying petroleum overland. Low handling costs and upkeep are among the advantages claimed.—R. J.

Aluminium Platters and Pans. —— (*Modern Metals*, 1952, **8**, (3), 49–50, 52, 54).—A comprehensive review of the use of Al for meat-handling equipment.—R. J.

Aluminium in General Line Containers. —— (*Modern Metals*, 1952, **7**, (12), 24–28, 30).—A description of the use of Al in general packaging, including an evaluation of the strength, corrosion-resistance, &c., of such packages and prodn. methods (deep drawing, impact extrusion, and built-up containers). —R. J.

Aluminium Foil Protects Aircraft Parts. —— (*Canad. Metals*, 1952, **15**, (12), 48).—A brief note on the use of Al foil for the protection of aircraft components during shipping and storage.—W. A. M. P.

Reflective Insulation [Aluminium Foil]. —— (*Modern Metals*, 1952, **8**, (4), 40–42).—The salient features of an insulating medium based on Al foil are described.—R. J.

Aluminium vs. Copper. F. L. Church (*Modern Metals*, 1952, **8**, (4), 25–28, 30–32).—A general review outlining the principal fields in which Al is successfully competing with Cu, particularly in elect. industries.—R. J.

Cast Bronzes and Gun-Metals: The Case for Fewer Specifications. E. Voce (*Tin and Its Uses*, 1952, **(26)**, 2–3, 12).—The advantages of reducing the number of alloys are reviewed, and V. suggests that the 12 tin bronzes and gun-metals in B.S. 1400 (1948) could be reduced to 6 without serious tech. disadvantages, but with considerable economy.—K. S.

Beryllium Copper as a Mould and Die Material. —— (*Machinery* (*Lond.*), 1952, **81**, (2092), 1277–1280).—The advantageous properties of Cu–Be alloys for mould prodn. are: (1) a relatively high thermal conductivity, (2) high resistance to corrosion, (3) high impact strength, (4) good flow characteristics, (5) structural homogeneity, and (6) considerable stability and long life under moulding conditions. The max. compressive stress for the alloy is given as 205,000 lb./in.^{2}. Al castings have been produced from dies of this alloy. Recommendations for the soldering, brazing, and welding of the alloy are included.—C. P. F.

Beryllium Copper Alloy Springs. J. Bourguignon (*Pro-Metal*, 1952, **5**, (28), 43–47).—[In French and German]. Cu–Be alloys combine the mech. properties of spring steel with the phys. properties of Cu alloys. 2% Be alloy is supplied as strip or wire in the soln.-treated condition and is aged after working. Grain orientation does not yield directional variations in bending properties. The ageing treatment ensures relief of internal stresses, giving very stable properties and low hysteresis; service at moderately high temp. leads to less deterioration than with springs whose properties depend on cold work; the same applies to soldering and brazing.—K. S.

Copper Alloy Springs. —— (*Pro-Metal*, 1952, **5**, (26), 986–991).—[In French and German]. Cold-rolled and cold-drawn Cu and brass are used for springs when special requirements regarding thermal and elect. conductivity and corrosion-resistance have to be met. In many cases springs are stamped from cold-rolled strip at an angle of 45° to the direction of rolling, so that the deflection characteristics are equal along and across the spring. A stress-relief anneal at 250°–300° C. is recommended before machining.—K. S.

***Stainless-Clad Copper for High-Temperature Service.** Joseph Kinney, Jr. (*Product Eng.*, 1952, **23**, (4), 129–133).—Results of tests on the lateral heat conductivity of clad strips with various proportions of cladding to core are given. Methods of sealing cut edges and welding procedures are described, and data on allowable working stresses and workability are given.—M. A. H.

Stainless-Clad Copper Promises Improved High-Temperature Service. —— (*Machine Design*, 1952, **24**, (6), 141–142).—An illustrated account is given of the properties of Rosslyn metal, a Cu "sandwich" consisting of a Cu core clad with stainless steel in order to improve the thermal conductivity of heat-resisting alloys. At temp. up to 1500° F. (870° C.) the lateral conductivity compares favourably with pure Cu, but the latter would oxidize to destruction at this temp. Details of the properties of the combination are given, and an account presented of its appn. in the prodn. of jet-engine combustion chambers and other heat-resisting components.—D. M. L.

Copperweld Fine Wire. F. E. Leib (*Wire and Wire Products*, 1952, **27**, (9), 878–879, 927).—Copperweld consists of steel wire with 30–40 wt.-% Cu welded to the surface. A bimetallic billet is cast, rolled, and drawn. It has been used in large gauges for over 35 years for overhead power lines, and is now available down to No. 26 A.W.G. for elect. and other purposes, including piano strings. It is 8% lighter than Cu wire, its U.T.S. is 60,000 lb./in.^{2}, and its conductivity 30 or 40% of that of Cu at power frequencies.—C. P. F.

Germanium, Produced as a By-Product, Has Become of Primary Importance. A. P. Thompson and J. R. Musgrave (*J. Metals*, 1952, **4**, (11), 1132–1137).—A report on Ge, discussing its: (1) early history; (2) occurrence; (3) properties; (4) recovery—U.S. and British processes producing crude $GeCl_4$, which is purified, hydrolysed to GeO_2 and reduced to powdered metal by heating in an atmosphere of H; and (5) uses—in electronic devices, e.g. Ge diodes, triodes, and rectifiers; in glasses; and in alloys, particularly those with Au. 30 ref.—E. N.

Lead in Modern Chemical Construction. Kempton H. Roll (*Chem. Eng.*, 1952, **59**, (1), 281–282, 284–286, 288–290).—R. describes the latest techniques and improvements in the use of Pb in the chem. industries, including methods of supporting sheet Pb, new methods of testing Pb linings and welds, the use of Pb bonded to steel (usually referred to as bonded or homogeneous Pb), Pb-covered Cu or steel heating coils, and the use of acid-proof brick with an impervious Pb interliner.—S. R. W.

Why Magnesium in Aircraft Construction? R. Smallman-Tew (*Modern Metals*, 1952, 7, (12), 33–35).—An assessment of the advantages and disadvantages of Mg in aircraft. High strength: weight ratio and greater stiffness without increased weight are the main features. S. quotes some interesting examples of how Mg has replaced Al in a jet-powered commercial plane.—R. J.

B-36 Experience with Magnesium. D. A. Tooley (*Modern Metals*, 1952, 7, (12), 49–50, 52–54).—The B-36 aircraft contains 8000–9000 lb. of Mg, and T. describes the various difficulties confronting the engineers responsible for the plane. They made particularly effective use of the good fatigue-resistance of Mg alloys. The test programmes carried out included mech. tests, protective treatments against corrosion, and the experimental use of new alloys. Future possibilities and requirements are briefly discussed.—R. J.

Details of Construction of the Magnesium Star at the Festival of Britain Exhibition in London. John L. Haughton (*Rev. Mét.*, 1952, 49, (12), 911–916).—The large Mg star suspended in Northumberland Avenue, London, had to fulfil, amongst others, the following conditions: (1) the panels of the star had to be truly plane, as the lighting both by day and night was oblique; (2) the steel supporting wires had to be as inconspicuous as possible; (3) it had to be as light in weight as possible; (4) there had to be no risk of the star's falling on the heavy traffic below; and (5) two of the arms of the star had to be mounted *in situ*, owing to difficulties in transport. H. gives the details of the construction and suspension of the star.—J. H. W.

Nickel and Its Alloys at the Industrial Chemical Show, Paris. L. Arbellot (*Rev. Nickel*, 1952, 18, (2), 27–35).—A. reviews various appn. of Ni alloys on view at the Industrial Chemical Show, Paris.—R. W. R.

Titanium and Its Alloys. John L. Everhart (*Materials and Methods*, 1952, 35, (5), 117–132).—The present and future appn. of Ti and its alloys are reviewed. Suitable techniques for machining, forming, heat-treatment, welding, cleaning, and finishing are discussed.—R. P. H. F.

Metallic Titanium and Its Industrial Applications. Hideo Nishimura (*Bull. Eng. Research Inst. Kyoto Univ.*, 1952, 2, (Sept.), 1–5).—[In Japanese]. Recent development of the metallurgy of Ti is briefly described. The indust. appn. of the metal are discussed in detail.—Author.

Research and Development on High-Temperature Materials. C. A. Bristow and H. Sutton (*Iron Steel Inst. Special Rep.*, 1952, (43), 289–292; discussion, 368–378).—The met. and supply factors which influence the choice of alloys for high-temp. service are reviewed and discussed, and the importance of avoiding the misuse of scarce elements is emphasized. Long-range research is essential, and examples of work in progress are given. 15 ref.—D. M. P.

High-Temperature Alloys for Gas Turbines.—I.–II. H. V. Kinsey (*Canad. Metals*, 1952, 15, (11), 28, 30; (13), 20, 22, 24).—[I.—] K. discusses the properties of ferritic-martensitic alloys and their gas-turbine appn. [II.—] Austenitic alloys are similarly reviewed and discussed. 42 ref.—W. A. M. P.

General Tendencies in the Development of Materials for Jet Engines in Great Britain. A. H. Waterfield (*Métaux, Corrosion-Ind.*, 1952, 27, (320), 156–157).—A brief review is given of the development of materials showing promise with regard to availability, cost, and properties.—M. A. H.

Problems Presented by the Application of Refractory Materials to Jet-Engine Components. R. Fleury (*Métaux, Corrosion-Ind.*, 1952, 27, (320), 160–163).—A summary of material properties required by the design engineer for blades, discs, combustion chambers, and distributors is followed by a list of difficulties encountered by the manufacturer in the mass production of such engines.—M. A. H.

The Problem of Heat-Resisting Alloys in the Construction of Automobiles. H. Godfroid (*Métaux, Corrosion-Ind.*, 1952, 27, (320), 158–159).—G. briefly compares this problem with that of refractory alloys in aero-engine construction.—M. A. H.

The Engine Bearing. D. G. Soutar (*J. Inst. Automotive Aeronaut. Eng.*, 1952, 12, (11), 253–258).—The properties of Pb-base, Sn-base, Cu–Pb, and Al–Sn bearing alloys are given, and their use in connecting-rod and main bearings in automotive engines is discussed. Typical failures are described, and their causes are given.—T. A. H.

Flexible Metal Tubes. O. Meyer (*Pro-Metal*, 1952, 5, (30), 84–88).—[In French and German]. Flexible metal tubing can withstand higher temp. and pressures than rubber, but is not flexible in torsion. In many cases the metal serves as a casing for rubber. Narrow brass strip is bent to shape, wound on a mandrel, and the interlocking portions are anchored. Crimped tubing, made from continuous drawn or welded tube, is a recent development which ensures complete freedom from leaks.—K. S.

Material-Selection Factor Significant in Bourdon Tubes. J. B. Giacobbe and A. M. Bounds (*J. Metals*, 1952, 4, (11), 1147–1148).—G. and B. discuss the various types of alloys used in the prodn of Bourdon tubes—their classification by temper, their drift hysteresis, and relaxation (cold creep, zero shift) characteristics, and their corrosion-resistance. Mention is made, also, of the methods of shaping and joining the tubes.—E. N.

The Role of Castings in the Agricultural Industry. William G. Gude (*Foundry*, 1952, 80, (11), 114–117, 228, 231, 234).—The appn. of ferrous and non-ferrous castings in the manufacture of agricultural implements are discussed; the possibilities in this connection of castings made by investment casting and the honing process are considered.—R. W. R.

Corrosion-Resistant Metals in the Pulp and Paper Industry. Daniel L. Horigan (*Paper Trade J.*, 1952, 135, (20), 261–262, 264–271).—Various types of corrosion are outlined, and corrosion-resistant ferrous and non-ferrous metals and alloys are discussed with special ref. to paper-industry appn. Suitable welding methods for tank, &c., liners are described and illustrated, and various processing stages in papermaking are enumerated, with annotations concerning the resp. corrosion-resistant metals used.—J. R.

24 — BIBLIOGRAPHY

(Publications marked * have been received.)

***Atomic Energy Research Establishment.** *Bibliography on Americium.* (A.E.R.E. Inf./Bib. 86). [Mimeographed]. F'cap. Pp. 6. 1952. London: H.M. Stationery Office. (1*s.* 3*d.*; 1*s.* 4½*d.* post free.)

***Azienda Minerali Metallici Italiani.** *Metalli non ferrosi e ferroleghe: Statistiche 1952.* (*Non-Ferrous Metals and Ferro-Alloys: Statistics 1952.*) [In Italian and English]. 27 × 22 cm. Pp. [vii] + 166. 1953. Rome: A.M.M.I., Via Molise 11.

[This volume contains data on the production, export, prices, and consumption of non-ferrous ores and metals and ferro-alloys in Italy and the leading producing and consuming countries.

The Italian statistics for production and foreign trade are given for the year 1952; those for prices are brought down to March 1953.

The statistics for other countries are up to the end of 1952 for production and March 1953 for prices.]

***Barnard, G. P.** *Modern Mass Spectrometry.* (Physics in Industry Series). 9¼ × 6 in. Pp. 326, with 153 illustrations. 1953. London: The Institute of Physics, 47 Belgrave Square, S.W.1. (50*s.*)

***Billiter, Jean.** *Technische Elektrochemie.* I. Band: *Elektrometallurgie wässeriger Lösungen.* Dritte, umgearbeitete Auflage. 24 × 16·5 cm. Pp. viii + 308, with 129 illustrations. 1952. Halle (Saale): Verlag Wilhelm Knapp. (Brosch., DM 19.60; geb., DM 21.60.)

***British Iron and Steel Research Association.** *Annual Report 1952.* 9½ × 6½ in. Pp. 132. [1953]. London: The Association, 11 Park Lane, W.1.

***Brooker, H. R.,** and **E. V. Beatson.** *Industrial Brazing.* 8½ × 5½ in. Pp. 344, with 203 illustrations. 1953. London: Iliffe and Sons, Ltd. (for *Welding and Metal Fabrication.*) (35*s.*)

***Cahn, R. W.** *The Preparation of Uranium Crystals.* (Atomic Energy Research Establishment Report M/R 744). [Mimeographed]. F'cap. Pp. 23. 1951. London: H.M. Stationery Office.

***Cazaud, R.** *Fatigue of Metals.* Translated by **A. J. Fenner.** 9¾ × 6 in. Pp. xiv + 334, with 245 illustrations. 1953. London: Chapman and Hall, Ltd. (60*s.*)

[A translation of the third edition of "La Fatigue des Métaux" (Paris: 1948), with some additional material by the translator.]

***Centro di Ricerche Spettrochimiche.** *Proceedings of the Second International Colloquium on Spectroscopy.* Organized by the Centro di Richerche Spettrochimiche dell' Associazione Italiana di Metallurgia and held in Venice in September 1951. (A special number of *Spectrochimica Acta.*) 9¾ × 7½ in. Pp. vii + 200, illustrated. 1952. London: Pergamon Press, Ltd., 2, 3, and 5 Studio Place, S.W.1.

[Contents: D. M. Smith, "Spectrographic Copper Standards"; H. Bückert, "Über einige Verbesserungen an den Apparaturen für die spektrochemische Analyse"; J. Orsag, "Nouvel appereillage simplifié utilisable par lecture directe"; G. Brucelle, "L'influence de l'énergie mise en jeu dans le décharge et du caractère de cette décharge sur l'émission des raies spectrales"; J. M. Lopez de Azcona, "Estudio espectral sobre la influencia del estado fisico en la 'Haynes Stellite Alloy, No. 30'"; J. van Calker, "Spektroskopische und elektrische Messungen an Niederspannungsfunken"; R. Baistrocchi, "Richerche spettrochimiche orientative su bronzi antichi Italiani"; A. Gatterer, "Über die Eignung von Gitter- und Prismenspektrographen für spektrochemische Arbeiten"; W. Seith und A. Kottmann, "Die Spektralanalyse von Nickel–Kobalt-Legierungen im Bereich von 0–100%"; A. Luszczak, "Technisch belangreiche Extinktionsregelmässigkeiten von Farbstoffen"; V. Gazzi, "Le 'esaltazioni' nell' analisi spettrochimica qualitativa"; A. Giavino, "Alcuni aspetti della taratura dei quantimetri"; F. X. Mayer, "Spektralanalytische Spurenuntersuchung in der Kriminalistik"; G. Piccardi, "Spettroscopia, archeologia e metallurgia"; S. Rosetta, "Determinazione spettrochimica del silicio nelle ghise ed osservazione della microstruttura corrispondente"; R. Berta e A. Palisca, "Osservazioni sull' analisi spettrografica della ghisa"; L. Benussi e A. Caroli, "L'impiego dell' analisi spettrochimica a lettura diretta per mezzo del quantometro nel controllo della produzione degli acciai speciali"; E. Arreghini e T. Songa, "Osservazioni sulla sensibilità di riconoscimento spettrale delle impurità nel piombo"; P. Mathiot, "Nouveau microdensitomètre enregistreur pour la spectrophotométrie"; O. Masi e B. Morello, "Ancora su talune determinazioni sensitometriche in spettrografia"; C. Rossi e R. Intonti, "Sulla unificazione nell' analisi spettrografica di acciai mediamente legati"; G. Zazini, "Metodi di analisi spettrografica quantitativa con spettrografo Hilger E 492"; W. Pasveer, "Le calcul spectrographique a l'aide de nomogrammes"; F. Gasparotti, "Purificazione dei solventi per uso spettroscopico"; F. C. Mathieu, "Le spectro-lecteur automatique comme instrument de recherche"; A. Portalupi, "Lavoro in collaborazione in corso per la unificazione di un metodo di analisi quantitativa spettrografica delle ghise"; L. Bartoli e C. Becchio, "Ricerca delle principali cause di errore nelle determinazioni quantometriche eseguite con quantometro A.R.L. (S.Q.A.)".]

***Darken, Lawrence S.,** and **Robert W. Gurry.** *Physical Chemistry of Metals.* (Metallurgy and Metallurgical Engineering Series). 9 × 6 in. Pp. ix + 535, illustrated. 1953. New York: McGraw-Hill Book Co., Inc. ($8.50); London: McGraw-Hill Publishing Co., Ltd. (61*s.*)

Dellwig, Friedrich, und **Wilhelm Esch.** *Grundlehrgang für Former.* Herausgegeben vom Verein Deutscher Giessereifachleute. 21 × 15·5 cm. Pp. 89, with 236 illustrations. 1952. Düsseldorf: Giesserei Verlag. (Brosch., DM 5.60.)

***Deutsche Gold- und Silber-Scheideanstalt.** *Aus Forschung und Produktion: Technische Berichte herausgegeben zum achtzigjährigen Bestehen der Deutschen Gold- und Silber-Scheideanstalt, vormals Roessler, 1873–1953.* 23 × 16 cm. Pp. 478, illustrated. 1953. Frankfurt am Main: The Company.

[Contents: I. METALLE.—A. Boettcher, "Metallforschung"; E. Raub und A. Engel, "Über das chemische Verhalten von Legierungen der Edelmetalle"; J. Leuser und E. Wagner, "Über den Einfluss verschiedenartiger Wärmebehandlung auf die Eigenschaften von Schmuckgold"; H. Holzmann, "Platinrückgewinnung bei der Ammoniakoxydation"; W. Seith und K. Budde, "Zur Diffusion im System Silber–Palladium"; J. Schatz, "Edelmetallegierungen mit besonderer Beständigkeit gegen starke Mineralsäuren"; O. Loebich, "Platinmetallhaltige Goldlegierungen in der Zahntechnik"; E. Gebhardt und M. Becker, "Über die innere Reibung schmelzflüssiger Metalle und Legierungen"; H. Rudolph und E. Wagner, "Das Löten mit Silberloten: Stand der Technik und neue Entwicklungen"; W. Schulenburg, "Seltene Metalle"; P. Pickhart, "Edle und unedle Katalysatoren"; W. Scheibe, "Der kernlose Induktionsofen"; K. Winterer, "Eine Vereinfachung der Wärmebehandlung von Einsatzstählen". II. ANORGANISCHE CHEMIE.—K. Andrich und O. Fuchs, "Cyan und Cyanide"; J. Müller, "Zur Geschichte der Perverbindungen"; L. Harant, "Zur Werkstoff-Frage in der Industrie der Perverbindungen"; W. Hundt und K. Vieweg, "Über die Perverbindungen und ihre praktische Verwendung"; E. Wagner, "Natriumchlorit"; E. Bergheimer, "Die Darstellung des Natriums"; H. Kloepfer, "Die Fabrikation der Russe unter besonderer Berücksichtigung des deutschen Aktivrusses"; F. Endter, "Die Herstellung der Corax-Russe"; F. Endter, "Weisse Kautschukfüllstoffe und ihre verstärkende Wirkung"; A. Weihe, "Zur Kenntnis der aktiven weissen Füllstoffe"; K. Dithmas, "Die Verwendung pyrogen gewonnener, kolloid disperser Oxyde von Metallen und Metalloiden in der Textil-Industrie". III. KERAMIK UND GLAS.—H. Kohl, "Die deutsche Industrie der keramischen Farben: Tradition und Fortschritt"; R. Liepack, "Der Reliefschablonendruck mit keramischen Farben"; M. Kollmar, "Flüssige Edelmetallpräparate zum Metallisieren von keramischem Material und Kunststoffen"; D. Frost und F. Klauer, "Die Messung von Dichtedifferenzen abgeschreckter Gläser als Mittel zur Beurteilung ihrer Temperaturwechselbeständigkeit"; G. Jaeger, "Oxydkeramik"; G. Jaeger, "Die Bestimmung des $\beta\text{-Al}_2\text{O}_3$-Anteiles in Schmelzkorund"; F. Stapelfeldt, "Gerät zum Aufzeichnen von Düsenkanälen". IV. ORGANISCHE CHEMIE.—F. Flügge, "Die Entwicklung der Holzverkohlungs-Industrie in Deutschland"; W. Kern und H. Hachenberg, "Die Charakterisierung des Paraformaldehyd und anderer Polyoxymethylene"; H. Schulz und H. Wagner, "Synthese und Umwandlungsprodukte des Acroleins"; K. H. Liedtke und W. Kaul, "Methionin: Chemische und medizinische Betrachtungen"; H. Schulz und H. Huemer, "Synthese von Cyanürchlorid"; T. Spreter von Kreudenstein, "'Palavit' in der Zahnheilkunde".]

Doehler, H. H. *Die-Casting.* 24 × 15 cm. Pp. vi + 502, with 275 illustrations. 1952. New York: McGraw-Hill Book Co. Inc.; London: McGraw-Hill Publishing Co. Ltd. (64*s.*)

Frede, Ludger. *Physik in der Giesserei.* Herausgegeben vom Verein Deutscher Giessereifachleute. 21 × 15·5 cm. Pp. 141, with 360 illustrations. 1952. Düsseldorf: Giesserei Verlag. (Brosch., DM 6.80.)

Fritz, J. C. *Das Flammspritzen von Stahl, Metallen und Kunststoffen.* 21 × 15·5 cm. Pp. 176, with 137 illustrations. 1953. Essen: W. Girardet.

***Garside, James E.,** and **R. F. Phillips.** *A Text-Book of Pure and Applied Chemistry.* 7½ × 5 in. Pp. ix + 1044, with 275 illustrations. 1953. London: Sir Isaac Pitman and Sons, Ltd. (25*s.*)

Guggenheim, E. A. *Mixtures: The Theory of the Equilibrium Properties of Some Simple Classes of Mixtures, Solutions, and Alloys.* (International Series of Monographs on Physics.) Pp. 270, illustrated. 1952. Oxford: University Press. (42*s.*)

***Hoyt, Samuel L.** *Metal Data.* (Revised edition of *Metals and Alloys Data Book*). 10 × 7 in. Pp. xiv + 526, illustrated. 1952. New York: Reinhold Publishing Corp. ($10.00); London: Chapman and Hall, Ltd. (80*s.*)

***"Iron and Steel".** *Iron and Steel Directory.* Seventh edition. 8½ × 5½ in. Pp. 386. 1953. London: The Louis Cassier Co., Ltd. (25*s.*; 25*s.* 8*d.* post free.)

***Milner, G. W. C.,** and **A. J. Wood.** *The Analysis of Uranium–Gallium Alloys.* (Atomic Energy Research Establishment Report C/R 1041). [Mimeographed]. Pp. 15. 1953. London: H.M. Stationery Office. (2*s.* 6*d.*; 2*s.* 7½*d.*, post free.)

***National Metallurgical Laboratory.** *Symposium on Electroplating and Metal Finishing.* Held at Jamshedpur on 7 and 8 March 1952. 9½ × 7½ in. Pp. 177, illustrated. [1953]. Jamshedpur, India: National Metallurgical Laboratory.

[Contents: T. Banerjee, " Impact of Modern Science in Plating Industries, with Special Reference to India "; G. P. Chatterjee, " Some Basic Concepts on the Rate of Film Formation on Metals and Alloys "; A. Goswami, " Anodic and Cathodic Crystal Growth and Structure "; T. Banerjee, " X-Ray Structure of Electrodeposited Alloys "; V. M. I. Nambissan, " Phase Structure of Cast and Electrodeposited Alloys "; A. A. Krishnan, " Influence of Structure of Electrodeposits on the Brightness of Plated Surfaces "; S. D. Gokhale, " Addition Agents in Electroplating "; S. C. Shome, " Prevention of Corrosion of Metals by Protective Coatings "; Hira Lal, " The Nature of the Electropolishing State "; B. N. Das and M. S. Mitra, " Influence of Surface Condition on the Fatigue of Metals "; D. R. Dhingra, G. N. Gupta, and M. G. Gupta, " The Electrodeposition on Non-Conducting Surfaces "; K. Chakraborty and T. Banerjee, " Plating Non-Metals "; S. S. Bhatnagar and B. R. Nijhawan, " Thickness of Anodic Films on Aluminium "; D. R. Dhingra, M. G. Gupta, and M. C. Bhattacharya, " Anodization and Multi-Colouring of Pure Aluminium "; D. S. Tandon and T. Banerjee, " Plating on Aluminium "; A. K. Bhimani, " Electro-Deposition—Its Importance and Necessity "; A. Goswami, " Specifications in Plating "; K. K. Majumdar, " Plating Materials—Their Availability in India "; T. L. Ramachar, " Electrodeposition of Silver from the Iodide Bath "; J. Balachandra, " Electrodeposition of Metals from Fluoborate Baths "; Vasant M. Dokras, " Codeposition of Nickel and Chromium "; S. K. Roy and T. Banerjee, " Industrial Brass Plating from a Non-Cyanide Bath "; J. McNeil, " Efficiency and Economy in the Electrodeposition of Nickel "; R. U. Khan, " Common Plating Troubles and Their Cures "; T. Banerjee and B. L. Sen, " Some Jari Plating Defects and Their Removal "; P. K. Gupta and B. R. Nijhawan, " Metal Surface Protective Coatings "; S. Hebel, " Rust-Proofing and Phosphatizing Treatment of Metals "; M. Roy and T. Banerjee, " Metal Finishing ".]

Shoenberg, D. *Supraconductivity.* (Cambridge Monographs on Physics.) Second edition. 8½ × 5½ in. Pp. 256, with 59 illustrations. Cambridge: University Press. (27*s.* 6*d.*)

Wagner, Erhard. *Chemie in der Giesserei.* Herausgegeben vom Verein Deutscher Giessereifachleute. 21 × 15·5 cm. Pp. 84, illustrated. 1952. Düsseldorf: Giesserei Verlag. (Brosch., DM 3.60.)

***Wilson, A. J. C.** Edited by. *Structure Reports for 1949. Vol. 12.* 9½ × 6½ in. Pp. viii + 478, illustrated. 1952. Utrecht: N. V. A. Oosthoek's Uitgevers MIJ. (for the International Union of Crystallography). (55 Dutch florins, post free.)

***Woodward, O. H.** *A Review of the Broken Hill Lead–Silver–Zinc Industry.* 9 × 6 in. Pp. 400, illustrated. 1952. Melbourne: Australasian Institute of Mining and Metallurgy (n.p.)

25 — BOOK REVIEWS

Physical Metallurgy for Engineers. By Donald S. Clark and Wilbur R. Varney. 9 × 6 in. Pp. xiii + 567, illustrated. 1952. New York: D. Van Nostrand Co., Inc. ($6.50); London: Macmillan and Co., Ltd. (48*s.*)

Students of all the many branches of engineering will find this well-written and clearly printed book helpful to their understanding of the metals and alloys with which they are inevitably concerned in their day-to-day work, thought, and calculations. The subject matter presented by the authors is that developed over a period of years for a course in metallurgy given to engineering students at the California Institute of Technology.

The authors have not quoted original papers, but each chapter ends with a list of references to such well-known modern text-books or monographs as would be easily accessible to American students.

No doubt the authors are not so parochially minded as would appear from their references, but it is significant of this book that its nineteen chapters include some 143 references of which only one stems from outside the U.S.A., namely Hume-Rothery. The contents list takes up nine pages and the index no less than 28 pages, and even then the latter is incomplete. However, both contents list and index are well done and most valuable. They indicate that the subject matter is so wide that it cannot be covered in detailed or other than dogmatic manner in a book of this convenient size. That is an indication of the thoroughness with which the authors have tried to cover the subject of physical metallurgy from the point of view of engineering students who must absorb the whole subject in one single semester. To help these student readers each chapter is given a tail piece of a dozen or more questions, and it will be a very good student who can answer them all satisfactorily after a semester, or indeed in his lifetime.

One may question the desirability of teaching men to use the discoveries of others without also giving them knowledge of those to whom they are indebted. It might surprise American engineering students to know that in other countries, Bessemer, Siemens, and Hadfield steels, Muntz metal, Duralumin, Elektron, and beryllium were first invented or produced; if so they must seek elsewhere for such knowledge. It may not be money-making knowledge, but it is part of a real education in metallurgy.

There is much in the book that will be of value to engineers, little that is irrelevant, and it offers excellent technical information.

T. Henry Turner.

Progress in Metal Physics. Vol. 4. Edited by Bruce Chalmers. 9¼ × 6¼ in. Pp. viii + 403, illustrated. 1953. London: Pergamon Press, Ltd., 2, 3, and 5 Studio Place, S.W.1. (60*s.*)

To workers in the various fields of metal physics, and indeed to most general metallurgists (for, after all, metal physics is no more than the more fundamental aspects of metallurgy), the volumes of this series are by now thoroughly familiar. The earlier volumes are undoubtedly referred to constantly, both for references and for subject matter, if the particular topic in which the worker is interested is one which has been dealt with. The latest volume comprises seven reviews, two of which are follow-up articles on subjects covered in the first volume of the series, the remaining five being on new subjects. The editor is fortunate in having been able to retain for the repeated subjects the same authors as prepared the original reviews, and continuity in style and treatment is thereby assured. This matter of style is particularly noticeable to a reviewer who studies the whole volume in a relatively short space of time and is thus forced to note the different methods of treatment of their subjects by the various authors. It would be unfair, however, to ascribe differences of this character solely to the authors, since the presentation of a logical and coherent story depends very much on the extent to which research has led to a well-established and unifying theory, and the subjects covered are by no means uniform in this respect.

The first chapter, by A. S. Nowick on " Internal Friction in Metals ", deals with the subject purely as a research tool to study the internal structure of metals and alloys and is not concerned with engineering applications of damping capacity. Experimental methods are referred to very briefly, and the article deals mainly with internal friction produced by atomic movements, i.e. stress-induced ordering, relaxation across interfaces, or the movement of dislocations. Other sources of internal friction on which less recent work has been done, such as thermoelastic and magnetoelastic effects, are covered less fully.

Karl Hauffe has contributed extensively to the current state of knowledge of the mechanism of high-temperature oxidation, and his chapter on this subject is an excellent review. The oxidation of alloys involves so many factors of diffusion rates, activities, &c., that it is not surprising that technically important cases are very imperfectly understood. The influence of fractional percentages of reactive elements in controlling the oxidation rate of alloys, mainly by modifying the cracking and flaking tendency of the scale, is not referred to in the review but is well worthy of fundamental study.

Chapter 3 on " Gases in Metals ", by C. R. Cupp, is largely a factual review of the effects of dissolved gases on the properties of solid metals. It includes a section on internal oxidation which might have been better included in the previous chapter.

" The Theory of Sintering ", by G. A. Geach, shows that the mechanism of this process is clearly a long way from being understood, and as the author implies in his last paragraph a good deal of carefully controlled experimental work is required.

A. H. Cottrell's chapter, " Theory of Dislocations ", is the second review of this title, and shows very clearly the important progress made in this field in the last few years. More direct evidence of the existence of dislocations has been obtained from the study of growth spirals, and the conception of the Frank–Read source has contributed to a knowledge of their method of generation. Advance has been made in the application of dislocation theory to problems of work-hardening, annealing, creep, &c., and these are dealt with in an admirably clear and logical manner. It is to be expected that a third article on this subject will be required in a few years' time, and it is hoped that nothing will prevent Professor Cottrell continuing as author, for a more lucid expositor of a complex subject could hardly be obtained.

The sixth chapter, by A. D. le Claire on " Diffusion in Metals ", is also a second review, and deals mainly with the experimental advances made in the study of the Kirkendall effect and of grain-boundary and surface diffusion and the theoretical implications of this work.

The final chapter, " Nucleation ", by J. H. Hollomon and D. Turnbull, deals with the theories developed to cover the growth of liquid phases from vapours and of solids from liquids and shows how they have been extended to describe the more complex cases of nucleation of new phases in solid-metal systems which can involve changes in composition and the development of strain in addition to the structural changes.

The volume is a most welcome and valuable addition to the series, and confirms the view that progress reviews of this type are perhaps the only medium by which a research worker can keep informed on developments in fields other than that of his own immediate interest. One cannot help feeling, however, that the standard is becoming rather high for the non-specialist reader. The specialist in any subject will presumably have studied the original publications and with his understanding of the subject can use the review rather to " recap ". The non-specialist, on the other hand, will not usually be able to spare the time for the close and intensive study which the more advanced of these reviews demand. It would be a great pity if competition in erudition between authors should lead to the reviews being read only by experts—for the volumes would then fail in their avowed purpose.

W. Betteridge.

Titanium Metal and Its Future. By R. M. Burston, C. D. Crosby, G. A. Goetz, W. W. Minkler, Ferd Nadherny, G. P. Little, G. J. Sella, W. W. Sherrill, and J. M. Wermuth. [Mimeographed.] 11 × 8½ in. Pp. 100, illustrated. 1952. Obtainable from Clifton D. Crosby, 9114 North Swan Circle, St. Louis 17, Mo., U.S.A. ($10.00.)

The specific object of " Titanium Metal and Its Future ", a report written in the early part of 1952 by a group of second-year students at the Harvard Graduate School of Business Administration, is to inform the entrepreneur of the present economic aspects and the future possibilities of titanium without too much emphasis on technology. The first half of the report deals with present-day aspects of titanium and the titanium industry and consists of an historical introduction; properties of commercial titanium and its alloys, largely taken from manufacturers' data books; raw material, extraction, melting, and fabrication; and information about companies producing, fabricating, and engaged in research. The treatment of the technical sections is perfunctory, and the specialist seeking new data or even a co-ordinated survey of available technical information will find little to interest him. A section on the American titanium industry, although interesting, is becoming out of date as month by month new names of interested companies are announced.

The second half of the report is devoted to the future of the titanium industry. The limitations of the Kroll process are discussed and alternative methods of extraction canvassed. The authors consider that an electrolytic process will eventually be chosen. However, few informed readers would agree that the cost of titanium could fall as low as the suggested value of 30 cents per lb., in view of the inherent difficulties involved in separating a solid, easily oxidizable product from a hot fused electrolyte. A section on future developments in titanium alloys dismisses existing alloys somewhat cavalierly and points to the necessity of obtaining better ductility with high strength, and if possible, an addition which will reduce the embrittling effects of oxygen and nitrogen.

The authors' significant contribution is to be found in the remainder of the report in which they discuss the future development of the industry and the ability of titanium to compete with other structural materials. The chief uses of titanium, they suggest, will be for those parts at present made in stainless steel. Competition by titanium in the field of aluminium, magnesium, and copper alloys and of plastics will be unimportant in the foreseeable future. The authors therefore examine in detail the fields in which it would pay to replace stainless steel sheet by titanium sheet at various prices, and calculate that the total demand for titanium on the basis of present prices ($20 per lb.), $5 per lb., and $3 per lb. would be 9,000, 24,000, and 86,000 tons per annum, respectively. The last price, they consider, would make it worthwhile to replace all stainless steel by titanium, a threat which some stainless-steel companies in the U.S.A. have recognized by interesting themselves in titanium production. A section is devoted to the location of a titanium industry, and although this is related to the economics and geography of the North American continent, the findings are worthy of note by those who will have the responsibility of setting up integrated titanium industries in other countries.

The report faithfully reflects the attitude of operators in the American industry at the beginning of 1952, and, though the position has somewhat changed since then, many of the authors' observations on the economic factors which will affect the development of the titanium industry still hold and are worthy of attention today.

J. W. Rodgers.

Treatise on Powder Metallurgy. Volume III.—**Classified and Annotated Bibliography.** By Claus G. Goetzel. 9 × 6 in. Pp. xxiv + 899. 1952. New York. Interscience Publishers, Inc. ($22.00); London: Interscience Publishers, Ltd. (176*s*.)

This large volume adequately rounds off Dr. Goetzel's really monumental work, the outstanding features of which have already been reviewed (*M.A.*, 17, 410; 19, 93). The bibliography is in two parts: a literature survey containing 5535 entries and a patent survey listing the astonishingly large number of 6330 patents or patent applications. Both of these surveys are classified chronologically according to subject in sections conforming with the chapter headings of the first two volumes; and each entry is annotated with up to ten lines of explanation and summary. Finally, there is a name index.

The period covered in both parts is up to January 1950, and the surveys are, as far as can be judged, both competent and remarkably thorough. It is only in the patent section that consistency is lacking. Here an apparently arbitrary choice has been made between similar patents filed in more than one country. The patent which has been selected is not always that filed in the country of origin; and unfortunately no cross-references are given to corresponding patents in other countries. Taken as a whole, however, there can be nothing but admiration for the painstaking labour and the judgment that have gone into the preparation of these volumes. Dr. Goetzel has brought a great work to a triumphant finish.

J. C. Chaston.

Die-Casting. By Charles O. Herb. Second edition. 9 × 6 in. Pp. [iii] + 310, illustrated. 1952. New York: The Industrial Press, ($4.50); Brighton: Machinery Publishing Co., Ltd. (37*s.* 6*d.*)

In accordance with American nomenclature, this book is mainly confined to the various means of producing pressure die-castings, and makes little or no reference to the gravity or permanent-mould die-casting. One chapter, devoted to die-casting in cast iron, confines itself to a description of a system which is very novel and, the reviewer believes, relatively unknown in this country at least.

The evolution of pressure die-casting machines is traced from the year 1838, when the original machines were capable of working only with lead and the Babbitt type of metals, to the present-day machines that are producing castings in zinc-, aluminium-, magnesium-, and copper-base alloys.

Operation of the early machines was by muscular effort. By contrast the modern machine is power-operated, usually with its built-in electric-motor-driven pump for an oil-hydraulic system operating at high unit pressures. Whereas injection pressures of the early pressure casting machines were in the region of a few hundred pounds per square inch, the modern cold-chamber machine seldom operates below 5000 lb./in.^{2} and frequently operates in the neighbourhood of 30,000 lb./in.^{2}. This single factor has done much to make possible sound, homogeneous pressure die-castings in a range of alloys adequate to meet modern industrial requirements.

The modern machines, with push-button control, semi- or fully-automatic cycles, and predetermined, accurately controlled solidification dwells, are largely responsible for production rates that are high judged by any normal manufacturing standards. The performance of the machine is, however, basically controlled by the quality of the tools contained therein; the main value of the book becomes apparent, therefore, when it is mentioned that it contains many excellent photographs and drawings of a wide assortment of die designs, and of some really outstanding large castings, particularly of an automobile radiator grille, oil sump, and door-frame.

Fundamental die design varies, firstly in respect of the alloy in which the castings are to be produced, secondly in respect of the injection system employed, and thirdly in respect of the geometrical and physical characteristics of the casting. Many of the problems, in numerous and varied forms, receive adequate mention, but it is perhaps a pity that practically all the designs illustrated are associated with the split-sprue systems of injection, whereas in practice, the centre-sprue system undoubtedly predominates throughout the world. This, however, does not detract from the many examples of mechanical devices employed for core pulling and various other features essential to the functioning of the tools.

The book is unpretentious in matters of theoretical considerations, but is written in an easily assimilated style, and perhaps its greatest value will be found in providing the student engineer with a working knowledge of the process, and will, it is hoped, whet his appetite for further, but more advanced, knowledge on the subject.

H. W. Fairbairn.

Handbuch der ältesten vorgeschichtlichen Metallurgie in Mitteleuropa. Von Helmut Otto und Wilhelm Witter. 29 × 21 cm. Pp. v + 222, with numerous illustrations, 33 plates and 31 tables. 1952. Leipzig: Johann Ambrosius Barth. (Brosch., DM 63.40; geb., DM 65.40.)

The term Bronze Age has no absolute chronological value; it is the name usually given to that period of human culture during which the alloying of copper with tin in regular proportions became a widespread practice. Archæologists generally are agreed that the manufacture of bronze implements and ornaments started at Hissarlik, near the Dardanelles. From Hissarlik the art spread in a very little while throughout Europe and beyond. The time was some 2000 or 3000 B.C., the age of the erection of Stonehenge and the megalithic remains at Carnac. The blowpipe, crucible, and alembic had already been invented in Egypt (although I note (p. 52) that the authors consider that the crucible was not available at that time—archæologists hardly ever agree !), so that apparatus for smelting and casting was to hand; for fashioning his metal early man had only a stone hammer and stone anvil.

The work before me shows how very widely throughout Germany, Hungary, Yugoslavia, and Northern Italy the arts of bronze making, smelting, and casting were practised in the so-called Bronze Age, for here are given analyses of 1374 pre-historic bronze implements and ornaments obtained from about 150 museums and private collections.

It has emerged, from studies carried out over the last 100 years or so, that copper and tin deposits in Europe differ slightly in composition among themselves, and these slight differences are reflected in the metal extracted from the respective ores and in articles made therefrom, so that an analysis of the finished article should lead to a knowledge of its place of origin. Hitherto, such analyses have been carried out by the time-consuming and destructive processes of customary qualitative and quantitative analysis. The authors now break comparatively new ground in determining the composition of these 1374 irreplaceable prehistoric ornaments and implements—some possessing considerable artistic merit—by spectrographic analysis. About 0·2 g. of material was removed from an inconspicuous place and fashioned into two electrodes of dimensions 5 × 5 mm., and the composition was determined spectrographically by the method of homologous paired spectral lines, using a condensed spark discharge. Occasionally, the specimen itself was used as an electrode, the patina having been previously removed. The authors remark very naïvely (p. 58) " with practice the bore-hole can be closed, so as not to be seen under careful inspection ". I certainly hope so, but . . .

The results are collected in 10 tables, giving the percentage content of the various alloys in Cu, Sn, Pb, Ag, Au, Ni, Co, As, Sb, Bi, Fe, and Zn. Truly a monumental achievement. The authors draw seven important conclusions from their work, the principal of which are: (1) that mid-Germany was a very considerable metallurgical centre during the Bronze Age, and (2) that Hungary, on the contrary, in that period, was not a metallurgical centre of any consequence, and relied principally upon *native* supplies of copper, of which considerable amounts were found even in historic times in that country.

This work of very considerable erudition is provided with adequate name and subject indexes, which, among other things, list the places where the various specimens were dug up. References to original papers number about 700, drawn from the scientific literature of all countries. The pioneering work of Dr. C. H. Desch (reported to the British Association for the Advancement of Science in 1928–38) relating to Sumerian copper is much praised (p. 16). The book is not as well got up as is usual in German publications: the paper is not too strong and, except for the art paper used for photographic reproductions, is not of good quality. The difference in price between the bound and unbound volumes is only 2 DM; I recommend anyone purchasing the book to choose the former.

J. S. G. Thomas.

METALLURGICAL ABSTRACTS

METALLURGICAL ABSTRACTS AUTHOR INDEX

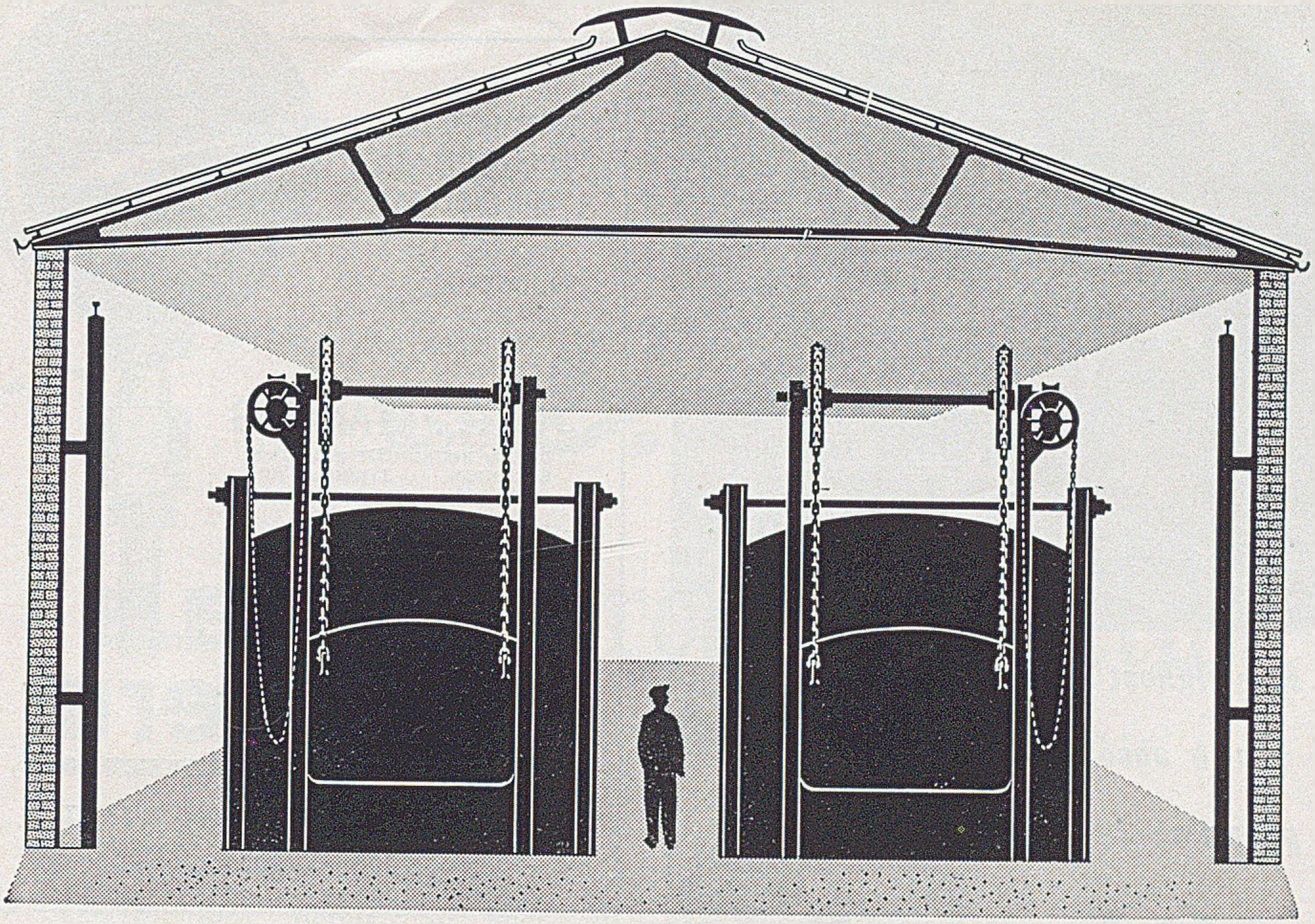

How many furnaces can you count — two or three?

"*You needed three to keep pace with the new production line. . . . Where's the third?*"

"In the other two. We've increased their capacity by fifty per cent. We get six charges per shift instead of four."

"*They look about the same.*"

"As a matter of fact, externally, they are exactly the same. A bit larger inside—thinner walls. But that's not the point; we've cut down the heat the walls soak up on every charge, it's that which has made the difference. They're built of a light-weight brick with a very low thermal capacity—and it's a good insulator into the bargain. We use no more fuel for six charges than we used for four."

"*The old hot face insulation, eh? Shouldn't have thought it would stand the temperature.*"

"The old stuff wouldn't. This is something new: stands 1540°C or 2800°F if you prefer it that way hence its name M.I.28. M. for Morgans of course."

MORGAN Refractories

ARE WORTH FAR MORE THAN THEY COST

THE MORGAN CRUCIBLE COMPANY LTD. (Refractories Group), Neston, Wirral, Cheshire. Tel: Neston 1406

N.E.26

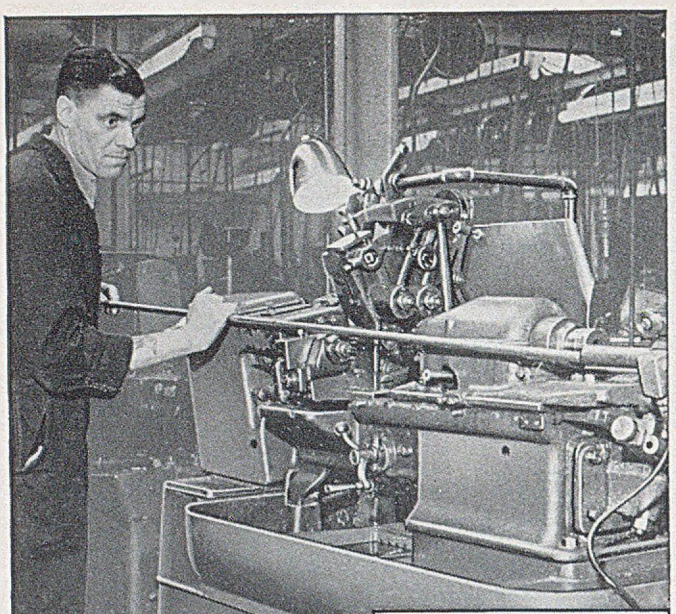

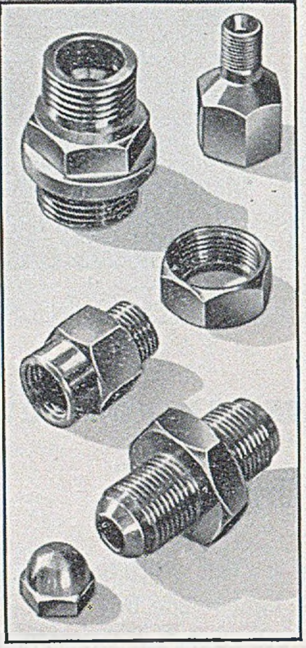


ROTOTHERM THERMOMETER
600
700
500
800
400
900
300
1000
200
°F
ROTOTHERM

Electrify production—

use G.E.C.

ELECTRIC Process Heating

FURNACES · INFRA RED · HIGH FREQUENCY

- Bold thinking about bigger production demands new methods of heat treatment. G.E.C. *electric* process heating ensures maximum output and true economy. The many heating equipments in its range are clean, safe, simple to operate, and heat rapidly to constant correct and controlled temperature. Its versatility is being proved every day.

- Its applications are many: for heat treating steel, setting resin glues, drying paint and numerous other processes. For example, the vertical cylindrical furnace is widely used in heavy industry for the bright annealing of most metals.

- G.E.C. has had many years' experience in the design and construction of heating plant. The Company's specialists welcome opportunities to discuss potential uses with engineers and metallurgists.

Furnace Plant

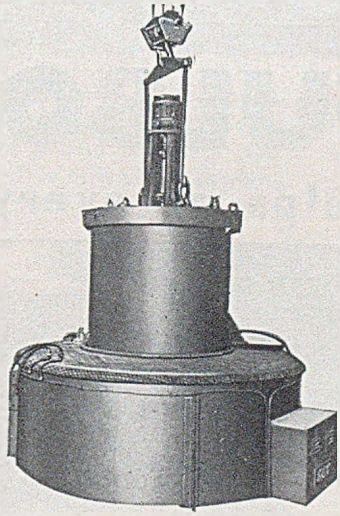

G.E.C.
VERTICAL CYLINDRICAL FURNACE

The charge is carried in the heat-resisting steel container. Rapid and uniform heating is ensured by the forced convection set up inside the container by the high-speed fan combined with the correct distribution of heating elements on the furnace wall.

Vertical cylindrical furnaces provide a perfect bright anneal for most ferrous and non-ferrous metal and alloys in coils of wire or strip.

THE GENERAL ELECTRIC CO. LTD., MAGNET HOUSE, KINGSWAY, LONDON, W.C.2

NON-DESTRUCTIVE TESTING

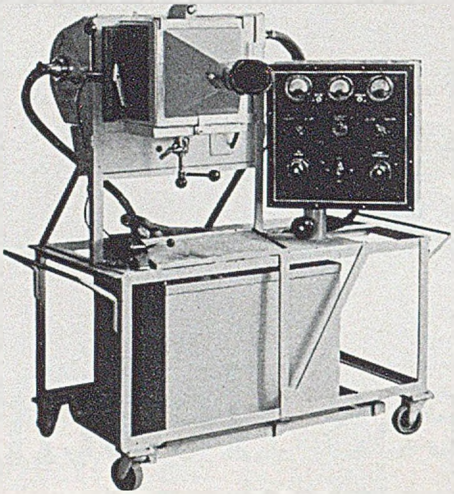

X-ray Fluoroscopic Equipment

EQUIPMENT

for X-radiography
Gamma radiography
Ultrasonic flaw detection
Magnetic Crack detection
Eddy Current Testing

N-D-TESTING SERVICE
at our laboratories at
BUSHEY and MATLOCK
or on Site

SOLUS-SCHALL LIMITED
18, NEW CAVENDISH STREET, LONDON W.1.
X-RAY. GAMMA RAY. ULTRASONIC. MAGNETIC.

'FULBOND'
TRADE MARK
helps at every stage

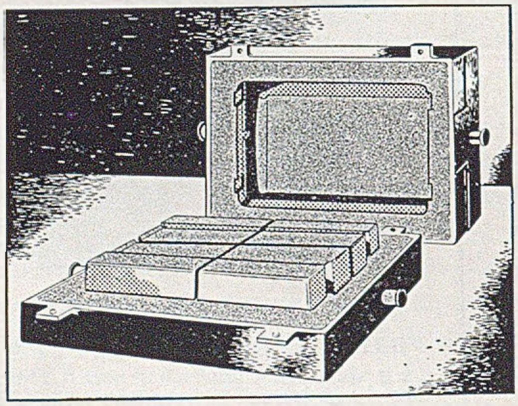

MOULDING
'FULBOND' improves the texture of natural and synthetic sands. It imparts many valuable properties.

For service and information write to:-
THE FULLERS' EARTH UNION LTD.
Patteson Court, Redhill, Surrey
Telephone REDHILL 3521
C.H.F.8

EQUIPMENT FOR THE
THERMAL TREATMENT
OF NON-FERROUS METALS AND ALLOYS

Cloth. 4to. 1952. Pp. 104, with 14 plates and numerous figures in the text. Price 15s. or $2.50, post free. (Members, one copy each at 7s. 6d. or $1.50, post free.)

CONTENTS: Electric Furnaces for the Thermal Treatment of Non-Ferrous Metals and Alloys; Gas Equipment for the Thermal Treatment of Non-Ferrous Metals and Alloys; Batch and Continuous Annealing of Copper and Copper Alloys; Bright Annealing of Nickel and its Alloys; Batch Thermal Treatment of Light Alloys; Flash Annealing of Light Alloys; Continuous Heat-Treatment of Aluminium Alloys of the Duralumin Type.

THE INSTITUTE OF METALS
4 Grosvenor Gardens, London, S.W.1

B
T-H

Rolling Mill Equipment

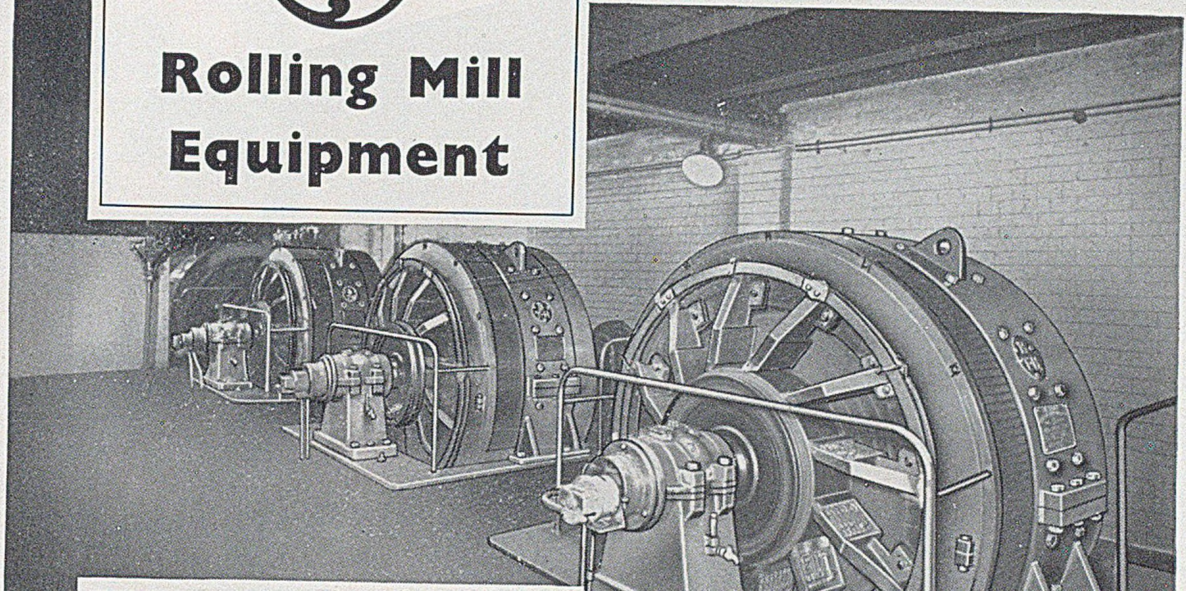

Three of the four 1,500-h.p., 300/600-r.p.m. D.C. motors, with appropriate control gear, driving the 4-stand tandem cold strip mill. The reel on this mill is driven by a 225-h.p., 225/900-r.p.m. D.C. motor.

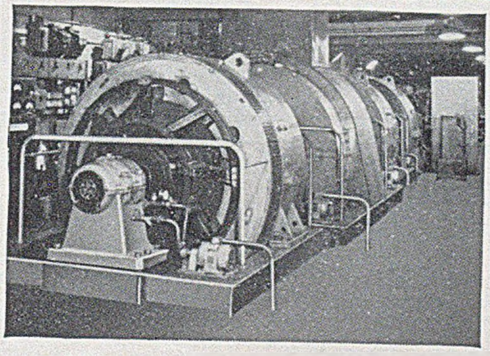

5,250-kW synchronous motor-generator set for the above mill.

750-h.p., 300/600-r.p.m. mill motor and 225-h.p., 225/900-r.p.m. reel motor, each with appropriate control gear, driving No. 1 skin pass mill.

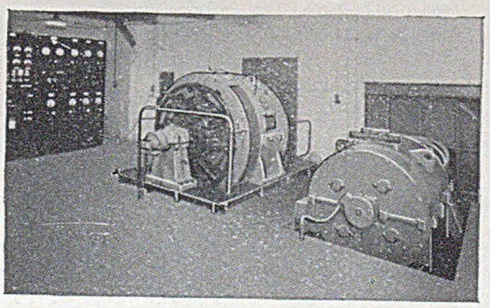

BTH manufacture electric drives for all types of rolling mills. The illustrations show some of the equipment installed in the Shotton Works of John Summers & Sons Ltd.

Over 500 Mazda Mercury Vapour lamps, complete with control boxes and auxiliary gear, were supplied for the lighting of the melting shop, scrap shop, and the maintenance workshop.

The services of BTH specialists in electric equipment for rolling mills are freely at the disposal of consulting and operating engineers.

Member of the AEI group of companies

THE
BRITISH THOMSON-HOUSTON
COMPANY LIMITED, RUGBY, ENGLAND

A4570

Index to Advertisers

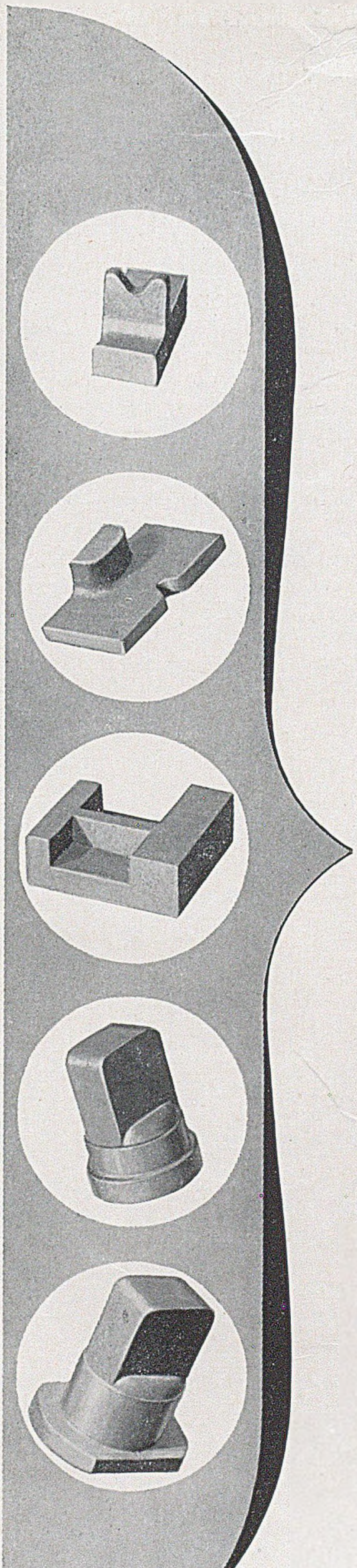

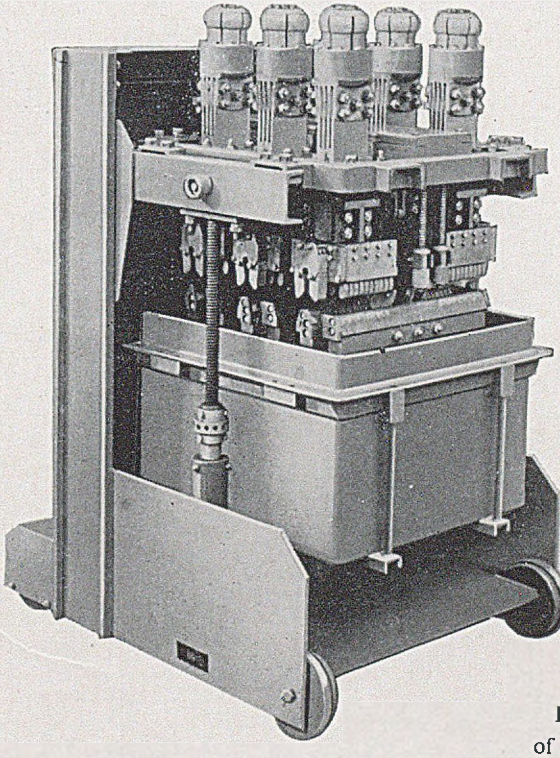

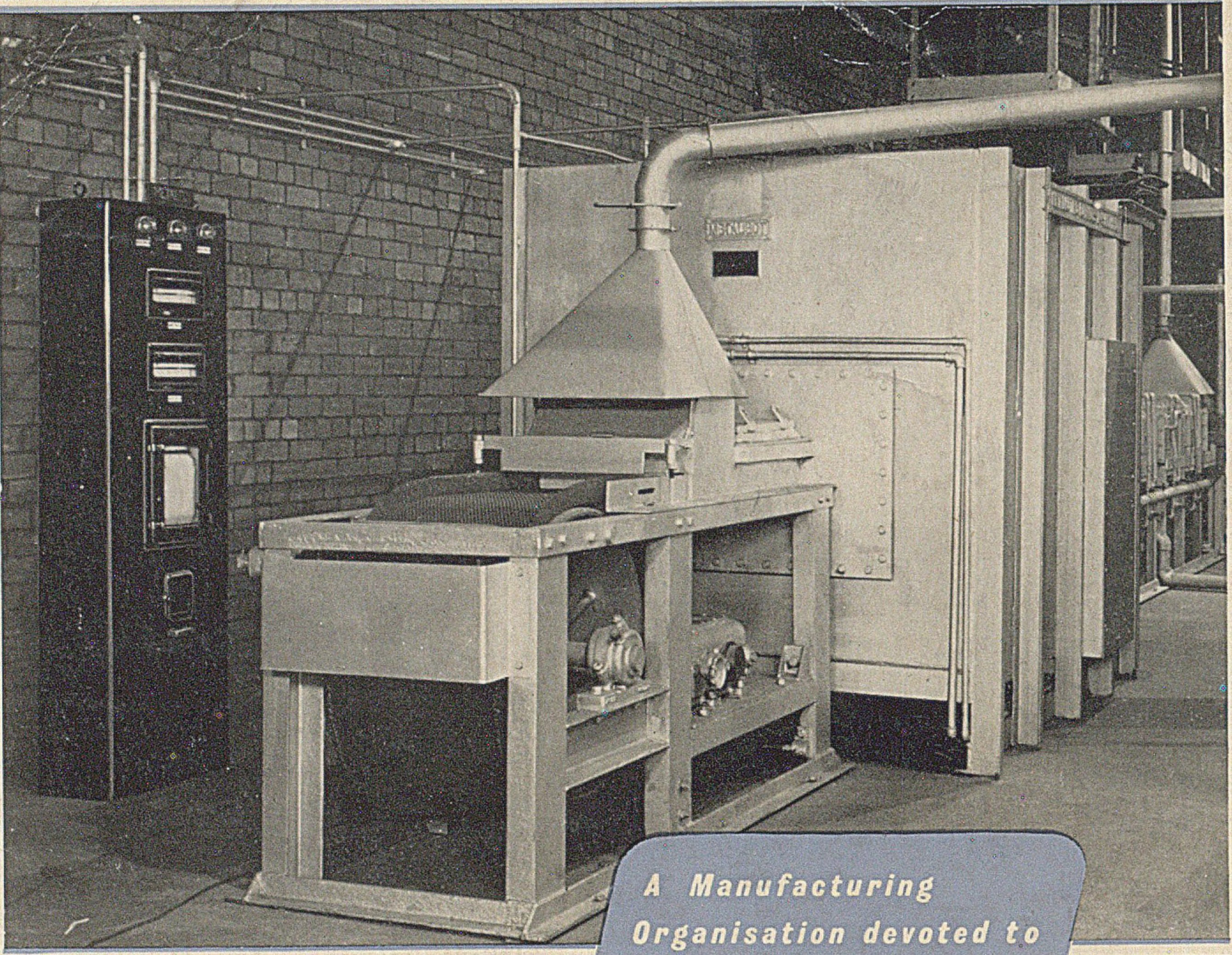

Electroflo Automatic Control Pyrometers with multi-point Recorder fitted to 2 zone electrically heated conveyor type furnace by Metalectric Ltd.

A Manufacturing Organisation devoted to the **DESIGN**
PRODUCTION
INSTALLATION
& SERVICING
of Industrial instrumentation and automatic control for all types of power and processing plants.

ELECTROFLO

METERS COMPANY LIMITED
Head Office: ABBEY ROAD, PARK ROYAL, LONDON, N.W.10
Factories: PARK ROYAL, LONDON, & MARYPORT, CUMBERLAND

All communications regarding Advertisements should be addressed to the Advertisement Department, 4 Grosvenor Gardens, London, S.W.1

Printed in Great Britain by Richard Clay and Company, Ltd., Bungay, Suffolk.